Novel approaches against pancreatic cancer based on adenoviral targeting and tumor ablation. Preclinical evaluation of antitumor efficacy.

Memòria presentada per

Anabel José Segarra-Martínez

Tesi dirigida per la Dra. Cristina Fillat Fonts, Investigador Senior ISIS, IDIBAPS. La tesi s'ha realitzat al Centre de Regulació Genòmica (CRG), Parc de Recerca Biomèdica de Barcelona (PRBB), programa Gens i Malaltia.

Dra. Cristina Fillat Fonts
Directora de la Tesi

Dra. Pura Muñoz-Cànoves
Tutor

Anabel José Segarra-Martínez
Doctoranda

TESI DOCTORAL UPF / 2011

Departament de Ciències Experimentals i de la Salut (CEXS)

CRG Centre de Regulació Genòmica

UNIVERSITAT POMPEU FABRA

A mis padres,

a mi yayi,

a Rubén.

Per a la realització d'aquesta Tesi Doctoral he gaudit, entre els anys 2007-20011, d'una beca del "Programa de Formación del Profesorado Universitario" (FPU) del Ministerio de Educación y Ciencia.

ABBREVIATIONS

ALT = Alanine Aminotransferase

AST = Aspartate Aminotransferase

ATCC = American Type Culture Collection

BE = Bystander Effect

CAR = Coxsackie and Adenovirus Receptor

CI = Combination Index

CMV = Cytomegalovirus

CPE = Cytopathic Effect

Cx = Connexin

ECM = Extracellular Matrix

eGFP = Enhanced Green Fluorescent Protein

ERCP = Endoscopic Retrograde Cholangiopancreatography

EUS = Endoscopic Ultrasonography

EUS-FNA = Endoscopic Ultrasound-Guided Fine-Needle Aspiration

EUS-FNI = Endoscopic Ultrasound-Guided Fine-Needle Injection

FBS = Fetal Bovine Serum

GCV = Ganciclovir

GCV-MP, GCV-DP, GCV-TP = GCV mono-, di- or tri-phosphorilated

GE, dFdC= Gemcitabine

GJIC = Gap Junctional Intercellular Communication

i.d = intraductal injection

i.p = intraperitoneal injection

i.v = intravenous injection

IRE = Irreversible Electroporation

HSV-1 = Herpes Simplex Virus Type 1

Luc = Luciferase

MCP = MMP Cleavable Peptide

MCP* = MMP Cleavable Peptide linked to fluorescein

MMP = Matrix Metalloproteinase

MTT = 3-(4,5- Dimethylthiazol-2-yl)-2.5-diphenyltetrazolium bromide

PanIN =Pancreatic Intraepithelial Neoplasia.

PDAC = Pancreatic Ductal Adenocarcinoma

PTD = Protein Transduction Domain

R.T = Room Temperature

RCAs = Replicative Competent Adenoviruses

RT-PCR = Reverse Transcription PCR

s.c = subcutaneous injection

TD-PCR = Touch Down PCR

TK = Thymidine Kinase

TSP = Tumor Specific Promoter

uPAR = urokinase Plasminogen Activator Receptor

UNITS OF MEASUREMENT AND SYMBOLS

bp, Kb = base pairs, Kilobase

cm, cm^2 = centimeter, square centimeter

°C = degrees Celsius

µF = microFaraday

g, mg, µg, ng = gram, milligram, microgram, nanogram

G = Gauge

x g = gravity

h = hour

KDa = KiloDalton

L, ml, µl = Liter, milliliter, microliter

λ = wave length

LU = Light Units

m, m^2, m^3 = meter, square meter, cubic meter

mm, mm^2, mm^3 = millimeter, square millimeter, cubic millimeter

M, mM, µM = Molar, millimolar, micromolar

min = minutes

nt = nucleotide

pfu = plaque forming units

RLU = Relative Light Units

rpm = revolutions per minute

s, ms, µs= seconds, milliseconds, microseconds

U/ml = Unitsper mililiter

V = volts

Vf = final volume

vp = viral particles

v/v = volume/volume

w/v = weight/volume

W = watts

Thomas Edison llegó a fracasar en 2.000 ocasiones antes de lograr el filamento de hilo de algodón carbonizado para su bombilla. Y cuando le preguntaron dijo: "no fracasé, descubrí 2.000 modos de cómo no se hace una bombilla, pero sólo debía encontrar un modo de que funcionara."

ABSTRACT

Novel therapies are needed to overcome the limited efficacy of current treatments in pancreatic cancer. Adenoviral gene therapy against pancreatic tumors is challenged by the limitation of viruses to reach the tumor mass, poorly distribute within the tumor and inefficiently transduce tumor cells. We show that intraductal administration of adenoviruses into the common bile duct of Ela-myc mice targets pancreatic tumors more efficiently than systemic delivery with relevant transduction of the bulk of the tumor and restricts expression to pancreatic tissue. Moreover, intraductal administration of AduPARTat8TK/GCV treatment significantly delayed tumor growth ameliorating tumor-associated toxicity. Noticeable the new generated MMP-activatable adenovirus AdTATMMP was susceptible to MMP2/9 activation, restored the transduction capacity of AdYTRGE *in vitro*, and increased 7.3 times tumor pancreas transduction. The multimodal treatment AduPARTat8TK/GCV and gemcitabine showed synergistic effects *in vitro;* however, did not enhance the antitumoral efficacy of single therapies. Interestingly, IRE treatment exhibited significant antitumor effects in BxPC-3-Luc orthotopic tumors and prolonged mice survival with minimal toxicity.

RESUM

Els tractaments actuals pel càncer de pàncreas presenten un eficàcia limitada de manera que es necessari el desenvolupament de noves teràpies antitumorals. La teràpia gènica pel càncer de pàncreas basada en l'ús d'adenovirus es troba limitada per la baixa capacitat dels virus d'arribar a les masses tumoral, de distribuir-se pel tumor i d'infectar les cèl·lules tumorals. Nosaltres hem observat que l'administració intraductal d'adenovirus al ducte biliar de ratolins Ela-myc permet arribar als tumors pancreàtics de manera més eficient que per la via sistèmica. A més a més permet transduir la majoria de la massa tumoral restringint l'expressió adenoviral al teixit pancreàtic. D'altre banda, l'administració intraductal del tractament AduPARTat8TK/GCV retarda significativament el creixement tumoral i disminueix la toxicitat associada al tumor. El nou adenovirus AdTATMMP és activat per les MMP2/9 restaurant la capacitat de transducció de l'AdYTGRE *in vitro*, i incrementant 7,3 vegades la infecció del tumor pancreàtic. El tractament combinat de l'AduPARTat8TK/GCV amb gemcitabina presenta un efecte sinèrgic *in vitro*, però no millora la eficàcia antitumoral de les teràpies simples. D'altre banda el tractament de l'electroporació irreversible presenta efectes antitumorals significatius en tumors ortotòpics de la línia cel·lular BxPC-3-Luc i allarga la supervivència dels ratolins provocant una toxicitat mínima.

PREFACE

Pancreatic cancer (PC) is one of the most devastating malignancies in developed countries. Patients with PC normally present with advanced disease and have a very poor prognosis. Due to the absence of early diagnosis and its highly invasive and metastatic feature, only 15-20% of patients have potentially resectable tumors and, unfortunately many of them experience recurrence of disease following surgery. Moreover, pancreatic cancer shows strong resistance to the current available chemotherapy and/or radiotherapy protocols. This figure has remained largely unchanged over the past 25 years, and the development of novel therapeutic approaches is urgently needed.

In this thesis we present novel antitumoral strategies for the treatment of pancreatic tumors. They are based on three major principles: i) improve adenoviral based therapies by exploring novel delivery routes and retargeting strategies, ii) search for synergistic treatments, and iii) evaluate novel approaches based on non-thermal ablative techniques.

Adenoviral vectors have been the most extensively vectors used in gene therapy clinical trials. They present a good safety profile and can be produced at high titers under GMP conditions, do not integrate and present high *in vivo* transduction efficiency. However, they face with several limitations when explored as anti-cancer agents. Following systemic administration they are trapped by the liver which limits tumor delivery and elicits hepatotoxicity. Moreover, malignant tumor cells express very variable levels of its primary receptor CAR, and thus Ad5 infection is often limited. The presence of a dense stroma and the poor vascularization of pancreatic tumors are physical barriers for virus delivery and spreading throughout the tumor.

In this thesis we have studied the potential of the intraductal injection of adenovirus into the common bile duct as a novel delivery route to efficiently arrive to pancreatic tumors, increase tumor transduction and improve adenoviral anti-tumor response in the TgEla-myc mouse model. With the aim to improve infectivity and tumor selectivity of adenoviruses we have engineered the metalloproteinase (MMP) activatable adenovirus AdTATMMP and evaluated its efficacy both *in vitro* and *in vivo*.

Multimodal therapies can become a strategy to act against pancreatic tumors, but it has to be demonstrated that they are more beneficial

when combined that as single agents. In the current work we evaluated the potential of the adenoviral therapy AduPARTat8TK/GCV to synergize with the first line treatment in pancreatic cancer, the chemotherapeutic agent gemcitabine.

Moreover, we have investigated the antitumoral efficacy of a novel technology known as irreversible electroporation (IRE), a loco-regional therapy in which high-voltage pulses induce plasma membrane defects leading to cellular death. We have studied the feasibility of the IRE procedure for the treatment of pancreatic tumors in an orthotopic mouse model.

TABLE OF CONTENTS

INTRODUCTION

"En algún sitio algo increíble espera ser descubierto."

Carl Sagan *(1934-1996)*

Astrónomo estadounidense.

1. THE PANCREAS

The pancreas is an organ of endodermal derivation uniformly lobulated of 14 to 20 cm length and weighting, on average, 100 g in adult. It is composed of four anatomic areas: the head, which comprises the bulk of the pancreas and includes the uncinate process; the neck; the body; and the tail. It is situated deep in the retroperitoneum and is enveloped by peritoneum and connective tissue. The organ is intimately associated with many different anatomic structures (Illustration 1A). Surgical access to the pancreas is further complicated because it lies behind the stomach and transverse colon. Moreover, the arterial blood supply to the pancreas is derived primarily from branches of the celiac trunk and the superior mesenteric artery. Within the pancreas, a large branch of the splenic artery, known as the great pancreatic artery or pancreatica magna, provides left and right branches that course parallel to the main pancreatic duct (Hruban et al. 2007b).

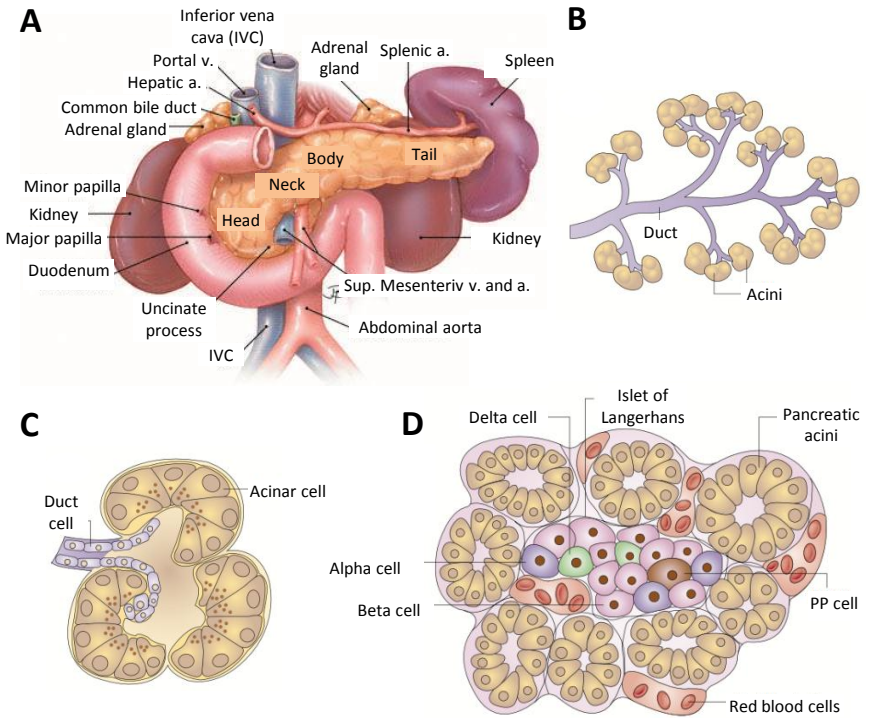

Illustration 1. Anatomy of the pancreas. A) Gross anatomy of the pancreas. a: artery, v: vein, Sup: superior. B) The exocrine pancreas. C) A single acinus. D) A pancreatic islet embedded in exocrine tissue. A panel adapted from (Hruban et al. 2007b). B,C and D panels adapted from (Hezel 2006).

The pancreas is composed of two separate functional units, the exocrine and endocrine pancreas, arranged in 1-10 mm lobules separated by connective tissue septa. It regulates two major physiological processes: digestion and glucose metabolism. The exocrine pancreas (80% of the tissue mass of the organ) consists of acinar and ductal cells. The acinar cells produce digestive enzymes and constitute the bulk of the pancreatic tissue. They are organized into grape-like clusters that are at the smallest termini of the branching duct system (Illustration 1B,C). The ducts, which add mucous and bicarbonate to the enzyme mixture, form a network of increasing size, culminating in main and accessory pancreatic ducts that empty into the duodenum (Bardeesy and DePinho 2002). The main pancreatic duct (of Wirsung) averages 3mm in diameter (range, 1.8 to 9.0 mm) and drains, along with the common bile duct, into the duodenum via the major papilla (ampulla of Vater). The common bile duct lies on the posterior-superior surface of the head of the pancreas or is embedded within the gland (Hruban et al. 2007b).

The endocrine pancreas, which regulates metabolism and glucose homeostasis through the secretion of hormones into the blood-stream, is composed of four specialized endocrine cell types gathered together into clusters called Islets of Langerhans (Illustration 1D). The α- and β-cells regulate the usage of glucose through the production of glucagon and insulin, respectively. Pancreatic polypeptide and somatostatin, that are produced in the PP and δ-cells, modulate the secretory properties of the other pancreatic cell types (Bardeesy and DePinho 2002; Hezel 2006).

2. PANCREATIC CANCER

With a 5-year survival rate inferior to 5% and a median survival of less than 6 months, a diagnosis of pancreatic adenocarcinoma carries one of the most dismal prognoses in medicine. Due to a lack of specific symptoms and limitations in diagnostic methods, the disease often eludes detection during its formative stages. Surgery is the only definitive cure as pancreatic cancer responds poorly to both chemotherapy and radiotherapy (Bardeesy and DePinho 2002).

2.1. Epidemiology

Pancreatic adenocarcinoma, although infrequent, has an exceptionally high mortality rate, making it one of the four or five most common causes of cancer mortality in developed countries. At the beginning of the 21st century, the estimated number of pancreatic cancers throughout the world was 110.000, with an estimated global mortality rate of 98% (Raimondi et al. 2009).

Pancreatic cancer is more common in elderly persons than in younger persons, in the USA the median age at diagnosis is 72 years and only about 5-10% of patients develop it before the age of 50 years (Raimondi et al. 2007). The majority of patients present with locally advanced or metastatic disease, showing a median survival of 6–10 months and 3–6 months, respectively. Although 10–15% of patients have potentially localized resectable tumors, many experience recurrence of disease following surgery. The overall 5-year survival rate among patients with pancreatic cancer is <5% (Wong and Lemoine 2009).

The causes of pancreatic cancer remain unknown. It is associated with only a few known environmental risk factors. Cigarette smoking has been associated to cause 20–25% of pancreatic cancer cases (Fuchs et al. 1996). Chronic pancreatitis and diabetes, two benign diseases, have also been linked to the disease (Luo et al. 2007b). High-fat, high-cholesterol diet, and previous cholecystectomy are associated with an increased incidence (Batty et al. 2009). More recently, an increased risk has been observed among patients with blood type A, B, or AB as compared with blood type O (Wolpin et al. 2009).

Approximately 5 to 10% of patients with pancreatic cancer have a family history of the disease (Shi et al. 2009). In some patients, pancreatic cancer develops as consequence of germline genetic alterations such as mutations in the tumor suppressor genes INK4A, BRCA2, LKB1, the DNA mis-match repair gene MLH1 and the cationic trypsinogen gene PRSS1. The incidence of pancreatic adenocarcinoma due to germline mutation is estimated in a 53-fold increase (Hezel 2006).

The major cause of pancreatic cancer results from the accumulation of somatic mutations in genes such as KRAS, CDKN2A, TP53, and SMAD4 (explained in detail in 2.2.2 section), that cause substantial genomic and transcriptional alterations that facilitate cell-cycle deregulation, cell survival, invasion, and metastases (Raimondi et al. 2009).

2.2. Biology of pancreatic cancer.

Pancreatic cancer responds to a histologic classification based on light microscopic examination of hematoxylin and eosin-stained sections, with recognition of the value of immunohistochemical labeling (Hruban et al. 2007b). Pancreatic ductal adenocarcinoma (PDAC), whose nomenclature derives from its histological resemblance to ductal cells, is the most common pancreatic neoplasm and accounts for >85% of pancreatic tumor cases (Warshaw and Fernandez-del Castillo 1992; Li et al. 2004). It is associated with non-invasive preneoplastic lesions that are thought to be precursors to the disease although the overwhelming majority does not progress to an invasive carcinoma within the lifespan of the individual (Hezel 2006). These precursor lesions are: pancreatic intraepithelial neoplasias (PanINs), mucinous cystic neoplasm (MCN), and intraductal papillary mucinous neoplasm (IPMN) (Brugge et al. 2004; Hruban et al. 2005; Maitra et al. 2005);

2.2.1. Histopathology

- ***Precursor lesions***

Pancreatic intraepithelial neoplasm (PanIN)

PanIN is the most common and extensively studied precursor lesion. It is found in the smaller-caliber pancreatic ducts, the epithelum is columnar, in contrast to the usual cuboidal ductal lining cells. It is histologically classified into three stages of increasing cellular and nuclear atypia. Stage I is characterized by the appearance of a columnar, mucinous epithelium and with increasing architectural disorganization and nuclear atypia through stages II and III. The high-grade PanINs ultimately transform into PDAC with evidence of areas of invasion beyond the basement membrane. Molecular studies have shown that the PanIN stage correlates with increasing mutation frequency and variety (Hruban et al. 2004; Feldmann et al. 2007; Hruban et al. 2007a).

Intraductal papillary mucinous neoplasm (IPMN)

IPMNs resemble PanINs at the cellular level but grow into larger cystic structures. Duct dilatation is accompanied by thick mucinous secretions, which can be visualized endoscopically as thick mucin extruding from the papilla of Vater (Hruban et al. 2004).

Mucinous cystic neoplasm (MCN)

MCNs are large mucin-producing epithelial cystic lesions that harbor a distinctive ovarian-type stroma with a variable degree of epithelial dysplasia and focal regions of invasion. It occurs predominantly in women and is the least common of the precursor lesions (Kern et al. 2011).

- ***Pancreatic adenocarcinoma (advanced stage).***

PDAC commonly arises in the head of the pancreas with infiltration into surrounding tissues including lymphatic nodules, spleen, and peritoneal cavity, and with metastasis to the liver and lungs. The cancer's lethal nature stems from its propensity to rapidly disseminate to the lymphatic system and distant organs.

PDAC primarily exhibits a glandular pattern with duct-like structures and varying degrees of cellular atypia and differentiation. Often within an individual tumor, there are regional differences in histology, tumor grade, and degree of differentiation.

The disease is characterized by the presence of a dense stroma of fibroblasts and inflammatory cells, termed desmoplasia (further explained below). Recently, it was described a hypovascularity of primary pancreatic cancers. Both characteristics possessed important clinical implications (Hezel 2006; Kern et al. 2011).

- ***Microenvironment. Cellular components of pancreatic cancer.***

Heterotypic microenvironmental cellular interactions seem to be important in the pathogenesis of pancreatic adenocarcinoma. Pancreatic cancers are composed of several distinct elements, including pancreatic-cancer cells, pancreatic-cancer stem cells, and the tumor stroma (Hidalgo 2010) (Illustration 2).

Pancreatic cancer stem cells are a subgroup of cancer cells (≤1%) that appear to have cancer stem-cell features, such as self-renewal and differentiation, enabling them to generate mature cells as well as cancer stem cells by asymmetric division. These stem cells may be identified by the expression of specific membrane markers, such as CD44, CD24, ESA and CD133, and can regenerate into full tumors on implantation in immunodeficient animals. Pancreatic-cancer stem cells are resistant to conventional treatments, probably due to the expression of multidrug-

resistant membrane transporters. They also present an increased capability to repair DNA and aberrant activation of developmental signaling cascades and antiapoptotic mechanisms (Hermann et al. 2007; Li et al. 2007; Sergeant et al. 2009).

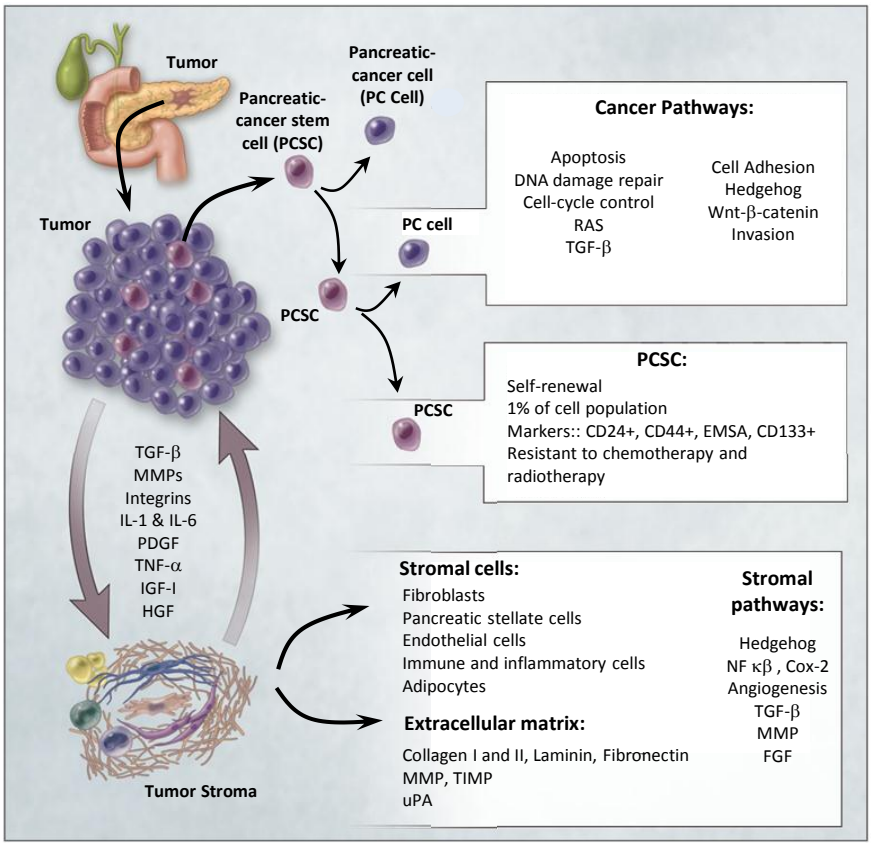

Illustration 2. Components of pancreatic cancer. Pancreatic cancers are composed of pancreatic-cancer cells, pancreatic- cancer stem cells, and the tumor stroma. Pancreatic cancer stem cells (PCSC) generate mature cells (pancreatic cancer cells) as well as cancer stem cells by asymmetric division. The tumor stroma consists on stromal cells embedded in an extracellular matrix. Autocrine and paracrine secretion of growth factors and cytokines results in continuous interaction between the stromal and cancer cells. Adapted from (Hidalgo 2010).

Tumoral stroma constitutes a dynamic and interacting compartment that is critically involved in the process of tumor formation, progression, invasion, and metastasis (Chu et al. 2007; Mahadevan and Von Hoff 2007). Pancreatic tumor stroma is dense and poorly vascularized, and

consists on invading tumor cells, inflammatory cells, and pancreatic stellate cells (PSCs). Pancreatic stellate cells, also known as myofibroblasts and characterized by α-smooth muscle actin expression, are a key cellular element in the formation and turnover of the stroma: they are stimulated by cytokines produced by the tumoral cells to synthesize collagen and other components of the extracellular matrix that contribute to tumor hypoxia. They also appear to be responsible for the poor vascularization that is characteristic of pancreatic cancer (Masamune and Shimosegawa 2009). Stromal cells express multiple proteins such as cyclooxygenase-2, PDGF receptor, vascular endothelial growth factor (VEGF), stromal cell–derived factor, chemokines, integrins, SPARC (secreted protein, acidic, cysteine-rich), and hedgehog pathway elements among others, which have been associated with a poor prognosis and resistance to treatment (Infante et al. 2007; Mukherjee et al. 2009). The degradation of surrounding matrix components and invasion into the nearby tissue is facilitated by upregulation of matrix-metalloproteases and plasminogen activator, which are highly expressed at the stroma-tumor border (Hidalgo 2010; Mihaljevic et al. 2010).

2.2.2. Molecular pathogenesis.

It has been proposed that malignant cells must fulfill some of the following criteria: i) self-sufficiency in growth signals, ii) insensitivity to antigrowth signals, iii) evasion of apoptosis, iv) limitless replicative potential, v) angiogenesis, and vi) invasion and metastasis. PDAC cells achieve this by accumulating genetic mutations in signaling pathways (Hanahan and Weinberg 2000) (Illustration 2).

A recent landmark paper described a set of core-signaling pathways altered in 69 to 100% of all PDACs analyzed (24 tumors) (Jones et al. 2008). In this study, an average of 63 genetic abnormalities per tumor, mainly point mutations, were classified as likely to be relevant. These abnormalities can be organized in 12 functional cancer-relevant pathways. However, not all tumors have alterations in all pathways, and the key mutations in each pathway appear to differ from one tumor to another. Some of these pathways are described below (Mihaljevic et al. 2010).

- ***Chromosomic instability.***

PDAC is characterized by genomic complexity and instability. Centrosome abnormalities are detected in 85% of PDAC samples, and there is a

correlation between levels of such abnormalities and the degree of chromosomal aberrations (Sato et al. 1999; Sato et al. 2001).

Telomere genetics have been implicated in cancer initiation in two ways: while telomerase-mediated preservation of telomere function has been shown to promote the development of advanced malignancies, the lack of telomerase activity and a transient period of telomere shortening and dysfunction during early neoplasia drives cancer initiation. Reactivation of telomerase activity has been observed later in PDAC progression and seems to be a critical step in cancer initiation (Hahn et al. 1999; Artandi et al. 2000; Mihaljevic et al. 2010).

- ***KRAS.***

K-RAS is a member of the RAS superfamily of GTPases and mediates a variety of cellular functions including proliferation, differentiation, and survival. 95% of tumors have activating mutations in the KRAS2 oncogene, frequently a glycine to aspartate mutation at codon 12 (K-RAS^{G12D}). Transcription of the mutant KRAS gene produces an abnormal Ras protein that is "locked" in its activated form, resulting in aberrant activation of proliferative and survival signaling pathways (Campbell et al. 1998; Malumbres and Barbacid 2003).

It is universally accepted a central role for K-RAS mutations in tumorigenesis, but some studies indicate that even though mutant KRAS is sufficient to initiate the PanIN–PDAC lineage in mice, there is some evidence that it may not be necessary (Morris et al. 2010).

- ***The 9p21 locus CDKN2A and INK4A and ARF tumor suppressors.***

The 9q21 locus encodes two overlapping tumor suppressors genes: INK4A and ARF, and their respective protein products $p16^{INK4A}$ and $p19^{ARF}$. Homozygous deletion of 9p21 is frequent (in ~40% of tumors). Loss of INK4A function occurs in 80%-95% of tumors, with the resultant loss of the p16 protein (a regulator of the G1–S transition of the cell cycle) and a corresponding increase in cell proliferation (Rozenblum et al. 1997; Sherr 2001).

- ***TP53.***

The TP53 tumour-suppressor gene is mutated, generally by missense alterations of the DNA-binding domain, in more than 50% of pancreatic adenocarcinomas. Its mutation permits cells to bypass DNA damage

control checkpoints and apoptotic signals, contributing to genomic instability (Rozenblum et al. 1997; Hidalgo 2010).

- ***The TGF-β/SMAD4 pathway.***

TGF-β is a cytokine that mediates a wide range of physiological processes, such as embryonic development, tissue repair, angiogenesis and immunosuppression. TGF-β also has a complex role in tumorigenesis: it acts as tumor-suppressor in epithelial cells, while promotes invasion and metastasis during the late stages of cancer progression. Mutations of the TGFBR1, TGFBR2 and SMAD4 genes are found in about 1%, 4% and 50% of patients with pancreatic cancers, respectively (Goggins et al. 1998). Inactivation of SMAD4, a transcriptional regulator that serves as a central component in the TGF-signaling cascade (Massague et al. 2000), abolishes TGF-β-mediated tumor-suppressive functions while it maintains some tumor-promoting TGF-β responses, such as epithelial–mesenchymal transition, which makes cells migratory and invasive (Levy and Hill 2005; Wong and Lemoine 2009).

- ***Embryonic development signaling pathways.***

PDAC is characterized by frequent reactivation of the embryonic signaling pathways Notch, Hedgehog (Hh), and Wnt–β-catenin, that are essential for embryonic development and tissue homeostasis. Not only do such pathways contribute to the ability of tumor cells to proliferate and evade cell death, but they also alter cell plasticity. Recent evidence points to temporal and spatial control of these pathways in PDAC development and maintenance (Morris et al. 2010).

- ***miRNA.***

miRNAs are small, endogenous, noncoding RNA molecules that negatively regulate gene expression post-transcriptionally and can be either oncogenic or tumor-suppressive, depending on their target mRNAs. Expression profiling showed that at least 100 miRNA precursors are aberrantly expressed in pancreatic cancer (Lee et al. 2007; Wong and Lemoine 2009). For example, miR-200a and miR-200b have been found overexpressed in the sera of patients with pancreatic cancer or chronic pancreatitis (Costello and Neoptolemos 2011).

2.2.3. Tumoral progression model.

As previously mentioned, various genetic risk factors predispose individuals to the development of pancreatic cancer. A new study has suggested that it takes at least 10 years from initiation of the tumor to the development of the parental clone and a further 5 years to the development of metastatic subclones, with patients dying an average of 2 years later (Illustration 3) (Yachida et al. 2010; Costello and Neoptolemos 2011)

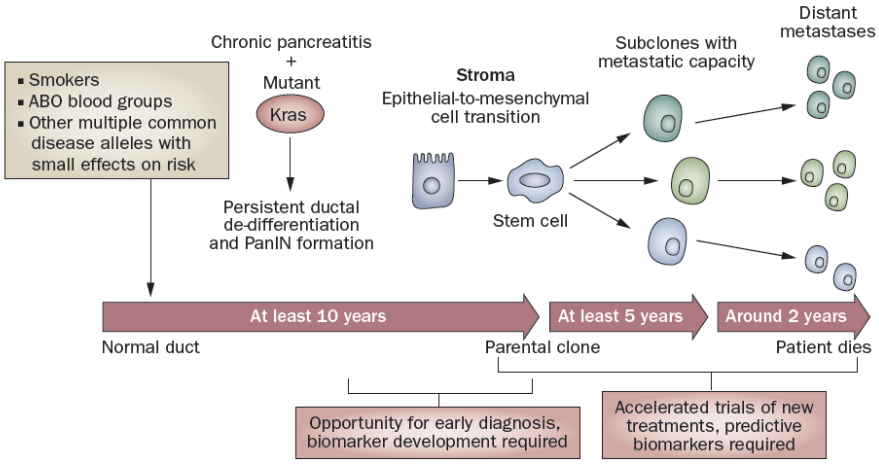

Illustration 3. Development and progression of pancreatic cancer. Various genetic risk factors predispose individuals to the development of pancreatic cancer. It takes at least 10 years from initiation of the tumor to the development of the parental clone and a further 5 years to the development of metastatic subclones, with patients dying an average of 2 years later. Adapted from (Costello and Neoptolemos 2011).

Similar to adenoma to carcinoma sequence seen in other types of tumors, a PanIN-to-PDAC progression model has been proposed (Hruban et al. 2000; Real et al. 2008): PanINs acquire increasing numbers of genetic alterations as they progress from early to late stages and finally to PDAC (Illustration 4). The normal pancreas is an organ with a low rate of cell proliferation. However, tissue damage, such as that originated by pancreatitis, results in a prominent proliferative response. This response might involve proliferation of the duct cells that are associated with disruptions in the basement membrane, inflammatory responses due to cytokine release and reactive oxygen species (ROS) production, and autocrine/paracrine release of growth factors (for example, TGF-α, HGF

and KGF). The proliferative response might result in regeneration of pancreatic tissue and return to quiescence when the stimulus is attenuated. This proliferative arrest is likely to involve INK4A and TGF-β/SMAD4 pathways. If the proliferative stimulus is maintained, there is a selective pressure for subsequent mutations in growth-inhibitory pathways that leads to PanIN and metastasis development (Bardeesy and DePinho 2002).

An initial genetic alteration is KRAS mutation. When KRAS activity is above a crucial threshold, differentiated pancreatic cells de-differentiate into a ductal state that persists in PanINs and PDAC. β-catenin signaling is maintained below a crucial low level, but once the PanIN state is established, β-catenin signaling is reactivated in parallel with increasing expression of Hedgehog (Hh) ligand, that activates target genes in stromal cells of the developing desmoplastic response (Morris et al. 2010). Most human somatic cells lack telomerase activity, hence telomeres are eroded as cells proliferate. Progressive telomere shortening activates DNA-damage responses, resulting in growth arrest. Loss of checkpoint responses, by TP53 mutations, allows cells to continue proliferating, leading to telomere dysfunction and genomic instability. Chromosome breakage–fusion cycles produce severe aneuploidy and chromosomal translocations that contribute to tumour progression. Telomerase reactivation subsequently stabilizes the genome and facilitates the immortal growth of the tumour cells development (Bardeesy and DePinho 2002).

Even after decades of research, the cell of origin of PDAC is still a topic of debate. Traditionally, pancreatic ductal cells have been viewed as the cell of origin since PDAC cells morphologically resemble ductal cells. However, nowadays is proposed that PDAC might originate from a number of different cells or cells in different conditions that reprogram into a 'ductal' cell type. This means that rather than having a common cellular origin, certain genetic alterations may lead to development of PDAC, independent of the cell type they occur in (Mihaljevic et al. 2010).

Another proposed origin/model is the cancer stem cell model, in which growth, regrowth and metastatic reconstitution of tumors is driven by a subpopulation of tumor cells (the cancer stem cells) that have self-renewal and multipotent capacity to generate progeny of various differentiation states that constitute the bulk of the tumor. Cancer stem cells originate from the tissue's normal stem cells by the accumulation of oncogenic mutations. In pancreas, centroacinar cells (CAC) are

considered a “stem cell”-like subpopulation, as express developmental markers and may differentiate into acinar as well as ductal cells. The oncogenic mutations alter the mechanisms that control normal stem-cell expansion in response to stimuli from the microenvironment, whereby stem cells become independent of their niche. Another theory implies that mutations in more differentiated cells affect genes responsible for stem-cell features and cell-cycle control, taking the more differentiated cells back to a stem-cell state. As a result, some subpopulations of the tumor bulk may adopt a cancer stem cell phenotype. The term cancer stem cell, therefore, does not refer to the cell of origin, but to the cell that sustains the tumor (Reya et al. 2001; Clarke and Fuller 2006; Sergeant et al. 2009).

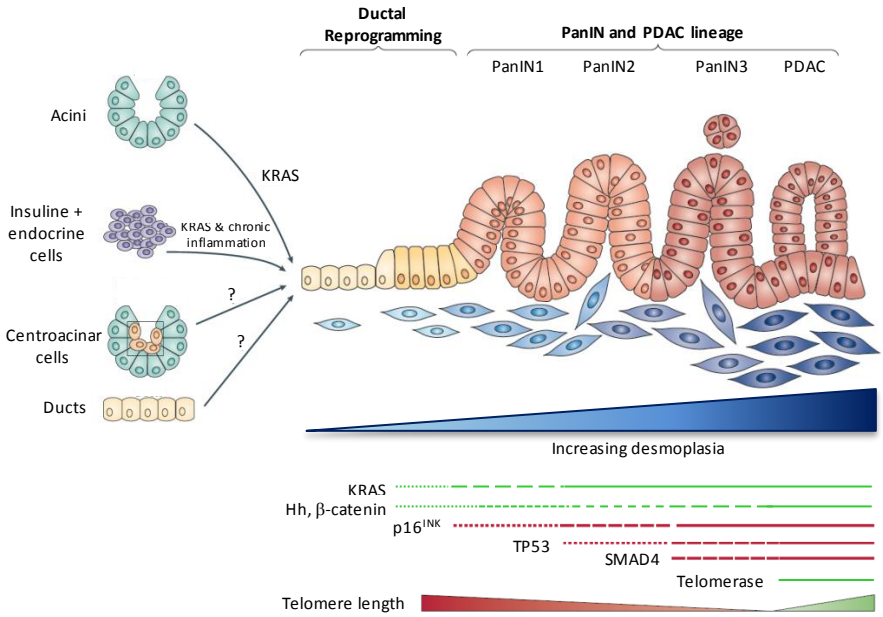

Illustration 4. Tumoral progression model of pancreatic cancer. Normal epithelium progress to infiltrating cancer (left to right) through a series of histologically defined precursors (PanINs). Changes in the epithelium are matched by desmoplastic changes in the stroma. Constitutively active KRAS is sufficient to initiate the development of PanIN and pancreatic ductal adenocarcinoma (PDAC). Acini, insulin-positive cells, centroacinar cells and ducts can give rise to PanINs after reprogramming into a ductal phenotype. PanINs are classified into three stages of increasing cellular atypia and, in humans, have been found to possess increasing numbers of mutations. Common mutations: initial point mutations in KRAS, reactivation of β-catenin signaling and Hedgehog (Hh) when PanIN are stablished, inactivation of p16 gene at an intermediate stage, late inactivation of TP53, SMAD4 and activation of telomerase. Adapted from (Bardeesy and DePinho 2002; Morris et al. 2010).

2.2.4. Proteases in pancreatic cancer.

The ability of cancer cells to migrate and invade surrounding tissues is mediated by molecular interactions of receptors with ligands and various proteases. The most common of these proteases are matrix metalloproteases (MMP) and serine proteases, such as Urokinase plasminogen activator (uPA). Moreover, MMP-2 and MMP-9 activation as well as uPA /uPAR (uPA Receptor) expression are significantly increased in metastatic pancreatic cancers compared with nonmetastatics (He et al. 2007; Gondi and Rao 2009).

- ***uPA-uPAR system.***

The uPA-uPAR system is involved in the regulation of several physiological and pathological conditions that exploit cell adhesion and migration including wound healing, neutrophil recruitment during inflammation as well as tumor invasion and metastasis. Importantly, uPAR expression in tumors can occur in tumor cells and/or tumor-associated stromal cells such as fibroblasts and macrophages (Gondi and Rao 2009; Smith and Marshall 2010).

The uPA-uPAR system consists of the serine protease uPA, its cell membrane-associated receptor (uPAR), the substrate plasminogen and the plasminogen activator inhibitors (PAI-1 and PAI-2) (Illustration 5). uPA is produced and secreted as an inactive enzyme, called pro-uPA, that is activated by binding to uPAR. uPA cleaves plasminogen, generating the active protease plasmin, that is involved in the degradation of the extracellular matrix (ECM) and basement membranes through direct proteolytic digestion, or the activation of other proteases including metalloproteases and collagenases. Binding of uPA with its receptor uPAR can activate downstream signaling pathways leading to cell proliferation, migration, and invasion (Mazar et al. 1999; Rao 2003; Gondi and Rao 2009).

- ***MMPs***

Matrix metalloproteinases (MMPs) are a highly conserved family of zinc-dependent endopeptidases able to degrade most components of the basement membrane and ECM. There are more than 21 human MMPs, the majority of them secreted, although a group of them are anchored to the cell membrane (MT-MMPs). They play a crucial role in various physiologic processes such as embryonic development, bone resorption,

angiogenesis and wound healing; as well as in pathologic processes such as rheumatoid arthritis, multiple sclerosis, periodontal disease and tumor growth and metastasis (Egeblad and Werb 2002; Gondi and Rao 2009).

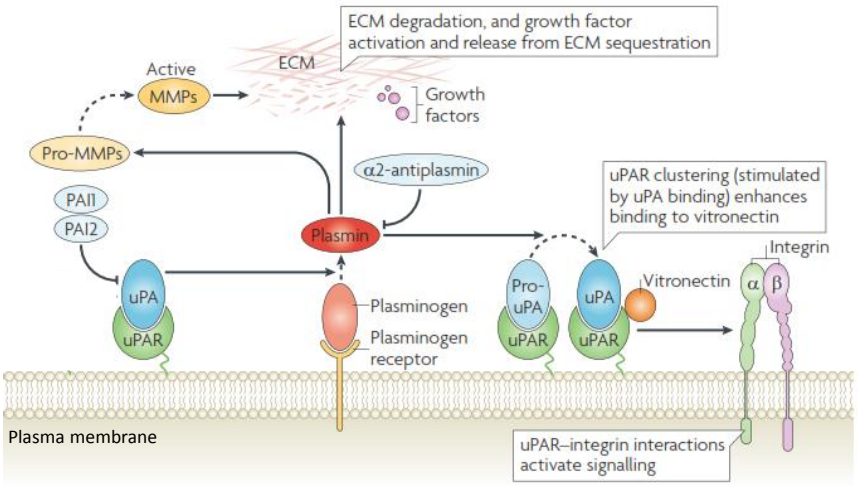

Illustration 5. Function and regulation of uPA/uPAR system and interaction with MMPs. Urokinase-type plasminogen activator receptor (uPAR) binds the protease urokinase-type plasminogen activator (uPA) in its active and zymogen (pro-uPA) forms. uPA cleaves plasminogen, generating the active protease plasmin. Plasmin can reciprocally activate pro-uPA. Plasmin cleaves and activates matrix metalloproteases (MMPs). Both plasmin and MMPs degrade many extracellular matrix (ECM) components and activate growth factors or liberate them from ECM sequestration. The proteolytic activities of uPA and plasmin are antagonized by the serine protease inhibitors plasminogen activator inhibitor 1 and 2 (PAI1 and PAI2) and α2-antiplasmin. uPA–uPAR binding promotes clustering of uPAR in the plasma membrane, and increases its ability to bind the ECM protein vitronectin. Complexes of full-length uPAR and its ligands interact with integrin co-receptors for intracellular signal transduction. Adapted from (Smith and Marshall 2010).

MMPs are secreted in an enzimatically inactive state (pro-MMPs), being activated by sequential cleavage steps which involve the removal of pro-peptide domains. Different proteinases such as other MMPs, plasmin, trypsin, chymotrypsin and cathepsins are implicated in MMP activation. MMP expression and proteolytic activity are tightly regulated at three stages: gene transcription, proenzyme activation and activity of natural inhibitors (tissue inhibitors of metalloproteinase: TIMPs) (Sternlicht and Werb 2001; Stefanidakis and Koivunen 2006).

In cancer, the major source of MMPs and TIMPs is from the different types of stromal cells infiltrating the tumor (Egeblad and Werb 2002). MMPs have been shown to regulate tumor cell invasion through extracellular matrix remodeling and downregulating cellular adhesion. Moreover they also affect multiple signaling pathways, such as cancer-cell growth, differentiation, apoptosis, migration and invasion, and the regulation of tumour angiogenesis and immune surveillance. The most important of these metalloproteases are MMP-9 and MMP-2, which have shown to be involved in invasion and angiogenesis (Itoh et al. 1998; Kessenbrock et al. 2010).

2.3. Diagnosis.

Pancreatic cancer, unfortunately, usually presents with nonspecific symptoms, and many patients are not correctly diagnosed until months or even years after tumor development. The symptoms of pancreatic cancer depend on the location of the tumor within the gland, as well as on the stage of the disease. The majority of tumors develop in the head of the pancreas and cause obstructive cholestasis (condition where bile cannot flow from the liver to the duodenum). The most common symptom is epigastric pain that radiates to the back. Other associated complications are the development of diabetes mellitus and pancreatitis. Anorexia, weight loss, gastric outlet obstruction and ascites are usually manifestations of more-advanced disease. Other less common manifestations include deep and superficial venous thrombosis, liver-function abnormalities and depression (Li et al. 2004; Hruban et al. 2007b; Maitra and Hruban 2008; Hidalgo 2010; Stathis and Moore 2010).

Currently, helical computed tomography (CT) with intravenous administration of contrast material is the imaging procedure of choice for the initial evaluation of pancreatic masses (Miura et al. 2006). This technique allows visualization of the primary tumor in relation to the superior mesenteric artery, celiac axis, superior mesenteric vein and portal vein, and also in relation to distant organs. In general, contrast-enhanced CT is sufficient to confirm a suspected pancreatic mass, and predicts surgical resectability with 80 to 90% accuracy (Karmazanovsky et al. 2005).

Some patients require additional diagnostic studies. Endoscopic ultrasonography (EUS) is useful in patients in whom pancreatic cancer is suspected although there is no visible mass identifiable on CT. Fine

needle aspiration biopsy can be used in conjuction with EUS (EUS-FNA) to obtain tissue for diagnostic purposes (Mizuno et al. 2011).

Magnetic resonance imaging (MRI) demonstrates the location of any duct lesion. It can be used to visualize the vascular anatomy and determine the resectability of pancreatic neoplasms (Hruban et al. 2007b).

Endoscopic retrograde cholangiopancreatography (ERCP) shows the pancreatic and bile-duct anatomy and can be used to guide ductal brushing and lavage, which provides tissue for diagnosis. ERCP is more invasive than the previously mentioned techniques, and is associated with a 2% complication rate, making it a less attractive first-line modality for the evaluation of pancreatic neoplasms. It is especially useful in patients with jaundice in whom an endoscopic stent is required to relieve obstruction (Dumonceau and Vonlaufen 2007).

The central problem with pancreatic cancer remains the lack of an effective screening test for early asymptomatic disease. There are many potential serum biomarkers for diagnosis, stratification of a prognosis, and monitoring of therapy; however, only a few have demonstrated clinical usefulness (Harsha et al. 2009). Serum carcinoembrionic antigen (CEA) and carbohydrate antigen (CA) 19-9 levels have proven to be ineffective screening tests for pancreatic cancer due to the lack of sufficient sensitivity and specificity (Ritts and Pitt 1998; Buxbaum and Eloubeidi 2010). Nonetheless, CA 19-9 levels have been used to prognosticate and to monitor the effectiveness of therapy, and are useful in conjunction with other diagnostic tests (Nishida et al. 1999).

Analysis of pancreatic biopsies is used for cancer evaluation and determination of the type of pancreatic neoplasm. Analysis of molecular markers in FNA tissue shows promise and is likely to be the strategy of the future (Buxbaum and Eloubeidi 2010).

Recently, Hoheisel and colleagues have described an extensive antibody microarray platform, including 810 antibodies, specifically selected against 741 cancer-related proteins. Dual-color measurements of proteins in blood and urine were achieved with excellent accuracy and reproducibility. Importantly, the antibody microarray platform could distinguish between urine samples from patients with pancreatic cancer and healthy individuals. This approach is promising and has the advantage that it could be readily converted into an immunodiagnostic

assay for routine use (Schroder et al. 2010; Costello and Neoptolemos 2011).

2.4. Treatment.

The management of patients with pancreatic carcinoma depends on the extent of the disease at diagnosis. Surgical resection followed by adjuvant therapy is the standard of care for patients diagnosed with early-stage disease. However, the majority of patients have locally advanced unresectable disease due to local vascular invasion; or present with advanced-stage disease or metastatic disease, which precludes surgery. Prognosis for these patients is extremely poor and the impact of standard therapy is minimal (Stathis and Moore 2010).

2.4.1. Early disease.

It is estimated that only 10–15% of patients present with early-stage disease that permits curative surgery (Heinemann and Boeck 2008). Depending on the location of the tumor, the operative procedures may involve cephalic pancreatoduodenectomy (the Whipple procedure), distal pancreatectomy, or total pancreatectomy. These patients also receive post-operative therapy, although no universal consensus exists as to the type of adjuvant therapy. Gemcitabine or 5-fluorouracil (5-Fu) chemotherapy without radiation are the most common treatments outside North America, while chemoradiation plus systemic chemotherapy is still widely used in the USA (Neoptolemos et al. 2004; Regine et al. 2008; Stathis and Moore 2010).

2.4.2. Locally-advanced and systemically advanced disease.

Patients with locally advanced disease represent almost 30% of newly diagnosed pancreatic carcinoma cases. These patients have a better outcome (median survival of 8–12 months) than patients with metastatic disease. The optimum treatment for patients with locally advanced disease has not yet been defined as data are limited; however, radiation combined with chemotherapy is often considered the standard treatment for these patients (Sharma et al. 2011).

The first line treatment for patients with systemically advanced pancreatic adenocarcinoma is gemcitabine. At present, there is no standard second-line treatment. The median overall survival is 5.65

months and the 1-year survival rate is 18%. Over the past decade, major efforts have been made to improve treatment outcomes in patients with metastatic disease, more than a dozen large randomized trials worldwide have been conducted (Burris et al. 1997). The most common approach has been to use gemcitabine as the control arm and gemcitabine combined with a second cytotoxic agent or, more recently, with a targeted agent, as the experimental arm (Stathis and Moore 2010).

Large randomized phase III trials were performed to evaluate the combination of gemcitabine with the cytotoxic agents cisplatin, oxaliplatin, 5-FU, capecitabine, irinotecan, exatecan and pemetrexed (Illustration 6A). The primary end point of overall survival was not improved in any of these trials. Combination chemotherapy resulted in an improved response rate and had some impact on progression-free survival in some of these trials; however, there was an absence of an overall survival benefit (Welch and Moore 2007; Merl et al. 2010b; Stathis and Moore 2010).

In the age of molecular targeted therapy, several drugs developed to specifically target those pathways/components altered in pancreatic cancer, such as RAS (Tipifarnib), MMPs (Marimastat, BAY 12-9566) angiogenesis (Bevacizumab, humanized anti-VEGF antibody), EGFR (Erlotonib, EFGR inhibitor; Cetuximab, anti-EGFR antibody) have been tested in phase II and randomized phase III trials (Illustration 6B). With the exception of erlotinib and gemcitabine, none of the targeted agents tested improved overall survival of patients. Gemcitabine plus erlotinib improved the median overall survival compared with those who received gemcitabine alone (6.24 months versus 5.91 months), and the respective 1-year survival rates (23% versus 17%, p=0.023) (Moore et al. 2007; Stathis and Moore 2010).

Recently, in the 2010 ASCO Annual Meeting, the phase III trial PRODIGE 4/ACCORD and the phase II trial TARGET were presented with a primary end point of overall survival (Merl et al. 2010a). The PRODIGE 4/ACCORD trial consisted on the administration of FOLFIRINOX (oxaliplatin, irinotecan, leucoviron and 5-FU) vs gemcitabine. The combined treatment showed statiscally significant longer median overall survival (10.5 months vs 6.9 months, p<0.001) and 1-year survival (48.8% vs 20.6%). However, it presented a higher incidence of toxicity, which would limit its use to patients with good performance status (Conroy et al. 2011). The phase II trial TARGET consisted on the combined inhibition of VEGF and EGFR pathway (bevacizumab and erlotinib) plus gemcitabine

and capecitabine. Patients with metastatic disease had an improved overall survival (11.1 months) and 1-year survival (49%) compared with historical data of standard therapy. These results may represent a start of a paradigm shift in the management of advanced pancreatic cancer.

A

Phase III trials of chemotherapy in advanced pancreatic cancer patients

Reference	Treatment	Number of patients	Median survival (months)
Heinemann *et al.* (2006)	Gemcitabine vs gemcitabine + cisplatin	195	6 vs 7.5 (P=0.15)
Colucci *et al.* (2002)	Gemcitabine vs gemcitabine + cisplatin	107	5 vs 7.5 (P=0.43)
Louvet *et al.*(2005)	Gemcitabine vs gemcitabine + oxaliplatin	313	7.1 vs 9 (P=0.13)
Poplin *et al.* (2009)	Gemcitabine vs gemcitabine FDR vs gemcitabine + oxaliplatin	832	4.9 vs 6.2 (P=0.04) vs 5.7 (P=0.22)
Berlin *et al.* (2002)	Gemcitabine vs gemcitabine + 5-FU	322	5.7 vs 6.5 (P=0.09)
Herrmann *et al.* (2007)	Gemcitabine vs gemcitabine + capecitabine	319	7.2 vs 8.4 (P=0.234)
Rocha Lima *et al.* (2004)	Gemcitabine vs gemcitabine + irinotecan	342	6.3 vs 6.6 (P=0.789)
Stathopoulos *et al.* (2006)	Gemcitabine vs gemcitabine + irinotecan	145	6.4 vs 6.5 (P=0.970)
Abou-Alfa *et al.* (2006)	Gemcitabine vs gemcitabine + exatecan	349	6.2 vs 6.7 (P=0.52)
Oettle *et al.* (2005)	Gemcitabine vs gemcitabine + pemetrexed	565	6.3 vs 6.2 (P=0.847)

Abbrevations: FDR, fixed dose rate; 5-FU, 5-fluorouracil.

B

Phase III trials of targeted agents in advanced pancreatic carcinoma

Reference	Treatment	Class of targeted agent	Target of targeted agent
Bramhall *et al.* (2001)	Gemcitabine vs marimastat	Broad-spectrum inhibitor of MMP	MMP
Bramhall *et al.* (2002)	Gemcitabine vs gemcitabine + marimastat	Broad-spectrum inhibitor of MMP	MMP
Moore *et al.* (2003)	Gemcitabine vs BAY 12-9566	Inhibitor of MMP-2, MMP-3, MMP-9, MMP-13	MMP
Van Cutsem *et al.* (2004)	Gemcitabine vs gemcitabine + tipifarnib	Inhibitor of FT	FT
Moore *et al.* (2007)	Gemcitabine vs gemcitabine + erlotinib	Tyrosine kinase inhibitor	EGFR
Kindler *et al.* (2007)	Gemcitabine vs gemcitabine + bevacizumab	Monoclonal antibody	VEGF
Philip *et al.* (2007)	Gemcitabine vs gemcitabine + cetuximab	Monocolonal antibody	EGFR
Vervenne *et al.* (2008)	Gemcitabine + erlotinib vs gemcitabine + erlotinib + bevacizumab	Tyrosine kinase inhibitor/ monoclonal antibody	EGFR/ VEGF

Abbrevations: FT, farnesyltransferase: MMP, matrix metalloproteinase; VEGF, vascular endothelial growth factor.

Illustration 6. Phase III clinical trials in advanced pancreatic adenocarcinoma. Adapted from (Stathis and Moore 2010).

3. MODELING PANCREATIC CANCER IN MICE.

In the last 10 years, there has been a relative explosion of new rodent systems that recapitulate both genetic and cellular lesions that lead to the development of pancreatic cancer. These mice models have been used to study causal signaling pathways and to evaluate novel detection, chemopreventative, and therapeutic measures. There are three primary groups of rodent models: carcinogen-induced, xenograft implanted and genetically engineered models.

3.1.1. Carcinogen-induced models.

Carcinogen-induced models rely on the administration of certain chemicals to generate cellular changes that rapidly lead to pancreatic cancer. The most widely used and studied model is Syrian gold hamster intraperitoneally injected with BOP (N-nitrosobis(2-oxopropyl)amine). These tumors are very similar to those in humans since they have a ductal phenotype with pronounced desmoplasia and predilection for perineural invasion; and at the molecular level, K-RAS and p53 mutations have been reported. Tumors in rats can be induced using a wide range of carcinogens, such as azaserine and DMBA. However, tumors in rats are biologically and phenotypically distinct from those in humans, grow relatively slow, infrequently metastasize and have different molecular changes. Carcinogens in mouse have rarely been used to model pancreatic neoplasia because they mostly induce cancers of acinar origin (Wei et al. 2003).

Carcinogens induced models resemble the human disease in their use of environmental factors to induce progressive tissue changes leading to cancer. However, the cancers that form are not of human origin and they lack a genetic definition; moreover, the administration of these compounds has broad effects in other tissues (Bardeesy et al. 2001; Ding et al. 2010).

3.1.2. Xenograft Models.

In general, nude and SCID mice are used to generate xenograft tumors as they are incapable of rejecting foreign tissues and cells. Nude mice display defective development of thymus and hair follicles, thus lack T lymphocytes and hair (Fidler 1986). Severe combined immunodeficient (SCID) mice lack mature B- and T lymphocytes because they carry a gene

mutation that impairs rearrangements of immunoglobulin and T-cell receptor genes (Bosma and Carroll 1991). Xenograft models develop by the inoculation of well-characterized pancreatic cancer cell lines (mostly of human origin) or from the implantation of primary or metastatic cancer tissue (Fogh et al. 1980; Kim et al. 2009).

- ***Subcutaneous xenograft tumors.***

Subcutaneous xenograft tumors are generated by implantation of tissue or cells in the subcutaneous pocket under the mouse skin, usually along the back or upper portion of the hind legs. This cancer model is relatively reliable, inexpensive, fast, and technically simple when establishing tumors to reach a defined end point for evaluation. The most notable limitation is that these cancer cells are forced to grow under the skin of immunocompromised mice, which ignores the contribution of the host's immune system in tumor growth modulation (Kim et al. 2009). Moreover, subcutaneous xenograft tumors usually show extensive local growth but rarely metastasize, in contrast to pancreatic cancer behavior in humans (Fogh et al. 1980).

- ***Orthotopic xenograft tumors.***

Pancreatic orthotopic tumors are generated by direct injection of cells into the pancreas, or by surgical implantation of 1 mm^3 tumor fragments. Orthotopic implantation of pancreatic cancer cells is more time-consuming, technically challenging and often requires image examinations or exploratory laparotomies to exclude or confirm the presence of tumor. However, the external milieu is more closely preserved in orthotopic tumors and theoretically better approximates the 'natural' setting of pancreatic cancer. Moreover, orthotopic implantation often results in higher metastasis efficiency and more relevant colonization patterns (similar to those of human cancer) than does ectopic implantation into mice; dissemination occurs in up to 60% of tumors to the peritoneum, liver, lungs, and lymph nodes (Wei et al. 2003; Loukopoulos et al. 2004).

Models initiated by direct orthotopic engraftment of primary human tumor samples into immunodeficient mice without a cell line intermediary are receiving increasing interest. Direct xenograft models better preserve tumor heterogeneity and limit the *ex vivo* manipulation inherent in the culturing of cancer cell lines. Most direct xenograft tumors grow with considerable stromal elements and recapitulate the

histological appearance of the original patient tumor over multiple passages in mice (Kim et al. 2009; Perez-Torras et al. 2011).

3.1.3. Genetically engineered models.

Genetically modified mice are generated by insertion of relevant genetic mutations into mouse genomic DNA in both a conditional and inducible format. Delivery of these genes is through transgenesis, embryo manipulation for knock-in/knockout technology, and retroviral delivery to somatic cells.

Currently, there are over a dozen models available, which range from homogeneous preneoplastic lesions with remarkable similarity to human PanINs, to PDAC models or to models with a more heterogeneous population of lesions including cystic papillary and mucinous lesions. The molecular features of these models may also vary in a manner comparable with the differences observed in lesion morphology (Grippo and Tuveson 2010; Morris et al. 2010). First mouse models generated were based on the expression of an oncogene under the control of the tissue-specific promoter Elastase-1. Activated H-Ras and SV40 T-antigen transgenes resulted in pancreatic acinar tumor formation, whereas c-myc overexpression triggered mixed acinar/ductal neoplasms (see next section for further details) (Ornitz et al. 1987; Quaife et al. 1987; Sandgren et al. 1991). Murine models of pre-neoplasms (earlier-stage lesions) displaying complete penetrance (all mice with a gene mutation have phenotypic manifestation of that disease) have been generated by expressing the oncogenic Kras allele in pancreatic exocrine and/or progenitor cells (Tuveson et al. 2006). When combined with various tumor suppressor mutations, such as p16, p53 and/or Smad4 (Aguirre et al. 2003; Hingorani et al. 2005; Izeradjene et al. 2007), these models often times give rise to invasive and metastatic PDAC and related epithelial histologies. Models using inducible alleles of Cre recombinase, such as estrogen receptor–Cre fusion genes (CreER or CreERT) and tetracycline-responsive Cre expression alleles (TRE-Cre), are capable of being temporally controlled and thus initiated selectively in adult pancreata, better reflecting the somatic acquisition of genetic mutations thought to occur in humans (Guerra et al. 2007; Gidekel Friedlander et al. 2009; Ji et al. 2009).

- ***Ela-myc.***

Transgenic Ela-myc mice was generated by Sandgren et al in 1991, by the insertion of the Ela1-myc cassete (Illustration 7A) in which the c-myc oncogene was under the control of the Elastase promoter, which targets c-myc expression to acinar cells (Sandgren et al. 1991). C-myc is a transcription factor implicated in growth and expansion of somatic cells, and is overexpressed in about 50% of human pancreatic ductal adenocarcinomas (Oster et al. 2002; Liao et al. 2006).

Mice develop mixed acinar/ductal pancreatic adenocarcinomas, with 100% penetrance and present a survival of 4-7 months. 10% of mice display tumor spread to peritoneal surfaces or liver (Sandgren et al. 1991). This Ela-myc mouse is the only single-transgene model that gives rise to pancreatic tumors with ductal elements in the shortest latency period (Liao et al. 2006). Other mouse models such as Ela-TGF-α, Ela-Kras or Mist-Kras develop acinar-to-ductal metaplasia but with a longer latency period (survival times: 12m, 18+ m and 11m, respectively) (Wagner et al. 2001; Grippo et al. 2003; Hruban et al. 2006; Tuveson et al. 2006).

Ela-myc mice at 2 months of age already present small cancer nodules (1–6 mm in diameter) in 40% of animals. At the time of sacrifice, multiple nodules are observed. Two different tumor colorations are found: a fish-meat-like white, a typical sign of solid cancer in humans, and a deep red color due to hemorrhage within the tumor (Illustration 7 B.A). Histologically, about one-half of the tumors are pure acinar cell carcinomas (Illustration 7 B.B and B.C), while the other one-half are mixed ductal and acinar carcinomas (Illustration 7 B.D). While acinar tumors can be either white or red in color, all ductal adenocarcinomas are white. Acinar cell tumors contained little stroma (Illustration 7 B.C), but invasive growth into the adjacent stroma, whilst ductal tumor cells were usually disseminated in the dense stromal tissue (Illustration 7 B.D and D.E), similar to the desmoplasia observed in human pancreatic ductal adenocarcinomas. The tumors are frequently associated with marked inflammatory cell infiltrates (Sandgren et al. 1991; Liao et al. 2006).

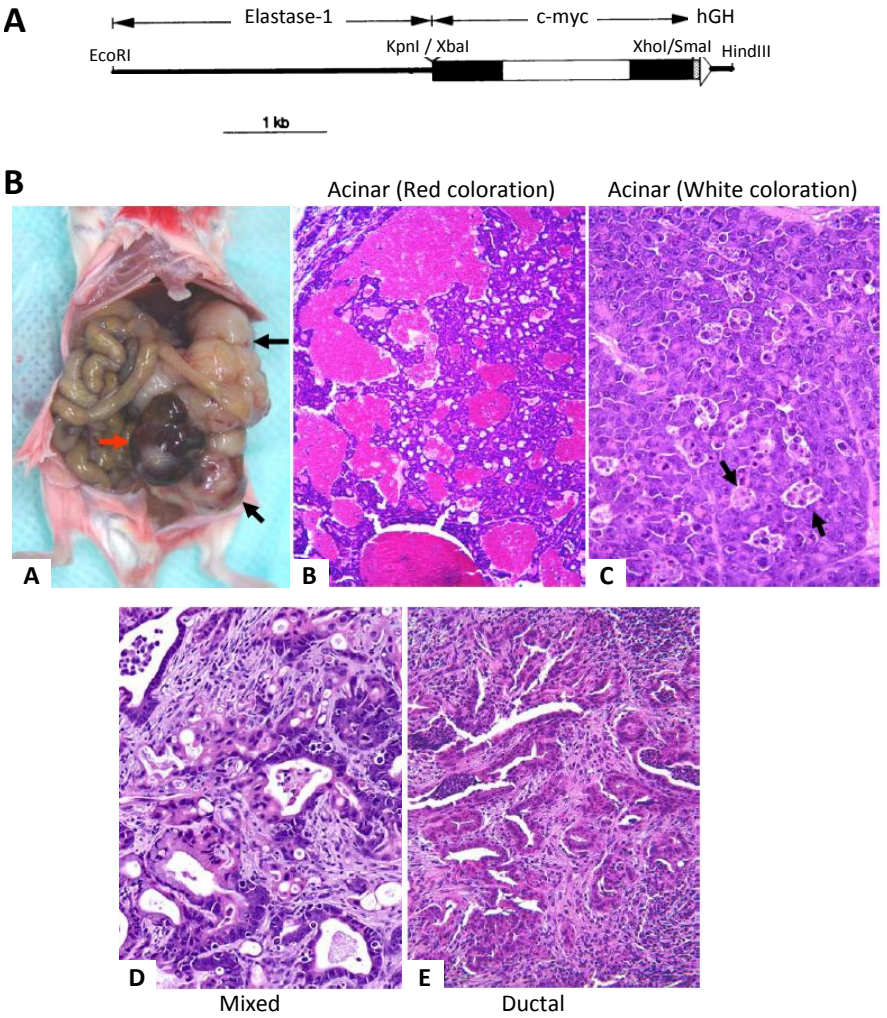

Illustration 7. Ela-myc mice. A) Construct of Ela-myc transgene. The 2.7 kb fragment of murine c-myc, which includes the entire protein coding region within exons 2 and 3, was cloned between the 3 kb rat Elastase-1 gene fragment, that includes the enhancer and promoter, and the 0.3 kb human growth hormone gene fragment that includes the 3' untranslated and poly(A) addition sequences. B) Gross morphology and histology. B.A) Black arrows indicate tumor nodules with white coloration. Red arrow indicates a tumor nodule with red coloration. B.B and B.C) Representative images of an acinar phenotype. Black arrows indicate apoptotic cells organized in clusters. B.D and B.E) Representative images of mixed and ductal phenotypes. Images adapted from (Sandgren et al. 1991) and (Liao et al. 2006).

4. NOVEL THERAPEUTIC MODALITIES.

4.1. Cancer Gene Therapy.

4.1.1. Concept

Gene therapy is an emerging advanced therapy that consists on the transfer of genetic material into cells in order to cure or at least ameliorate the course of a disease. The main objective of cancer gene therapy is to eliminate cancer cells or to restore their normal phenotype by restoration or inhibition of usually mutated genes in pancreatic cancer such as silencing of KRAS, or functional rescue of p53 or p16 (Calbo et al. 2001; Miura et al. 2005; Bardeesy et al. 2006).

The success of a gene therapy will largely depend on the activity induced by the introduced gene and the efficiency of gene delivery resulting from the combined effects of the delivery vector and the applied delivery route.

4.1.2. Therapeutic systems.

Different gene therapy approaches exist according to the different therapeutic genes transferred. A large number of genes have been tested for their therapeutic efficacy against pancreatic tumors.

- ***Apoptotic genes.***

Some approaches consist on targeting hallmarks of cancer such as apoptosis resistance or angiogenesis. The re-engagement of the disrupted apoptosis program in pancreatic cancer cells is a general strategy for effective and tumor-cell-specific cancer therapy. Studies on single apoptosis-associated gene deregulated in pancreatic cancer have shown encouraging results; for example, downregulation of the anti-apoptotic gene BCL-2 triggered anti-proliferative and pro-apoptotic effects in tumoral cells but not in non-malignant tissues (Ocker et al. 2005). Overexpression of pro-apoptotic genes such as BAX and TRAIL also showed antitumoral effects and sensitization to gemcitabine chemotherapy (Wack et al. 2008). Interestingly, inhibition of particular inhibitors of apoptotic proteins (IAPs) such as cIAP-2 and XIAP proved to be very efficient to induce sensitivity to cisplatin, doxorubicin and plaxitaxel (Lopes et al. 2007; Vogler et al. 2007).

- ***Antiangiogenic gene therapy.***

Development of antiangiogenic gene therapies includes the suppression of angiogenic molecules and the upregulation of antiangiogenic molecules. A replication-deficient retrovirus encoding truncated VEGF-RII was used to block VEGF signaling through dominant-negative inhibition, and significantly reduced the growth rate of subcutaneous tumors in three pancreatic cancer cell lines (Buchler et al. 2003). On the contrary, a recombinant adenovirus expressing the angiogenesis inhibitor NK4 suppressed the number and growth of pancreatic cancer metastasi foci in the liver after viral intrasplenic injection and reduced the development of pancreatic tumors in a mouse peritoneal model after viral intraperitoneal injection (Saimura et al. 2002; Murakami et al. 2005).

- ***Restoration or inhibition of gene mutated functions.***

The inhibition of oncogene expression and restoration of tumor suppressor functions have also been studied in pancreatic cancer gene therapy. Strategies involving the silencing of mutated K-ras and/or the functional rescue of p53 or p16 tumor suppressor genes have shown significant antitumoral responses in mouse models. Adenoviruses carrying a dominant negative H-ras mutant that competed with K-ras for a guanine nucleotide exchange factor, or an antisense K-ras RNA reduced the dissemination of pancreatic cancer in rodent models (Takeuchi et al. 2000; Miura et al. 2005). Similarly, an adenovirus containing the wt-p16 cDNA or/and the wt-p53 cDNA decreased cell proliferation and increased the level of apoptosis (Cascallo et al. 1999; Calbo et al. 2001). Due to the fact that mutational activation of K-ras is such a common event in pancreatic cancer, targeting of key signaling pathways downstream of mutant K-ras has also been explored through gene therapy approaches (Fillat et al. 2011). Other oncogenes and tumor suppression genes used as therapeutic targets include Notch-1, survivin, SMAD4 and cyclin D1, among others (Xu et al. 2010).

- ***Suicide gene therapy.***

Suicide or prodrug-converting cancer gene therapy conform another important group of anti-cancer therapies. This strategy is based on the transfer of an enzyme able to transform a prodrug into a toxic metabolite, resulting in cell death. This approach provides low systemic but high local intratumoral toxicity since the non-toxic prodrug is systemically administered, but the enzyme is specifically delivered to tumoral cells (Lanuti et al. 1999). Some examples of suicides systems are

the TK/GCV system, CD/5-FC and CYP2B1/CPA. In this thesis the TK/GCV system has been employed as antitumoral strategy. A detailed description of the TK/GCV system is presented in section 4.1.6.

- ***Immunotherapy.***

The objective of immunotherapy is to stimulate the immune system to target and destroy cancer cells and confront the fact that pancreatic cancer cells have low immunogenicity. Tumor gene transduction of tumor specific antigens, costimulatory molecules or inflammatory cytokines constitute the major type of molecules assessed to facilitate the presentation of pancreatic tumor cells to the immune system. Vectors expressing IL-1, IL-2, IL-12, TNF-α, GM-CSF have shown significant antitumoral responses (Mazzolini et al. 2005; Meng et al. 2010). Combination of restricted replication-competent adenovirus with an adenovirus carrying IL-2 led to a remarkable inflammatory response and almost complete regression of established tumors (Motoi et al. 2000). IFN-γ viral administration provoked an activation of antitumor immunity resulting in complete eradication of both primary and distant tumors (Sarkar et al. 2005). Tumor regression/stabilization was achieved in 50% of treated mice after *in vivo* lentiviral administration of hIFN-α (Ravet et al. 2010). A Phase I trial of intratumoral injection of an adenoviral vector encoding human IL-12 for pancreatic cancer showed to be well-tolerated but exerted only mild antitumor effects (Sangro et al. 2004).

Another promising strategy is the development of cancer cell vaccines, in which cells, usually antigen presenting cells (APC) such as dendritic cells, are manipulated to be more recognizable by the immune system via introduction of one or more transgenes, which include cytokines, costimulatory molecules and specific tumor associated antigens (Xu et al. 2010).

- ***Oncolytic virus therapy.***

Growing interest relies on the efficacy of virotherapy. Virotherapy is based on the viral replication itself as a mean to destroy cancer cells in a process referred to as viral oncolysis. The safety and efficacy of this approach depends on the selectivity of the virus to replicate only in cancer cells. To increase the antitumoral potency, replication-competent viruses can be further modified to express a transgene, originating "armed oncolytic viruses". Several types of virus have been studied as

replication agents, some of them have been engineered to selectively replicate in tumoral cells, such as adenovirus (Ad), herpes virus (HSV) or measles virus (McAuliffe et al. 2000; Zhang et al. 2006; Huch et al. 2009), while others possess a natural oncolytic capacity as for example vaccinia viruses or reovirus (Kelly et al. 2009; Yu et al. 2009). The first virotherapy-based clinical trial in pancreatic cancer was a Phase I/II carried out with repeated intratumoral administrations of ONYX-15 adenovirus by EUS-guided. ONYX-15 was developed to selectively replicate and lysate in p53 deficient cancer cells. The trial showed the feasibility and tolerability of the therapy; however, its very limited replication capacity compromised its antitumoral effect (Hecht et al. 2003). A Phase I study is ongoing to assess the safety and effectiveness of intratumoral injections of the oncolytic herpes simplex virus, OncoVEX GM-CSF into unoperable patients with pancreatic cancer (NCT00402025). A Phase I study combining suicide gene therapy delivered by the replication competent adenovirus expressing the TK and the CD enzymes (Ad5-yCD/mutTKSR39rep-ADP) with chemoradiation therapy is currently recruiting patients with non-metastatic pancreatic adenocarcinoma (NCT00415454) (Fillat et al. 2011).

- ***Combined therapies.***

The pathogenesis of pancreatic cancer is complex and single gene therapy approach is unlikely to achieve a cure. Therefore, nowadays many studies are based on the combination of gene therapy approaches, such as virotherapy with immunotherapy (Hu et al. 2006; Bortolanza et al. 2009), or combination of gene therapy with chemotherapy and radiotherapy (Freytag et al. 2007; Oberg et al. 2010). The replication deficient Ad-NK4 combined with gemcitabine significantly reduced tumor volume of orthotopically implanted SUIT-2 tumors and completely suppressed peritoneal dissemination and liver metastases, compared with Ad-NK4 or gemcitabine alone (Ogura et al. 2006). Similarly, the AdDeltaE1B19K replicative adenovirus synergized with gemcitabine to selectively kill cultured pancreatic cancer cells and xenografts *in vivo* with no effect in normal cells (Leitner et al. 2009). The combination of the replicative adenovirus 5/3COX2CRAdF with gemcitabine or 5-fluorouracil also showed improved antitumoral effect (Nelson et al. 2009).

4.1.3. Delivery vectors.

Delivery vectors can be classified into three main groups: viral vectors, non-viral vectors and cellular vectors.

Viral vectors are biological systems deficient in replication, derived from naturally evolved viruses capable of transferring their genetic material into the host cells. Basically, viruses are transformed to viral vectors capable of delivering genes by substituting key genetic components of the viral genome by the transgene of interest and providing viral genes in *trans* to generate recombinant viral particles (Morille et al. 2008). Many viruses, either with RNA or DNA genomes, enveloped or no-enveloped, integrative or non-integrative, with the ability to transduce both diving and non-diving cells, have been engineered as vectors. The most commonly used are adenovirus, retrovirus, lentivirus, herpes simplex virus (HSV) and adeno-associated virus (AAV). In particular, adenoviruses are leading gene therapy clinical trials (Illustration 8).

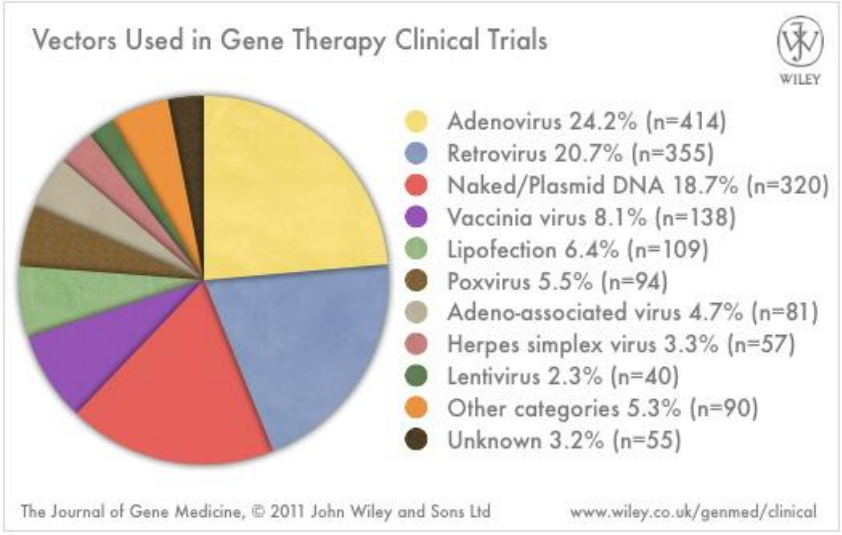

Illustration 8. Vectors used in gene therapy clinical trials in 2011. Image from Wiley Gene Therapy Clinical Database.

Viral vectors are very effective in achieving high efficiency for both gene delivery and expression. However, the limitations associated with viral vectors in terms of safety, immunogenicity, low transgene size and high cost, have encouraged researchers to focus on alternative systems. Non-viral vectors are safe, low immunogenic and easy to produce at large-scale; they can carry large inserts but they are quite inefficient at transfecting cells *in vivo* (Morille et al. 2008; Atkinson and Chalmers 2010). Non-viral vectors include naked DNA, cationic liposomes (lipoplexes) and synthetic polymers (polyplexes). Naked DNA can be directly injected to the tumor site but it results in poor transfection

efficiency; alternatively it can be systemically delivered, although then it is rapidly degraded by serum nucleases. Physical methods that increase the permeability of cell membrane to facilitate the introduction of naked DNA into cells such as electroporation (EP) or ultrasounds have shown to improve its transfection efficiency (Niidome and Huang 2002). Lipoplexes and polyplexes are generated by interaction of cationic liposomes and synthetic polymers with negatively charged DNA through electrostatic interactions. Non-viral vectors have yet to consistently demonstrate transfection efficiency comparable to that of viruses, regardless of gene or target cell type (Morille et al. 2008). Recently, the use of nanoparticles to deliver DNA molecules has strongly emerged in the development of non-viral gene therapy approaches.

Growing attention is paid on cellular vectors. Dendritic cells, fibroblasts, mesenchymal stem cells (MSC) and blood outgrowth endothelial cells (BOECs) have already been tested as delivery vectors. MSC are pluripotent progenitor cells that are actively recruited to the tumor environment (Kallifatidis et al. 2008). It has been shown that systemic delivery of TK transfected MSC to mice carrying orthotopic syngenic pancreatic tumors significantly reduced the primary tumor growth and the incidence of metastases (Zischek et al. 2009). Similarly, intraperitoneal administration of MSC-IFN suppressed tumor growth of orthotopic pancreatic tumors (Kidd et al. 2010).

4.1.4. Adenovirus biology.

Adenoviruses are non-enveloped icosahedral viruses with a double stranded DNA genome of 30 to 40 kb enclosed in a capsid comprised predominantly of hexon, penton base and fiber proteins. Hexon is the most abundant structural component and constitutes the bulk of the mature virion. Five subunits of the penton base are found at each of the twelve vertexs of the capsid and form the platform for the twelve fiber homo-trimers that protrude from the virion. At the distal tip of each linear fiber is located the globular knob domain (Illustration 9B). Hexon appears to play structural role as a coating protein, while the penton base and the fiber are responsible for the key virion-cell interactions that constitute Ad tropism (Curiel and Douglas 2002). Recently, hexon protein has also been described as a major mediator of *in vivo* liver transduction by interaction with coagulation factor X (FX) (Kalyuzhniy et al. 2008; Vigant et al. 2008; Waddington et al. 2008).

There are about 50 serotypes of human Ad, most of which can recognize the cellular Coxsackie B virus-adenovirus receptor (CAR) as the primary receptor. For Ad2 and Ad5, the first step of Ad uptake occurs primarily through high affinity binding of the viral fiber protein to CAR. The second step of virus uptake is mediated by low affinity binding of the Arg-Gly-Asp (RGD) residues of Ad penton base to integrin molecules $\alpha v\beta 1$, $\alpha v\beta 3$ or $\alpha v\beta 5$ on the cell surface. Integrin binding induces internalization of Ad through receptor-mediated endocytosis in clathrin-coated vesicles. Ad is then released from the endosome and progresses through cytosol to the nuclear pore complex. Here the remainder of the capsid is disassembled as the genome enters the nucleus. Viral transcription, replication and packaging occur in the nucleus (Meier and Greber 2004; Sadeghi and Hitt 2005).

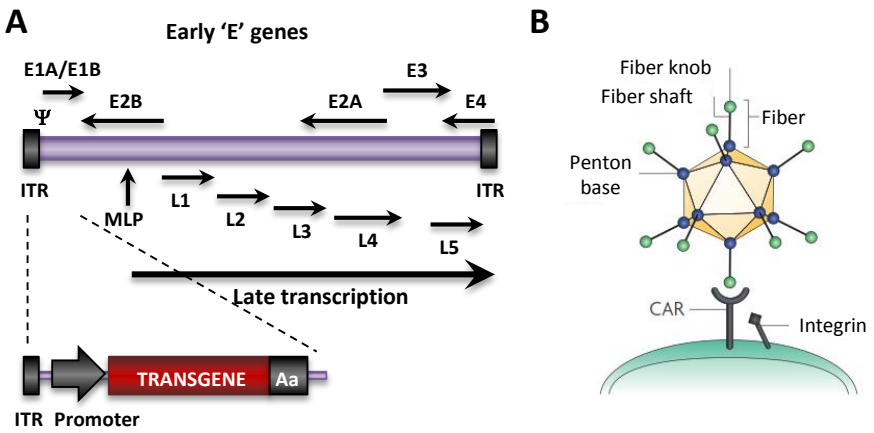

Illustration 9. Adenovirus biology. A) Adenoviral genome. E1A induces the other viral regions included E1B (encodes proteins that block host mRNA transport, and inhibit E1A-induced apoptosis), E2 (encodes the DNA polymerase, terminal protein and DNA binding protein that mediate viral replication), E3 (encodes several proteins that modulate the host immune response to infection) and E4 (encodes proteins involved in DNA replication, late gene expression, and host protein shut off). Most late genes are transcribed under the control of the Major Late Promoter (MLP), in a single primary transcript that is multiply spliced. The late mRNAs encode most of the structural proteins of the virion. B) Native entry mechanism of adenovirus. Ad5 binds to its receptor CAR through its fiber knob, and integrins interact with the RGD peptide motif in the penton base and facilitate cell entry by endocytosis. Panel B adapted from (Waehler et al. 2007).

Adenovirus genome consist on a linear molecule flanked by inverted terminal repeats (ITRs) carrying the replication origin (Illustration 9A).

The viral packaging signal is located near the “left” end of the genome. The ITRs and packaging signal are the only sequences required in *cis* for Ad production. Viral coding sequences are divided into early (transcribed before viral DNA replication) and late (expressed after the onset of replication) regions. Early region 1A (E1A) is the first transcription unit expressed after Ad infection and induces the other viral early regions. E1A region is deleted in replication-defective adenoviral vectors, preventing lysis of the infected host cell and vector dissemination, and in addition, creates space for gene insertions (Sadeghi and Hitt 2005).

Ad5 serotype has been the most extensively vector used in gene therapy. It presents low pathogenicity in humans causing mild acute respiratory infections. Ad vectors have a good safety profile and can be produced at high titers under GMP conditions, do not integrate, can transduce dividing and non-dividing cells and present high *in vivo* transduction efficiency. When administered systemically they are trapped by the liver, which limits tumor delivery and elicits hepatotoxicities. The fact that many individuals have pre-existing neutralizing antibodies against the most common vector strains (Ad2 or 5) can limit gene transfer. Moreover, residual expression of viral genes also causes direct toxicity and the activation of a cellular immune response that leads to the clearance of vector-transduced cells and to short duration of transgene expression (Fillat et al. 2011). Nevertheless, strategies to overcome such limitations are under development and include transductional and transcriptional targeting.

4.1.5. Adenoviral targeting.

To achieve therapeutic success, gene therapy vehicles must be capable of transducing target cells while avoiding harming non-target cells. Despite the high transduction efficiency of viral vectors, their tropism frequently does not match the therapeutic need. Many efforts are being conducted to modify current vectors to efficiently and specifically target pancreatic cancer cells. We will focus on adenoviral vector targeting towards pancreatic tumors although other tumor types are briefly mentioned.

4.1.5.1. Transcriptional targeting.

Transcriptional targeting of Ad transgene expression or replication exploits the unique transcriptional profile of the target cell by employing target cell-specific regulatory sequence elements to restrict the

therapeutic transgene expression or replication to target cells. In addition to promoter elements providing tissue- specific gene activation, tumor-associated regulatory sequences are also used for transcriptional targeting to cancer cells. A number of candidate tumor/tissue-specific promoters (TSPs) have been studied for pancreatic cancer gene therapy, but some promoters lack sufficient activity, specificity, or both. Therefore, recent research has focused on the evaluation of candidate promoters with regard to these attributes.

Tumor-specific promoters (TSP) have been tested to drive the expression of either cytotoxic genes, such as TK or the pro-apoptotic genes Bax and TRAIL, or to control the expression of viral essential gens, such as are E1A and/or E4, in oncolytic adenovirus (Hoffmann and Wildner 2006b; Liu et al. 2007; Wack et al. 2008; Huch et al. 2009). Examples of TSP altered in a broad number of tumor types and in pancreatic cancer in particular, include the cyclooxygenase-2 (COX-2), midkine (MK), E2F1, cancer specific progression elevated gene-3 promoter (PEG-prom), human telomerase reverse transcriptase (hTERT), carcinoembryonic antigen promoter (CEA), urokinase-like Plasminogen activator receptor (uPAR), among others (Sadeghi and Hitt 2005; Fillat et al. 2011).

Several features of tumor-associated vasculature are different from normal vasculature providing candidate targets for tumor-selective 'transcriptional targeting'. Tumor endothelia-selective expression of transgenes has been afforded using native promoters of genes such as VEGF, pre-endothelin-1 (PPE-1), ICAM-2, Flt-1, E-Selectin and KDR (Bazan-Peregrino et al. 2007).

Another strategy for cancer gene therapy involves restricting gene expression with a conventional treatment methodology, such as chemotherapy or radiation. For example, the early growth response gene 1 (EGR-1) promoter is inducible via external beam ionizing radiation or an iodine-125-labeled thymidine analog. The TNFerade (Ad.Egr-TNF) adenoviral vector has been evaluated in trials for patients with sarcomas, melanomas and cancers of the pancreas, esophagus, rectum and head and neck (Weichselbaum and Kufe 2009).

Many enhancer-promoters derived from tissue-specific genes have been assessed for their ability to transcriptionally target first generation Ad vectors. Unfortunately, *cis*-acting viral sequences can sometimes distort the specificity of promoters and enhancers inserted into these vectors. Specificity can be restored in some cases by flanking the expression

cassette with additional polyadenylation signals or with insulator sequences, although these strategies are no successful with all enhancer-promoters (Sadeghi and Hitt 2005).

TSPs have the potential to decrease the toxicity of gene therapy for cancer and represent a powerful tool for the specific targeting of transgene expression to neoplastic cells. However, they do not modify the capacity of Ad infection since viruses are dependant on CAR for entry.

4.1.5.2. Transductional targeting.

Targeting therapeutic transgenes to the primary tumor and distant metastases requires delivery of the gene vector via the bloodstream. Unfortunately, following intravenous injection, adenoviral vectors are cleared very rapidly into the liver. Moreover, many viral vectors have an intrinsic tropism for non-target cells. Vectors capable of efficient delivery to tumoral cells must therefore usually be 'detargeted' in order to permit their persistence in the bloodstream sufficiently to enable access to target sites, and also 'retargeted' to enable infection of their target cells and tissues (Waehler et al. 2007).

Several approaches have been developed to modify the vector tropism and redirect viral entry towards abundant receptors in tumoral cells. Two major strategies have been employed: i) targeting achieved via genetic-structural manipulation of the Ad capsid, and ii) adapter molecule-based targeting.

- ***Genetic modification of the proteins participating in viral entry.***

Several genetic attempts have been made to detarget Ad5 from murine liver by ablating CAR-binding, integrin-binding, heparan sulfate proteoglycan-binding sites and blood factors-binding via fiber modifications (Smith et al. 2002; Akiyama et al. 2004; Shayakhmetov et al. 2005; Bayo-Puxan et al. 2009). Results have shown that some detargeting can be achieved using genetic modifications, although the variety of infection pathways operative *in vivo* makes this less successful than expected. As previously mentioned, hexon protein mediates *in vivo* liver transduction; substitution of hexon protein of Ad5 for hexon protein of Ad3 has demonstrated reduced FX binding, decreased liver tropism, and improved antitumor efficacy (Short et al. 2010).

Genetic manipulation of capsid proteins is a conceptually elegant targeting approach, but genetic targeting efforts must work within narrow structural constraints since Ad tropism has to be modified without disrupting native molecular interactions indispensable for proper biological function. Rigorous structural analysis of adenoviral particles has exploited two separate locations within the knob domain that tolerate genetic manipulation without loss of fiber function, the C-terminus and the HI-Loop. The introduction of the Arg-Gly-Asp (RGD) peptide into the HI loop of the knob domain of the fiber protein has been shown to target adenovirus to alpha-beta integrins and improves adenoviral transduction in pancreatic carcinoma (Jacob et al. 2005). Poly-lysine ligand introduction into the C-terminal have successfully targeted adenovirus to heparan sulfates (Koizumi et al. 2003). Insertion of the protein transduction domain TAT into the HI-loop or C-terminus of fiber protein has also demonstrated enhanced infectivity of CAR-negative cell lines *in vitro* and *in vivo* (Han et al. 2007; Kurachi et al. 2007).

Pseudotyping is the process of changing the natural tropism of a virus to that of another virus by switching their surface proteins. Genetic replacement of either the entire fiber or knob domain with other from another human Ad serotype that recognizes a cellular receptor other than CAR has been achieved. Adenovirus serotypes 11 and 35 present enhanced infectivity compared to Ad5 in pancreatic cancer (Glasgow et al. 2004). The combination of different fibers in the adenovirus, such are fibers 5 and 35, or fibers 16 and 50 mediate more efficient and specific gene transfer to pancreatic cancer cells (Toyoda et al. 2008; Kuhlmann et al. 2009).

- ***Adapter molecule-based targeting.***

The adapter molecule-based concept is based on the formulation of molecular conjugates that link the vector with specific cellular receptors. Bispecific conjugates bear one component recognizing a region of the adenoviral vector and the other component specific for a cellular receptor, bypassing the native CAR-based tropism. They mainly consist on the fusion or conjugation of antibody fragments (Fab) with cell-selective ligands or antibodies against target cell receptors such as EGFR (Glasgow et al. 2004). The fusion of a Fab fragment against the adenovirus knob region with the fibroblast growth factor (FGF-2) ligand, resulted in retargeting to FGFR positive cells, leading to improved transduction of pancreatic tumor cells *in vitro* and *in vivo* (Kleeff et al. 2002; Huch et al. 2006). Adenoviruses retargeted with a bispecific fusion

protein composed of a soluble form of truncated sCAR fused to the EGF ligand led to enhanced gene transfer efficiency in pancreatic carcinoma cells (Wesseling et al. 2001).

Although adapter-based targeting studies have shown promising results for retargeting adenovirus to new receptors, these Ad based delivery systems have more complex pharmacodynamics and kinetics. Therefore, one-component systems may be more easily applicable to human gene therapy trials.

4.1.6. The therapeutic system TK/GCV.

4.1.6.1. Mechanism of action.

The herpes simplex virus thymidine kinase gene/ganciclovir prodrug system (TK/GCV) is a well-studied gene-directed prodrug activation approach for the treatment of cancer, presenting promising results against some malignant conditions (Immonen et al. 2004). It consists on a first step where the TK gene is delivered into to the tumoral cells, and a second step where the prodrug GCV is administered and is selectively activated by the TK enzyme (Moolten 1986).

GCV, an acyclic analog of the natural nucleoside 2'-deoxyguanosine, is an antiviral agent used against human cytomegalovirus, herpes simplex type 1 and 2, varicella zoster virus and Epstein-Barr virus (Faulds and Heel 1990). In the TK/GCV system, the HSV-TK enzyme converts the nucleoside analog GCV to its monophosphate form, which is later converted by the cellular enzymes guanylate kinase and phosphoglycerate kinase, into GCV triphosphate (GCV-TP), which competes with endogenous dGTP for subsequent incorporation into DNA. GCV-treated cells undergo a round of DNA replication, doubling in number and incorporating GCV-TP into the nascent DNA strand. However, the lack of a complete sugar ring makes GCV a poor substrate for continuing chain elongation, triggers the formation of double-strand breaks and, finally, cause cell death by apoptosis (Fillat et al. 2003; Abate-Daga et al. 2010). Incorporation of GCV-TP also leads to cell death as a result of chromosomal aberrations and sister chromatid exchange. Adverse effects are minimal because of the selective cytotoxicity of the prodrug for HSV-TK expressing cells, since GCV is not phosphorylated by mammalian cellular kinases. Moreover, since the toxicity of the prodrug is associated with DNA replication, cell killing will mainly occur in rapidly

dividing cells (e.g. tumor cells) and not in normal tissue (van Dillen et al. 2002).

One of the most important findings in the validation of the HSV-TK/GCV system as a potentially powerful tool in cancer gene therapy was the discovery of the bystander effect (BE). BE is mediated by the transfer of GCV metabolites from the TK-expressing cells to the adjacent cells (Illustration 10). Early studies have shown that a transfection percentatge of only 1% was sufficient to kill virtually the complete cell population *in vitro* (Moolten 1986), and that complete tumoral regression was achieved when 10-50% of cells expressed TK (Culver et al. 1992; Caruso et al. 1993). The more accepted mechanism by which the bystander effect occurs is through gap junctions (GJIC) and is mediated by connexins (Vrionis et al. 1997). The reintroduction of connexins into poor communicating cells can help reestablish gap junction intercellular communication and enhance TK/GCV toxicity (Carrió et al. 2001; Jimenez et al. 2006). It has also been demonstrated that cell adhesion molecules as for example E-cadherin, have a marked influence on gap junction assembly and communication and consequently on the magnitude of the bystander effect (Garcia-Rodriguez et al. 2011).

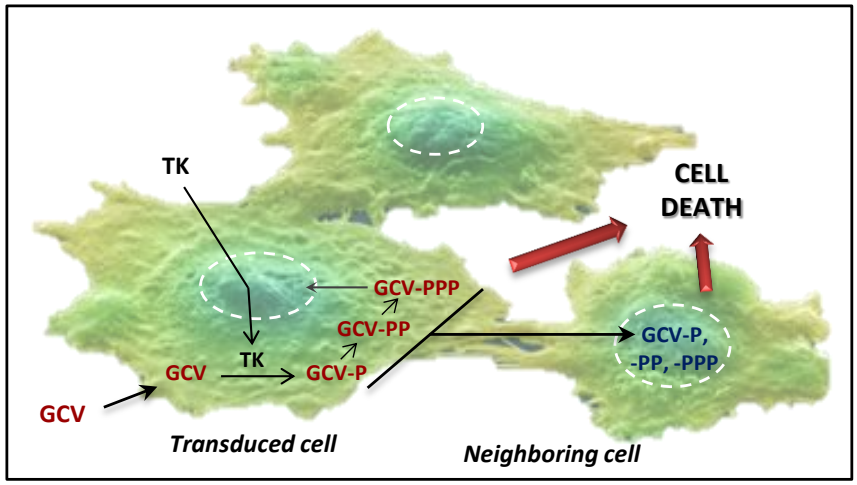

Illustration 10. TK/GCV mechanism of action and bystander effect. TK enzyme phosphorylates GCV to its monophosphate form (GCV-P), while cellular kinases phosphorylate GCV-P to di and triphosphate forms (GCV-PP, GCV-PPP). Then, GCV-PPP enters to the nucleus competing with dGTP for incorporation into DNA, blocks DNA synthesis, generates DSB and triggers apoptotic cell death. Bystander effect is produced by the transfer of GCV metabolites from transduced cells to neighboring cells producing then their death by apoptosis.

Another proposed mechanism to mediate BE was through phagocytosis of apoptotic bodies. Apoptotic vesicles generated from dying TK-expressing cells would be phagocytized by nearby intact unmodified tumor cells provoking their death (Freeman et al. 1993).

In vivo experiments have demonstrated that the immune system also plays a role in the bystander effect. The immune response, generated due to the expression of non-human proteins or due to the death of transduced cells, can stimulate recognition of tumor antigens triggering the immune system and finally ending up with the death of non-transduced cells (Barba et al. 1994).

4.1.6.2. Strategies to enhance the therapeutic response of the TK/GCV system.

Different approaches have been studied to augment the efficacy of the TK/GCV system. Some examples are the use of TK mutants, the improvement of GJIC facilitating TK intercellular spreading and the use of combined therapies. TK mutants have been engineered to overcome the low sensitivity of cells to GCV or other nucleoside analogues (Kokoris et al. 2000; Qiao et al. 2000; Black et al. 2001). Improvement of GJIC has been achieved pharmacologically by the use of drugs such as lovastatin or retinoic acid (Hossain and Bertram 1994; Touraine et al. 1998), or by the overexpression of connexins, such as Cx43 or Cx26 (Estin et al. 1999; Carrió et al. 2001), or E-cadherin (Garcia-Rodriguez et al. 2011). The use of combined therapies and the improvement of TK intercellular spreading are explained in detail below.

- ***Combined therapies; TK/GCV and chemotherapy.***

Different combined therapies have been used to enhance the cytotoxic effect of the TK/GCV system. One strategy has been the combination of two suicide genes such as TK and Cytosine deaminase (CD) or TK and Cytochrome P450, that proved to be synergistic (Carrio et al. 2002; Freytag et al. 2007). Another strategy explored by several authors has been the combination with radiotherapy. Studies have reported that the TK/GCV treatment sensitizes the cell to radiation *in vitro* and *in vivo* (Nishihara et al. 1997; Hodish et al. 2009; Chen and Tang 2010). A triple combined strategy include the application of the replicative adenovirus Ad5-yCD/mutTK(SR39)rep-ADP expressing a mutant TK and the suicide gene (CD) together with radiotherapy (Freytag et al. 2007). The authors demonstrated that this suicide gene therapy strategy had the potential

to augment the effectiveness of pancreatic radiotherapy without resulting in excessive toxicity.

Several chemotherapeutic agents have also been combined with the TK/GCV system. Some of them have afforded synergistic toxicity, such as topotecan, UCN-01, gemcitabine or temozolomide, while others were antagonistics such as Taxol or camptothecin (Fillat et al. 2003). The final effect of the combined therapy will very much depend on the interference or synergy between the operating mechanisms of action of each treatment and the genetic background of the tumor cell. In this line, Abate-Daga and collaborators demonstrated that TK/GCV –UCN-01 combined therapy synergized or antagonized *in vitro* in different pancreatic cancerous cells depending on its sensitivity to the TK/GCV system (Abate-Daga et al. 2010).

Two recent studies have demonstrated that the combination of TK/GCV with gemcitabine synergize *in vitro* and *in vivo* in cultured SW620 human colon carcinoma cells as well as in murine xenograft models (Boucher and Shewach 2005; Fridlender et al. 2010).

- ***Intercellular spreading: the optimized Tat8TK/GCV system.***

It has been described that certain proteins or peptides, termed translocatory proteins, can efficiently translocate across the membrane of mammalian cells and are able to mediate the intracellular delivery of heterologous proteins fused to them, suggesting that a new type of bystander effect might take place in a given tissue. Examples of such proteins are the TAT protein of the human immunodeficiency virus, *Drosophila* antennapedia and herpes simplex virus VP22 (Harada et al. 2006). The intercellular transfer function has been related to short peptides of highly basic residues that have been termed protein transduction domains (PTDs) (Beerens et al. 2003; Leifert and Whitton 2003). The most widely used domain responsible for TAT translocation corresponds to the short basic region of 11 aa comprised by the residues 47-57:YGRKKRRQRRR (Vives et al. 1997). However, Cascante et al showed that an 8 aa peptide also had PTD properties (Cascante et al. 2005). The common feature among these peptides is their highly cationic nature due to their high proportion of basic aminoacids. Several therapeutically active macromolecules have been fused to these PTDs and have shown to successfully transduce living cells, such as peptides, proteins, oligo DNAs, super magnet beads, liposomes, λ phages and adenovirus (Harada et al. 2006). To date, fusion proteins with TAT_{PTD} have shown markedly

better cellular uptake than similar fusions with antennapedia or VP22 (Wadia and Dowdy 2005).

An approach to increase the cytotoxic effect of the TK/GCV therapy has been to provide the system with a new type of bystander effect resulting from the transduction capacity of an engineered TK protein. It consisted on the modification of the TK enzyme, by the fusion with the 8 aa TAT_{PTD} to generate the TAT8-TK protein. The increased cytotoxicity of the system was associated to a remarkable antitumor effect in pancreatic xenograft tumors (Cascante et al. 2005).

4.2. Tumor ablation techniques.

Several image-guided ablation techniques have been developed to treat patients with cancer not elected for surgery. These minimally invasive procedures can achieve effective and reproducible tumour destruction with low morbidity. Over the past two decades, several methods for chemical ablation or thermal tumor destruction have been developed and clinically tested. These include the injection of ethanol or acetic acid and the administration of localized heating (radiofrequency, microwave, laser ablation) or freezing (cryoablation) (Crocetti and Lencioni 2008).

Ethanol injection induces coagulation necrosis of the lesion as a result of cellular dehydration, protein denaturation, and chemical occlusion of small tumour vessels. Its major limitation is the high local recurrence rate (about 30-40%). It is a well-established technique for the treatment of nodular-type hepatocellular carcinoma (HCC), leading to complete necrosis of about 70% of small lesions (Lencioni et al. 1995).

Radiofrequency ablation (RFA) induces thermal injury to the tissue through electromagnetic energy deposition. RFA ablation has been the most widely assessed alternative to ethanol injection for local ablation of HCC (Lencioni and Crocetti 2005). Studies with patients with unresectable pancreatic adenocarcinoma have shown that RFA is a feasible palliative treatment that leads to tumor reduction and improved quality of life. However, its safety remains still under debate, with a high complication rate without a clear benefit of survival (D'Onofrio et al. ; Pezzilli et al. 2011).

Microwave ablation is the term used for all electromagnetic methods using devices with frequencies greater than or equal to 900 kHz.

Although no statistically significant differences were observed in the efficacy when compared with RFA, a tendency favoring RFA was observed in local recurrences and complications rates (Lu et al. 2001).

Cryosurgery uses freezing temperature to produce ice crystals which removes water from the cells and leads to deleterious events. Freeze-thaw cycles produce cell death by necrosis in the central part of the cryogenic lesion and by induces apoptosis at the periphery (Gage et al. 2009).

Although some ablative techniques, such as RFA and microwave ablation, have been widely used in treating patients with liver, lung, and kidney tumors, they are limited in that they rely upon the indiscriminate use of thermal energy to induce necrosis of tumor cells, a process that can result in damage to nearby structures including blood vessels, bile ducts, and nerves. In addition, the blood flow of large vessels creates a heat sink effect that severely inhibits the ability to ablate cancer cells in the vicinity of large vessels (Patterson et al. 1998). These limitations are especially relevant to the pancreas which lies immediately adjacent to the superior mesenteric artery, portal vein, and common bile duct. Furthermore, the use of ablative therapies in the pancreas has largely been avoided altogether due to the possibility of thermal injury induced pancreatitis (Bower et al. 2011).

Electrolytic ablation (EA) is a non-thermal technique that produces localized necrosis through local pH and electrochemical changes in the local microenvironment induced by a low voltage direct current. The technique is particularly safe especially close to major vessels. Although some clinical studies were carried out in patients with HCC, no clinical study has been performed in patients with pancreatic cancer (Gravante et al. 2011).

Irreversible electroporation (IRE) is an emerging technology for non-thermal tumor ablation. Electroporation utilizes targeted delivery of millisecond electrical pulses to induce permeabilization of cell membranes through nanoscale defects (Rubinsky et al. 2007).

4.2.1. Irreversible electroporation.

Electroporation is a non-thermal phenomenon in which cell membrane permeability to ions and macromolecules is increased by exposing the cell to high electric field pulses. If short pulses of low electric field

magnitude are applied, such permeabilization will be reversible and the treated cells will be viable after the procedure. However, when such artificially induced permeabilization is too high (range, 1500 to 3000 volts), it causes a disruption of cellular homeostasis through dismantling the cell membrane wall with innumerable nanopores, and cells end up dying by necrotic or apoptotic processes (Rubinsky 2007). Optimum results are achieved when more than 80 electrical pulses are delivered, contrasting with the 8 pulses used in most reversible electroporation settings (Lee et al. 2010c).

Studies in animal models have shown that IRE can ablate substantial volume of tissues and the efficacy of IRE to target breast, brain and hepatocarcinomas has already been evaluated and reported anti-tumor efficacy (Neal and Davalos 2009; Guo et al. 2010; Ellis et al. 2011). Recently, IRE has been proposed as a method for solid tumor ablation and it is now being assayed clinically for liver tumors (Lee et al. 2010b), lung tumors and kidney tumors (Ball et al. 2010). A Phase I clinical study to treat renal carcinomas with IRE has shown to be a safe technique that can offer some potential advantages over current ablative techniques (Pech et al. 2011).

- ***Characteristics of IRE procedure.***

Several unique characteristics of IRE distinguish it from other currently available tumor ablative techniques, such as radiofrequency ablation, cryoablation or microwave ablation.

Short ablation time: a typical IRE procedure for a solid tumor, with a size of approximately 3 cm in diameter takes less than one minute. If three or four overlapping ablations are required, total IRE treatment time is below 5 minutes. The time required for RFA or Cryo range 15 to 60 min. This correlates with reduced anesthesia time, reduced post-ablation pain and decreased ablation-related complications (Solbiati et al. 2001; Lee et al. 2010c).

Preservation of vital structures within IRE-ablated zone: extracellular matrix is not damaged by IRE ablation. This has been proposed to lead to the preservation of structural scaffoldings of vessels and ducts (Maor and Rubinsky 2010).

Avoidance of heat/cold-sink effect: IRE treatment uses multiple ultra-short pulses with brief intervals which increases therapeutic effect and decreases thermal effects (Davalos et al. 2005).

IRE-induced complete ablation with well-demarcated margin: other thermal methods, such as RFA or MWA, create a "grey-zone" of ablation, where the most outer margin of ablation contains some living cells that can cause residual tumor or recurrence (Guo et al. 2010; Lee et al. 2010c).

OBJECTIVES

"El motivo no existe siempre para ser alcanzado, sino para servir de punto de mira."

Joseph Joubert *(1775-1824)*

Ensayista francés

The general objective of this thesis has been the development of novel antitumoral strategies for the treatment of pancreatic tumors.

The work has focused on three major principles: i) improve adenoviral based therapies by exploring novel delivery routes and retargeting strategies, ii) search for synergistic treatments, and iii) evaluate novel approaches based on non-thermal ablative techniques .

The specific objectives have been:

I. To explore the effectiveness of adenovirus to transduce pancreatic tumors by a pancreatic intraductal injection method.

II. To determine the efficacy of the antitumoral cytotoxic AduPARTat8TK/GCV gene therapy to treat Ela-myc pancreatic tumors by intraductal or intravenous delivery.

III. To analyze the impact of the combined therapy AduPARTat8TK/GCV and gemcitabine in pancreatic tumors from Ela-myc mice.

IV. To study the tumor selectivity of the matrix metalloproteinase activatable adenovirus AdTATMMP.

V. To evaluate the efficacy of irreversible electroporation to treat pancreatic tumors.

MATERIALS AND METHODS

"Experiencia es el nombre que damos a nuestras equivocaciones."

Oscar Wilde *(1854-1900)*

Dramaturgo irlandés

1. METHODS RELATED TO ADENOVIRUS MANIPULATION.

All the adenoviruses used in this thesis are deficient in replication and derived from human adenovirus serotype 5 (Ad5). Their origin and characteristics are shown in Table 12. Some of them were generated as part of this thesis, while others were previously generated in our laboratory or kindly ceded by Dr. Ramon Alemany (IDIBELL-Institut Català d'Oncologia).

1.1. Adenoviral vectors generation.

We followed the protocol described by the group of Dr. Vogelstein (He et al. 1998) (Luo et al. 2007a) to generate adenoviral vectors. Two slightly different protocols were used to generate the adenoviral vectors depending on the type of viral modification assessed. In general terms, the gene of interest was cloned into a plasmid called *pShuttle* that contains homologous regions to the adenoviral genome. After homologous recombination between the recombinant *pShuttle* plasmid and a plasmid that contains the adenoviral genome (called *pBackbone*), the recombinant vector was generated. Then, the recombinant vector was linearized and transfected to HEK 293 cells, that produce the recombinant adenoviral particles.

1.1.1. Generation of plasmid DNA constructs.

In this thesis we have generated the viruses AduPARTat8TK, AdTAT and AdTATMMP. To generate the AduPARTat8TK virus, the cassete uPARp-Tat8TK-SV40 polyA was cloned into the pShuttle vector (AdEasy™ XL Adenoviral Vector System, Stratagene) in three consecutive steps. Briefly, Tat8TK was inserted into the NotI/XhoI sites of the pShuttle vector; next, SV40 polyA tail was cloned into the XhoI/XbaI sites of the previously generated plasmid, and lately uPAR promoter fragment was inserted into the NotI sites, generating the plasmid **pS-uPAR-TTK-pA**.

To generate AdTAT and AdTATMMP vectors we followed the protocol shown in Ilustration 11.

A

Peptide sequences:

TAT = YGRKKRRQRRR

TATMMP = YGRKKRRQRRR-GG-AKGLYK-GG-EEEGEEEEE

Nucleotide sequences:

TAT = TATGGCAGCAAGAAGCGGAGACAGCGACGAAGATAAAGAATCGTTTGTGTTATGTTT
CAACGTGTTTATTTTTCAATTGC

TATMMP = TATGGCAGCAAGAAGCGGAGACAGCGACGAAGAGGCGGCGCCAAGGGCCTGT
ACAAGGGCGGCGAGGAAGAGGGCGAGGAGGAAGAGGAGTAAAGAATCGTTT
GTGTTATGTTTCAACGTGTTTATTTTTCAATTGC

Legend:

TAT, MMP-cleavable linker, Blockage.
TAA: STOP codon fiber sequence.
In grey: 3' UTR fragment fiber sequence.
CAATTGC: MfeI restriction site.

B

1- TD-PCR 1. TAT insertion & **Ligation into T-vector**

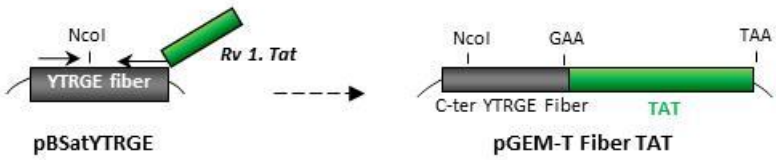

2- TD-PCR 2. 3'UTR / MMP linker – Blockage-3'UTR insertion & **Ligation into T-vector**

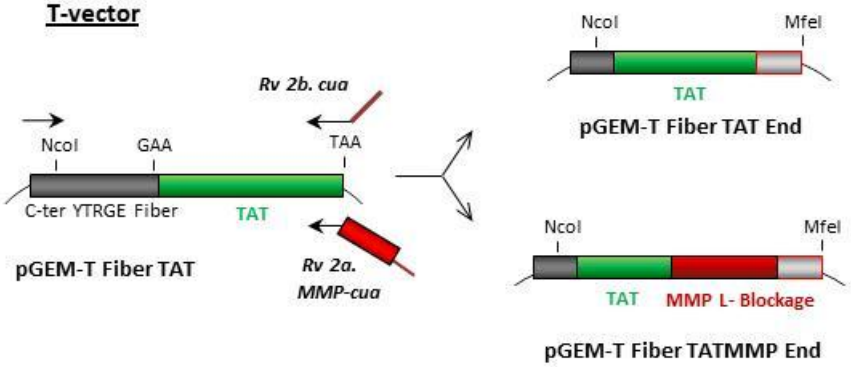

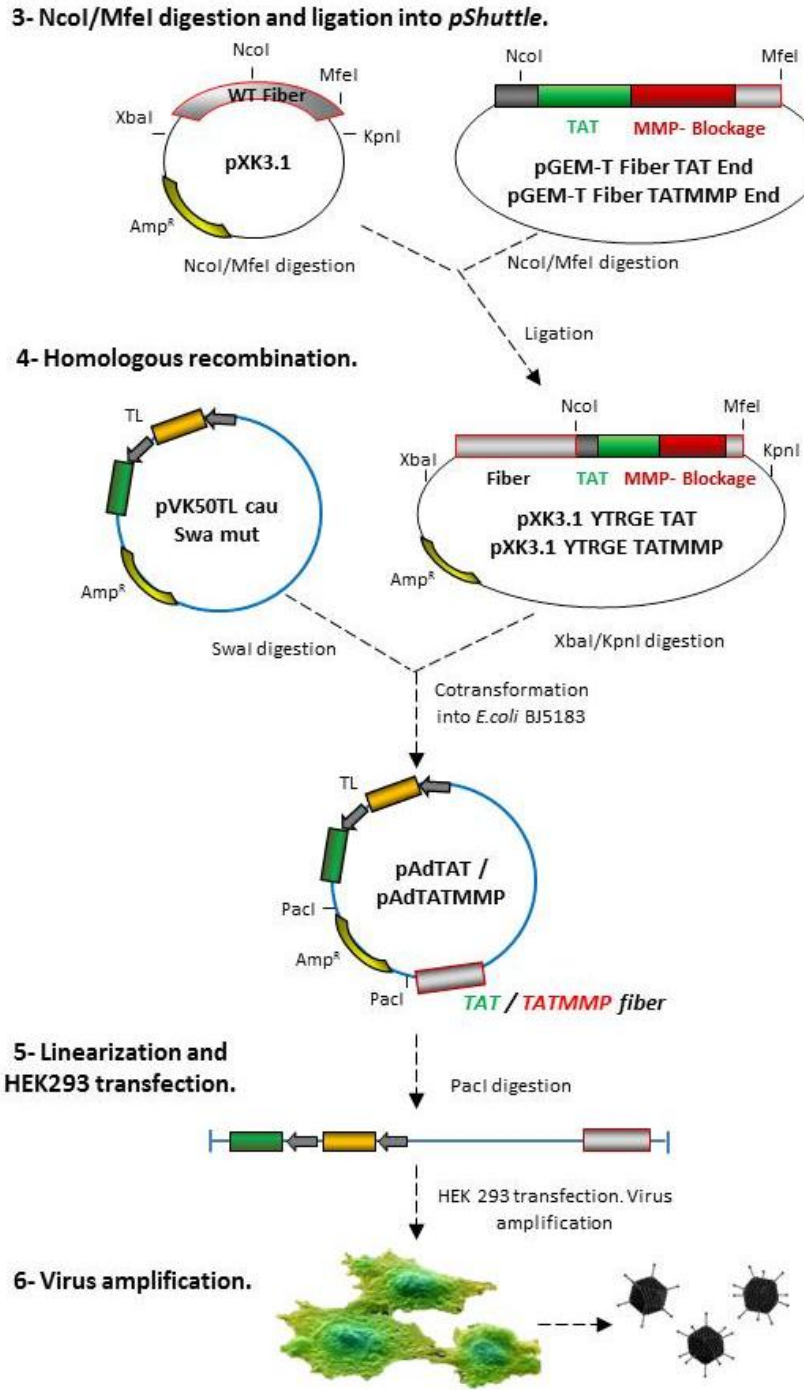

Ilustration 11. AdTAT and AdTATMMP generation scheme. pBSatYTRGE, pXK3.1 and pVK50TL swa mut plasmids were kindly ceded by Dr. Ramon Alemany (IDIBELL-Institut Català d'Oncologia).

TAT and TATMMP sequences were cloned at the end of fiber sequence by two consecutive Touch-Down PCRs (TD-PCR), a modified PCR technique that reduces nonspecific amplifications. TAT sequence was amplified from the plasmid pBSatYTRGE by TD-PCR using the primers Fibra 1Fw and Rv 1.Tat and the PCR conditions listed in Table 1 and Table 2, respectively. The PCR product, that contained the YTRGE mutations and TAT sequence, was cloned into a T-vector following the manufacturer instructions (pGEM®-T Easy Vector System I, Promega), generating the plasmid pGEM-T fiber TAT. Next, a second TD-PCR was employed to introduce the 3'-UTR region or the MMP-cleavable linker-Blockage-3' UTR region. We used the primers Fibra 1Fw and Rv2b.cua or Fibra 1Fw and Rv 2a.MMP-cua and the PCR conditions listed in Table 1 and Table 2 to generate the plasmids pGEM-T Fiber TAT end and pGEM-T Fiber TATMMP end, respectively, after ligation of the PCR product into a T-vector. Confirmation of the correct sequence was assessed by direct sequencing. The cloned sequences were then digested with NcoI/MfeI and ligated to the pXK3.1 plasmid, a plasmid containing the wt fiber, generating the *pShuttles* **pXK3.1 YTRGE TAT and pXK3.1 YTRGE TATMMP**.

	Primer sequences	Primer Length
Fibra 1Fw	GCACCAAACACAAATCCC	18 nt
Rv 1.Tat	GCGCCGCCTCTTCGTCGCTGTCTCCGCTTCTTGCTGCCATA TTCTTGGGCAATGTATGA	59 nt (18 nt)
Rv 2a. MMP-cua	GCAATTGAAAAATAAACACGTTGAAACATAACACAAACG ATTCTTTACTCCTCTTCCTCCTCGCCCTCTTCCTCGCCGCCC TTGTACAGGCCCTTGGCGCCGCCTCTTCGTCGCTGTCT	119 nt (23 nt)
Rv 2b.cua	GCAATTGAAAAATAAACACGTTGAAACATAACACAAACG ATTCTTTATCTTCGTCGCTGTCTCCG	69 nt (22 nt)

Table 1. Primer sequences employed to generate TAT and TATMMP fibers. Nucleotides complementary to template sequence are underlined; the remaining nucleotides correspond to primer tail.

	TAT	MMP/End	Cycles
Step 1	95 °C, 5 min	95 °C, 5 min	
Step 2	95 °C, 1 min	95 °C, 1 min	14
Step 3	55,6 °C, decrease 0,5 °C/cycle, 30 s	60,2 °C, decrease 0,5 °C/cycle, 30 s	
Step 4	72 °C, 70 s	72 °C, 80 s	
Step 5	95 °C, 1 min	95 °C, 1 min	19
Step 6	48.6 °C, 30 s	53.2 °C, 30 s	
Step 7	72 °C, 70 s	72 °C, 80 s	
Step 8	72 °C, 5 min	72 °C, 5 min	

Table 2. TD-PCR conditions to generate TAT and TATMMP fibers.

1.1.2. Homologous recombination in E.coli BJ5183 strain and transfection to HEK293 cells.

To generate pAduPARTat8TK plasmid, 300 ng of pS-uPAR-TTK-pA were digested with 50 U of PmeI at 37°C for 30h and purified using the QIAquick® PCR purification kit (QIAGEN). The digested plasmid was co-transformed into *Escherichia coli* BJ5183, together with the *pBackbone* plasmid p3602 that contains the full length Ad5 genome. Positive clones corresponding to pAduPARTat8TK plasmid were identified by PacI digestion, and transformed into *E.coli* DH5α. Correct sequence was verified by direct sequencing.

To generate pAdTAT and pAdTATMMP plasmid, 1 µg of pXK3.1 YTRGE TAT or pXK3.1 YTRGE TATMMP were digested with 4U of XbaI and 4U of KpnI in two consecutive steps. The digested fragment was obtained from an agarose gel and purified using the QIAquick® Gel extraction kit (QIAGEN). In parallel, 4 µg of the *pBackbone* plasmid pVK50TL swa mut, that contains the full length Ad5 genome with the expression cassete CMVpGFPCMVpLuc cloned into the E1A region, were digested with 4U of SwaI enzyme at 37°C for 16h, and purified by chloroform extraction and DNA precipitation with sodium acetate 3M. The digested fragments TAT or TATMMP and the linearized plasmid pVK50TL swa mut were co-transformed into *Escherichia coli* BJ5183, and positive clones were identified by Fiber PCR (Primer sequences and PCR conditions listed in Table 6 and Table 5) and HpaI digestion, and transformed into *E.coli* DH5α. Correct sequence was verified by direct sequencing.

		AduPARTAT8TK	AdTAT/AdTATMMP
pShuttle	Plasmid	pShuttle	pXK3.1
	Digested with	PmeI	XbaI/KpnI
pBackbone	Plasmid	p3602	pVK50TL cau Swa mut
	Digested with	---	SwaI
DNA quantities insert:vector		- 45 ng : 100 ng - 80 ng: 100 ng	- 2,5 ng: 10 ng - 40 ng: 160 ng
Electroporation conditions		200 Ohms, 25 μF, 2500 V	
Antibiotic of selection		Kanamycin	Ampicillin
Screening by		Digestion with PacI	- PCR of fiber - Digestion with HpaI

Table 3. Conditions of homologous recombination

20 μg of pAduPARTat8TK, pAdTAT and pAdTATMMP were linearized by PacI digestion and 5μg of purified digestions were transfected into 450.000 (AduPARTat8TK) or 250.000 (AdTAT and AdTATMMP) HEK293 cells with SuperFect transfection reagent (QIAGEN). Cells and supernatant were harvested when cytophatic effect (CPE) was observed, then they were exposed to three cycles of freeze-thaw-vortex and centrifuged at 600 x g. The obtained supernatant corresponded to the first viral lysate (p1).

1.1.3. Adenovirus large scale amplification.

Large scale viral amplification was performed from viral lysate p1 as well as from purified virus. AduPARTat8TK vector was propagated on 911 cells and HEK293 cells, and the rest of the viruses in HEK293 cells.

Several steps of viral amplification were carried out until obtaining a viral lysate able to lysate a HEK293 cell plate of 150 mm diameter (p150) in 36-72h. To generate AduPARTat8TK virus, 30 p150 plates of HEK293 cells were infected with 0.5 mL of viral lysate p3 and CPE was complete at 40h. To generate AdTAT and AdTATMMP viral vectors, we required much more steps of viral amplification as these viruses expressed modified fibers that hampered virus generation. Moreover, cells were infected at lower densities with the help of polybrene (4μg/mL), and they initially

required 5 days to show CPE. After several steps of viral amplification, 30 p150 plates of HEK293 cells were infected with 0.5-2 mL of viral lysate p11 and CPE was complete at 48h. Cells were harvested, pelleted at 600 x g, resuspended in PBS^{++}exposed to three freeze-thaw-vortex cycles and centrifuged at 600 x g. The obtained supernatant corresponded to the crude extract. Fiber sequence integrity was verified by PCR and sequencing at different steps.

To amplify a viral vector from the purified virus, a p150 plate of HEK293 cells was infected with 1-4µl of purified virus. The obtained viral lysate was named as p1. 30 p150 plates of HEK293 cells were infected with 0.5-1 mL of p1 or p2, and CPE was observed in 36-72h. Crude extract was obtained as previously described.

REAGENTS:

- PBS^{++}: PBS 1x supplemented with 0.68 mM $CaCl_2 \cdot 2H_2O$ and 5 mM $MgCl_2 \cdot 6H_2O$.

1.2. Adenovirus purification.

Adenoviral purification was performed in accordance with the standard method described by Becker et al in 1994 (Becker et al. 1994), based on ultracentrifugation of a cesium chloride (CsCl, Calbiochem) density gradient, which allows viral particles separation from non-desired elements present on the crude extract (empty viral capsids, cellular debris…).

A CsCl gradient was carefully prepared in ultracentrifuge tubs (Beckman) as it is shown in Illustration 12. Tubs were centrifuged for 1.5 h at 35.000 rpm, 15°C in a SW41Ti (Beckman) rotor. Viruses were separated from the cellular debris in a blue-whitish band located between 1.25 and 1.35 g/ml CsCl solutions. Virus was collected with the help of a micropipette, mixed with CsCl 1.35 g/ml and centrifuged for at least 18h in the same conditions as before, which allows virus separation from empty viral capsids. Viral vector band was collected with the help of a micropipette, and desalted by filtration in a prepacked Sephadex™ G-25 column (PD-10 Desalting columns, GE Healthcare). The eluted virus was mixed with 10% glycerol for its correct conservation.

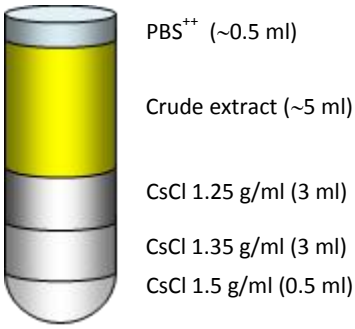

Illustration 12. Scheme of CsCl gradient density tub.

1.3. Titration of adenovirus.

1.3.1. Titration by O.D at 260nm (vp/ml).

Viral titration by optical density determines the number of viral particles without distinguish between infective and defective particles as the method is based on the absorbance by viral DNA at λ=260 nm.

Purified virus diluted in lysis buffer (10 mM Tris, 1 mM EDTA, 0.1% SDS) was incubated for 10 min at 56°C and centrifuged 30 s at 10.000 rpm. Supernatant $O.D._{260}$ was determined in a spectrophotometer (Nanodrop®) and viral titer was calculated as follows:

$$^{vp}/_{ml} = O.D._{\cdot 260} \times dilution \times virus\ extinction\ coefficient\ (1.1 \cdot 10^{12})$$

1.3.2. Titration by hexon staining (pfu/ml).

Viral titration by hexon staining determines the number of infective particles, and it is based on the number of hexon-positive cells of an infected monolayer after immunostaining against the viral protein hexon.

50.000 HEK-293 cells previously seeded in a 96-well plate, were infected with 100 µl of a viral serial dilution bank (10^4-10^{12}) in triplicate, and incubated for 20h at 37°C. Hexon immunodectection was performed at this time. Briefly, cells were fixed with cold MeOH 20 min at -20°C, washed three times 5 min with PBS^{++} 1% BSA, and incubated for 1h at 37°C with mouse anti-hexon hybridoma (dilution 1/3). Then, cells were

washed and incubated with the secondary antibody anti-mouse Alexa Fluor® 488 (Invitrogen) (dilution 1/400), 1h at R.T. After 3 washes with PBS^{++} 1% BSA, positive cells were counted under a fluorescence microscope (Observer/Z1; Zeiss). The titer of virus was calculated according the following formula:

$$pfu/_{ml} = \frac{n \times virus\ dilution}{0.1\ ml}$$

1.4. Adenovirus characterization.

Purified viruses were tested for Replicative Competent Adenovirus (RCAs) absence by E1A PCR. AdTAT and AdTATMMP fiber integrity was also tested by PCR and sequencing. Moreover, fiber integrity was also analyzed at protein level by electrophoresis of the capsid proteins of adenovirus.

1.4.1. Viral DNA extraction, PCR and sequencing.

Viral DNA was obtained from cells previously infected with 1 µl of purified virus or 1 ml of viral lysate. To analyze E1A expression, cells were different from HEK293 or 911. Infected cells were harvested and centrifuged 5 min at 1200 rpm. Pelleted cells were resuspended in 700µl of HIRT's 1X solution and incubated for 1h at 56°C. Then, 200 µl of NaCl 5M were added in agitation, and incubated 16h at 4°C. Cellular debris were separated by centrifugation 30 min, 13.000 rpm at 4°C. Supernatant was collected and DNA was extracted with phenol-chloroform and precipitated with ammonium acetate 3M. DNA was resuspended in 25 µl H_2O.

PCR was done to amplify the E1A and the fiber genes from the adenoviral genome. PCR reagents, reactive conditions and primer sequences are listed in Table 4, Table 5 and Table 6.

Reagents	Final concentration
DNA	250 ng
dNTP's 1.25 mM	200 μM
Primer Fw 10 μM	1 μM
Primer Rv 10 μM	1 μM
Buffer 10x	1x
Taq DNA pol 5U/μl	0.025 U
H_2O	Up to 20 μl

Table 4. PCR reagents.

	Fiber	E1A
1. Initial Denaturalization	94 °C, 5 min	94 °C, 3 min
2. Denaturalization	94 °C, 30 s	94 °C, 15 s
3. Annealing	55 °C, 30 s	58 °C, 15 s
4. Elongation	72 °C, 30 s	72 °C, 30 s
5. Final elongation	72 °C, 5 min	72 °C, 5 min
Cycles (Step 2-4)	35	35

Table 5. Reaction conditions for Fiber and E1A viral gene PCR amplification.

		Primer sequences	Product size	
Fiber	Fibra 1Fw	GCACCAAACACAAATCCC	WT fiber YTRGE fiber TAT fiber MMP fiber	799 nt 823 nt 856 nt 913 nt
	Fibra 4Rv	GTATAAGCTATGTGGTGGTGG		
E1A	E1A Fw	ATCGAAGAGGTACTGGCTGA	416 nt	
	E1A Rv	CCTCCGGTGATAATGACAAG		

Table 6. Primer sequences of Fiber and E1A PCR.

Fiber sequencing was carried out using as a template the fiber PCR product purified with the commercial QIAquick® PCR purification Kit (QUIAGEN). Sequencing mixture was prepared mixing 5 μl of purified PCR with 1.5 μl of primer 3.2 μM (Fibra 1Fw or Fibra 4Rv) and 3 μl of Big Dye 3.1 (Applied Biosystems; contains dNTPs, polymerase and marked ddNTPs). Reaction conditions were:

- Initial Denaturalization: 94°C, 5min.
- 35 cycles: 94°C 30s ; 50°C 15s ; 60°C 4min.
- Final elongation: 60°C, 7min.

Sequence reactions were purified in a Sephadex G-50 column and dried out in a SpeedVac® concentrator (Thermo Electron Corporation). Sequences were analyzed in an automatic DNA sequencer by *Unitat de Seqüenciació i Anàlisi* from the *Servei de Genòmica* of the Universitat Pompeu Fabra.

REAGENTS:

- HIRT's 2X solution: 10 mM Tris pH 8.0, 20 mM EDTA, 1.2% SDS. 200 μg/ml proteinase-K was added to HIRT's 1x.

1.4.2. Electrophoresis of the capsid proteins of Ad.

10^{10} purified viral particles were diluted in 6x Laemmli buffer, incubated for 5 min at 95°C and separated by 10% SDS-polyacrylamide gel. Proteins were detected by silver staining, which allows protein detection in the ng range. Silver staining was carried out as described in (Chevallet et al. 2006). Briefly, proteins were fixed with Fixation solution for 3h in agitation. After three washes with EtOH 50% of 20 min each, the polyacrylamide gel was soaked in Pretreatment solution for 1 min at R.T to increase sensitivity and contrast of the staining. Gel was washed three times with deionized water for 20s. Staining was performed by gel incubation in pre-cooled Staining solution for 16h at 4°C. Gel was washed three times with deionized water for 20s and incubated in Development solution at R.T until bands appeared (5-10 min). Development reaction was stopped by incubation with deionized water for 2 min and Fixation solution for 10 min. Gel was scanned using a flat-bed scanner set in the transillumination mode (Epson Expression 1680 Pro).

REAGENTS:

- Laemmli 6X buffer: 350 mM Tris-HCl pH 6.8, 30% glycerol, 10% (w/v) SDS, 0.6 M DTT, 0.012% Bromophenol Blue
- Fixation solution: 40% EtOH, 10% acetic acid.

- Pretreatment solution: 0.02% $Na_2S_2O_3$, 30% EtOH, 6.8% sodium acetate.
- Staining solution: 0.02% AgNO3, 0.015% formaldehyde.
- Development solution: 6% Na_2CO_3, 0.0004% $Na_2S_2O_3$, 0.02% formaldehyde.

2. METHODS RELATED TO RNA MANIPULATION.

2.1. RT-PCR.

RT-PCR technique was used to analyze gene expression of Keratin7, Keratin 19, Elastase-2, Trypsin, c-Myc, and uPAR genes on Emyc primary cultures and mouse pancreatic tissue. Gdx and 15S genes were used as controls.

Total RNA was prepared from adherent cell cultures and mouse pancreatic tissue using RNeasy® Mini kit (QIAGEN). To avoid genomic contamination of pancreatic tissue samples, they were treated with DNAse (TURBO DNA-*free*™, Ambion®), as described by manufacturer's protocol.

1 µg of total RNA from each sample was reverse transcribed with a RETROscript® kit (Ambion®). 2 µl of cDNA was PCR amplified using 200 µM dNTPs, 1X PCR buffer (Roche Diagnostics), 0.025 U Taq DNA pol (Roche Diagnostics) and 2 µM of the corresponding primers listed in Table 7. PCR conditions used to characterize Emyc primary cultures were the same for the analyzed genes and consisted on an initial denaturation step of 5min at 94°C followed by 30 cycles of 94°C 30 s, 57°C 30 s, 72°C 30 s, and a final elongation step of 5min at 72°C. PCR conditions used to analyze uPAR gene expression in pancreas of Ela-myc and C57Bl6/J mice were slightly different and consisted on 40 cycles of 94°C 30 s, 60°C 30 s, 72°C 30 s; initial denaturation step and final elongation step conditions were mantained. PCR products were run in a 2% agarose gel stained with ethidiumbromide.

	Gene	Primer sequences		Product size
Keratin 7 (K7)	Krt7	Fw	CACGAACAAGGTGGAGTTGGA	100 bp
		Rv	TGTCTGAGATCTGCGACTGCA	
Keratin 19 (K19)	Krt19	Fw	CCTCCCGAGATTACAACCACT	110 bp
		Rv	GGCGAGCATTGTCAATCTGT	
Elastase-2 (Ela)	Cela2a	Fw	ATTGCCTCAGCAACTATCAGA	200 bp
		Rv	TGTCTGGATGTTCTTGCTCA	
Trypsin (Tryp)	Try	Fw	GATGACAAGATCGTTGGAGGA	308 bp
		Rv	ACTCTGGCATTGAGGGTCAC	
c-Myc	Myc	Fw	AGTGCATTGACCCCTCAG	431 bp
		Rv	CCTGCCACTGTCCAACTTG	
uPAR	Plaur	Fw	CAGGACCTCTGCAGGACCAC	529 bp
		Rv	CCTTGCAGCTGTAACACTGG	
Gdx	Gdx	Fw	GGCAGCTGATCTCCAAAGTCCTGG	260 bp
		Rv	AACGTTCGATGTCATCCAGTGTTA	

Table 7. Primers used for RT-PCR analyses and PCR product sizes. Underlined mismatch with mouse cDNA template. 15S gene primers were supplied by the RETROscript® kit (Ambion®).

3. METHODS RELATED TO PROTEIN MANIPULATION.

3.1. Western Blot.

Western Blot technique was used to analyze the expression of Connexin 43 (Cx43) and matrix metalloproteinase 2 and 9 (MMP2/9) in cell extracts and cell supernatants, respectively.

Cell extracts were obtained as follows: confluent cultures were collected at 4°C and resuspended in Cx43 lysis buffer containing 1% Complete Mini Protease Inhibitor (Roche Diagnostics) and phosphatase inhibitors (20 mM $Na_4P_2O_7$ and 100 mM NaF) and sonicated for 5 s at 50 W three times. Cell lysates were centrifuged for 15 min at 14000 rpm and protein concentration determined from the cleared lysate (BCA assay; Pierce-Thermo Fisher Scientific).

Cell supernatants were obtained from confluent cultures grown in plates of 60 mm of diameter with 1 ml of medium without FBS. Conditioned media samples were concentrated using Microcon® centrifugal filters (ultracel YM-30 membrane, Millipore) up to a final volume of 30 µl.

60 µg of total protein from cell extracts, 15 µl of concentrated supernatant or 100 ng of purified MMP2 plus 100 ng of purified MMP9 (Calbiochem) were mixed with loading Laemmli 6x buffer and incubated at 98°C for 10 min.

Proteins were separated in a 12% or 8% SDS-PAGE gel (Cx43 or MMP2/9, respectively) and transferred onto nitrocellulose membranes (Hybond™ C Extra, Amersham Biosciences) by standard methods. The membranes were blocked in 10% non-fat dried milk dissolved in TBS-T for 1 h at room temperature and then incubated overnight at 4°C with the primary antibody anti-Connexin43 or anti-MMP2 diluted in 5% powdered milk in TBS-T (specific antibodies, dilutions and incubation conditions are shown in Table 8). Protein loading from cell extracts was monitored using a mouse antibody against α-tubulin. Incubation with anti-mouse IgG/HRP (horseradish peroxidase) antibodies (Dakocytomation) was performed at room temperature for 1 h. Membranes were rinsed in TBS-T and antibody labeling was detected by chemiluminescence with an ECL detection system (Promega) following the manufacturer's instructions. Chemiluminiscence was determined with a LAS-3000 image analyzer (Fuji PhotoFilm Co.). MMP9 expression was analyzed after MMP2 detection with the ECL system. The membrane was washed 3 times in TBS-T for 30 min and incubated with the primary antibody anti-MMP9 for 2h at R.T. The following steps were the same as before.

	Commercial house	Catalog number	Specie	Dilution	Incubation conditions
Cx43	Chemicon	MAB3068	Mouse	1:1000	O/N, 4 °C
MMP2	Santa Cruz Biothecnology	sc-53630	Mouse	1:100	O/N, 4 °C
MMP9	Santa Cruz Biothecnology	sc-21733	Mouse	1:100	2h, R.T
α-tubulin	Sigma	T9026	Mouse	1:2000	1h, R.T
Mouse IgG	Dakocytomation	P0260	Rabbit	1:2000	1h, R.T

Table 8. Antibodies and incubation conditions used in WB.

REAGENTS:

- Cx43 lysis buffer: 10 mM Na_2HPO_4 (pH 7.2), 150 mM NaCl, 2 mM EDTA, 1% Triton X-100, 1% sodium deoxicholate, 1% SDS.
- Laemmli 6X buffer: 350 mM Tris-HCl pH 6.8, 30% glycerol, 10% (w/v) SDS, 0.6 M DTT, 0.012% Bromophenol Blue.
- Electrophoresis running buffer: 25 mM Tris Base, 200 mM glycine, 0.1% (w/v) SDS.
- Transference buffer: 25 mM Tris-HCl pH 8.3, 200 mM glycine, 20% (v/v) methanol.
- TBS-T: 10 mM Tris HCl pH 7.5, 100 mM NaCl, 0.1% Tween-20.

3.2. Zymography.

10^6 cells were seeded in plates of 60 mm of diameter and allowed to adhere. Next day media was replaced by 1 ml of serum-free medium. Conditioned medium was harvested 24h later and concentrated using Microcon® centrifugal filters (ultracel YM-30 membrane, Millipore) up to 30 µl. 15 µl of concentrated supernatant or 2 ng of purified MMP-2 plus 2 ng of purified MMP9 were mixed with 15 µl of zymography loading buffer 2x and incubated for 10 min at R.T. Gelatin zymography was performed as described in (Kleiner and Stetler-Stevenson 1994; Leber and Balkwill 1997). Briefly, total proteins were separated on 10% SDS-PAGE gels containing 0.1% gelatin. Next, gels were treated with 2.5% Triton X-100 at R.T for 1h to remove SDS and then incubated overnight at 37°C in Developing buffer. Gels were stained with 5% Coomassie Blue R-350 (Phastgel™ Blue R-350, GE Healthcare Life Science) in 30% methanol, 10% glacial acetic acid at room temperature for 30-90 min. The activities of enzymes were identified as clear gelatin-degrading bands against the blue background. Gels were scanned using a flat-bed scanner set in the transillumination mode (Epson Expression 1680 Pro).

REAGENTS:

- Zymography loading buffer (2x): 125mM Tris–HCl pH 6.8, 20% (v/v) glycerol, 4% (w/v) SDS, 0.005% (w/v) bromophenol blue.
- Developing buffer: 10x Zymogram Development Buffer (Bio-Rad) (50 mM Tris-HCl, pH 7.5, 200 mM NaCl, 5 mM $CaCl_2$) diluted in water.

3.3. Luciferase Assay.

Firefly luciferase transgene expression was measured in cell lysates or in liver and pancreatic tissues. Cell lysates were prepared with 50 µl of Reporter Lyses buffer (RLB, Promega) in accordance with the manufacturer's instructions (Luciferase Assay System; Promega). Liver or pancreatic tissues were mechanically homogenized in a cold potter with liquid nitrogen to obtain a fine powder. Powder was mixed with lyses buffer (Cell culture Lysis Reagent, Promega) (400 µl of lyses buffer per 100 mg of tissue) and incubated for 15 min at 25 C. Samples were centrifuged for 10 min, 16000 x g at 4 C and supernatants were collected. Luciferase activity from 10 µl of *in vitro* or *in vivo* samples was measured in a Centrol LB 960 microplate luminometer (Berthold Technologies) or a tube luminometer Autolumat Plus LB953 (Berthold Technologies) respectively, and normalized to total protein levels. Protein concentration was determined with a BCA protein assay (Pierce Biotechnology).

3.4. MMP-Cleavable-Peptide (MCP).

3.4.1. MCP and MCP* preparation.

The MMP-Cleavable-Peptide (MCP) and the MCP peptide linked to fluorescein (MCP*) were produced by the group of Dr. David Andreu (Proteomics and Protein Chemistry Unit, Department of Experimental Health Sciences). Lyophilized peptides were dissolved in Tris-HCl 100 mM pH 7.4 and prepared at 0.5 mM and 1 mM respectively.

	Concentration	Quantity	Molecular Weight (MW)	Volume of Tris-HCl
MCP	0.5 mM	1.075 mg	3528,78 Da	600 µl
MCP*	1 mM	1.5 mg	4010 Da	374.1 µl

Table 9. MCP and MCP* properties.

3.4.2. MCP and MCP* cleavage by MMP2.

30 µl of MCP or MCP* were incubated with 2.5 µg of recombinant MMP2 (Calbiochem) in 45 µl of 50 mM Tris-HCl pH 7.4 at R.T for 4h or 9h respectively. MCP samples were obtained at 30 min, 60 min and 240 min and reaction was stop by the addition of an acidic solution. MCP cleavage

was analyzed by HPLC (High-Performance Liquid Chromatography) by the group of Dr. David Andreu (Proteomics and Protein Chemistry Unit, Department of Experimental Health Sciences).

4. CELL CULTURE.

4.1. Cell lines. Maintenance and culture conditions.

1) Cell lines used to generate and amplify adenoviral vectors:

HEK293: cell line derived from human embryonic kidney tissue, established by Graham et al (Graham et al. 1977).

911: cell line derived from human embryonic retinoblasts. It was generated by the group of Dr. Van Der Erb (Fallaux et al. 1996).

The two cell lines express the E1A gene of the Adenovirus type 5. They are commonly used for the generation, amplification and titration of recombinant adenoviruses. 911 cell line is used because reduces the probability of E1A recombination with the transgene cloned into the E1A region of the produced adenovirus. Both cell lines were kindly provided by Dr. Ramon Alemany's laboratory (IDIBELL-*Institut Català d'Oncologia*, Barcelona).

2) Cell lines derived from human tumors:

PANC-1: cell line derived from a human pancreatic ductal carcinoma. ATCC nº: CRL-1469.

RWP-1: cell line derived from a hepatic metastasis originated from a human pancreatic ductal adenocarcinoma. It was generated by subcutaneous implantation of an hepatic metastasis fragment in nude mice (Dexter et al. 1982). This cell line was kindly provided by Dr. FX. Real (IMIM, Barcelona).

BxPC-3: cell line derived from a human pancreatic adenocarcinoma. ATCC nº: CRL-1687.

NP18: cell line derived from a hepatic metastasis originated from a human pancreatic ductal adenocarcinoma. It was generated by orthotopic implantation of an hepatic metastasis fragment in the pancreas of nude mice. This cell line was generated and kindly ceded by *Servei Digestiu* of the *Hospital de la Santa Creu i Sant Pau de Barcelona* (Reyes et al. 1996).

HT-1080: cell line derived from a fibrosarcoma. ATCC nº: CCL-121™. This cell line was kindly provided by Dr. Ramon Alemany (IDIBELL-*Institut Català d'Oncologia*, Barcelona).

PANC-1-Luc and BxPC-3-Luc: luciferase-expressing cells previously generated in our laboratory. Parental cells (PANC-1 and BxPC-3) were transduced with luciferase recombinant retrovirus, selected in 0.2 mg/ml hygromycin, cloned and tested for luciferase expression.

3) Cell lines derived from mouse tumors:

266-6: pancreatic acinar cell line derived from a pancreatic tumor grown in a transgenic mice that express the SV40 T antigen under the control of Elastase I promoter (Ornitz et al. 1985). This cell line was obtained from the cell bank at the IMIM-*Hospital del Mar*.

Emyc-1, Emyc-3 and Emyc-10: these cell lines were established in our laboratory from pancreatic tumors of Ela-myc transgenic mice. Three Emyc cell lines were generated from eleven primary cultures of pancreatic tumors from six independent Ela-myc mice of 2.5-4 months of age. In this work tumor characteristics, medium conditions, type of plates and passage dilutions were assessed. Fragments from different parts of the pancreatic tumor (white or red) were mechanically minced and incubated in primary culture medium in p60 plates at 37°C, in a humid atmosphere of 5% CO_2. Media was first changed at 4-8 days after establishing the primary culture and first passaged at 11-20 days. Cells were trypsinized for 30-60 min, resuspended in primary culture medium and filtered in a cell strainer (ref 352350, BD Falcon™); cells were plated in special dishes (ref 353803, BD Falcon™). Medium was changed once per week, and cells were passed when reached confluence. Cultures generated from a white tumor produced a viable primary culture; however, it was not possible to establish any primary culture from red fragments. Cultures required about 10 passages to get rid of

fibroblasts. Around passage 20, a primary culture was considered an established cell line (4-5 months after initial plating).

4) Non tumoral cell lines:

NIH-3T3: cell line derived from mouse embryo fibroblasts. ATCC nº: CRL-1658.

All cell lines were maintained at 37°C in a humid atmosphere of 5% CO_2.

- DMEM: all previously mentioned cells, except NP18, were growth in Dulbecco's Modified Eagle Medium (DMEM), that contains L-glucose (4500 mg/l), L-glutamine and sodium piruvate; supplemented with 10% FBS, 100 U/ml penicillin, 100 μg/ml streptomycin and 2 mM L-glutamine (Gibco-Invitrogen).

- RPMI: NP18 cells were grown in RPMI 1640 medium (Roswell Park Memorial Institute), that contains L-glucose (4500 mg/l), glutamax and sodium piruvate; supplemented with 10% FBS, 100U/ml penicillin, and 100 μg/ml streptomycin (Gibco-Invitrogen).

- Primary culture medium: DMEM supplemented with 20% FBS, 1x Non Essential Aminoacids (NEA), 20 ng/mL EGF, 200 U/ml penicillin, 200 μg/ml streptomycin and 0.25 μg/mL fungizone.

4.2. Drug treatments.

4.2.1. Ganciclovir (*Cymevene®*, Roche)

- *In vitro* experiments (10 mg/ml): stock solution (1000x) was prepared diluting 10 mg of the commercial *Cymevene®* (Roche) in 1 ml of injectable water (B.BRAUN), and filtered with 0.22 μm filters.

- *In vivo* experiments (10 mg/ml): GCV was administered to mice at 100 mg/kg. Stock solution was prepared at 10 mg/ml in saline (B.BRAUN) and filtered with 0.22 μm filters.

4.2.2. Gemcitabine (*GEMZAR®*, Lilly Co.)

- *In vitro* experiments (10 mM): 10 mM stock solution was prepared diluting 6.18 mg of *GEMZAR®* in 1 mL of injectable water (B.BRAUN), and filtered with 0.22 μm filters. The commercial drug *GEMZAR®* contains 43.8 g of active principle in 100 g of *GEMZAR®*. The stock solution was stored at RT for 35 days.

- *In vivo* experiments (16 mg/ml): GE was administered to mice at 160 mg/kg. Stock solution was prepared at 16 mg/ml in saline (B.BRAUN) and filtered with 0.22 μm filters. The solution was stored at RT for 35 days.

4.2.3. Dose-response analyses.

Cells were treated with gemcitabine alone, AduPARTat8TK plus GCV alone or gemcitabine plus AduPARTat8TK and GCV. Three days later, cell viability was measured and quantified by a colorimetric assay system based on the tretrazolium salt 3-(4,5-dimethylthiazol-2-yl)-2,5-diphenyl tetrazolium bromide (MTT; Roche Molecular Biochemicals), in accordance with the manufacturer's instructions. Results were expressed as the percent absorbance determined in treated wells relative to that in untreated wells. ID_{50} values were estimated from dose–response curves by standard non-linear regression, using an adapted Hill Equation (GraFit v3.0, Erithacus Software).

4.2.4. Drug interaction analysis.

The induction of synergism, addition or antagonism between gemcitabine (GE) and TK/GCV treatments was analyzed by Combination Index (CI) analysis as previously described (Chou and Talalay 1984). Combination Index analysis is one of the most popular methods for studying *in vitro* drug interactions in combination cancer chemotherapy. Dose–response curves were constructed for the treatments with either GE, TK/GCV or a combination of both, from which Hill coefficient and ID_{50} values were calculated by non-linear regression based on a modified Hill Equation using the GraFit v3.0 software. Estimated equation was used to calculate the doses of each treatment, administered independently or in combination, necessary to induce an inhibition (IF: Inhibitory Fraction) of 10%, 20%, 30%, 40%, 50%, 60%, 70%, 80% and 90%.

Combination Index value was calculated as indicated below. CI values <1 indicates synergism, CI values =1 indicates addition, and CI values >1 indicates antagonism between treatments.

$$CI_{FI} = \frac{D_{AdTK,GE}}{D_{AdTK}} + \frac{D_{GE,AdTK}}{D_{GE}}$$

CI_{FI} = Combination index, for a given IF.

$D_{AdTK,GE}$= Dose of AduPARTat8TK/GCV needed to produce given IF when applied in combination with GE.

D_{AdTK} = Dose of AduPARTat8TK/GCV needed to produce given IF when applied alone.

$D_{GE,AdTK}$ = Dose of GE needed to produce given IF when applied in combination with AduPARTat8TK/GCV.

D_{GE} = Dose of GE needed to produce given IF when applied alone.

5. METHODS RELATED TO ANIMAL MANIPULATION.

Animal procedures met the guidelines of European Community Directive 86/609/EEC and were approved by the *Comité de Experimentación Animal (CEEA)* of the PRBB (*Parc de Recerca Biomèdica de Barcelona*).

5.1. Animals

Animals were housed in plastic cages in controlled environmental conditions of humidity (60%), temperature (22°C ± 2°C) and light with food and water ad libitum. Transgenic Ela-myc mice and immunodeficient nude mice (Athymic Nude-*Foxn1*^{nu}, Harlan) were used in this thesis. Immunodeficient mice were males of 6 weeks of age and 20-30 g of weight. TgEla-myc mice were males and females of 11-17 weeks of age and 16-30 g of weight. To maintain the Ela-myc colony, Ela-myc males were mated to C57Bl/6J females and progeny was genotyped by PCR analysis.

5.1.1. Ela-myc mice genotyping.

Mouse DNA was extracted from a tail fragment by heating in 300 µl of basic solution (50 mM NaOH) for 30-60 min at 98°C. 30µl of neutralization solution (1M Tris-HCl pH 8.0) was added and tail debris were centrifuged at 13000 rpm for 5 min. Genotyping of the progeny was performed by multiplex PCR analysis using 1 µM c-Myc primers and 0.5 µM Gdx primers (primer sequences shown in Table 10). PCR conditions are indicated below. Products of PCR were run in a 2% agarose gel for 30-60 min at 95V.

- Initial Denaturalization: 94°C, 5min.
- 35 cycles: 94°C, 20 s ; 63°C 20 s ; 72°C 20 s.
- Final elongation: 72°C, 7 min.

		Primer sequence	Product size
c-Myc	Fw	CACCGCCTACATCCTGTCCATTCAAGC	240 nt
	Rv	TTAGGACAAGGCTGGTGGGCACTG	
Gdx	Fw	GGCAGCTGATCTCCAAAGTCCTGG	260 nt
	Rv	AACGTTCGATGTCATCCAGTGTTA	

Table 10. Primers for Ela-myc mice genotyping.

5.2. Orthotopic tumor model.

Orthotopic human pancreatic cancer xenografts were generated as previously described (Kim et al. 2009). Nude mice were anesthetized with a mixture of isofluorane and oxygen, and placed on their right side. Buprenorphine (0.05-0.1 mg/Kg) was administered intraperitoneally 20 min before surgery. The left side was sterilized with iodine solution and a minilaparatomy of 1 cm was performed. The spleen/pancreas was externalized and $5x10^5$ BxPC-3-Luc cells (50 µl) were injected using a 29G needle into the tail of the pancreas and passed into the body/head region. Cell injection formed a fluid-filled region within the pancreatic parenchyma. The needle was removed and Histoacryl® (B.Braun) was added to avoid leakage. Pancreas/spleen was internalized, the muscle layer was closed with interrupted 4-0 silk suture and the overlying skin with Autoclips® (Stoelting Europe). Iodine solution was applied to the

region of surgery, and animals were maintained under a heating source. Autoclips® were removed 4-7 days after surgery.

5.3. Delivery routes.

Buprenorphine, meloxicam, D-luciferin, ganciclovir and gemcitabine were administered intraperitoneally (i.p) with a 26G needle.

Saline solution or glucosaline was administered subcutaneously (s.c) or intraperitoneally with a 26G needle.

Viruses were systemically or locally administered. For systemic administration, $5{\cdot}10^{10}$ vp of virus diluted in saline (200µl) were injected intravenously into the lateral vein of the tail with a 29G needle. For locally administration, 10^{10} vp, $5{\cdot}10^{10}$ vp or 10^{11} vp of virus diluted in saline (50 µl) were intraductally administered with a 30G needle.

5.3.1. Intraductal injection into the common bile duct.

Ela-myc mice received i.p 20 min before surgery an analgesia mixture composed of buprenorphine (0.05-0.1 mg/Kg) and meloxicam (1-2 mg/Kg). Mice were anesthetized with a mixture of isofluorane and oxygen. The abdominal region was shaved and sterilized with iodine solution. A laparatomy of 2 cm was done in the abdominal region below the xiphoid. Skin and muscular layers were maintained separated by the use of a colibri retractor of 9 mm of teeth width (Fine Science Tools, FST). With a pair of ring forceps duodenum was exposed and the ampulla of Vater (also named as hepatopancreatic ampulla) was localized. Common bile duct was clamped with a micro serrefine (FST) near to the liver to avoid infection of the liver. Then a 30G needle was inserted into the ampulla of Vater, passed through the common bile duct a pair of mm and clamped. 50 µl of virus were slowly injected (approximately 10 µl every 10 s), and 1 min was left before removing the duodenal clamp to avoid virus regression into the duodenum. Histoacryl® (B.Braun) was added with the help of a 26G needle to close the wound on the papilla. One minute later, the clamp of the bile duct was removed, the organs were internalized

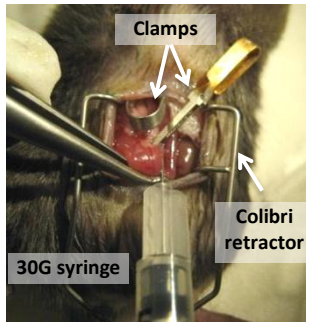

Illustration 13. Intraductal duct injection.

and the muscle layer was closed with interrupted 4-0 silk suture and the overlying skin with Autoclips® (Stoelting Europe). Iodine solution was applied to the region of surgery, and animals were maintained under a heating source.

Meloxicam was readministered the day after surgery to avoid pain. Autoclips® were removed 4-7 days after surgery.

5.4. Irreversible Electroporation (IRE)

Animals received buprenorphine (0.05-0.1 mg/Kg) 20 min before surgery. Nude mice were anesthetized with a mixture of isofluorane and oxygen. A minilaparotomy incision in the left dorsal side of the mouse was performed to expose the BxPC-3-Luc tumor within the body/tail of the pancreas. Tumor nodules were identified visually or by palpation and were measured with an electronic caliper. A partially conductive gel (Aquasonic 100 Sterile, Parker Laboratories) was applied and the nodule was gently squeezed between the tweezertrodes. Two electrode setups were employed depending on the size of the tumor nodule. Then, an IRE pulse train was applied (see below). Pancreas/spleen were internalized and the muscle layer was closed with interrupted 4-0 silk suture, and the overlying skin with Autoclips® (Stoelting Europe). Iodine solution was applied to the region of surgery, and animals were maintained under a heating source.

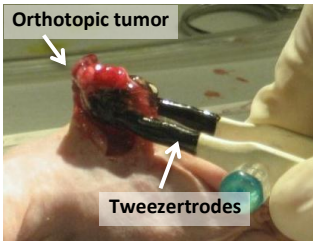

Illustration 14. IRE procedure.

The IRE pulse was delivered by a commercial electroporator (ECM830, BTX Instrument Division). The pulse consists on deliver sequences of ten pulses of 2500 V/cm (i.e. distance between plates × 250 V) with duration of 100 µs and repetition frequency of 1 Hz. The whole electroporation treatment consisted of ten of those ten pulses sequences (i.e. 100 pulses in total). Between those sequences, a manual pause of 10 seconds was introduced for allowing Joule heat to dissipate.

IRE pulse train = 10 x Sequences. *10s between sequences.*

Sequence = 10 pulses x 2500V/cm. *100µs each pulse and 1s between pulses (1Hz).*

5.5. Bioluminescence.

In vivo luciferase expression was visualized and quantified in living animals using an *in vivo* bioluminescent system (IVIS50; Xenogen). Briefly, the substrate firefly D-Luciferin (Xenogen) was administered i.p (32 mg/kg) and 10 min later animals were anesthetized with a mixture of isofluorane and oxygen preparation. Mice were introduced into the IVIS50 coupled to an inhaled anesthesia system, and images were captured. All images from the same experiment were obtained under the same measurement conditions. To study *ex vivo* luciferase expression, organs were rapidly removed from animals recently measured in the IVIS system, placed in a dish and introduced inside the black cage to capture the images.

Luciferase activity was quantified from non-saturated captured images using the software Living Image 2.20.1 Igor Pro4.06A. Images were represented as photons per second per square centimeter and per steradian. ROI quantification was expressed as total flux (photons/s).

5.6. Mouse sample analysis.

5.6.1. Organs and tumors dissection.

Animals were euthanized by cervical dislocation or by CO_2 inhalation, organs and tumors were collected and in some cases photographs were taken. Depending on their posterior analysis, tissue was frozen at -80ºC, fixed on 4% Phosphate-buffered formaldehyde (PFA) or included/frozen in OCT (Tissue Tek, Akura Finetek).

5.6.2. Measurement of Ela-myc pancreas/tumor volume.

Pancreas of Ela-myc mice was measured with an electronic caliper and volume was calculated according to the following formula:

$$Volume = \frac{a \times b \times c}{2}$$

a = length
b = width
c = height
} of pancreas + tumor

5.6.3. Biochemical analysis in serum samples.

Blood samples were collected by cardiac puncture or from the orbital sinus. In both cases the animal was anesthetized with a mixture of isofluorane and oxygen. Cardiac puncture was a terminal procedure, while retro-orbital puncture was performed in time-course experiments. Cardiac puncture was done using a 26 gauge needle. Retro-orbital puncture was done using a micro haematocrit blood tube (BRAND); 200 µl of glucosaline (B.BRAUN) were injected s.c to hydrate the animal.

To obtain the serum, blood samples were allowed to clot for 30 min at R.T and then were centrifuged at 3600 rpm 15 min. Serum was collected and stored at -20°C until its analysis. Serum levels of ALT, AST, lipase, amylase and glucose were analyzed by *Servei de Bioquímica Clínica Veterinària* of the *Facultat de Veterinària* of the *Universitat Autònoma de Barcelona.*

6. HISTOLOGICAL TECHNIQUES.

6.1. Sample processing.

Preparation of paraffin embedded samples, as well as their sectioning and sectioning of frozen samples were done by the Histology Unit of the CRG (*Centre de Regulació Genòmica*). Paraffin-embedded sections were 5 µm thick and frozen sections were 10 µm thick.

Hematoxylin/eosin staining of paraffin-embedded sections was used to evaluate tissue structure and was performed by the Histology Unit of the CRG (*Centre de Regulació Genòmica*).

6.2. Immunohistochemistry (IHC).

Five-micrometer paraffin-embedded sections were deparaffinized, rehydrate, permeabilized in PBS-T (PBS supplemented with 0.3% Triton X-100) and treated 25 min with boiling 10 mM citrate buffer (pH 6.0) for antigen retrieval. After washing twice with PBS-T, tissue sections were incubated with blocking solution for 1 h at R.T. Sections were then incubated overnight at 4°C with the primary antibody in diluting solution. Subsequently, sections were washed twice in PBS-T and incubated in

Peroxidase blocking solution for 5 min. Sections were processed by the avidin–biotin-peroxidase method (LSAB+2 system-HRP, Dako). Briefly, after washing, sections were incubated for 30 min with biotinylated secondary antibody against mouse and rabbit IgGs, followed by incubation for 30 min with a Streptavidin–HRP solution. Following washing, peroxidase activity was visualized by incubation of tissue sections with DAB+ (Dako, diaminobenzidine in hydrogen peroxide). Tissue sections were counterstained with Harris's hematoxylin, dehydrated and mounted with EUKITT® (Sigma-Aldrich). Images were captured with a microscope (Leica DM6000 B) and digital camera (Leica DFC300 FX; Leica Microsystems) and processed with Leica Application Suite software.

To analyze uPAR expression incubation with blocking solution was for 48h and incubation with primary antibody account for 72h.

	Commercial house	Catalog number	Specie	Antigen Retrieval	Dilution
Luciferase	Sigma	L0159	Rabbit	Yes	1/500
GFP	Invitrogen	A6455	Rabbit	Optional	1/500
uPAR	R&D	AF534	Goat	Yes	15 µg/ml
Anti-human Ki67	Dako	M7240	Mouse	Yes	1/200
Active caspase-3	BD Pharmingen	559565	Rabbit	Yes	1/500

Table 11. Primary antibodies used for immunohistochemistry.

REAGENTS:

- Citrate Buffer (for 1L): 2.1 g citric acid, 1 g NaOH in dH_2O, pH 6.0.
- Diluting solution: 1% BSA (w/v), 0.2% Tween-20 in PBS.
- Blocking solution: 10% FBS in Diluting solution.
- Peroxidase Blocking solution: 3% hydrogen peroxide in methanol.

6.3. Immunofluorescence (IF).

Immunofluorescence was performed to detect CD31 expression. Briefly, 10 µm frozen tissue sections were air-dried during 30 min and fixed in

cold acetone for 5 min, acetone/chloroform 1:1 treatment was applied for 5 min and then acetone during 5 min. After washing in PBS, sections were blocked for 1h in PBS-10% FBS and incubated with anti-mouse CD31 antibody clone MEC 13.3 (dilution 1/50, BD Pharmingen) for 16h at 4°C. The following day, samples were rinsed 3 times with PBS and incubated with the secondary antibody Alexa Fluor 488 goat anti-rat antibody (dilution 1/500, Molecular Probes). Nucleus were counterstained with 5 µg/ml bis-benzimide (Hoechst 33342, dilution 1/1000; Sigma) and slides were mounted with VECTASHIELD® Mounting Media (Vector Laboratories). Sections were visualized under a fluorescent microscope (Observer/Z1; Zeiss) and images were captured with a digital camera (AxioCamMRm; Zeiss).

7. STATISTICAL ANALYSIS.

The statistical analysis was performed using the SPSS 12.0 software. Results are expressed as the mean ±SEM (Standard Error of the Mean). A Mann-Whitney nonparametric test was used for the statistical analysis (2-tailed) of *in vitro* and *in vivo* studies. Differences were considered statistically significant (*) when p value≤0.05, and highly statistically significant (**) when p value≤0.01.

Differences between more than two independent samples/means were analyzed using the nonparametric Kruskal-Wallis test with Mann-Whitney U test for post hoc analyses. P value≤0.05 for the Kruskal-Wallis test indicates that the analyzed samples belong to different populations.

Survival analyses were performed to analyze time-to-event probability by the Kaplan-Meier test. The survival curves obtained were compared for the different treatments. Animals that were alive at the end of the experiment or leave the study to be used in other experiment were included as right censored information. A log-rank test was used to determine the statistical significance of the different treatments. Differences were considered statistically significant (*) when p value≤0.05, and highly statistically significant (**) when p value≤0.01.

8. LIST OF EMPLOYED ADENOVIRUS.

AdCMVGFPLuc

Reporter adenovirus that expresses the eGFP gene under the control of the constitutive promoter CMV, and the Luciferase gene under the control of a second CMV promoter. This cassette is named as TL. The eGFP gene encodes for the Enhanced Green Fluorescent Protein, a mutated form of the GFP from *Aequorea Victoria*. The gene Luciferase encodes the Firefly Luciferase protein. This virus was kindly ceded by Dr. Ramon Alemany (IDIBELL-Institut Català d'Oncologia).

AduPARLuc

Reporter adenovirus that expresses the eGFP gene under the control of the constitutive promoter CMV, and the Luciferase gene under the control of the uPAR promoter. The genes eGFP and Luciferase are described above. The uPAR promoter corresponds to a 450 bp fragment of the promoter region of the human gene PLAUR, that encodes for the urokinase Plasminogen Activator Receptor (uPAR). This virus was previously generated in the laboratory by Dr. Meritxell Huch.

AdTK

Therapeutic adenovirus that expresses the TK transgene under the control of the constitutive promoter CMV. The TK gene encodes for the Thymidine Kinase enzyme from the Herpes Simplex Virus 1 (HSV-TK). This virus was previously generated in our laboratory in collaboration with Dra. Ana Mª Gomez.

AduPARTat8TK

Therapeutic adenovirus that expresses the Tat8TK transgene under the control of the uPAR promoter. The uPAR promoter is described above. The Tat8TK gene encodes a modified form of the HSV-TK with enhanced cytotoxicity, previously described in our laboratory by Dr. Anna Cascante (Cascante et al. 2005). In particular, TK gene is fused to the 8nt reduced variant of the protein transduction domain TAT.

AdYTRGE

Reporter adenovirus that expresses the TL cassette and presents specific fiber mutations that significantly reduce binding to CAR and to the blood factors C4BP and FIX, resulting in a low efficient liver transduction and in a reduced hepatotoxicity *in vivo* (Shayakhmetov et al. 2005). The fiber mutations were:

- Y477A single point mutation: ablates Ad binding to CAR.
- TAYT: deletion of amino acids 489 to 492 (TAYT) in the FG loop; changes the overall conformation of the knob domain without disturbing its ability to trimerize.
- RGE: peptide insertion (SKCDCRGECFCD) into position 547 of the HI loop; creates additional sterical hindrances, preventing interaction with natural ligands.

This virus was kindly ceded by Dr. Ramon Alemany (IDIBELL-Institut Català d'Oncologia).

AdTAT

Reporter adenovirus that expresses the TL cassette, carries the YTRGE fiber mutations and expresses the 11 nt TAT_{PTD} into the C-ter of the fiber protein.

AdTATMMP

Reporter adenovirus that expresses the TL cassette, carries the YTRGE fiber mutations and expresses the 11 nt TAT_{PTD} blocked with a glutamic tail into the C-ter of the fiber protein. The glutamic tail was linked to TAT_{PTD} by the MMP-cleavable linker sequence AKGLYK.

	Fiber mutations	Casette in E1A region	Origin:
AdCMVGFPLuc	Wt	- CMVpGFP - CMVpLuc	(Alemany and Curiel 2001)
AduPARLuc	Wt	- CMVpGFP - uPARpLuc	(Huch et al. 2009)
AdTK	Wt	CMVpTK	(Carrio et al. 1999)
AduPARTat8TK	Wt	uPARpTat8TK	This work
AdYTRGE	- Y, T, RGE	- CMVpGFP - CMVpLuc	(Shayakhmetov et al. 2005)
AdTAT	- Y, T, RGE - TAT in C-ter	- CMVpGFP - CMVpLuc	This work
AdTATMMP	- Y, T, RGE - TAT-MMP cleavable linker-Blockage in C-ter	- CMVpGFP - CMVpLuc	This work

Table 12. Adenovirus used in this thesis and their characteristics.

RESULTS

"El genio se compone del 2% de talento y del 98% de perseverante aplicación."

L. Beethoven *(1770-1827)*

Músico Alemán

1. EVALUATION OF THE EFFICACY OF INTRADUCTAL DELIVERY OF ADENOVIRUS TO TREAT PANCREATIC TUMORS.

The success of gene therapy is largely dependent on the viral transduction efficiency of the tumor. This relies in one hand on the delivery vector and in the other hand on the delivery route of vector administration. Three major delivery routes are commonly used to administer adenovirus for tumor treatment: intravenous (i.v) administration, intratumoral (i.t) injections and intraperitoneal administration. Systemic delivery (i.v) is specially indicated for pancreatic tumors that present with distant metastasis, while locoregional delivery is restricted to non-advanced carcinomas (Fillat et al. 2011).

All routes face with difficulties to achieve optimal delivery. In theory, vascular delivery of vectors will lead to a larger distribution of virus within the tumor. However, often blood vessels are confined to the tumor stroma, and therefore several layers of stromal cells must be passed before viruses reach malignant cells (Kuppen et al. 2001). Moreover, 90% of the adenovirus are sequestered into the liver by Kupffer cells and by hepatocyte transduction through interaction with clotting factors (Di Paolo et al. 2009). Another hurdle of systemic delivery is the preexistence of a humoral response that could compromise gene transfer (Harvey et al. 1999).

Intratumoral injections also show limitations to reach the bulk of tumoral cells. The stromal compartment and extracellular matrix components in the tumor act as physical barriers limiting the spread of the vector within the tumor (de Vrij et al. 2010). To improve on vector distribution, multiple injections in different parts of the tumor mass are often applied (Calbo et al. 2001; Roig et al. 2004).

After intraperitoneal administration, the vectors do not interact with the components of the vascular system, which reduces some of the hurdles of systemic delivery, but the physical barriers to reach the bulk of the tumors are increased (Hoffmann and Wildner 2006a).

In light of the lack of efficacy to reach the bulk of pancreatic tumors by the usually applied delivery routes, in this thesis we have studied an alternative delivery route to target pancreatic tumors.

1.1. Evaluation of the transduction efficiency of pancreatic tumors by intraductal administration of reporter adenoviruses.

Intraductal (i.d) or retrograde administration to pancreas is an adaptation of the endoscopic retrograde colangio-pancreatography (ERCP) technique, used in humans for the evaluation and treatment of diseases of the bile duct and pancreas (Dumot 2006). Intraductal administration consists on the introduction of a 30G needle into the common bile duct through the Vater's papilla to retrograde deliver virus to the pancreas (Figure 1A). Previously to virus administration, the common bile duct and the needle are clamped to avoid liver infection and regression of the liquid into the duodenum. When the virus is administered, it spreads across the pancreas through the branching duct system. As a proof of concept, Evans Blue dye was intraductally administered to the pancreas. As shown in Figure 1B, the pancreas stained blue suggesting that Evans Blue dye reached the whole pancreas.

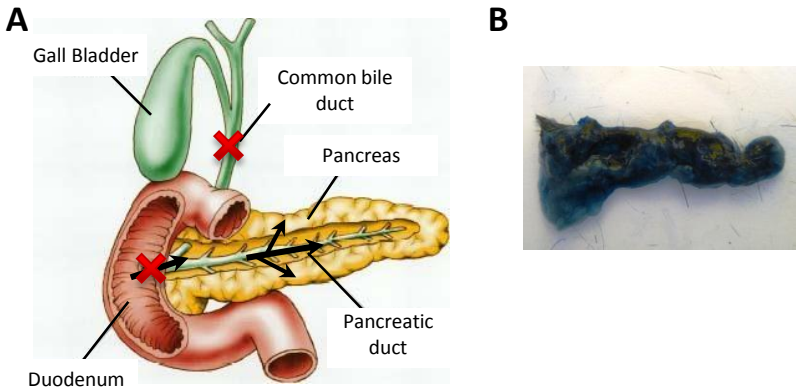

Figure 1. Intraductal administration into the common bile duct. A) Scheme of the surgical technique. Crosses indicate clamping points. Arrows indicate viral distribution. B) Pancreas of C57Bl/6 mice after Evans Blue intraductal injection.

1.1.1. The pancreatic cancer mouse model Ela-myc.

To evaluate the capacity of adenovirus to reach the pancreas and pancreatic tumors upon intraductal delivery, C57Bl/6 wt mice and the transgenic mouse model Ela-myc at 11 weeks of age were used in this study.

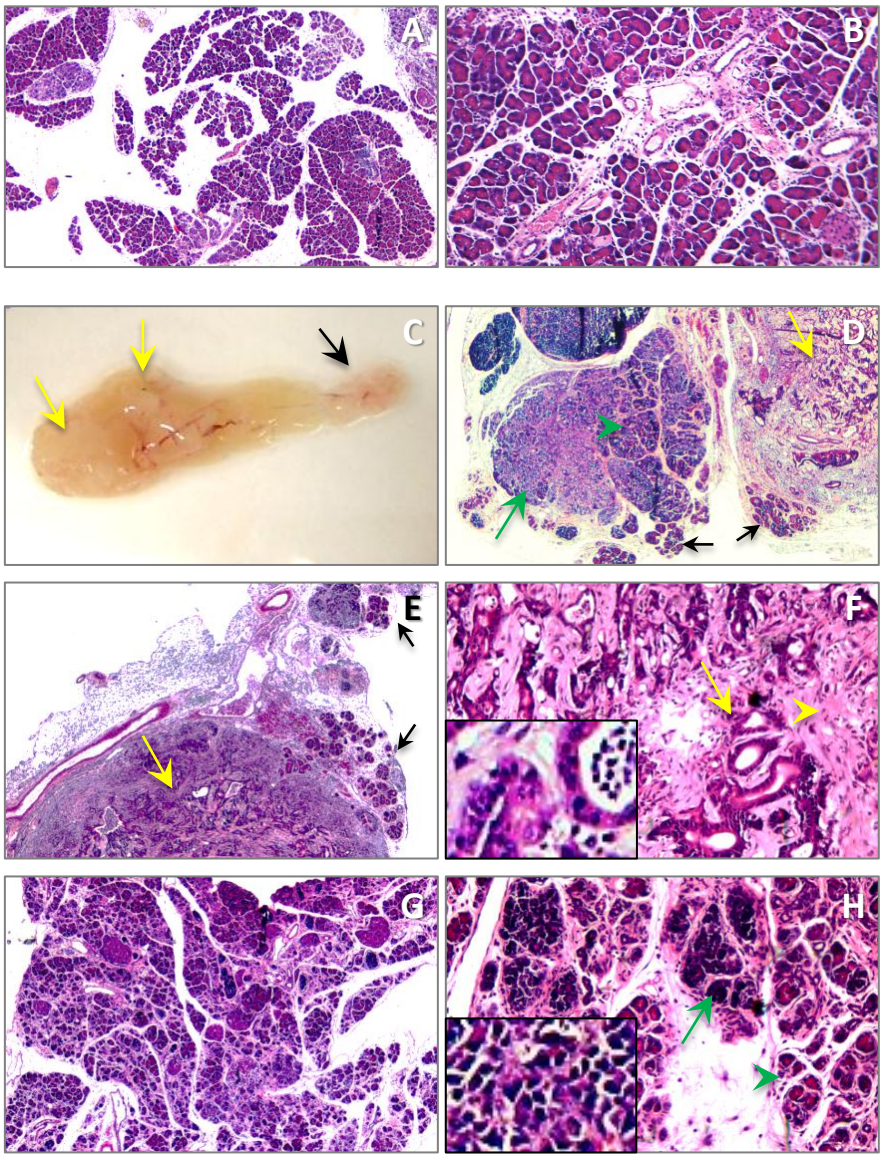

Figure 2. Pancreas of Ela-myc mice at 11 weeks of age. Representative images of wt (A,B) and Ela-myc (C-H) pancreas. Black arrows indicate non-tumoral areas, yellow arrows indicate solid regions that show a ductal phenotype, yellow arrow head indicates dense stroma, green arrow heads indicate preneoplasic regions and green arrows indicate tumoral regions showing an acinar phenotype. Original magnification, 2.5x (A, D,E, G), 10x (B, F, H), 40x (insets).

Transgenic Ela-myc mice of 11 weeks of age exhibited a preneoplasic pancreas with, in some cases, tumor nodules of 3-7 mm in diameter

(Figure 2C). Preneoplasic and tumoral pancreas shows a white coloration and a grained structure at the macroscopic level (Figure 2C). The preneoplasic pancreas is microscopically visualized as disorganized and deformed acinus within a well-organized parenchyma (Figure 2G), and some areas already exhibit a tumoral acinar phenotype (Figure 2H). At this time, non-tumoral areas can be observed surrounding or within the preneoplasic areas (Figure 2D, E, black arrows). Solid tumor nodules appear lately in tumor development. They present a ductal phenotype and a dense stroma (Figure 2F), and preneoplasic/acinar tumoral regions can be detected adjacent to them (Figure 2D), constituting the so-called mixed acinar/ductal phenotype. When solid nodules appear at early times, they are embedded within a healthy parenchyma (Figure 2E). Ela-myc mice present a survival of 19.6±0.7 weeks.

1.1.2. Biodistribution study after intraductal delivery of the reporter adenovirus AdCMVGFPLuc.

The reporter adenovirus AdCMVGFPLuc, that expressed the reporter genes luciferase and GFP, was intraductally administered into the common bile duct of wt C57Bl/6 or transgenic Ela-myc mice. Expression of luciferase by bioluminescence analyses was carried out as an indicator of viral biodistribution.

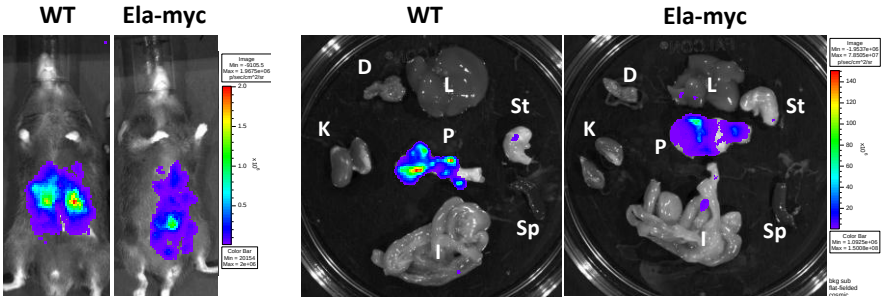

Figure 3. Biodistribution study of AdCMVGFPLuc intraductally administered into the common bile duct. Representative bioluminescent images of animals and isolated organs from wt C57Bl/6 (n=7) and transgenic Ela-myc (n=9) mice i.d injected with $5{\cdot}10^{10}$ vp of AdCMVGFPLuc. Bioluminescence was measured four days later in living animals and in isolated organs (K: kidney, D: diafragm, L: liver, St: stomach, Sp: spleen, I: intestine and P: pancreas).

Five$\cdot10^{10}$ vp of AdCMVGFPLuc were intraductally delivered to wt and Ela-myc mice 11 weeks old and four days later, *in vivo* and *ex vivo* luciferase expression was analyzed by bioluminescent imaging IVIS50 system

(Xenogen). As it is observed in Figure 3 luciferase expression was restricted to the pancreas both in wt and Ela-myc animals. In a small number of mice, punctual luciferase expression was detected in stomach or intestine, probably corresponding to pancreas fragments not correctly isolated during necropsy.

1.1.3. Persistence of transgene expression following AdCMVGFPLuc intraductal injection.

Next, we analyzed the persistence of transgene expression in the pancreas of wt and Ela-myc mice that received intraductally 10^{10}vp of AdCMVGFPLuc. At 4, 7 and 10 days after virus administration animals were sacrificed and luciferase expression was quantified in pancreatic tissue extracts.

Maximum transgene expression was obtained at day 4 in both groups that decreased at days 7 and 10 (Figure 4). Luciferase activity in Ela-myc mice was lower than that of wt mice at all the times analyzed. This could probably be explained by the presence of tumoral stroma that hindered viral distribution through the neoplasic pancreas.

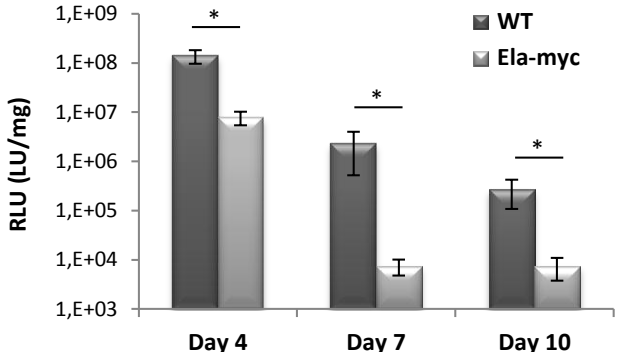

Figure 4. Time-course study of luciferase expression in the pancreas of wt and Ela-myc mice after AdCMVGFPLuc intraductally administered into the common bile duct. 10^{10} vp of AdCMVGFPLuc were intraductally administered to wt (n=4 per day) and Ela-myc (n=5 per day) mice. Animals were sacrificed 4, 7 and 10 days later, pancreas was removed and luciferase expression was measured in tissue extracts. Results are represented as the mean ± SEM and expressed as RLU (LU/mg of protein). * $p<0.05$.

1.1.4. Comparative analyses of AdCMVGFPLuc biodistribution following intraductal or intravenous delivery.

Next we evaluated whether intraductal delivery was providing with any advantage to intravascular delivery to target adenovirus to the pancreas or pancreatic tumors. To this end, $5{\cdot}10^{10}$ vp of the reporter adenovirus AdCMVGFPLuc were intraductally or intravenously administered in 11 weeks old wt and Ela-myc mice. Four days later, animals were sacrificed and luciferase expression was measured in the pancreas and the liver.

Luciferase expression was mainly observed in the liver after Ad intravascular delivery, whereas it was localized in the pancreas after intraductal administration (Figure 5A). Interestingly, quantification of bioluminescence images showed a 5-40 fold increase in pancreatic luciferase expression upon intraductal delivery when compared to intravenous delivery. On the contrary, liver transduction was reduced 3 logs upon i.d administration when compared to i.v administration. To confirm these results luciferase expression was quantified in tissue extracts from animals intraductally delivered with AdCMVGFPLuc. As shown in Figure 5B, transgene expression was significantly higher in the pancreas than in the liver of mice i.d injected with Ad.

These results indicated that intraductal delivery of Ad increased pancreatic transduction and reduced liver sequestration when compared to intravenous delivery. Thus, the application of intraductal delivery provides with pancreatic selectivity.

1.1.5. AduPARLuc expression analyses after intraductal administration.

To restrict adenoviral activity to pancreatic tumoral cells we decided to test the activity of AduPARLuc, a reporter adenovirus with the tumor specific promoter uPAR driving the luciferase gene. Previous studies in the laboratory had demonstrated that uPAR promoter was highly active driving transgene expression and presented good oncoselectivity for pancreatic tumors (Huch et al. 2009).

First, we analyzed uPAR expression in tumor-presenting pancreas of 11 weeks old Ela-myc mice (Figure 6). Elevated levels of Plaur mRNA were detected in the pancreas of Ela-myc mice. IHC analysis showed uPAR

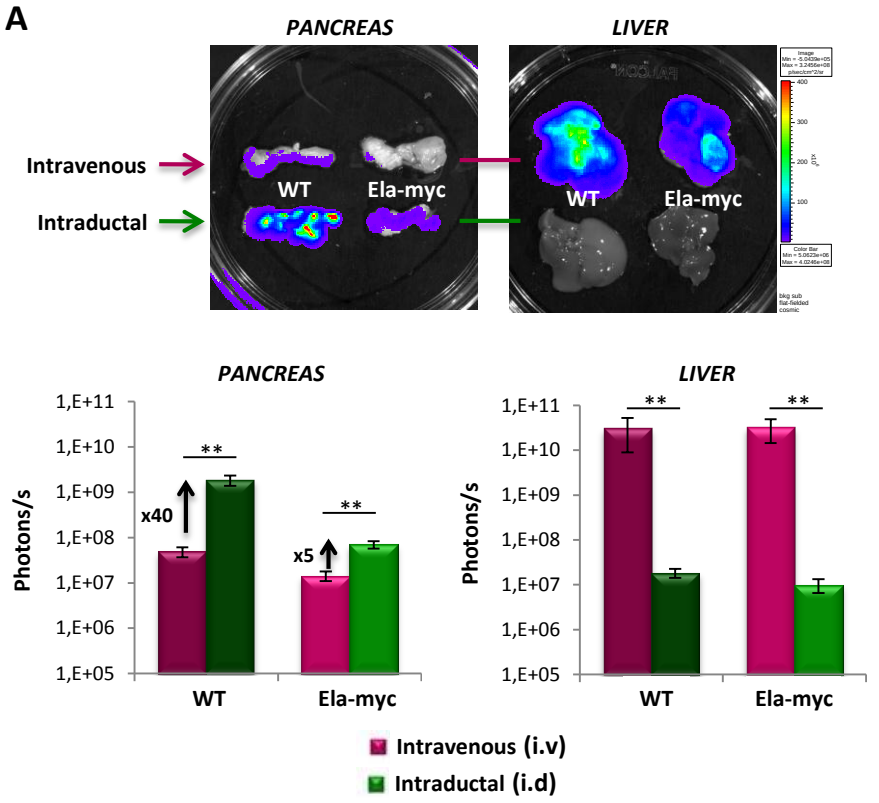

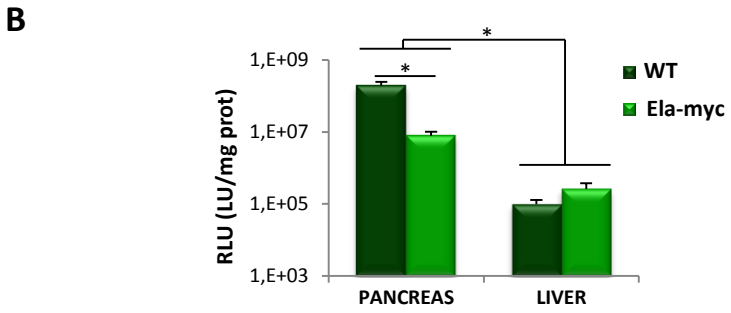

Figure 5. Luciferase expression analysis of AdCMVGFPLuc intravenously or intraductally administered to wt or Ela-myc mice. A) $5{\cdot}10^{10}$ vp of AdCMVGFPLuc were intravenously or intraductally administered to wt (n=7, n=7, respectively) and Ela-myc mice (n=7, n=9, respectively). Four days later animals were sacrificed and liver and pancreas luciferase expression was measured. Top panel: Representative bioluminescent images. Bottom panel: Quantification of luciferase expression from captured bioluminescence images. Results are expressed as photons/s. B) 10^{10} vp of AdCMVGFPLuc were intraductally administered to wt (n=4) and Ela-myc mice (n=5), and four days later luciferase expression was measured in tissue extracts. Results are expressed in RLU (LU/mg of protein). All the results are represented as the mean ± SEM. * p<0.05, ** p<0.01.

expression in ductal and acinar cells of preneoplasic areas, and abundant staining was also detected in the stromal cells.

The observation that endogenous expression of the Plaur gene was elevated in the pancreas of Ela-myc mice suggested that factors regulating the uPAR promoter were active in Ela-myc tumors. This could be an indicator that AduPARLuc adenovirus could be highly regulated in this context.

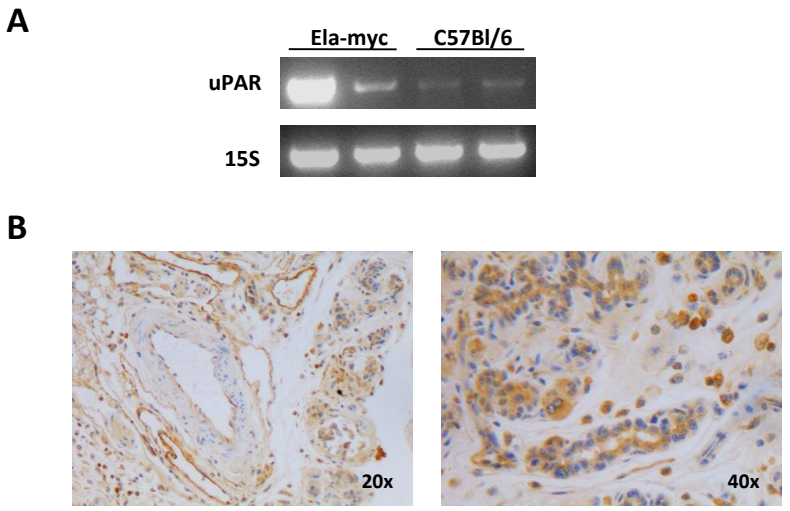

Figure 6. uPAR expression in the pancreas of Ela-myc mice. A) RT-PCR of Plaur gene (uPAR) and the control 15S gene in the pancreas of Ela-myc and wt mice. B) Representatives images of anti-uPAR immunostaining in Ela-myc pancreas. Left panel: 20x magnification; Right panel: 40x magnification.

To test this hypothesis, 10^{10} vp of AdCMVGFPLuc or AduPARLuc were i.d administered to wt mice and luciferase expression was analyzed four days later (Figure 7B). AduPARLuc expression was 80 times lower than that of AdCMVGFPLuc. This could probably be explained by the low uPAR expression observed in the pancreas of wt mice that would correspond with a low uPAR promoter activity, contrasting with the highly active constitutive promoter CMV.

To achieve therapeutic success, the adenoviral vector must present selectivity for the tumoral tissue while avoiding harming non-tumoral cells. To test uPAR promoter oncoselectivity we took advantage of the double cassette that expressed the AduPARLuc vector (Figure 7A). We analyzed by immunohistochemistry the expression of GFP, controlled by

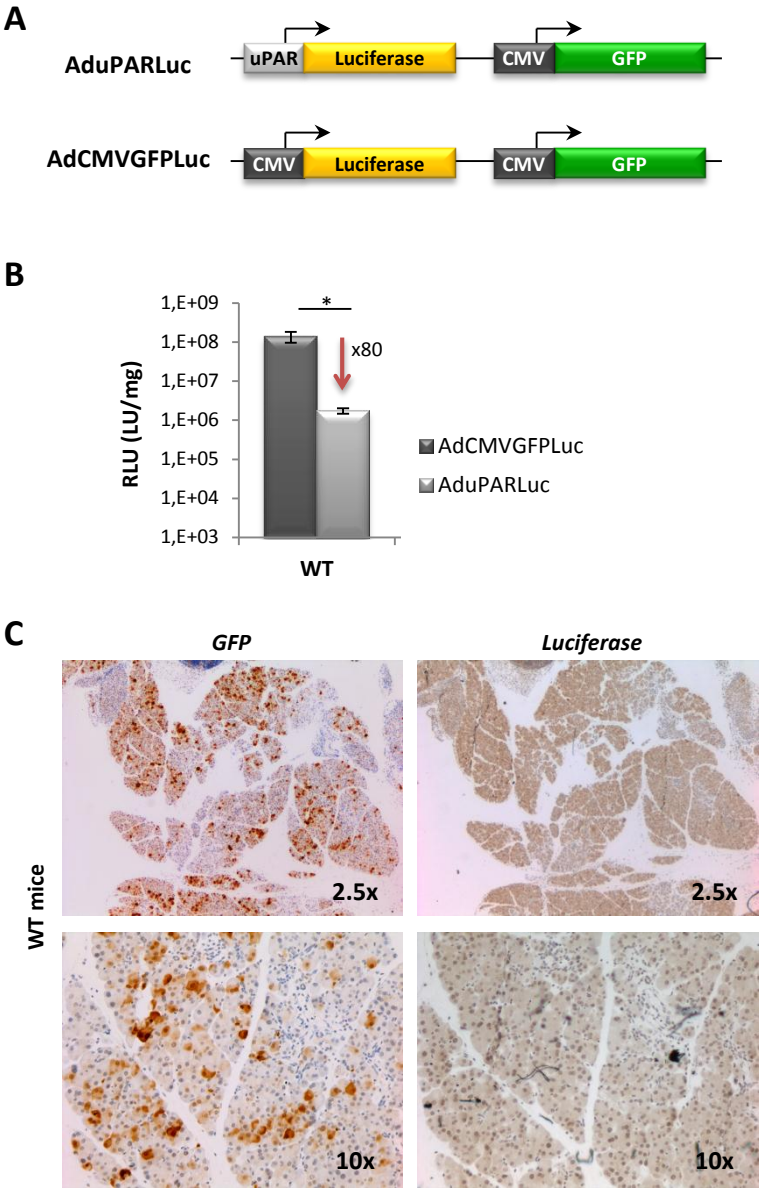

Figure 7. AduPARLuc expression after intraductal administration to wt mice. A) Scheme of AduPARLuc and AdCMVGFPLuc (AdCMVGFPLuc) viruses. B) 10^{10} vp of AdCMVGFPLuc or AduPARLuc were intraductally administered to wt (n=7, n=4, respectively), and four days later luciferase expression was measured in tissue extracts. Results are represented as the mean ± SEM and expressed as RLU (LU/mg). * $p<0.05$. C) Representative images of anti-GFP and anti-luciferase immunostaining in pancreas of wt mice four days after 10^{10} vp of AduPARLuc were i.d administered.

the CMV promoter, and the expression of luciferase, controlled by the uPAR promoter, in the pancreas of wt mice i.d injected with AduPARLuc. Analyses of the same pancreatic regions showed strong GFP immunoreactivity but absence of luciferase staining (Figure 7C), indicating that although AduPARLuc virus transduced the majority of the wt pancreas (as suggested by the strong GFP staining), the transgene controlled by the uPAR promoter was not expressed (lack of luciferase staining). These results suggested that AduPARLuc transduce normal pancreas, but transgene expression driven by the uPAR promoter was very low, and undetectable by anti-luc inmunostaining.

Next, we studied the capability of the AduPARLuc to drive luciferase expression in Ela-myc pancreatic tumors when intraductally administered. 10^{10} vp of AduPARLuc were i.d delivered to Ela-myc mice, and luciferase expression was analyzed four days later. uPAR promoter activity resulted in 10% that of the CMV promoter in the Ela-myc pancreas compared to the 1.2% observed in the wt pancreas (Figure 8A). Furthermore, as shown in Figure 8B, luciferase expression was detected in preneoplasic and tumoral areas with an acinar phenotype (upper panel) as well as in the core of solid tumoral masses with ductal phenotype and dense stroma (middle and bottom panels).

In conclusion, the results showed that intraductal delivery of AduPARLuc into the common bile duct led to the efficient transduction of Ela-myc mice pancreatic tumors.

1.2. Evaluation of the AduPARTat8TK/GCV therapy to treat pancreatic tumors.

To evaluate the feasibility of intraductal adenoviral delivery to treat Ela-myc pancreatic tumors we generated the cytotoxic adenovirus AduPARTat8TK, in which the cytotoxic gene Tat8TK was regulated by the uPAR promoter. First we tested the cytotoxic effect of AduPARTat8TK/GCV in primary Emyc tumor cultures.

Figure 8. Luciferase expression of AduPARLuc in the pancreas of Ela-myc mice after intraductal delivery. 10^{10} vp of AdCMVGFPLuc or AduPARLuc were intraductally administered to wt (n=7, n=4, respectively) and Ela-myc mice (n=4, n=4, respectively), and four days later luciferase expression measured in tissue extracts (A) or analyzed by immunohistochemistry (B). A) Results are represented

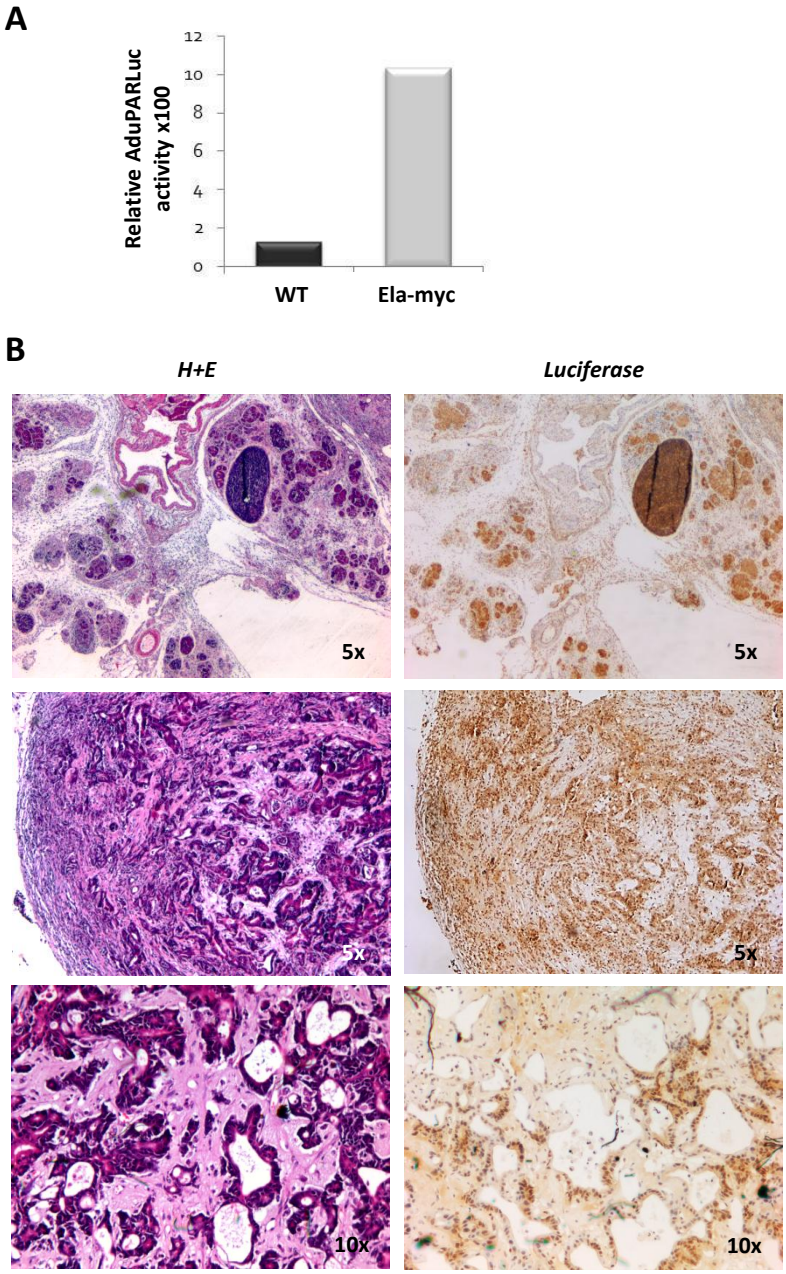

as the ratio x100 between the mean of AduPARLuc expression and the mean of AdCMVGFP expression. B) Representative images of luciferase immunostaining and hematoxilyn&eosin staining corresponding to the same pancreatic area (except for the bottom panel).

1.2.1. Generation and molecular characterization of Emyc cell lines.

Eleven pancreatic tumor fragments from six Ela-myc mice of 2.5-4 months of age were processed to generate primary cultures. From three of them we established the independent cell lines: Emyc-1, Emyc-3 and Emyc-10, all them deriving from white tumoral areas.

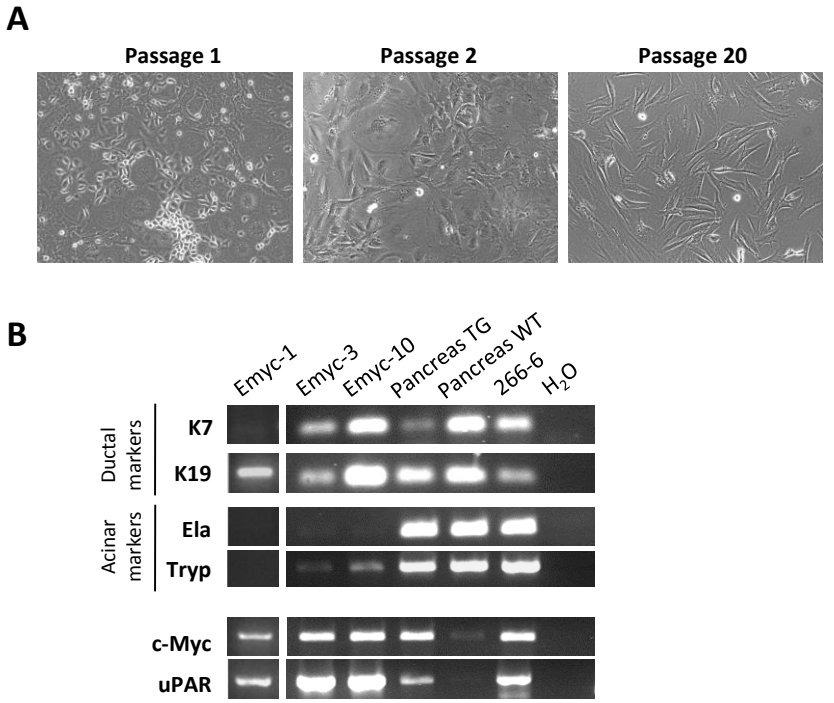

Figure 9. Characterization of Emyc cell lines. Primary cultures were generated from pancreatic tumor nodules of Ela-myc mice of 2.5-4 months of age. Primary cultures were considered established cell lines from 20 passages. A) Representative images of Emyc primary cultures at different passages. B) Molecular characterization of Emyc cell lines by RT-PCR analyses. RT-PCR of the ductal markers keratin 7 and keratin 19 (K7 and K19), acinar markers elastase and trypsin (Ela-myc and Tryp), and c-Myc and Plaur (uPAR) genes in Emyc-1, Emyc-3 and Emyc-10 cell lines, and in the controls: pancreas from TgEla-myc mice and wt C57Bl/6 mice, and the acinar pancreatic tumoral cell line 266-6.

Cell line morphology and expression of phenotypic markers were analyzed at several passages of the primary culture. Different morphologies were found within and through passages (Figure 9A). Initial cell population was a mixture of cells, e.g. fibroblasts, polygonal cells,

refringent cells, etc. Cultures required about 10 passages to get rid of fibroblasts. Around passage 20, a primary culture was considered an established cell line (4-5 months after initial plating).

Cell lines characterization was performed by examining acinar and ductal cell-specific markers by RT-PCR analysis. Expression of the oncogenes c-Myc and uPAR was also analyzed (Figure 9B). RT-PCR analysis revealed the expression of ductal markers (Keratin 7 and/or Keratin 19) in all three Emyc cell lines. The acinar marker elastase was not detected in any of the Emyc cell lines, although some expression of the acinar marker trypsin was detected in Emyc-3 and Emyc-10 cells. Interestingly, all Emyc cell lines showed stronger uPAR gene expression.

The stronger expression of Keratin 7 and 19 and lower expression of trypsin seemed to indicate that Emyc cell lines exhibited a more prominent ductal phenotype. This result is in accordance with the study carried out by Biliran et al in which they generated a cell line derived from Ela-myc mice and observed expression of acinar and ductal markers but prevailed the ductal phenotype (Biliran et al. 2005).

1.2.2. Susceptibility of Emyc cells to viral transduction and response of Emyc cells to uPAR promoter controlled adenovirus.

To test the capacity of AduPAR controlled adenovirus to drive expression in the pancreatic cancer Emyc cell line. Emyc, Panc-1 and RWP-1 cultures were exposed to 10^4 vp/cell of AduPARLuc or the control AdCMVGFPLuc and GFP and luciferase expression was analyzed three days later. Emyc-1 cells were susceptible to adenoviral transduction as GFP emission was similar to that of RWP-1 cells (high susceptible to adenoviral transduction) and highly different from Panc-1 (low adenoviral transduction) (Figure 10A).

All pancreatic cancer cells transduced with the AduPARLuc virus showed high levels of luciferase activity, indicating that the uPAR promoter was active in all the pancreatic cancer cells, although it was lower than that of CMV promoter (Figure 10B). It is not surprising since it has been described that tumor specific promoters show lower transcriptional activity than that of CMV promoter. Thus, these results indicated that AduPARLuc was highly active and efficiently transduce Emyc cell lines.

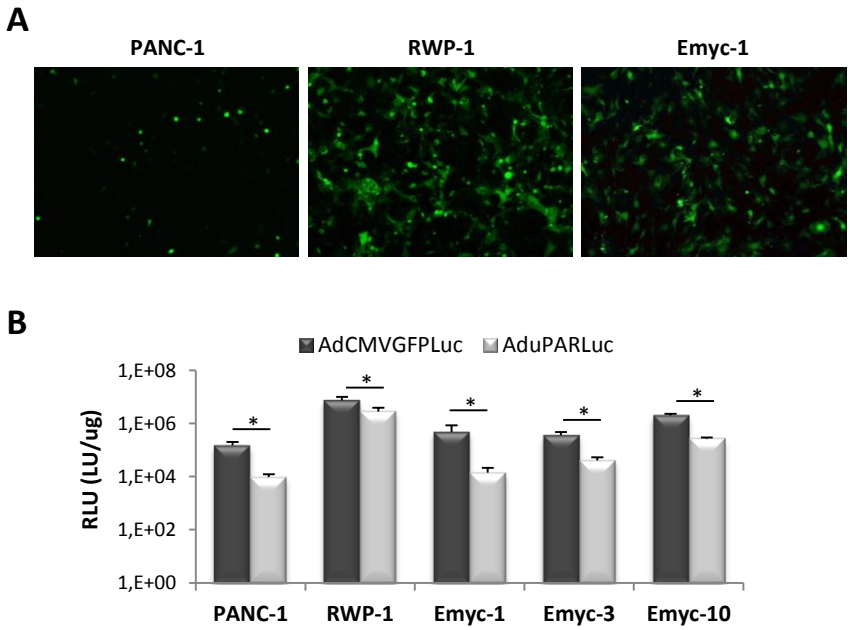

Figure 10. AduPARLuc activity in Emyc cell lines. 10.000 cells were seeded in triplicate in a 96-well plate. Cells were infected with 10000 vp/cell of AdCMVGFPLuc or AduPARLuc, and four hours later medium was changed to fresh medium. Transgene expression was measured 3 days later. A) Representatives fluorescent images of GFP expression. B) Luciferase expression of AdCMVGPLuc and AduPARLuc. Results are represented as the mean ± SEM of at least 3 independent experiments and expressed as RLU (LU/µg). * $p<0.05$.

1.2.3. Evaluation of the sensitivity of Emyc cells to the Tat8TK/GCV system

- ***AduPARTat8TK/GCV ID_{50} value determination.***

Next, we evaluated the response of the Emyc cell lines to the Tat8TK/GCV cytotoxic therapy. Six pancreatic cancer cell lines were infected with increasing doses of AduPARTat8TK (Figure 11A) and four hours after transduction, cells were treated with GCV for 3 days and cell viability was then assessed by MTT assay. Dose-response curves were obtained (Figure 11B) and vp/cell corresponding to the ID_{50} values were determined (Figure 11C).

We observed that AduPARTat8TK displayed an important cytotoxic effect in pancreatic tumor cells and, interestingly, Emyc cell lines showed the

lowest ID_{50} values, indicating that Emyc cell lines were highly sensitive to the AduPARTat8TK/GCV therapy.

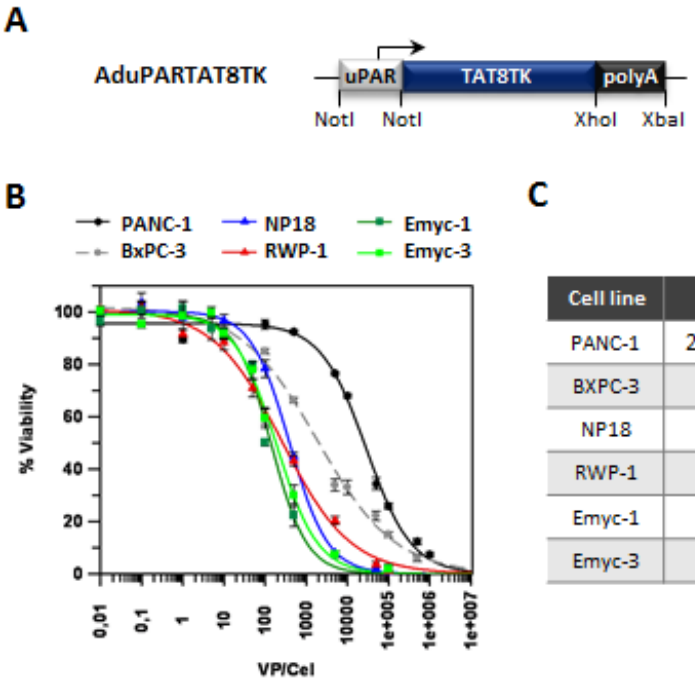

Cell line	ID_{50} (VP/Cel)
PANC-1	28755.1 ± 2196.8
BXPC-3	1864.7 ± 250.4
NP18	390.1 ± 30.6
RWP-1	258.6 ± 33.1
Emyc-1	140.5 ± 15.9
Emyc-3	187.2 ± 22.2

Figure 11. TK/GCV cytotoxic study. A) Schematic representation of AduPARTat8TK adenovirus. B) Dose-response curves of pancreatic cancer cells transduced with AduPARTAT8TK and treated with GCV. 3.000 cells were seeded in triplicate in a 96-well plate and infected with a dose range of 0 to 10^6 vp/cell. Four hours post-infection medium was replaced by complete medium supplemented with 100 µg/ml GCV. Viability was measured 3 days later by MTT. C) ID_{50} values±SEM of at least four independent experiments.

- ***Study of the bystander effect of Tat8TK/GCV on the Emyc-3 cell line.***

To further analyze the cytotoxicity of the TK/GCV system in Emyc cells, we tested for the presence of a bystander effect (BE) in Emyc cells and compared to a battery of cell lines. To this end, PANC-1, RWP1, Emyc-3 and NP18 pancreatic cancer cells were transduced with the recombinant adenoviral vector AdTK at a viral dose corresponding to approximately the IC_{90}, and designated as TK^+ cells. Cocultures of 50% TK+ cells and 50% TK- cells were established at high confluence and treated with GCV for 3 days. Cell survival was assessed by MTT assay and the percentage of cell viability with respect to PBS-treated cells was calculated. As shown in

Figure 12B the percentage of cell survival in the cocultures derived from all four pancreatic cancer cell lines was significantly lower than 55%, indicating that BE was participating in the TK/GCV cytotoxicity. Specifically, coculture of Emyc cells showed very low cell survival values, suggesting that BE was a contributing factor to the higher cytotoxicity exerted by the TK/GCV system on the Emyc cell lines.

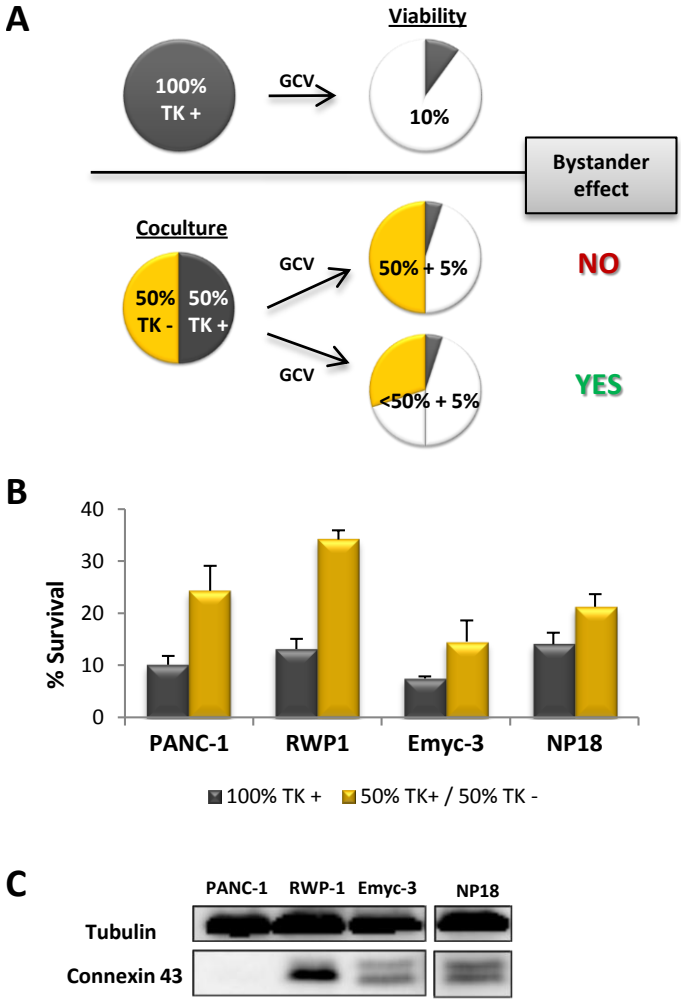

Figure 12. Evaluation of TK/GCV bystander effect in Emyc cells. A) Scheme of the experiment performed to study the bystander effect of TK/GCV system on cellular models. B) TK/GCV bystander effect. 200.000 cells seeded in a 60 mm plates were transduced with AdTK (PANC: 5.000 vp/cell; NP18: 100 vp/cell; RWP1 and Emyc-3: 50 vp/cell). The following day, cocultures (50% TK+/50% TK-) or 100% TK+ cultures were generated by seeding 5000 cells (RWP1, Emyc-3 and NP18) or 9000 cells (PANC-1) in 96-well plates. At 6h GCV treatment was initiated.

It is well documented that the TK/GCV bystander effect is mediated by the transfer of phosphorylated GCV from TK+ cells to neighboring cells through gap junctions (Carrió et al. 2001). To corroborate the implication of BE on TK/GCV toxicity, we studied the expression of the structural proteins connexins constituting the gap junctions; in particular we studied Connexin 43 (Cx43) expression, a connexin expressed in the pancreas. Immunoblot analysis of confluent cell cultures showed high Cx43 expression in NP18 cells, moderate expression in RWP1 and Emyc-3 cells and no expression in PANC-1 cells (Figure 12C). NP18 and PANC-1 Cx43 expression levels were in accordance with previous studies described in our laboratory (Garcia-Rodriguez et al. 2011). The presence of Cx43 in Emyc cells suggest that Cx43 could probably be facilitating TK/GCV BE in Emyc cells, although other connexins not analyzed in the current study could also be involved.

1.2.4. Evaluation of AduPARTat8TK/GCV treatment on Ela-myc pancreatic tumors.

Next, we studied the antitumoral effect of AduPARTa8TK/GCV therapy on pancreatic tumors of Ela-myc mice. First, we evaluated the antitumoral effect of the therapy at two different doses of AduPARTat8TK when intraductally delivered. Five groups of Ela-myc mice were established (PBS, GCV, AduPARTat8TK, AduPARTat8TK$_{Low}$+GCV and AduPARTat8TK$_{High}$+GCV). Ela-myc mice were i.d injected with PBS, $5{\cdot}10^{10}$ vp or 10^{11} vp of AduPARTat8TK. Three days later, a daily dose of 100 mg/kg of GCV was administered for 6 consecutive days in the control group (GCV) and in the AduPARTat8TK$_{Low}$+GCV and AduPARTat8TK$_{High}$+ GCV groups. Six weeks after viral administration animals were sacrificed and the pancreatic volume was determined. We evaluated the pancreatic volume instead of the tumoral volume because a defined tumoral nodule was not always detected at the time of virus administration and, in addition, the Ela-myc pancreas was preneoplasic in its totally.

Non-treated Ela-myc pancreas showed tumor progression with a pancreatic volume of 444 mm^3 (PBS group in Figure 13B). AduPARTat8TK or

After 72h, cell viability was determined by an MMT assay. Values represent the mean ± SEM of 3 independent experiments. C) Connexin 43 expression analyses by Western blot. 60µg of total protein extract from confluent cell cultures were loaded. Tubulin expression was used as a control.

GCV treatments independently administered had no effect on the pancreatic volume (423 mm^3). On the contrary treatment with both high and low viral AduPARTat8TK combined with GCV resulted in a significant reduction on the pancreatic volume, with values similar to those of wt mice. These results indicated that i.d. adenoviral delivery of AduPARTat8TK followed by GCV treatment, significantly reduced Ela-myc tumor progression.

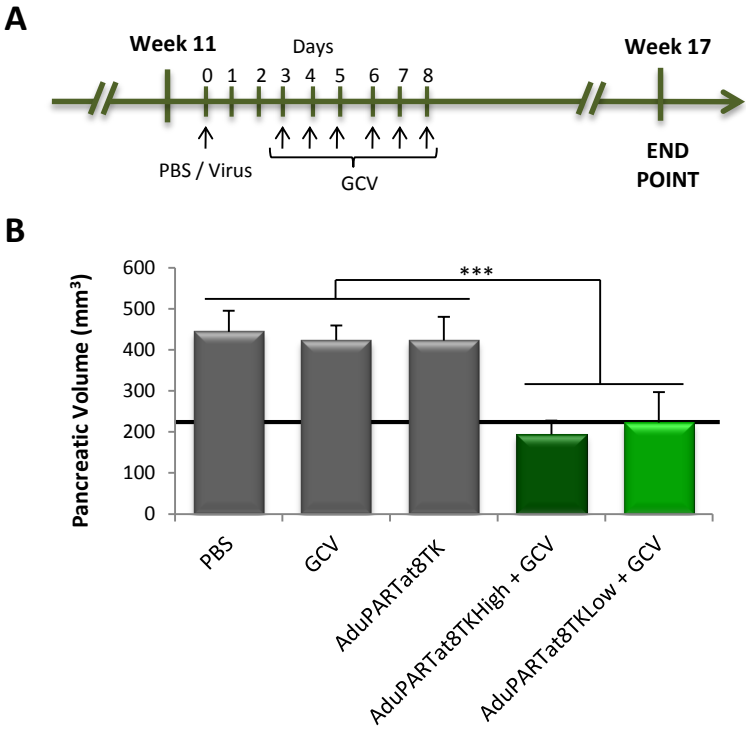

Figure 13. Antitumoral effect of AduPARTat8TK/GCV treatment, upon virus intraductal delivery, on Ela-myc pancreatic tumors. A) Schematic representation of the therapeutic protocol. $5{\cdot}10^{10}$ or 10^{11} vp of AduPARTat8TK (Low (n=10) and High (n=9), respectively) were intraductally injected to 11 weeks old Ela-myc mice. Three days later, GCV treatment (100 mg/kg) was i.p administered for 6 days. Six weeks after virus administration, animals were sacrificed and pancreatic volume was measured. The control groups received PBS (n=10), GCV (n=11) or virus at high dose (n=10). B) Pancreatic volume of Ela-myc mice upon i.d delivery of AduPARTat8TK/GCV therapy. Black line corresponds to C57Bl6 (n=8) pancreatic volume (221.3 ± 8.7 mm^3). *** $p<0.005$.

We have previously observed (Figure 5) that adenoviral transduction of pancreatic tumors in Ela-myc mice with AdCMVGFPLuc was more efficient when administered intraductally than following intravascular

delivery. To analyze whether this different transduction effect impacts differently on the antitumoral response of a therapeutic virus we intraductally or intravenously administered $5{\cdot}10^{10}$ vp of the cytotoxic AduPARTat8TK virus, followed by six daily doses of GCV initiated three days after virus administration. Pancreatic volume was measured six weeks later. As shown in Figure 14, both treated groups showed reduced pancreatic volume compared to non-treated mice, suggesting that AduPARTat8TK/GCV therapy, administered either i.d or i.v, reduced Ela-myc tumor progression. Interestingly, intraductal virus delivery reduced pancreatic volume to lower values than intravenous delivery. These results seemed to indicate that AduPARTat8TK/GCV therapy upon i.d delivery was a good candidate therapy to treat Ela-myc pancreatic tumors.

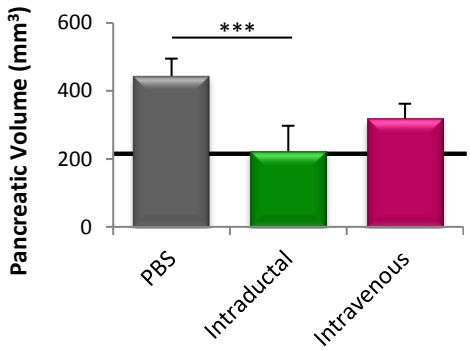

Figure 14. Antitumoral effect of AduPARTat8TK/GCV therapy, upon intraductal or intravenous viral administration, on Ela-myc mice. $5{\cdot}10^{10}$ vp of AduPARTat8TK were intraductally (n=10) or intravenously (n=7) delivered to 11 weeks old Ela-myc mice. Three days later, GCV treatment (100 mg/kg) was i.p administered for 6 days. Six weeks after virus administration, animals were sacrificed and pancreatic volume was measured. The control group PBS (n=10) intraductally received PBS solution. Black line corresponds to C57Bl6 (n=8) pancreatic volume (221.3 ± 8.7 mm^3). *** $p<0.005$.

1.2.5. Toxicity analysis of AduPARTat8TK/GCV therapy.

After intravascular injection, adenoviruses liver tropism leads to liver toxicity caused by an immune response to the viral proteins as well as transgene expression. In addition, the pancreas is a delicate organ and intraductal injection can lead to pancreatitis. Therefore, we evaluated the potential toxicity of AduPARTat8TK/GCV therapy after i.v or i.d viral administration in Ela-myc mice.

First, we determined serum biochemical parameters of liver and pancreatic function in non-treated Ela-myc mice at different times (Figure 15). Pancreatic damage was assessed by measuring amylase, lipase and glucose levels, and liver damage was assessed by measuring ALT and AST levels. Non-treated Ela-myc mice presented altered pancreatic parameters at all the time points analyzed (Figure 15B). Specifically, amylase levels were over the reference range in mice at 12 weeks of age and rapidly increased at later times (17 weeks of age), probably related to an exponential growth of the pancreatic tumor. Lipase values were in the close vicinity to the lowest reference value and, similarly to amylase, rapidly increased at later time points. On the contrary, glucose levels were always below the reference range and rapidly decreased at later times. These results indicated that Ela-myc mice already presented pancreatic damage at 11-12 weeks of age that exponentially increased with time. Ela-myc mice also presented elevated AST values whereas ALT levels were within the reference suggesting minor liver damage associated to the tumor.

Next, we evaluated serum biochemical parameters of pancreatic function in Ela-myc mice intraductally (i.d) or intravenously (i.v) treated with $5{\cdot}10^{10}$ vp of AduPARTat8TK plus six doses of GCV. Schedule of blood sample acquisition is shown in Figure 15A. As shown in Figure 15B, the AduPARTat8TK/GCV therapy reduced the levels of the pancreatic parameters analyzed at all the time points compared to that of non-treated mice. Whereas amylase levels were reestablished within the reference range aside from the latest time, lipase and glucose levels were stabilized below the reference range. These results suggested that AduPARTat8TK/GCV therapy ameliorated pancreatic tumor-associated toxicity in Ela-myc mice.

We also evaluated the hepatotoxicity produced by the AduPARTat8TK/GCV therapy. Transaminases levels were maintained or reduced to the reference range, indicating that AduPARTat8TK/GCV therapy produced no hepatotoxicity either upon i.v or i.d administration. Probably the use of the uPAR promoter was restricting the hepatotoxicity associated to the systemic administration of adenoviruses.

Therefore, these results indicated that the AduPARTat8TK/GCV therapy was not toxic and, moreover, reduced the tumor-associated toxicity in Ela-myc mice.

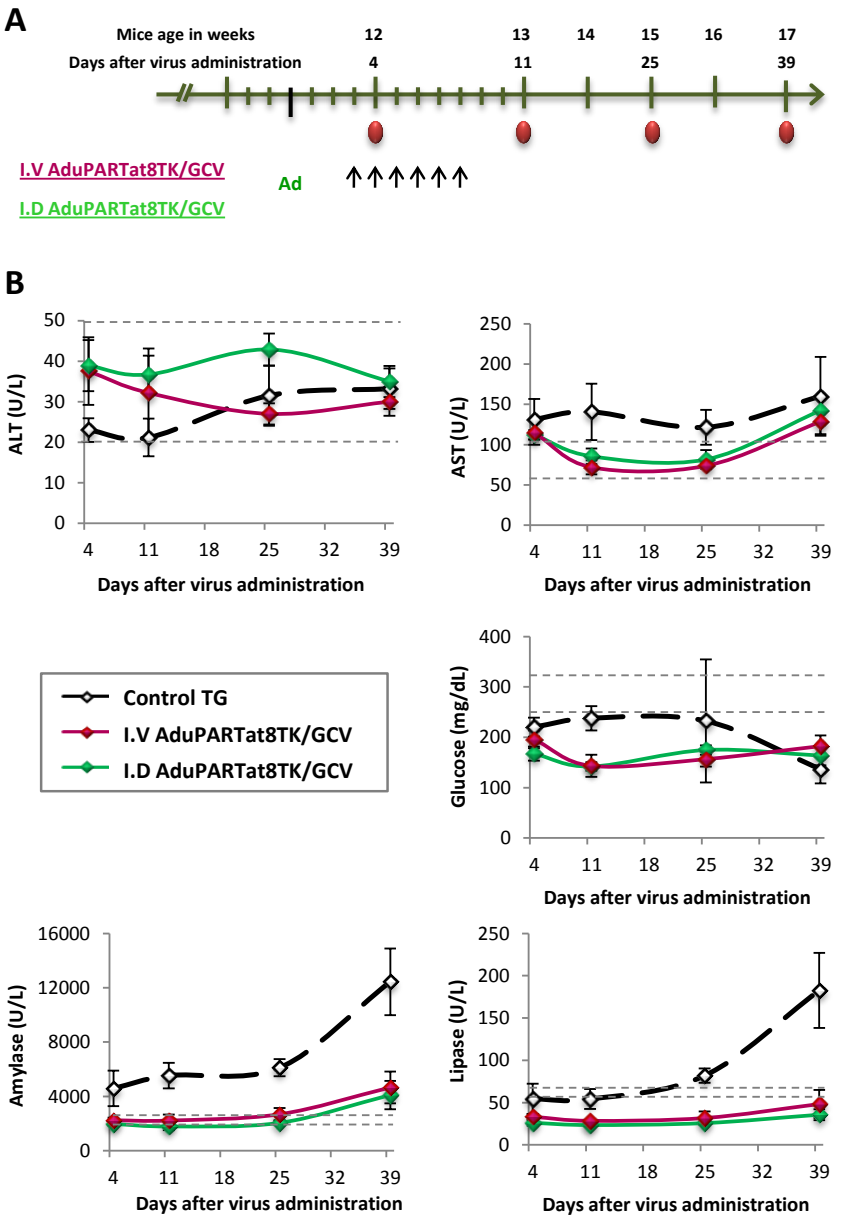

Figure 15. AduPARTat8TK/GCV toxicity studies in Ela-myc mice. A) Protocol for evaluation of pancreatic and liver toxicity of AduPARTat8TK/GCV therapy. Times of blood sample acquisition are indicated with red circles. B) Analysis of ALT and AST, amylase, lipase and glucose serum levels in treated Ela-myc mice at 4, 11, 25 and 39 days after virus administration or at their corresponding times in non-treated Ela-myc mice. AduPARTat8TK/GCV therapies followed the same protocol than in Figure 14. Non-treated mice n=4-6, Treated mice n=5 per group. Dash lines indicate reference values from untreated C57Bl/6 mice (n=6).

2. ANALYSIS OF THE THERAPEUTIC EFFICAY OF AduPARTat8TK/GCV THERAPY COMBINED WITH GEMCITABINE TO TREAT PANCREATIC CANCER.

Gemcitabine (GE) is a nucleoside analogue used for the treatment of solid cancers, such as pancreatic cancer; in fact it is the first line treatment for patients with systemically advanced pancreatic adenocarcinoma. Nowadays, a large number of works are trying to improve the activity of gemcitabine by its combination with other agents (Vonhoff 2006). Some of these regimens, such as gemcitabine plus erlotinib (EGFR kinase inhibitor) or gemcitabine plus capecitabine (nucleoside analogue), have shown to moderately improve survival over the use of gemcitabine alone (Moore et al. 2007; Cunningham et al. 2009). However, others such as gemcitabine plus bevacizumad (VEGF inhibition) plus cetuximab (EGFR inhibition) have shown lack of sufficient efficacy (Ko et al. 2011).

We were interested to study the activity of the combined treatment gemcitabine and TK/GCV in the Ela-myc mouse model. Both GE and GCV are nucleoside analogues that interfere with DNA replication causing cell death by apoptosis (Wong et al. 2009), but GE is also an inhibitor of the ribonucleotidase reductase. We hypothesized that GE, through its activity as inhibitor of ribonucleotidase reductase, will lead to the reduction on the dNTP pool facilitating triphosphorilated-GCV incorporation into the DNA and consequently improving TK/GCV cytotoxicity. Moreover, Boucher et al demonstrated that GE enhanced the GCV-mediated bystander cytotoxicity *in vitro* and *in vivo* in s.c colon tumors (Boucher and Shewach 2005).

2.1. Evaluation of the anticancer effect of gemcitabine in cellular models and Ela-myc pancreatic tumors.

First, we determined the response to gemcitabine therapy *in vitro* and *in vivo* in the Ela-myc model. Emyc-3, NP-18 and RWP-1 pancreatic cancer cell lines were exposed to increasing doses of GE (0-10^5 μM) and three days later cell viability was determined by MTT assay. Dose-response curves were generated (Figure 16A) and ID_{50} values were calculated (Figure 16B).

The results showed that the ID_{50} value for the Emyc cell lines was significantly higher than that of the other pancreatic tumoral cell lines analyzed, suggesting that Emyc-3 cells were more resistant to gemcitabine cytotoxicity.

A

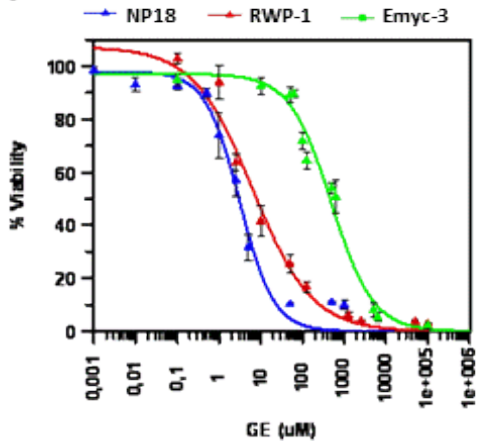

B

Cell line	ID_{50} (µM)
NP18	3.12 ± 0.37
RWP-1	6.37 ± 1.27
Emyc-3	489.27 ± 61.05

Figure 16. Gemcitabine cytotoxic study. A) Dose-response curves to gemcitabine (GE) in the pancreatic tumoral cell lines NP18, RWP-1 and Emyc-3. 3.000 cells were previously seeded in triplicate in a 96-well plate. Cells were treated at different GE concentrations. Cell viability was determined by an MTT assay 72h later. Values represent the mean ± SEM of at least 4 independent experiments. C) ID_{50} values of gemcitabine in the different tumoral cell lines.

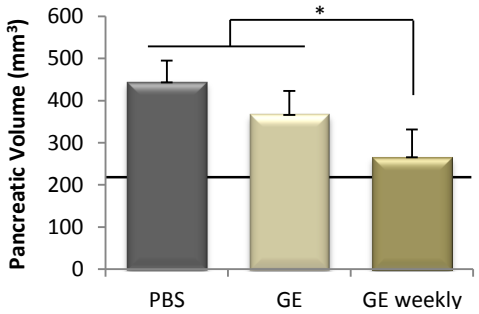

Figure 17. Antitumoral effect of gemcitabine in Ela-myc mice. Ela-myc mice of 11 weeks of age were treated with a single dose (160 mg/kg) or four doses of gemcitabine (160 mg/kg, once per week), corresponding to GE (n=9) and GE weekly (n=9) groups respectively. Non-treated PBS group received saline (n=10). Animals were sacrificed and pancreatic volume was measured six weeks after initial treatment. Black line corresponds to C57Bl6 (n=8) pancreatic volume (221.3 ± 8.7 mm^3). * $p<0.05$.

Next, we tested the antitumoral capacity of gemcitabine on Ela-myc pancreatic tumors. Two different gemcitabine treatments were applied to Ela-myc mice: animals received a single dose of gemcitabine (GE group, 160 mg/kg) or four doses of gemcitabine scheduled once per week (GE weekly group). Pancreatic volume was measured six weeks after the initial GE dose. As shown in Figure 17, GE weekly treatment significantly reduced the pancreatic volume of Ela-myc mice, whereas the reduction achieved by a single dose of GE was not statiscally significant. These data indicated that a weekly dose of gemcitabine (4 doses in total) showed antitumoral capacity.

2.2. Evaluation of the cytotoxic effects of the combination AduPARTat8TK/GCV plus gemcitabine in cellular models.

We evaluated whether the combination of gemcitabine and AduPARTat8TK/GCV therapy exerted a synergistic, additive or antagonistic effect on the Emyc cellular model. To this end, pharmacological interaction between gemcitabine and AduPARTat8TK/GCV treatments was assessed by Combination Index analysis (CI) in Emyc, NP18 and RWP-1 cell lines. Combination Index analysis is one of the most popular methods used to study *in vitro* drug interactions in combination cancer chemotherapy. A CI value <1 indicates synergism, =1 additivity and >1 antagonism between the drugs.

Cells were treated with either GE, AduPARTat8TK/GCV or a combination of both, and cell viability was determined by MTT assay three days later. Dose-response curves were constructed for each treatment alone or combined (Figure 18A) and Hill coefficient and ID_{50} value were calculated. These values were used to calculate the CI values for each Inhibitory Fraction (10%-90%) (Figure 18C). Dose-response curves corresponding to the combined therapy showed a shift to the left compared to single treatments, supposing a reduction in the ID_{50} value of each drug. Interestingly, this effect was higher in the Emyc cell line.

Figure 18. GE and AduPARTat8TK/GCV treatment interaction analysis. A) Dose-response curves for either gemcitabine (GE), AduPARTAT8TK/GCV or the combination of both treatments (TK+GE). 3.000 cells were seeded in triplicate in

A

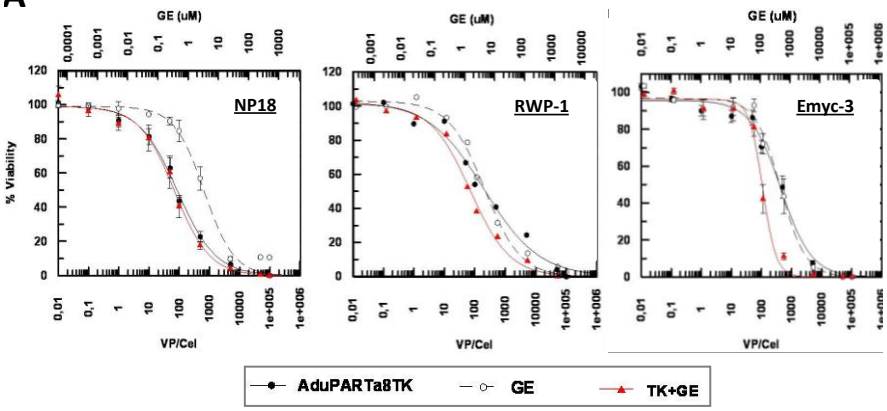

B

$$CI = \frac{\text{Combined TK doses}}{\text{Alone TK doses}} + \frac{\text{Combined GE doses}}{\text{Alone GE doses}}$$

>1: Antagonism
=1: Additivity
<1: Synergy

C

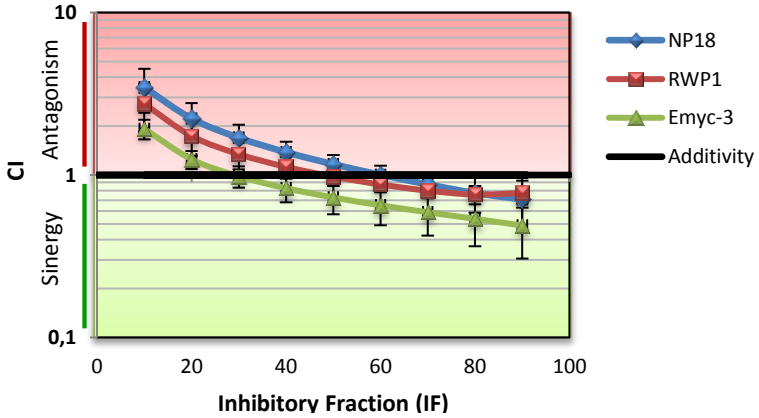

a 96-well plate. For single treatments, cells were transduced with a dose range of gemcitabine or AduPARTAT8TK, and four hours post-infection 100 µg/ml GCV was added. For the combined treatment cells were transduced with a dose range of AduPARTAT8TK (the same than in single treatment) and at 4h medium was replaced by fresh medium supplemented with GCV (100 µg/mL) and GE at the same dose range than in single treatment. Cell viability was determined by an MTT assay 72h later. Values represent the mean ± SEM of at least 4 independent experiments. B) Equation of Combination Index value for a specific Inhibitory Fraction. C) CI values for the interaction of gemcitabine and AduPARTat8TK/GCV treatments are depicted as a function of Inhibitory Fractions. Values represent the mean ± SEM of at least 3 independent experiments.

CI analysis revealed CI values lower than 1 for the majority of the Inhibitory Fractions in Emyc cells, indicating a synergistic effect of gemcitabine cytotoxicity when combined with AduPARTat8TK/GCV. On the contrary, CI values for NP18 and RWP-1 cells were higher than 1 or lied close to the additivity line, indicating that the combination of both treatments induced an antagonistic effect at low Inhibitory Fractions and only slightly improved drug cytotoxicity at higher IFs.

2.3. Evaluation of the antitumoral effect of gemcitabine combined with AduPARTat8TK/GCV therapy in Ela-myc pancreatic tumors.

Next, we studied whether the synergism between gemcitabine and AduPARTat8TK/GCV treatments identified *in vitro* was also observed *in vivo.* With this objective, two different treatment schedules were applied to Ela-myc mice (Figure 19A). Both protocols consisted on the i.d delivery of $5{\cdot}10^{10}$ vp of AduPARTat8TK followed by six doses of GCV plus three weekly doses of gemcitabine, and the posterior analyses of the pancreatic volume six weeks after initial treatment. In the COMB I protocol, the first dose of GE was co-administered with the fourth dose of GCV; whereas in the COMB II protocol the first dose of GE was administered the day previous to virus administration. The two protocols differed in the co-administration of both drugs with the objective to study possible differences in the outcome of the therapy due to GCV and GE interactions.

As shown in Figure 19B, both combined treatments significantly decreased the pancreatic volume of Ela-myc mice similarly to GE weekly and AduPARTat8TK/GCV treatments. This result suggested that the combined therapy of gemcitabine plus AduPARTat8TK/GCV showed an additive effect since no improvement nor diminution of single treatment antitumoral capacity was observed when combined. Moreover, no statiscally significant differences were found between the combined protocols assessed.

2.4. Toxicity analysis of the combined therapy AduPARTat8TK/GCV plus gemcitabine.

We had previously demonstrated that AduPARTat8TK i.d administered and combined with GCV did not produce pancreatic nor liver toxicity.

However, previous studies had demonstrated that gemcitabine administration led to an increase in the transaminases levels producing liver failure in particular cases (Fossella et al. 1997; Robinson et al. 2003). Therefore, we evaluated the potential toxicity of AduPARTat8TK/GCV therapy when combined with gemcitabine in Ela-myc mice (Figure 20).

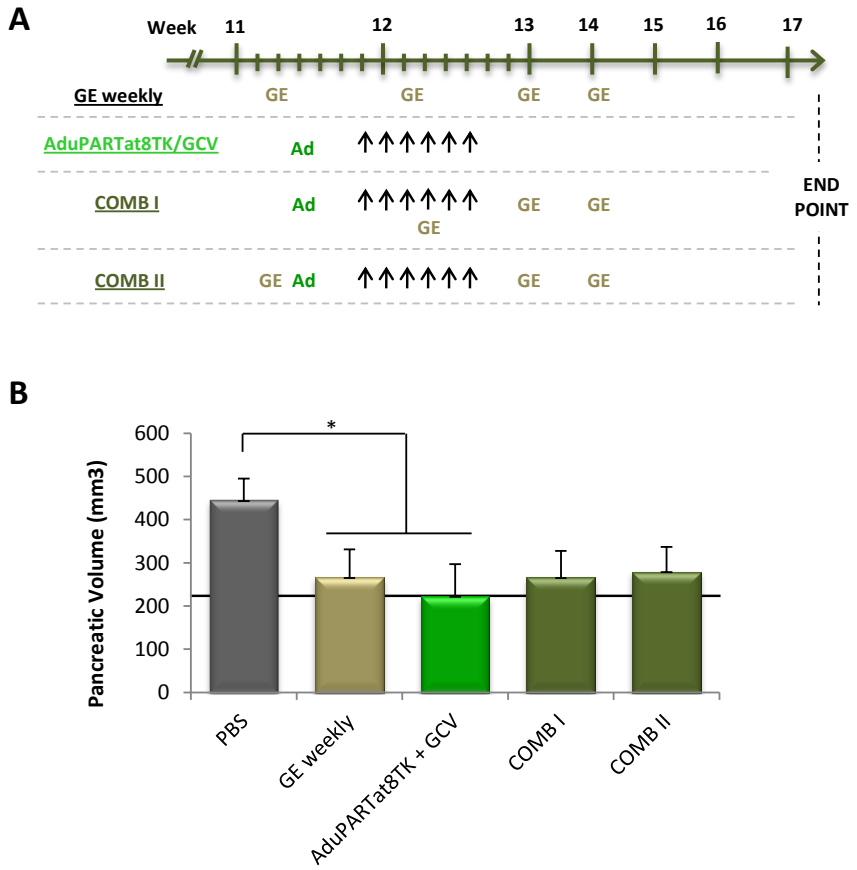

Figure 19. Antitumoral effect of gemcitabine and AduPARTat8TK therapy on Ela-myc pancreatic tumors. A) Protocol for evaluation of the combined therapy. B) Ela-myc mice of 11 weeks of age were treated with the indicated protocols and pancreatic volume was determined six weeks after initial treatment. PBS non-treated mice received i.d PBS. GE Weekly group (n=9) received four doses of gemcitabine (160mg/Kg, once per week). AduPARTat8TK/GCV group (n=10) received i.d $5{\cdot}10^{10}$vp of AduPARTat8TK and three days later GCV treatment (100 mg/kg, 6 doses) was initiated (arrows). COMB I (n=7) and COMB II (n=8) groups received i.d $5{\cdot}10^{10}$vp of AduPARTat8TK plus six doses of GCV (100 mg/kg) scheduled as indicated in A). Black line corresponds to C57Bl6 (n=8) pancreatic volume (221.3 ± 8.7 mm^3). * $p<0.05$.

Gemcitabine addition to the AduPARTat8TK/GCV therapy led to an increase in the transaminases levels although only AST values were over the reference range. Interestingly, lower values were found at day 25 and 39 after virus administration probably related to the finalization of the gemcitabine treatment. GE addition also increased the serum levels of amylase and lipase although to a lesser extent than with transaminases values.

These data indicated that the combined therapy of AduPARTat8TK/GCV plus gemcitabine ameliorated tumor-associated toxicity but produced minor liver damage.

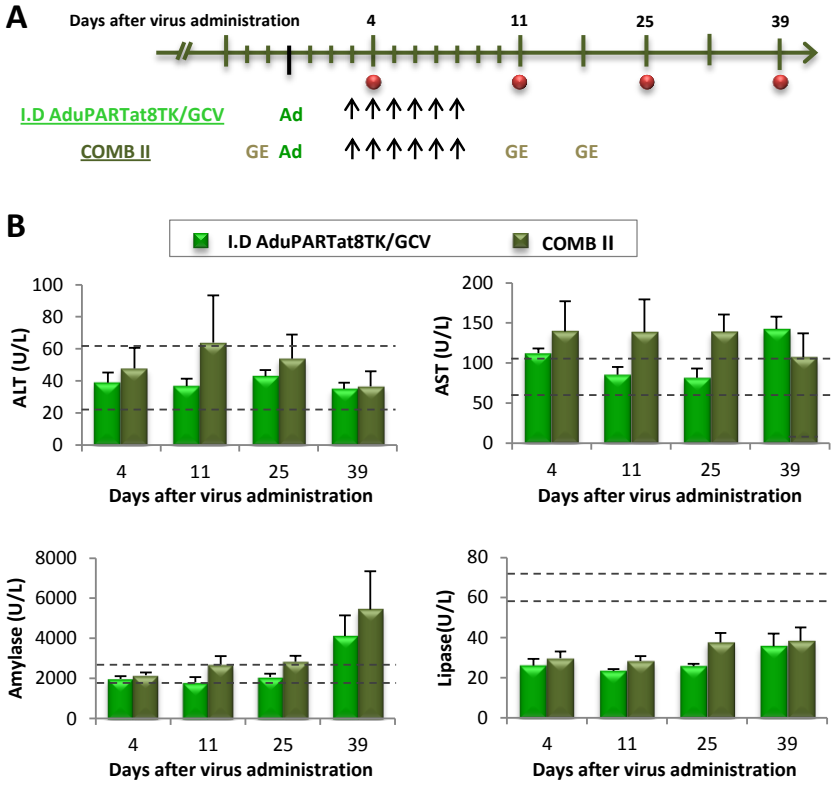

Figure 20. AduPARTat8TK/GCV toxicity studies in Ela-myc mice. A) Protocol for evaluation of pancreatic and liver toxicity of AduPARTat8TK/GCV combined therapy. Times of blood sample acquisition are indicated with red circles. B) Analysis of ALT, AST, amylase and lipase serum levels in treated Ela-myc mice at 4, 11, 25 and 39 days after virus administration. AduPARTat8TK/GCV therapies followed the same protocol than in Figure 19. Treated mice n=5 per group. Dash lines indicate reference values from untreated C57Bl/6 mice (n=6).

3. DEVELOPMENT OF A TRANSDUCTIONAL TARGETING STRATEGY TO IMPROVE ADENOVIRUS INFECTIVITY AND PROVIDE WITH PANCREATIC TUMOR SELECTIVITY.

To confer adenoviral-based therapies with improved antitumoral activity we have designed genetically engineered virus with specific fiber modifications in order to increase adenoviral tumor cell transduction and tumor selectivity.

Previous studies had demonstrated the capacity of the protein transduction domain TAT to successfully transduce living cells when fused to several therapeutically active macromolecules (Kashiwagi et al. 2007; Essafi et al. 2011; Yu et al. 2011). In this thesis, we have genetically introduced the 11aa TAT_{PTD} into the C-terminal end of the fiber protein of AdTAT and AdTATMMP with the objective to improve adenovirus infectivity in a CAR independent manner.

To achieve tumor-selectivity we have benefit of the elevated expression of matrix metalloproteases (MMPs) found in primary and metastatic tumors (Matsuyama et al. 2002). We have generated the MMP activatable adenovirus AdTATMMP which expressed the TAT_{PTD} blocked by a polyanionic sequence. This blocking sequence was linked to TAT_{PTD} by an MMP cleavable sequence which would lead to vector tumor selectivity by restricting virus activation to MMP2/9 presence.

To reduce adenovirus liver sequestration we have incorporated the YTRGE mutations into the fiber protein of AdTATMMP. These mutations have been shown to significantly reduce adenovirus binding to CAR receptor and to the blood factors C4BP and FIX, resulting in decreased liver transduction and hepatotoxicity *in vivo* (Shayakhmetov et al. 2005).

3.1. Characterization of MMP2/9 expression in a battery of cell lines.

First we analyzed the expression of MMP-2 and MMP-9 in a battery of cell lines in order to identify cellular models to test the activity of the new engineered MMP-activatable adenovirus. MMP2/9 expression was analyzed by western blot and gelatin zymography. MMPs are secreted by cells as inactive zymogens requiring of its posterior activation. Western

blot and zymography techniques detect the different forms of MMP generated during its activation: zymogen, pre-active and active forms.

Confluent cell cultures of PANC-1, RWP-1, Emyc-3, HT1080 and NIH-3T3 cell lines were grown for 24h in serum free medium. Then, the conditioned medium was harvested, concentrated up to 30 µl and the same sample was analyzed by WB and zymography (Figure 21). Immunoblot analyses revealed elevated MMP9 expression in PANC-1 cells, and moderate and low expression levels in HT1080 and Emyc-3 cell lines, respectively. No MMP9 expression was detected in NIH-3T3 cells. By contrast, zymogram analyses detected MMP9 expression in all the studied cell lines, although intense bands were shown for active MMP9 in PANC-1 cells and the zymogen forms in HT1080 and RWP-1 cells.

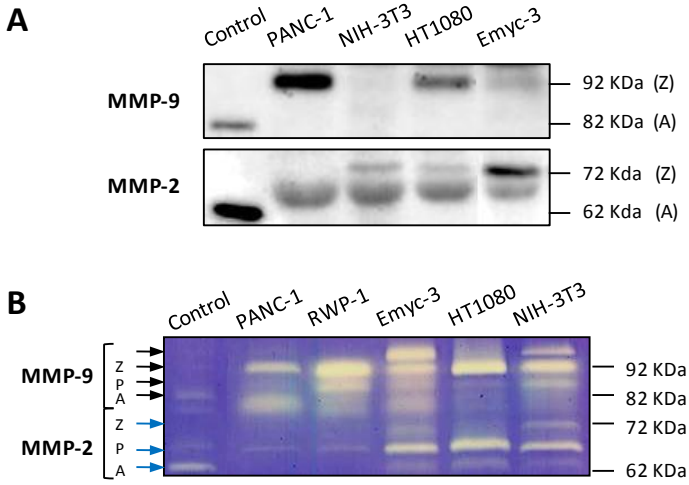

Figure 21. MMP-9 and MMP-2 expression analysis. A) Western blot analysis of MMP-9 and MMP-2 levels in concentrated conditioned media. Control lanes correspond to 50 ng of MMP-9 or MMP-2. B) Gelatin zymography analysis of MMP-9 and MMP-2 activity levels in concentrated conditioned media. Control lane corresponds to 2 ng of MMP-9 and 2ng of MMP-2. Z: zymogen form, P: pre-active form, A: active form.

MMP2 expression was detected in all the studied cell lines by WB and zymography. High expression levels were observed in HT1080, Emyc-3 and NIH-3T3 cells. Differences observed in MMP expression between WB or zymography analyses may be due to the highest zymography sensitivity as its detection limit is in the range of nanograms.

3.2. Proof of concept: the MCP peptide.

To test the feasibility of the engineered system, in which the TAT peptide would be initially blocked and only exposed upon MMP activation, the Metalloproteinase Cleavable Peptide (MCP) was synthetized by the group of Dr. David Andreu (Proteomics and Protein Chemistry Unit, Department of Experimental Health Sciences, Universitat Pompeu Fabra). MCP peptide consisted on 11 Aa corresponding to TAT_{PTD} linked by a MMP2/9 target sequence to a polyanionic sequence whith the aim to neutralize the polycations of the TAT sequence by forming intramolecular hairpins (Figure 22). We used an optimized MMP2/9 cleavable linker that was demonstrated to efficiently and specifically recognize MMP-2 and MMP-9 proteins (Szecsi et al. 2006).

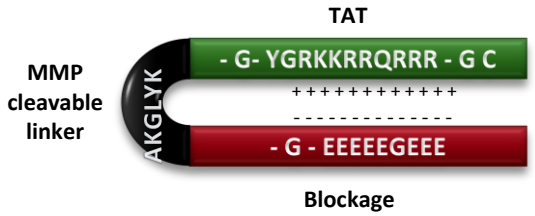

Figure 22. MCP peptide scheme.

First, we tested the capacity of the MMP linker to be recognized and cleaved by MMPs. The MCP peptide was incubated in the presence of recombinant MMP-2 for 4h. At specific time points samples were collected and analyzed in an HPLC (Figure 23). Three separated peaks were detected in the HPLC chromatograms corresponding to the MCP peptide and the products resulted as a consequence of its cleavage: the TAT and the polyanionic sequences. At 240 min, only the two peaks corresponding to TAT and polyanionic sequences were detected, indicating that the MCP peptide was completely cleaved.

These results indicated that the MMP target sequence of the MCP peptide was recognized by recombinant MMP-2, producing MCP peptide complete cleavage in 4h.

Next, we studied whether the MMP cleavable linker was recognized and cleaved by endogenous MMPs, and whether the MCP peptide was able to introduce a cargo molecule (fluorescein) into cells. To this end, the MCP* peptide was generated by linking fluorescein to the TAT domain of the MCP peptide. PANC-1 and NIH-3T3 cells were incubated with the MCP* peptide for 3 hours and then were visualized under a fluorescence

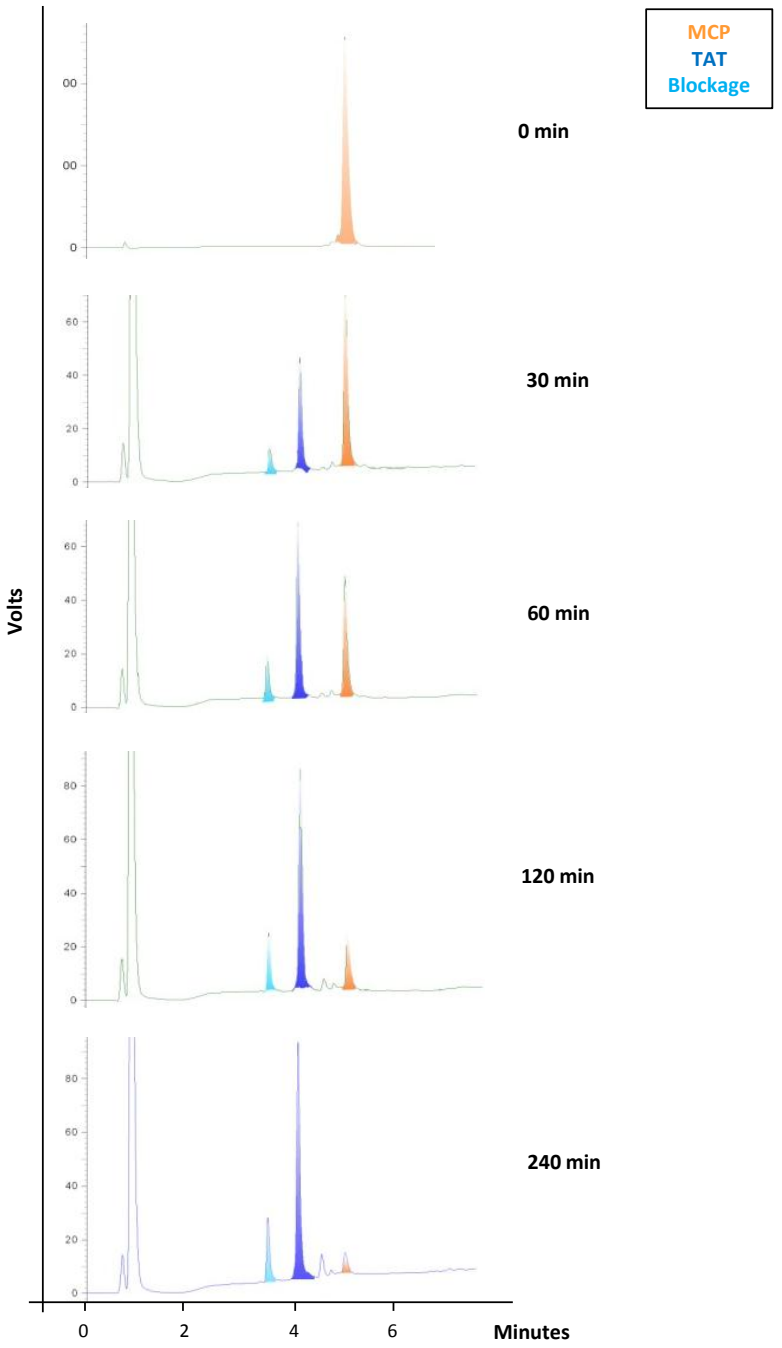

Figure 23. MCP cleavage by recombinant MMP-2. 0.5 mM MCP was incubated with 2.5 µg recombinant MMP-2 at room temperature for 4h. Samples were obtained at 0, 30, 60, 120 and 240 min and were analyzed by HPLC. Each graphic corresponds to the HPLC chromatogram obtained for each time of analyses.

microscope (Figure 24). Fluorescence emission was detected in PANC-1 cells but not in NIH-3T3 cells indicating that MCP* peptide entered in PANC-1 but not in NIH-3T3 cells. Considering the different content of MMP in PANC-1 (elevated) and NIH-3T3·cells (low) these results suggested that the MCP* peptide was recognized and cleaved by endogenous MMPs triggering MMP2/9 specific cell transduction.

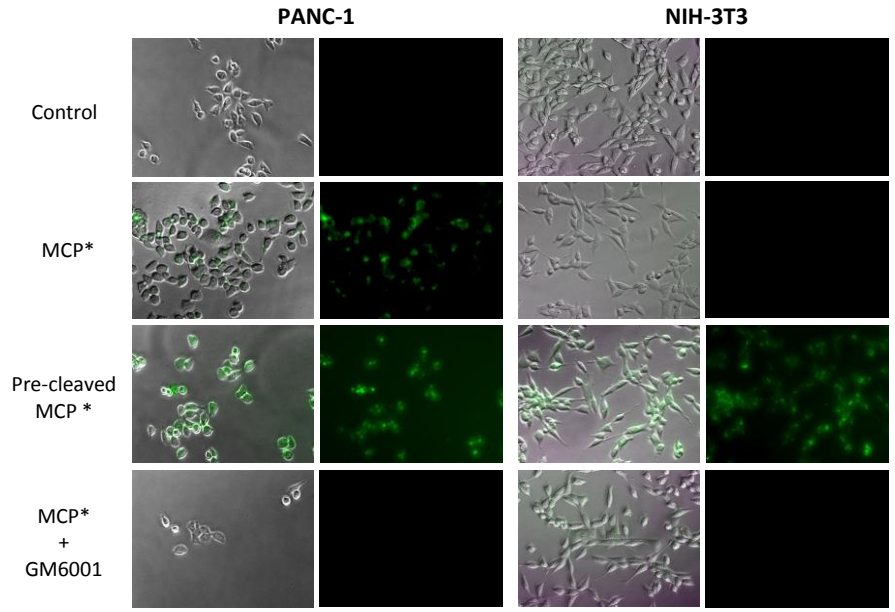

Figure 24. Study of MCP cleavage by cells. 10.000 cells were seeded in triplicate in a 96-well plate. 16h later, medium was removed and 100 µl of serum free medium containing 10 µM MCP*, 10 µM pre-cleaved MCP* or 10 µM MCP* plus 20 µM GM6001 were added. Three days later, cells were visualized under a fluorescence microscope. Pre-cleaved MCP* resulted from the incubation of MCP* peptide with 2.5 µg of MMP2 for 9h. Representative fluorescent images from one of three independent experiments are shown.

To further analyze MMP2/9 dependent entrance of the MCP* peptide, cells were incubated with pre-cleaved MCP* or with MCP* in the presence of the GM6001 MMP inhibitor. Pre-cleaved MCP* entered in both PANC-1 and NIH-3T3 cells independently of MMP expression. By contrast, MCP* was not able to enter PANC-1 cells in the presence of GM6001. These results suggested that MCP* peptide was recognized and cleaved by endogenous MMPs and that its transduction capacity was dependent on MMP presence.

3.3. AdTATMMP transduction efficiency in cellular models.

3.3.1. AdTAT and AdTATMMP generation.

In light of the obtained results, we generated the reporter adenoviruses AdTAT and AdTATMMP (Figure 25A) as explained in section of Materials and Methods. We incorporated in our studies the AdYTRGE as a control virus of the mutated fiber and AdCMVGFPLuc as control of non-mutated fiber. AdCMVGFPLuc, AdYTRGE, AdTAT and AdTATMMP viruses expressed the reporter cassette CMVGFPCMVLuc that consisted on the GFP and firefly luciferase genes controlled by the CMV promoter (Figure 25). To verify correct fiber gene expression, HEK293 cells were infected with adenoviral vectors, and two days later total DNA was obtained and the fiber gene was analyzed by PCR (Figure 25B). Fiber PCR fragments of different sizes corresponding to fiber specific mutations were identified. Correct fiber sequences were verified by the sequencing of PCR products.

To confirm that the mutated fibers were correctly incorporated into the viral capsid, purified viruses were resolved in an SDS-polyacrylamide gel and silver stained. No changes in protein content of the viral capsid were observed (Figure 25C).

These results demonstrated the integrity of the viruses and confirmed that the modified fibers were correctly expressed and incorporated into the viral capsids of AdYTRGE, AdTAT and AdTATMMP.

3.3.2. Analysis of AdTATMMP transduction efficiency after activation by MMP2/9.

We evaluated the capacity of AdTATMMP to be activated by MMPs. AdTATMMP was incubated with 10 ng/µl of recombinant MMP2 or MMP9 at 37° for 2h. HT1080, PANC-1 and NIH-3T3 cells were then cultured in the presence of AdTATMMP or the MMP2 and MMP9 pre-cleaved viruses, and three days later luciferase expression was measured. As shown in Figure 26A, MMP2 and MMP9 pre-cleaved AdTATMMP exhibited higher luciferase expression than AdTATMMP in all the studied cell lines, indicating higher transduction efficiency of AdTATMMP upon MMP cleavage. The highest luciferase expression was detected upon MMP9 cleavage, probably because the MMP target sequence was better recognized by MMP9 than by MMP2 (Liu and Muruve 2003; Greenlee et al. 2006). In non-precleaved AdTATMMP experiments HT1080 cells were

the most efficiently transduced followed by PANC-1 and NIH-3T3 cells; this could be related to the activity of endogenous MMPs.

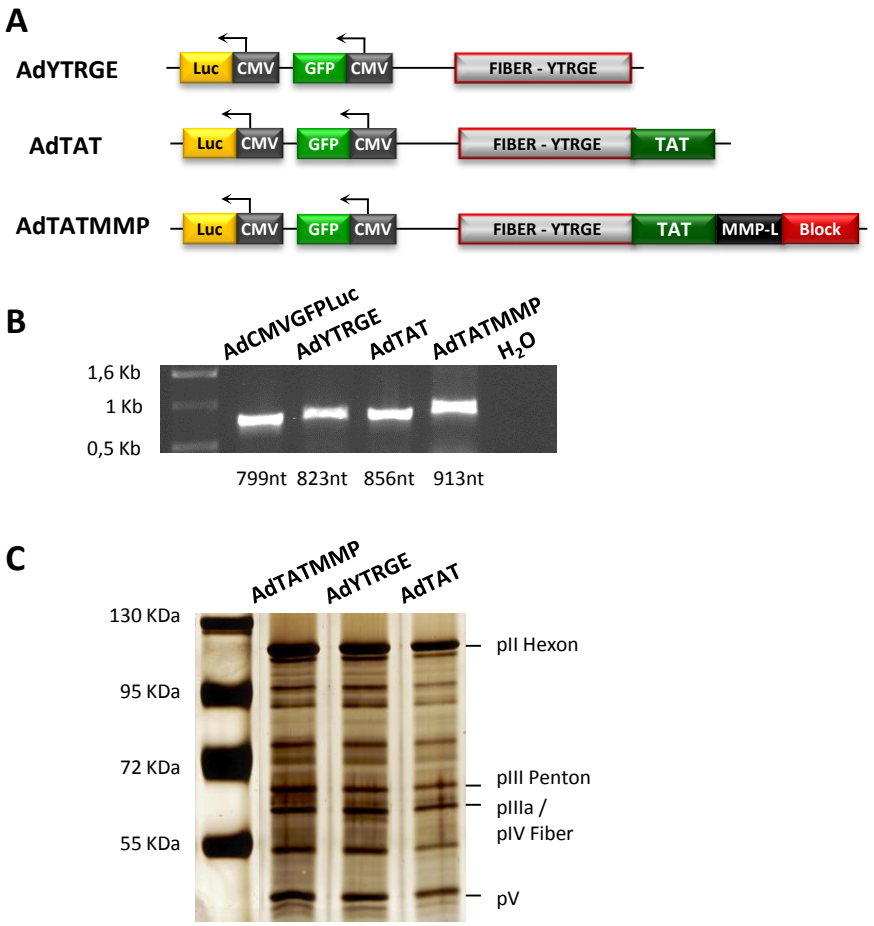

Figure 25. AdTAT and AdTATMMP fiber characterization. A) Schematic representation of AdYTRGE, AdTAT and AdTATMMP adenoviruses. B) Fiber analyses by PCR. HEK-293 cells were infected with 2µl of purified adenovirus. Two days later, cells were harvested and total DNA was obtained and used for PCR analyses. C) 10^{10} vp of purified viruses were lysed, resolved in a 10% SDS polyacrylamide gel and silver stained.

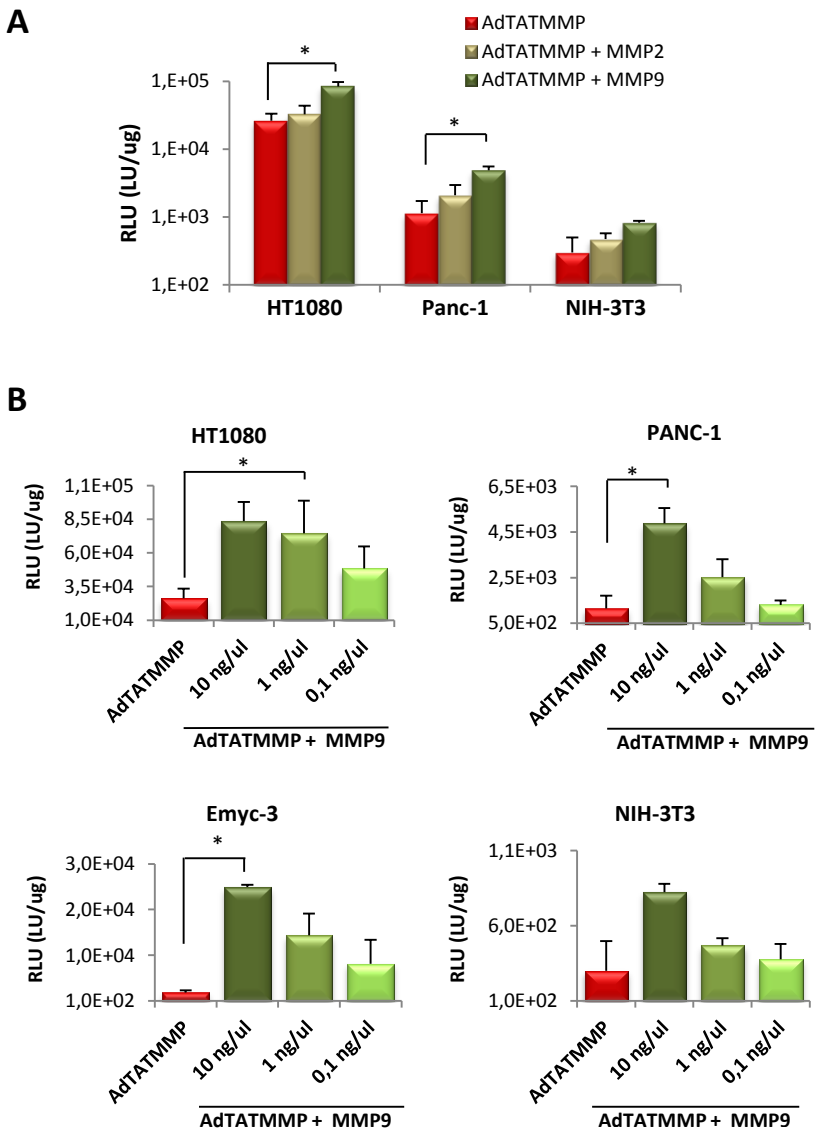

Figure 26. AdTATMMP infection after MMP2/9 pre-cleavage. A) 10.000 cells were seeded in triplicate in a 96-well plate. The next day, AdTATMMP was incubated with 10ng/µl MMP9 or MMP2 in FBS-depleted medium at 37°C for 2h. Cells were infected at 1.000 vp/cell with AdTATMMP or the pre-cleaved AdTATMMP and 6h later, virus was removed and cells were further cultured in FBS medium. Luciferase expression was measured 3 days later. Results are represented as the mean ± SEM of 2 independent experiments. B) The experiment was done as in panel A but MMP-9 doses were 10 ng/µl, 1 ng/µl or 0.1 ng/µl. Results are represented as the mean ± SEM of 3 independent experiments. * $p<0.05$

To further evaluate the MMP–dependent activation, cells were infected with AdTATMMP pre-cleaved with three different doses of MMP-9 (10ng/µl, 1 ng/µl and 0.1 ng/µl), and three days later luciferase expression was measured. A dose response effect was observed in all the cell lines analyzed being the maximum luciferase activity detected at the highest MMP-9 dose used (Figure 26B).

These results suggested that AdTATMMP was cleaved by MMP2/9 leading to an increase in the viral transduction capacity of AdTATMMP.

3.3.3. Evaluation of AdTATMMP transduction efficiency. Comparative study with AdTAT, AdYTRGE and AdCMVGFPLuc.

Next, we studied the transduction capacity of AdTATMMP in a battery of cell lines that exhibited different MMP9/2 activities and compared to the CAR-ablated viruses AdYTRGE and AdTAT and to the CAR-dependent AdCMVGFPLuc. Cells were transduced with 1.000 vp/cell of AdCMVGFPLuc, AdYTRGE, AdTAT or AdTATMMP in the absence of FBS. After 6h the medium was changed for fresh FBS+ medium, and luciferase expression was measured three days later.

A very low transduction capacity was observed for AdYTRGE when compared to AdCMVGFPLuc in all the cell lines analyzed in agreement with the knowledge that CAR ablation hindered adenoviral infection *in vitro* (Figure 27A). AdTAT and AdTATMMP viruses rescue adenovirus transduction capacity. Interestingly, AdTATMMP transduced cells more efficiently than AdTAT. A possible explanation could rely on structural differences in the modified fibers resulting in conformational changes that facilitate TAT domain presentation in AdTATMMP adenovirus. However, this remains to be demonstrated. Interestingly, AdTATMMP transduction capacity was from 2 to 4-folds higher than AdTAT and differences increased in cells that express MMP9/2 (Figure 27B). These results indicated that TAT_{PTD} insertion restored the transduction capacity of a CAR ablated adenovirus and that AdTATMMP presents with improved transduction than AdTAT.

To further analyze the infection capacity of AdTATMMP, we evaluated its transduction efficiency in a battery of cell lines with different susceptibility to adenoviral CAR mediated infection. To this end, cells were exposed to

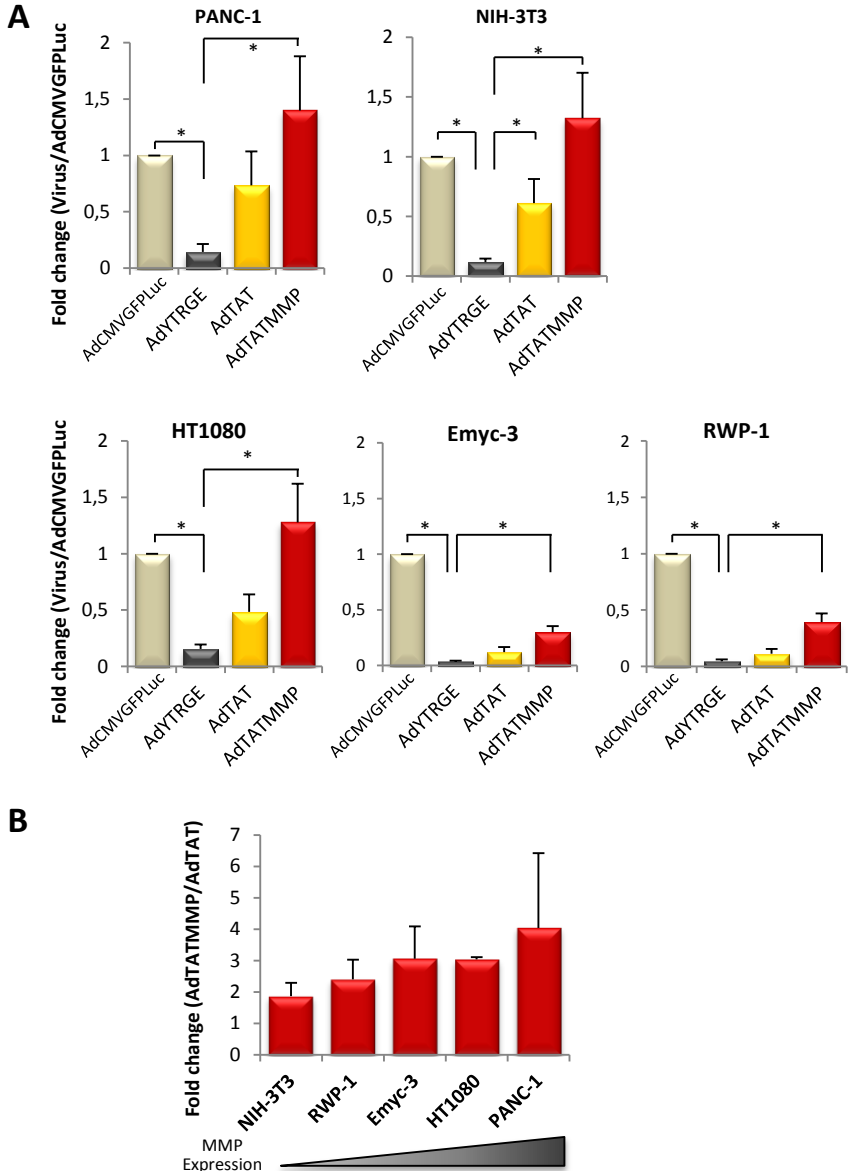

Figure 27. Transduction efficiency of AdTATMMP, AdTAT, AdYTRGE and AdCMVGFPLuc at 1.000 vp/cell. 10.000 cells were previously seeded in triplicate in a 96-well plate. Cells were infected with 1.000 vp/cell of AdCMVGFPLuc, AdYTRGE, AdTAT or AdTATMMP in medium FBS-. 6h later, virus was removed and FBS+ medium was added. Luciferase expression was measured 3 days later. Results are represented as the mean ± SEM of 3 independent experiments. A) Luciferase expression relativized to that of AdCMVGFPLuc. * $p<0.05$. B) Luciferase expression of AdTATMMP relativized to that of AdTAT. Cell lines were plotted according to their MMP expression levels.

AdCMVGFPLuc or AdTATMMP at 10^4 vp/cel and luciferase expression was measured three days later (Figure 28).

Luciferase activity in PANC-1 and NIH-3T3 cells transduced with AdTATMMP adenovirus was significantly higher than that achieved with AdCMVGFPLuc indicating that transduction with AdTATMMP virus was more efficient than with AdCMVGFPLuc. However, similar luciferase activity was detected in HT1080 and Emyc-3 cells between the two viruses whereas decreased levels were detected in RWP1 cells transduced with AdTATMMP.

These data indicates that AdTATMMP improved adenoviral infection in cell lines with low susceptibility to CAR-mediated infection.

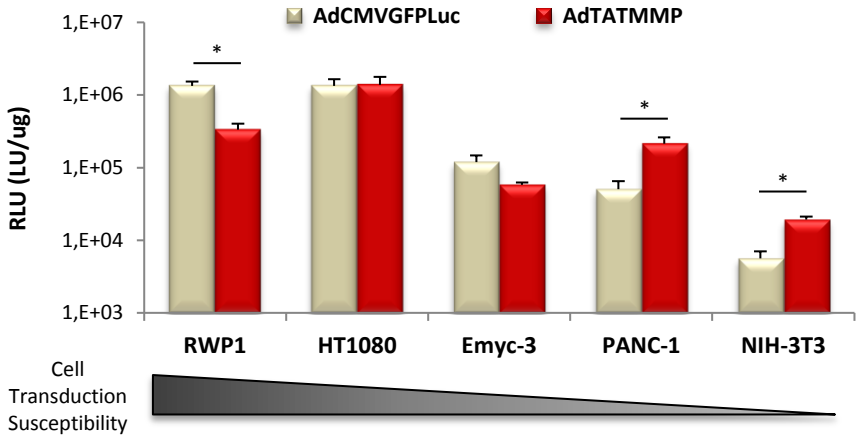

Figure 28. Transduction efficiency of AdTATMMP and AdCMVGFPLuc at 10.000 vp/cell. 10.000 cells were seeded in triplicate in a 96-well plate. Cells were infected with 10.000 vp/cell of AdCMVGFPLuc or AdTATMMP in medium FBS-. 6h later, virus was removed and FBS+ medium was added. Luciferase expression was measured 3 days later. Results are represented as the mean ± SEM of 3 independent experiments.

3.4. AdTATMMP biodistribution after systemic administration to Ela-myc mice.

The next step was to evaluate AdTATMMP onselectivity *in vivo* in Ela-myc mice. $5{\cdot}10^{10}$ vp of AdYTRGE or AdTATMMP were intravenously administered into Ela-myc mice at 11 weeks of age and four days later luciferase activity in liver and pancreatic tissue was measured in the bioluminescent system IVIS50. AdTATMMP led to a slight increase in liver

transduction of 1.4 times respect to AdYTRGE (Figure 29). Interestingly, luciferase activity in the pancreas of Ela-myc mice with tumor nodules was 7.3 times higher than that of AdYTRGE. Thus, AdTATMMP increased tumor/pancreas transduction probably through tumor MMP viral activation.

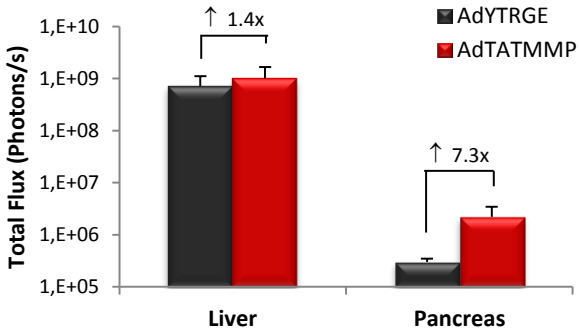

Figure 29. Liver and pancreas AdTATMMP transduction efficiency in Ela-myc mice. $5 \cdot 10^{10}$ vp of AdYTRGE (n=3) or AdTATMMP (n=4) were intravenously administered into Ela-myc mice at 11 weeks of age. Four days later bioluminiscence emission of isolated organs was measured. Luciferase expression was quantified from captured images and expressed as photons/s.

4. EVALUATION OF THE EFFICACY OF IRREVERSIBLE ELECTROPORATION (IRE) TO TREAT PANCREATIC TUMORS.

It is estimated that from the 85% of patients with unresectable PDAC, 25% present locally advanced PDAC, and the rest are metastasic (Kern et al. 2011). Irreversible electroporation (IRE) has been proposed as a method for solid tumor ablation. This technology is based on the application of high-voltage pulses with a duration of microseconds to milliseconds to induce plasma membrane defects leading to cellular death. Interestingly, this method does not affect large blood vessels (Rubinsky 2007), which make it suitable for treatment of unresectable cancers with a complicated anatomical situation, as in pancreatic cancer

In this thesis, we decided to evaluate the feasibility of IRE for the treatment of PDAC in an orthotopic mouse model. This work was done in collaboration with Dr. Luciano Sobrevals.

4.1. Generation and characterization of BxPC-3-Luc orthotopic tumor model.

To study the therapeutic effect of irreversible electroporation (IRE) on pancreatic tumors, we developed a pancreatic cancer model by orthotopic implantation of BxPC-3-Luc cells in the body of the mouse pancreas (Figure 30A). The expression of luciferase by BxPC-3-Luc cells allowed us to follow-up the tumoral growth, as well as the dissemination of tumoral cells to other organs, through the use of the *in vivo* bioluminescent system IVIS50. BxPC-3 xenografts were very aggressive tumors when implanted orthotopically (Lee et al. 2010a), the tumor growth rate was elevated and, in the majority of animals, the tumor ended up disseminating through the peritoneal cavity. Histologically, BxPC-3 tumors showed the ability to infiltrate the pancreatic parenchyma (Figure 30B).

4.2. Evaluation of IRE treatment on tumor progression and mice survival.

With the objective to follow-up tumor growth, luciferase expression of BxPC-3-Luc tumor-bearing mice was monitored once a week until the dead of the animal. Animals were irreversible electroporated (IRE

treated group) or sham electroporated (Untreated group) when the luciferase counts were within the range of 10^6-10^7 photons/s, that corresponded to day 32-43 after tumor implantation and to a tumor volume of 95.79±29.59.

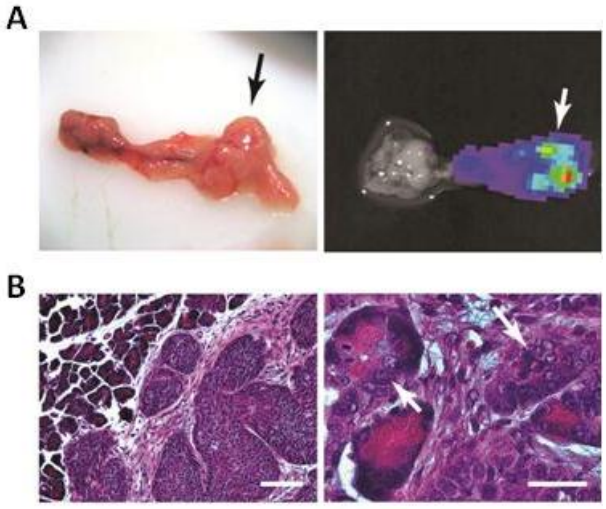

Figure 30. BxPC-3-Luc orthotopic human tumoral model. A) Representative images of tumor aspect (left panel) and luciferase signal (right panel) of orthotopic pancreatic BxPC-3-luc tumors. Black arrow indicates tumoral masses within the pancreas and white arrow indicates luciferase positive area, corresponding to the tumoral masses. B) H&E staining of representative orthotopic BxPC-3-Luc tumors. Left and right scale bar: 100 µm and 25 µm, respectively. White arrows indicate tumoral cells invading healthy acinar cells.

IRE treatment consisted on the application of an IRE pulse train to a pancreatic tumor situated between the tweezertrodes. The process is described in detail in section 5.4 of Materials and Methods. The IRE pulse train consisted on 10 sequences of 10 pulses each, separated by 10s each sequence. Each pulse was of 2500 V/cm diameter tumor, with duration of 100 µs and separated by 1s each pulse. The whole electroporation treatment consisted on 100 pulses in total.

IRE pulse train = 10 x Sequences. *10s between sequences*.

Sequence = 10 pulses x 2500 V/cm. *100µs each pulse and 1s between pulses (1Hz).*

Four days after IRE treatment, the treated group presented significantly lower luciferase activity than control mice. For most of the animals luciferase values remain low or undetectable for all the period analyzed, suggesting a reduced tumor progression or tumor eradication; however in a small subset of mice, 30 days post-IRE treatment luciferase activity increased, indicative of tumor regrowth (Figure 31).

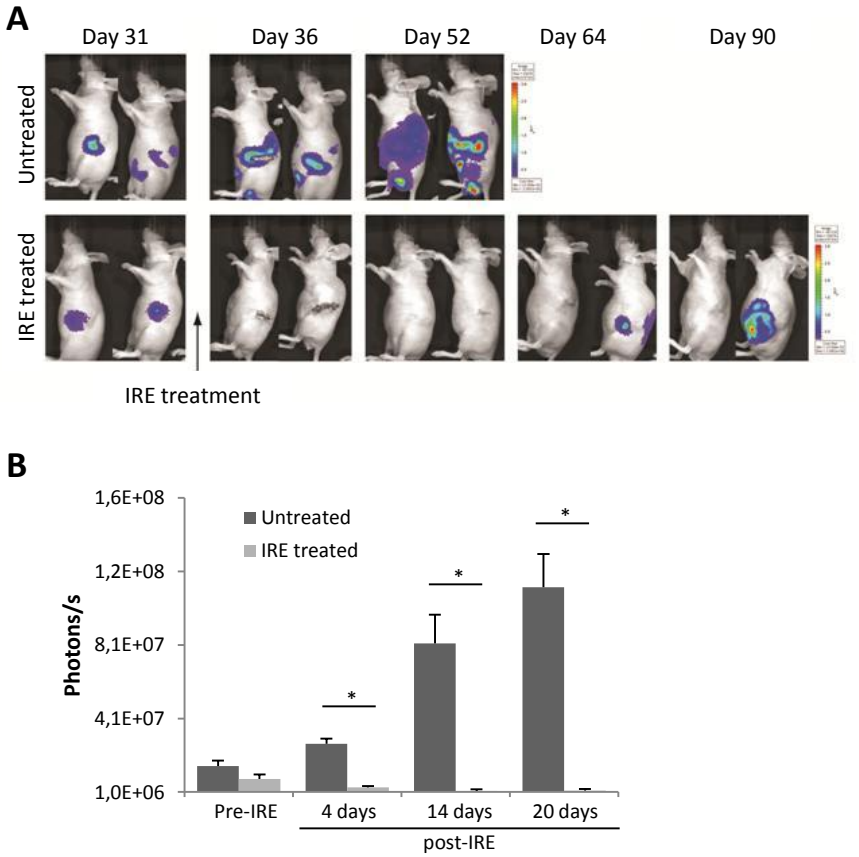

Figure 31. IRE treatment effect on tumor progression. BxPC-3-Luc orthotopic tumors were generated in nude mice. When the luciferase counts were within the range of 10^6-10^7 photons/s, animals were irreversible electroporated. A) Representative images of bioluminescent emission from untreated or IRE-treated BxPC-3-Luc tumor-bearing mice, at different time points. B) Luciferase quantification of bioluminescent emission images from untreated (n=7) and IRE-treated (n=12) BxPC-3-Luc tumor-bearing mice, before (pre-IRE) and after 4, 14 and 20 days of IRE treatment. Results are expressed as photons per second. Values are represented as mean ± SEM. *$p < 0.01$

IRE treatment prolonged mouse survival and increased the median survival time from 42 days in untreated mice, up to 88 days in the IRE-treated group (Figure 32). At the end of the experiment 25% of mice presented complete tumor eradication.

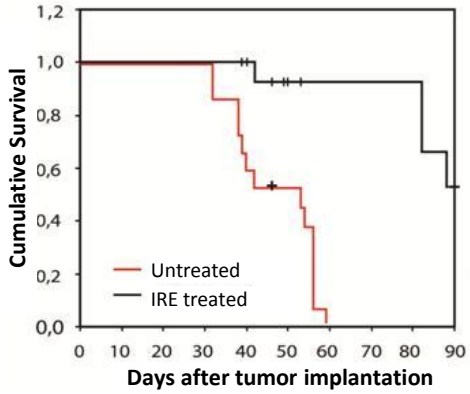

Figure 32. Survival analysis of BxPC-3-Luc tumor bearing mice after IRE treatment. BxPC-3-Luc orthotopic tumors were generated in nude mice and irreversible electroporated when the luciferase counts were within the range of 10^6-10^7 photons/s. Kaplan-Meier analyses survival curve (log-rank test, $p<0.01$). Untreated group n=15, IRE treated group n=18. Crosses indicate censored mice.

4.3. Evaluation of the pancreatic pathological alterations produced by IRE treatment.

Next, we analyzed the pathological alterations produced in the pancreas by irreversible electroporation. For this, we assessed gross morphology, histological analysis and immunohistochemical studies in the pancreas of treated animals at days 1, 7 and 14 post-IRE, as well as in non-treated animals.

4.3.1. Gross morphology and histological analysis.

With the objective to analyze the effect of IRE treatment on tumor/tissue morphology, pancreas/tumors from untreated and IRE-treated mice were obtained at 1, 7 and 14 days after electroporation. Tumors of untreated animals were visualized as a mass of white bright color. In contrast, treated tumors at days 1 and 7 post-IRE revealed an intense brown area covering the tumor, suggestive of blood accumulation. At day 14 post-IRE a yellow mass of strong intensity in the periphery was

observed defining a well-demarcated tumor, indicative of necrosis (Figure 33A).

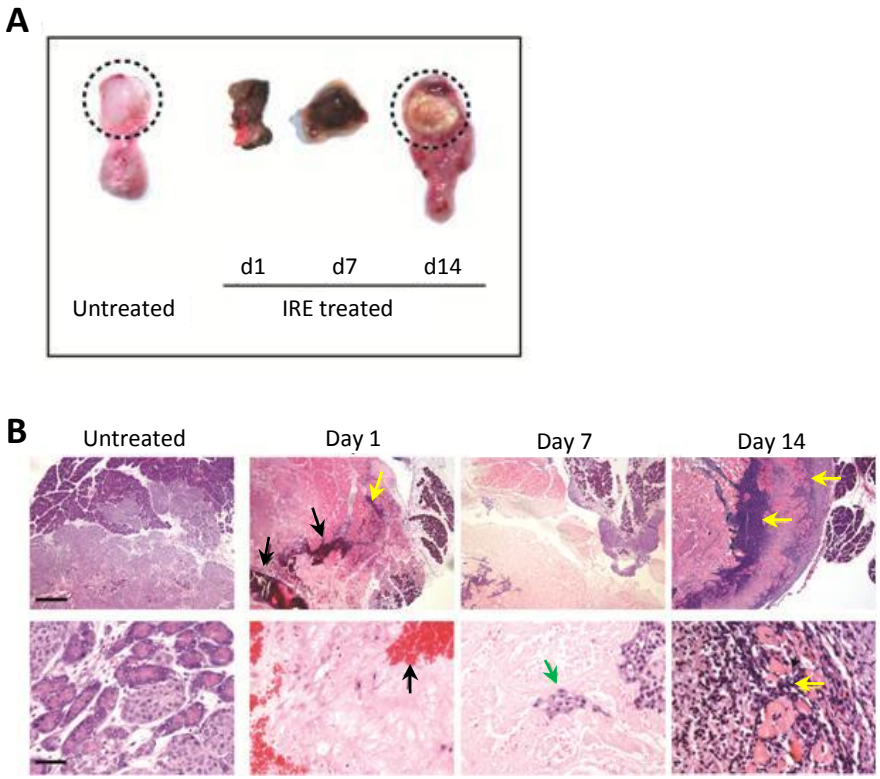

Figure 33. IRE treatment effect on tumor morphology. BxPC-3-Luc orthotopic tumors were generated in nude mice and IRE treated when the luciferase counts were within the range of 10^6-10^7 photons/s. Animals were sacrificed at the indicated time points, and the pancreas was obtained. A) Representative tumors from untreated (n=2) and IRE-treated mice, showing the macroscopic effect of electroporation at day 1 (n=2), 7 (n=4) and 14 (n=4). B) H&E staining of BxPC-3-Luc tumors untreated and IRE-treated at 1, 7 and 14 days. Black arrows indicate hemorrhagic reaction, green arrow indicates islands of tumoral cells immersed into necrotic tissue and yellow arrows point at lymphocytic infiltrates. Scale bar 400 µm (top panel) and 50 µm (bottom panel).

Histological tissue examination after IRE treatment (Figure 33B) revealed an extensive necrotic area, evident since day 1. At day 1 post-IRE a large number of red blood cells were visualized suggesting vascular disruption as a consequence of the procedure. At day 7 post-IRE extensive areas of necrotized tissue were observed, as well as the presence of lymphocytic infiltrates and histiocytes, that was much more remarkable at day 14.

In some animals residual viable tumoral cells were present within the electroporated tumor, and curiously, at day 14 post-IRE, small non-electroporated nodules were also found distant to the electroporated tumor suggesting that at the moment of IRE procedure these nodules were not detected. These nodules could be a factor implicated on the tumor regrowth detected in some animals despite a good response to IRE treatment.

Regions of non-viable epithelium of the pancreatic parenchyma were also observed in some animals, probably due to the inclusion of a portion of normal pancreas between the plate electrodes during the IRE procedure.

4.3.2. Analysis of tumor cell viability in IRE treated mice.

We next analyzed the effect of IRE treatment on tumoral cell proliferation by staining with Ki67, a well-known marker of cell proliferation, in sectioned pancreas. Strong immunoreactivity was observed in untreated tumors, indicative of active proliferating tumors. In contrast, most of the treated tumors analyzed were Ki67 negative at all the time-points. In particular, some remnant proliferating cells positive for Ki67 were identified within or at tumor periphery, especially at day 1 post-IRE, probably indicating an incomplete IRE effect (Figure 34).

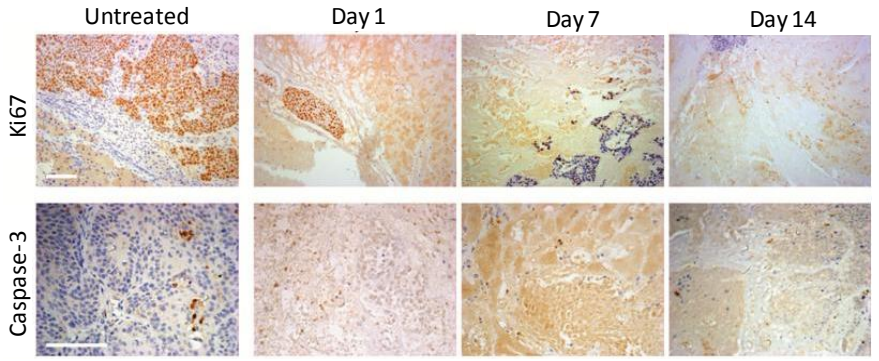

Figure 34. IRE treatment effect on proliferation and apoptosis. BxPC-3-Luc orthotopic tumors were generated in nude mice and IRE treated when the luciferase counts were within the range of 10^6-10^7 photons/s. Animals were sacrificed at the indicated time points, and the pancreas was obtained and embedded in paraffin. Immunohistochemical analysis in untreated and IRE-treated mice at days 1 (n=2), 7 (n=4) and 14 (n=4) after treatment was performed. Representative images of anti-Ki67 and anti-active caspase-3 immunostaining are shown. Scale bar: 100 µm.

To study whether IRE treated tumors suffer from apoptotic cell death, we analyzed the presence of activated caspase-3. No caspase-3 positive cells in any of the analyzed tumors were detected indicating that IRE was not activating apoptotic cell death. However, some isolated caspase-3 positive cells could be identified in untreated tumors, corresponding to normal tumor development (Figure 34, bottom panel). At day 14 some polymorphonuclears cells in the tumor burden were also positive for caspase-3.

4.3.3. Analysis of tumor vascular architecture in IRE treated mice.

We also analyzed the effect of IRE treatment on tumor vascular architecture. Immunostaining against the endothelial cell marker CD-31 was performed. Anti-CD31 staining nicely showed microvessel-density in the BxPC-3Luc xenograft model. Disruption of the small vascular architecture was clearly observed since day 1 post-IRE and was present at all time-points post-IRE treatment (Figure 35). At day 14, images seem to indicate that there was a vascular regrowth.

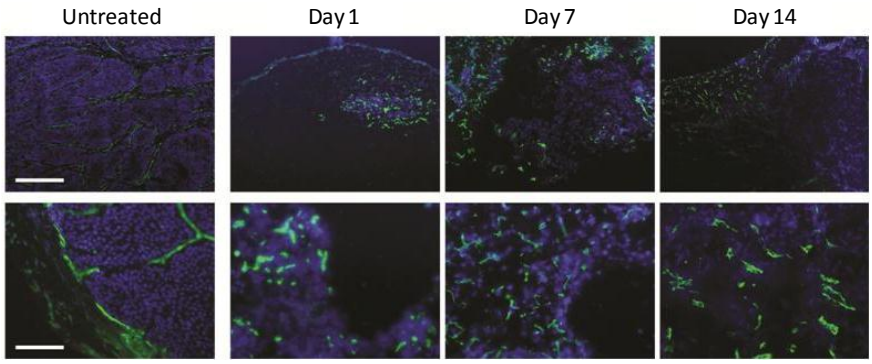

Figure 35. IRE treatment effect on tumor vasculature. BxPC-3-Luc orthotopic tumors were generated in nude mice. When the luciferase counts were within the range of 10^6-10^7 photons/s, animals were irreversible electroporated. Animals were sacrificed at the indicated time points, and the pancreas was obtained and included in OCT. Representative images of anti-CD31 immunohistochemical analysis in untreated and IRE-treated mice at days 1 (n=2), 7 (n=4) and 14 (n=4) after treatment are shown. Top panel scale bar: 400 μm; bottom panel scale bar: 100 μm.

4.4. Evaluation of IRE procedure-associated toxicity.

We next evaluated the safety of the IRE procedure by analyzing serum biochemical parameters of liver and pancreatic function at 1h, 6h, 24h, 7 days and 14 days after IRE procedure. Liver damage was assessed by measuring serum AST and ALT levels at different time-points after IRE application. As shown in Figure 36A a peak in serum levels of liver transaminases was detected at 6h. However, at one day post-treatment ALT values were already within the normal range and AST levels were almost completely recovered. At days 7 and 14 post-IRE ALT and AST values were both within the reference range.

Pancreatic function was assessed by measuring serum amylase and lipase levels (Figure 36B), as well as serum glucose levels (Figure 36C). A transient increase in both amylase and lipase enzymes was detected at 6h post-IRE that completely normalized at 24h. Normal values were also detected at days 7 and 14 post-IRE treatment.

A 2-fold increase in the glucose levels was detected in the first hour post-IRE, followed by a slight hypoglycemia at 6h that resolved at 24h. The transient increase in the glucose levels in the first hour could be an indication of the glucose release from dying tumor cells. Normal glucose values were maintained at 7 and 14 days post-treatment.

These data indicated that IRE pancreatic tumor treatment generated minimal damage in the first hours post-treatment that resolved at 24h.

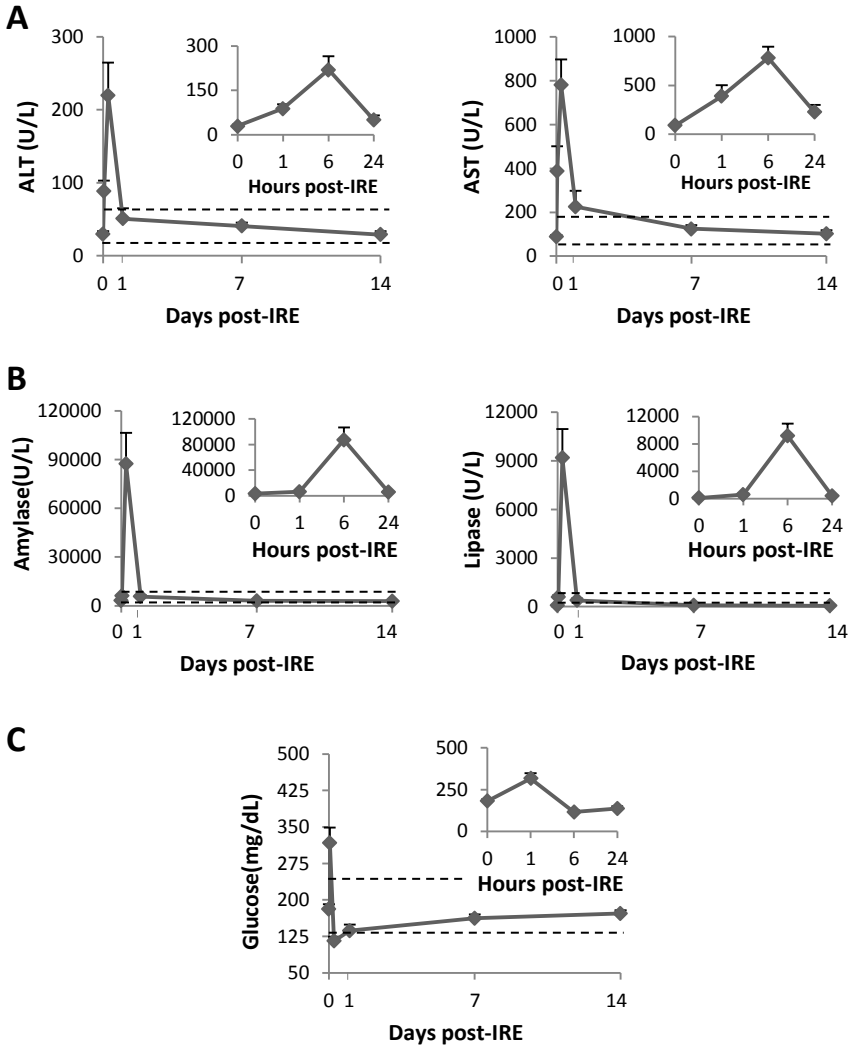

Figure 36. Liver and pancreatic function studies in IRE treated mice. Analysis of ALT and AST (A), amylase and lipase (B) and glucose (C) serum levels in IRE-treated mice before (n=18) and after 1h (n=6), 6h (n=6), 24h (n=7), 7 d (n=12) and 14 d(n=9) IRE treatment. Graphic insets correspond to the first 24h after IRE-treatment. Dash lines indicate reference values from untreated BxPC-3-Luc tumor-bearing mice.

DISCUSSION

"Es mejor debatir una cuestión sin resolverla, que resolver una cuestión sin debatirla."

J. Joubert *(1754-1824)*

Ensayista francés

Pancreatic cancer is one of the most devastating malignancies with a 5-year survival rate lower than 5%. Pancreatic cancer (PC) is classified in 3 clinically important categories: i) localized cancer, ii) locally invasive disease, and iii) unresectable PC. The criteria for unresectability of PC include tumor vascular involvement (celiac axis or superior mesenteric artery) and the presence of distant metastasis (Edge et al. 2010). The 5-year survival directly correlates to the stage at diagnosis (Table 13) since surgical treatment is the only potential cure of PC. Due to the absence of early diagnosis and its highly invasive and metastatic features, only 10-15% of patients with pancreatic cancer are candidates for surgical resection. However, even after resection, the 5 year survival rate is only 20% or less as PC has a high loco-regional recurrence rate and a tendency towards early liver metastasis, requiring the employment of adjuvant therapy in combination with surgical resection (Fatima et al. 2010). Unresectable and metastatic patients are treated with chemo and radiotherapy (Sharma et al. 2011); however, PC shows strong resistance to the currently available chemotherapy and/or radiotherapy protocols. In the recent years clinical trials with FOLFIRINOX (oxaliplatin, irinotecan, leucoviron and 5-FU) or with the combined treatment (gemcitabine, capecitabine, bevazicumab and erlotinib) have shown a small improvement on survival (from a median survival of 6.9 months with standard therapy to 10.5 and 11.1 respectively) in patients with advanced disease. This still represents very limited success for treatment, thus, novel therapeutic modalities are urgently needed.

Stage at diagnosis	Stage distribution (%)	5 year relative survival (%)
Localized (confirmed to primary site)	8	22.5
Regional (spread to regional LNs)	26	8.8
Distant (cancer had metastasized)	53	1.9
Unknown (unstaged)	14	5

Table 13. Stage distribution of pancreatic cancer and 5-year relative survival by stage at diagnosis for 1999-2006. LNs : lymphatic nodules.

Gene therapy is a potential and promising therapeutic modality for the treatment of cancer. Effective treatments must be capable of efficiently target tumoral nodules destroying tumoral cells without harming non-tumoral cells, and without being inactivated by components of the blood stream nor rapidly sequestered into non-target tissues. Tumor anatomy represents a challenge to gain access to tumoral cells, especially in

pancreatic tumors, where the dense stroma and the poor tumor vascularization limited the arrival of viruses to the bulk of the tumor. One of the objectives of this thesis has been the improvement of adenoviral gene delivery to pancreatic tumors by exploring a novel delivery route and by enhancing tumor transduction through a retargeting strategy.

The success of a gene therapy-based tumoral treatment not only relies on the viral transduction efficiency of the tumor, but also on the capacity of the therapeutic agent to destroy tumoral cells. Hence, a second objective of this thesis has been the evaluation of the therapeutic efficacy of the antitumoral AduPARTat8TK/GCV gene therapy and its combination with the chemotherapeutic gemcitabine.

Following the general objective of this thesis of developing novel antitumoral strategies for the treatment of pancreatic cancer, we have evaluated the antitumoral efficacy of the novel non-thermal ablative technique irreversible electroporation.

1. STRATEGIES TO IMPROVE ADENOVIRAL TUMOR TARGETING.

1.1. Intraductal injection into the common bile duct as a novel delivery route to target pancreatic tumors.

The success of gene therapy relies, among others, on the delivery route of vector administration since therapeutic efficiency has been clearly associated with the ability of the viral agent to spread throughout the tumor (Heise et al. 1999). The location and stage of the tumor will influence the choice of the optimal route of administration. Systemic delivery by intravenous administration is specially indicated for pancreatic tumors with distant metastasis; whereas intratumoral injection is a locoregional route to target primary tumors. However, all routes face with difficulties to achieve optimal delivery.

Direct injection of anticancer therapies into the pancreas, although tested, are limited by the relative inaccessibility of the organ and the potential for causing pancreatitis. CT-guided injection of the replicative adenovirus ONXY-015 in a Phase I trial demonstrated the safety and feasibility of the adapted technique (Mulvihill et al. 2001); however, CT-guided injection was cumbersome and it was difficult to perform

repeated intratumoral injections during a given treatment session. EUS-guided injection of ONYX-015 (Hecht et al. 2003) and TNFarade, a replication-deficient adenovirus carrying the TNF-α gene (Chang et al. 2008; Chang and Irisawa 2009) have shown encouraging results in clinical trials; unfortunately, this technique has also presented several complications from the injection procedure such as infection, perforation of the duodenum or the stomach, risk of pancreatitis and the potential for malignant seeding (Seo 2010). Then, nowadays clinical trials on top of evaluating the safety and the efficacy of therapeutic agents, they also analyze for the safety and efficacy of novel delivery routes to treat pancreatic tumors.

Systemic administration of adenoviral vectors is limited by the sequestration of adenovirus by the liver (Lieber et al. 1997; Di Paolo et al. 2009) which produces hepatotoxicity and reduces the amount of therapeutic vector targeting the tumor. Moreover, the preexistence of neutralizing antibodies can lead to the clearance of the viral vector (Harvey et al. 1999). In addition a great obstacle to the clinical application is the innate immune response towards the vector that occurs upon adenovirus administration that depends entirely on virus capsid interaction with host cells (Liu and Muruve 2003). Such response has been observed both after intravenous delivery and upon direct injection of adenovirus into the pancreas (McClane et al. 1997).

ERCP is an imaging technique used in human for the diagnoses of bile and pancreatic duct diseases and in some cases for the diagnoses of pancreatic neoplasms. Intraductal injection is an adaptation of the ERCP technique and has been used for the delivery of compounds to the pancreas of animal models, to generate rat models of pancreatitis after administration of sodium taurocholate, or to generate animal models of pancreatic cancer after administration of tumoral cells or carcinogen agents (Kamano et al. 1991; Jonsson and Ohlsson 1995; Folch et al. 2000; Tsuji et al. 2006; Gea-Sorli and Closa 2009). The technique has also been used for the treatment of diabetes after adenovirus or adenoassociated virus administration to mouse models (Tokui et al. 2006; Jimenez et al. 2011). In this thesis, we have evaluated the effectiveness of the intraductal injection method for the delivery of adenovirus to target pancreatic tumors. We have shown that adenoviral delivery through the common bile duct restricted transgene expression to pancreas and, when compared to systemic administration, intraductal injection increased pancreatic viral transduction with significantly reduced liver infection.

Importantly, adenoviruses efficiently reached the bulk of pancreatic tumors in Ela-myc mice upon intraductal delivery.

Our data showed that by adenoviral intraductal administration transgene expression from the adenoviral vector was detected in the whole pancreas probably because adenoviruses distribute through the pancreatic branching duct system to the whole organ. To restrict viral antitumor activity to cancerous cells we have used the uPAR promoter controlling transgene expression. Previous studies had demonstrated that the PLAUR gene (uPAR) was overexpressed in pancreatic tumors and PLAUR gene amplification was a highly significant adverse prognostic marker (Hildenbrand et al. 2009). Moreover, uPAR-based adenoviruses present with oncoselectivity for pancreatic tumors (Huch et al. 2009). In the pre-neoplasic Ela-myc pancreas we have shown that uPAR mRNA expression was upregulated compared to wt pancreas, similarly to what has been shown in high-grade PanIN lesions of clinical samples (Hildenbrand et al. 2009). These data suggest that the factors driving uPAR transcription may be highly active in the tumoral context. Indeed, we have observed that the AduPARLuc reporter adenovirus showed 80 times lower luciferase activity than AdCMVGFPLuc in wt mice whereas this reduction was only of 10 times in the Ela-myc tumoral model. This difference in luciferase activity was probably caused by the elevated expression of uPAR in the Ela-myc pancreas that led to the activation of the uPAR promoter in the adenoviral context. This oncoselectivity was further confirmed by the elevated and broadly distributed expression of GFP, driven by the CMV promoter in the pancreas of wt mice contrasted with the lack of luciferase expression, controlled by the uPAR promoter. On the contrary, in Ela-myc mice luciferase expression was detected in the core of solid pancreatic tumors demonstrating that AduPARLuc targeted the bulk of pancreatic nodules upon i.d administration.

The interest of the intraductal delivery as a target route against pancreatic tumors was demonstrated by showing the antitumoral efficacy of the cytotoxic adenovirus AduPARTat8TK/GCV. The antitumoral capacity of Tat8TK-based adenovirus for the treatment of pancreatic subcutaneous tumors upon intratumoral injection has been previously demonstrated by our group (Cascante et al. 2007; Garcia-Rodriguez et al. 2011). Interestingly, the i.d. delivery of AduPARTat8TK showed major reduction on the tumoral growth of Ela-myc pancreatic tumors than the intravascular delivery. These results were in line with the data from the reporter experiments where we demonstrated that AdCMVGFPLuc

adenovirus targeted Ela-myc tumors more efficiently upon intraductal injection.

Importantly, no pancreatic toxicity was observed upon intraductal administration of AduPARLuc to Ela-myc mice demonstrating that the intraductal injection into the common bile duct was a safe delivery route for the administration of adenoviruses to the pancreas. Moreover, the lack of hepatotoxicity found upon AduPARLuc systemic administration confirmed the specificity of the uPAR promoter for tumoral tissue and demonstrated the safety of the AduPARTat8TK/GCV therapy.

An interesting aspect of this route of administration is the potential feasibility of being applied for repeated adenoviral administrations. It has been reported that intraductal delivery of adenovirus into the common bile duct (two and three times) led to successful re-expression of the transgene into the liver despite the existence of neutralizing antibodies in serum. Interestingly, no neutralizing antibodies were present in the duct (Tominaga et al. 2004). This technique was similar to the one employed in the present work, but differed in the clamping of the bile duct. The absence of bile duct clamping would allow for adenovirus reaching the liver. Thus, intraductal administration seems to be a good option to overcome an important limitation of the adenoviral vectors, the inability of vector re-administration. Neutralizing antibodies have also been detected following direct injection of adenoviral vectors into the pancreas what induced a systemic response that prevented local direct re-administration of the vector (McClane et al. 1997). Noticeable, the mechanisms that triggered a systemic immune response upon direct Ad injection were not activated upon intraductal injection. Therefore, it would be interesting to evaluate the feasibility of AduPARTat8TK/GCV intraductal re-administration and its therapeutic effect on Ela-myc pancreatic tumors.

Altogether, our results indicate that intraductal administration of adenovirus into the common bile duct efficiently targeted pancreatic tissue. Moreover, AduPARTat8TK/GCV therapy is capable of great activity and selectivity for pancreatic tumors, reducing the tumoral growth of Ela-myc tumors with no toxicity and ameliorating tumor-associated toxicity. The intraductal administration delivery route of cytotoxic adenovirus to pancreatic tumors would mostly applied for the treatment of localized tumors or locally invasive pancreatic tumors. Nevertheless, because the application of this technique in the absence of bile duct clamping has been shown to allow for the virus to reach the liver, it could be

speculated that in such conditions small pancreatic liver metastasis could be targeted with an appropriate adenovirus through this route. This remains to be demonstrated; however, if so, it will enlarge the potential application of the intraductal delivery route.

1.2. Infectivity and selectivity of the metalloprotease activatable adenovirus AdTATMMP.

Human adenovirus serotype 5 has been widely exploited as a gene delivery vector owing to its superior gene delivery efficacy, minor pathological effects on humans and easy manipulation *in vitro*. However, they present inefficient transduction of cancerous tissue due to low levels of CAR expression, and the innate hepatotropism and toxicity of Ad5 *in vivo* following intravenous delivery (Lieber et al. 1997; Hamdan et al. 2011). Thus, Ad vectors which combine liver detargeting with high efficiency CAR-independent gene delivery to cancer-specific receptors would improve the adenoviral tumor delivery and, consequently, their antitumoral capacity. In this thesis we have generated the MMP activatable adenovirus AdTATMMP. On one hand, AdTATMMP virus carried the previously described YTRGE mutations to provide with liver detargeting by eliminating the binding to coagulation FIX and the complement factor C4BP (Shayakhmetov et al. 2005). The virus was also mutated in its motif for CAR receptor binding recognition leading to an adenovirus with a CAR-independent cell entry. On the other hand, AdTATMMP virus expressed the protein transduction domain TAT into the fiber protein to mediate viral infection. To provide the virus with tumor selectivity, we have blocked the TAT_{PTD} with a polyanionic tail linked by a MMP cleavable linker.

AdTATMMP virus showed to be activatable by metalloproteases. Incubation of the virus in the presence of recombinant MMP2 or MMP9 demonstrated that AdTATMMP was able to transduce cells in a dose-response manner being more efficient at the highest concentration of MMP9 tested. Interestingly, cell lines with higher content of MMP2/9 also were more susceptible to AdTATMMP transduction. This MMP-activation could provide to the virus with oncoselectivity, suggesting that in environments with high MMP activity, such are the pancreatic tumors (Jimenez et al. 2000; Giannopoulos et al. 2008), the virus could be activated. This selectivity has also been observed for other virus such are Retrovirus, Sendai virus and Measles virus which had been successfully engineered to be activated by MMPs and had demonstrated to

selectively transduce MMP-rich cells and subcutaneous tumor models after intratumoral administration (Schneider et al. 2003; Kinoh et al. 2004; Springfeld et al. 2006; Szecsi et al. 2006; Duerner et al. 2008). However, all these viruses were enveloped virus and, upon activation, viral entrance was mediated by the env proteins.

AdTATMMP is a CAR-ablated virus, thus, the entrance to the cell was engineered to be through the TAT domain with the aim to improve CAR-mediated tumor transduction. The TAT_{PTD} incorporation into the C-ter of the YTRGE fiber protein was probably mediating viral entry because both AdTAT and AdTATMMP adenoviruses restored viral transduction capacity. As a cell penetrating peptide, TAT_{PTD} is capable to translocate across the plasma membrane of mammalian cells and mediate the intracellular delivery of heterologous proteins fused to them after their systemic delivery (Schwarze et al. 1999; Beerens et al. 2003; Orii et al. 2005). TAT_{PTD} had already been used to facilitate virus infection; in particular, bi-specific adaptor proteins consisting of TAT_{PTD} fused to the extracellular domain of CAR were used to coat Ad vectors, which resulted in enhanced gene delivery (Kuhnel et al. 2004). However, genetic fusion of TAT_{PTD} to the fiber protein possesses major advantages such as the stable interaction between Ad5 and TAT_{PTD}, and the possibility of retarget replicative adenovirus. During the development of this thesis Han et al and Kurachi et al developed adenoviruses that incorporated the TAT_{PTD} domain into the HI-loop or the 3' end of the fiber gene (Han et al. 2007; Kurachi et al. 2007). They demonstrated that the recombinant vectors combined cell entry mediated by CAR with that mediated by TAT. TAT-modified viruses resulted in improved gene delivery efficacy in cellular models as well as in subcutaneous tumor models after Ad intratumoral administration. No biodistribution differences were found between systemic administration of TAT-modified or non-modified adenoviruses. By contrast, in this thesis we have evaluated the transduction capacity of a CAR-ablated TAT-modified adenovirus when introduced at the 3' end of the fiber protein. The resolution of the crystal structure of the Ad5 knob domain by X-ray crystallography has identified the HI loop region as a region suitable for peptide incorporation (Xia et al. 1995), and to date this site has been shown to tolerate the insertion of ligands up to 83 amino acids with negligible effects on structural integrity (Belousova et al. 2002). The 3' end of the fiber gene has also been used for peptide incorporation. Indeed, the suitable location for peptide incorporation seemed to be dependent on the peptide itself. RGD motif insertion improved adenoviral transduction more efficiently when incorporated at the HI-loop whereas polylysine (pK7) insertion improved transduction

efficiency when incorporated at the C-terminus (Koizumi et al. 2003). Kurachi et al incorporated TAT_{PTD} both at the HI-loop and at C-terminus of the fiber knob and reported better transduction efficiency in HI-loop modified vectors. But Han et al cloned the TAT_{PTD} at the C-terminus of the fiber protein and also observed enhanced transduction capacity. In the case of AdTATMMP, we were forced to introduce the TAT-MMP linker-blockage peptide at the C-terminus of the fiber protein since the blocking domain had to be released after cleavage by MMPs.

Transduction experiments in this study indicated that AdTATMMP exhibited enhanced transduction capacity compared to that of AdTAT. Although there is not a clear explanation for that it could be speculated that the TAT peptide acquired a conformation in the YTRGE-TATMMP fiber that facilitated its interaction with the cell membrane more efficiently that in the YTRGE-TAT fiber. We hypothesize that YTRGE mutations hindered TAT_{PTD} exposure since it was predicted that YTRGE mutations changed the overall conformation of the knob domain and created sterical hindrances preventing interaction with ligands (Shayakhmetov et al. 2005). On the contrary, the presence of the blocking domain in the YTRGE-TATMMP fiber could facilitate the correct folding and exposure of TAT_{PTD} after its cleavage by MMPs.

The systemic administration of the MMP-activatable retrovirus in mice with s.c tumors showed an improved ratio tumor/bone marrow, but the retargeted vector was less potent than the control retrovirus (Duerner et al. 2008). Interestingly, AdTATMMP was 7.3 folds more potent than its control virus AdYTRGE to target pancreatic tumors when administered intravenously. On the other hand, only a 1.4-fold increase in liver transduction was observed suggesting that AdTATMMP vector exhibited selectivity for tumoral tissue.

Despite containing the YTRGE mutations both AdYTRGE and AdTATMMP significantly transduced hepatic cells when administered systemically. Its transduction capacity was much lower than that from the AdCMVGFPLuc adenovirus, carrying a non-modified fiber. Luciferase counts in the liver after AdYTRGE or AdTATMMP intravenous administration were about 2-logs less than those from AdCMVGFPLuc. Thus YTRGE mutation contributed to minimize liver transduction but there was not a complete liver detargeting effect. This is not surprising because during the development of this thesis, Kalyyuzhniy et al and Waddington et al demonstrated that hexon protein is a major mediator of liver transduction by interaction with coagulation factor X (Kalyuzhniy et al.

2008; Waddington et al. 2008). Indeed, hexon hypervariable region five (HVR5) substitution or pseudotyping with serotype 3 hexon protein dramatically reduced liver transduction and associated toxicity (Vigant et al. 2008; Short et al. 2010). Therefore, the introduction of hexon modifications to AdTATMMP virus would be a possible strategy to reduce to a greater extent liver transduction and increase the tumor/liver ratio.

2. EFFECTS OF THE COMBINED TREATMENT AduPARTat8TK/GCV GENE THERAPY AND GEMCITABINE.

The pathogenesis of pancreatic cancer is complex and single therapies are unlikely to achieve a cure. The chemotherapeutic gemcitabine (GE) is the first line treatment for pancreatic cancer; however, the survival benefit for advanced pancreatic cancer remains limited. Nowadays many studies are evaluating the therapeutic efficacy of combined therapies such as gemcitabine plus a gene therapy agent. Previous studies reported a synergistic effect between gemcitabine and GCV; in particular, it was described that gemcitabine enhanced the bystander effect of GCV *in vitro* and *in vivo* (Boucher and Shewach 2005).

In this work we have observed a synergistic effect between GE and AduPARTat8TK/GCV *in vitro* that was remarkable in the Emyc cell line. To understand the basis of this synergism we have to pay attention to the mechanism of action of GE and GCV. Both drugs are nucleoside analogues that incorporate into the DNA during its synthesis, blocking chain elongation and finally causing cell death by apoptosis. In addition, GE is an inhibitor of the ribonucleotide reductase, through this activity GE reduces dNTPs pool, increasing in this way the ratio triphosphorilated-GE (dFdCTP)/dCTP (its nucleoside analogue) and, consequently, enhancing gemcitabine (dFdCTP) incorporation into the DNA. Therefore, GE can synergize with GCV reducing the endogenous dGTP pool (GCV nucleoside analogue) and consequently facilitating the incorporation of GCV-TP into the DNA. On the contrary, GE can antagonize with GCV by inhibiting DNA syntheses and then hindering TP-GCV incorporation into the DNA. The outcome of the combined therapy will depend on which of these two additional mechanisms would prevail.

Unfortunately, we could not appreciate any synergism when both therapies were applied *in vivo* in the Ela-myc mice in any of the two

protocols applied. The two protocols differentiate in the order of application of GE, AduPARTat8TK and GCV. The initial idea was that by giving GE first, this would reduce the dNTP pool, what will potentially enhance the posterior incorporation of GCV into the DNA. Moreover, the administration of GE first could also affect the uPAR promoter activity influencing the cytotoxicity of the TK/GCV. It is known that GE treatment can modify the expression pattern of some genes showing for example enhanced expression of transcription factors such as Wilms' tumor (Takahara et al. 2011), a positive regulator of the uPAR promoter (Dra. Maria Victoria Maliandi, personal communication). Hence, we cannot rule out that gemcitabine treatment could modulate uPAR promoter activity influencing on the output of the TK/GCV therapy with consequences in the combined treatment. It will be interesting to study whether this translates in an activation of the promoter, similar to what has been proposed for the CMV promoter (Onimaru et al. 2010) or on the contrary it limits its activity. Although the upregulation of the uPAR positive regulator Wilm's tumor might suggest an activated uPAR mediated transcription, we could not discard the induction of other mediators that could negatively regulate the uPAR promoter.

The results of the *in vivo* combined therapy have to be also contextualized to the characteristics of the mouse model utilized. As we observed in the Emyc cultures these tumor cells are much more resistant to gemcitabine than any of the human derived cancer cells tested in the study (with an ID_{50} 160 to 80 times higher). Thus, in an *in vivo* situation the option that tumor cells would be receiving sufficient amount of GE inducing an effect that could synergize with activated GCV metabolites could be suboptimal. However, the fact that Ela-myc mice have an intact immune system could provide with potent biological activity to gemcitabine. It is well known that GE presents with immunostimulatory functions by the alteration of the local immunosuppressive microenvironment of the tumor. It has been described that GE releases tumoral antigens inducing an antitumor response (Suzuki et al. 2005), prevents tumor-induced systemic immunosuppressive cells (Gallina et al. 2006; Curiel 2008) and can augment trafficking and activation of immune cells in tumor sites (Pardoll 2003).

The immune system has a dual role in the outcome of an adenoviral therapy. On one hand, replication-deficient adenoviruses induce a rapid inflammatory response that define dose limiting toxicity (Lieber et al. 1997) and T cell mediated killing of infected cells can reduce transgene expression (Dai et al. 1995). On the other hand, AduPARTat8TK/GCV

combined therapy could have an immunostimulatory role by eliciting an antitumor immune response. Several studies have demonstrated that cell killing via suicide gene therapy can stimulate the immune system and generate antitumor immunity (Vile et al. 1997; Shibata et al. 2008; Neves et al. 2009). Interestingly, the stimulation of an antitumor immune response following adenoviral suicide therapy was demonstrated in patients with prostate cancer in which an increased frequency of T cells recognizing prostate-specific antigens (PSA) or prostate-specific membrane antigen (PSMA) was observed after intratumoral suicide therapy (Onion et al. 2009). Importantly, it has been proposed that chemotherapy delivered after viral immunogene therapy (AdTK+GCV) augmented antitumor efficacy via multiple immune-mediated mechanisms (Fridlender et al. 2010). The authors proposed a primed-boost vaccine effect in which AdTK+GCV could "primed" an initial strong antitumor immune response, and sequential courses of chemotherapy would act as "boost" by the release of immunostimulatory tumor antigens. In our studies (COMB I protocol), AduPARTat8TK /GCV followed by gemcitabine was administered so that this priming-boost effect could be happening in such combined protocol.

It is worth to note that in our experiments single therapies of GE and AduPARTat8TK already showed a good response and reduced the pancreatic volume of Ela-myc mice to an average similar to that of wt mice. To observe for a synergistic effect we might test for doses leading to partial responses in the individualized treatments. In addition, a third combined protocol in which GE and the first dose of GCV were co-administered could be of interest to test. In fact, with this co-administration protocol Boucher et al described synergism between GE and GCV in subcutaneous tumors (Boucher and Shewach 2005); however, these experiments were carried out in nude mice, thus eluding what can be an important contributor, the immune response effect.

Toxicity studies of the combined treatment revealed some liver damage that resolved at the end of gemcitabine treatment. In fact, the elevation of hepatic transaminases has already been reported as a secondary effect of gemcitabine, especially when used in combination with other chemotherapeutics (Fossella et al. 1997). On the contrary, the combined treatment did not produce pancreatic toxicity but ameliorated the pancreatic tumor-associated toxicity.

3. ANTICANCER EFFECTS OF IRREVERSIBLE ELECTROPORATION ON PANCREATIC TUMORS.

Irreversible electroporation is an emerging technology for non-thermal tumor ablation. In this study we have investigated the efficacy of irreversible electroporation to achieve antitumoral effects in a pancreatic cancer mouse model. We have demonstrated efficacy of IRE by showing potent reduction in tumor growth from day 4 post-IRE with increased mice survival and complete tumor regression in the 25% of animals at 90 days post-treatment. Moreover, we have shown a rapid recovery of pancreatic function from an initial damage probably associated to IRE in non-tumoral areas.

These data have been achieved in a preclinical orthotopic model based on the pancreatic inoculation of the BxPC-3 pancreatic cancer cell line modified to express the luciferase gene. Several works have already demonstrated the use of bioluminescence to measure tumor biometrics after antitumor therapy in orthotopic pancreatic xenografts and highlight the utility of the technology to monitor tumor response in longitudinal studies (Kim et al. 2009; Lee et al. 2010a; McNally et al. 2010). It is worth mentioning that the BxPC-3 xenografts is a highly aggressive tumor model when implanted orthotopically (Lee et al. 2010a). Importantly, we have observed a very early response to IRE treatment, already detected at one day post-treatment. However, in certain tumors limited viable cells were detected within the ablated area as well as secondary tumors were lately localized in the pancreas distant to the primary electroporated tumor in particular animals. These remaining proliferating cells could be the responsible of the tumor regrowth shown in some animals. A second round on the application of the procedure could help to act against secondary nodules detected in later examinations.

We have shown that IRE procedure produced a disruption of the microvascular architecture with a rapid release of red blood cells and the appearance of a bloody tumor in accordance with other studies (Al-Sakere et al. 2007; Tracy et al. 2011). At days 7 and 14 post-IRE necrosis was much more evident than at day 1 and inflammatory cell reaction was observed. It has been proposed that the IRE pulses induced vascular congestion, which should also cause tissue hypoxia and may further contribute to tumor cell death. Disaggregation of the membranes starts a

couple of hours after the pulse delivery and is completed at 24 h when necrosis can be already detected (Al-Sakere et al. 2007).

Efficacy of IRE treatment has also been recently reported in a rat model of hepatocellular carcinoma with a necrotic response similar to the one we have observed (Guo et al. 2010). By contrast, the authors also reported extensive caspase-3 activation, suggesting an apoptotic cell death at one day post-IRE that was no longer visible later on. Similarly, a recent study in normal pig pancreas has reported an increase in the apoptotic index after IRE procedure determined by a TUNEL assay (Bower et al. 2011). In our model we did not detect caspase-3 activation in the tumor cells at any of the periods analyzed which is in agreement with other studies performed on renal tissue, lung tissue and fibrosarcoma subcutaneous tumors which reported cell death caused by necrosis (Al-Sakere et al. 2007; Deodhar et al. 2011; Tracy et al. 2011). Some of these studies described an increase in the number of nuclei stained by TUNEL reaction at 1 h after treatment that was no longer detected at later times. The authors argumented that TUNEL staining was not indicative of apoptosis since irreversible electroporation could affect the nuclear envelope, exposing the DNA to extracellular nucleases generating double strand breaks that are the seeding point for the TUNEL assay. In fact, there is a debate about the cause of cell death induced by IRE procedure. This is not surprising since studies were performed in different tumor models with different susceptibility to apoptotic cell death. Nevertheless, we cannot discard that the IRE protocol that we applied presents with different kinetics on the response to cell death as we have used different type of electrodes and applied a pulse train with different number and frequency of pulses. Thus caspase-3 activation could be an earlier event that escaped from our analysis.

The IRE procedure that we used in addition to ablate the tumor area produced some damage to the adjacent parenchyma, also showing small necrotic areas. Nevertheless the effects on pancreas and liver functionality were only transiently affected. Most damage occurred in the first to 6h and at one day post-IRE, despite necrosis in small pancreatic areas, enzyme serum levels were normalized. Thus no major adverse effects were observed in treated mice proving for the low toxicity of the procedure. Our data is in agreement with a recent study in which IRE was applied to the pancreas of swine pigs and only transient increases in pancreatic enzymes were observed (Bower et al. 2011). In that study, as in ours, all animals tolerated the procedure without immediate complications and no associated cardiac dysrhythmias.

Other ablative techniques such as radiofrequency RFA are currently performed for locally advanced pancreatic neoplasms in a combined therapeutic plan. Improvement in the quality of life due to the achievement of pain relief has been reported (Wu, J. Surgical Oncology 2006; Girelli Br. J. Surg. 2010), nevertheless significant results on increased survival are still missing (D'Onofrio. Word J. Gastroenterol. 2010). However these techniques are based on the use of thermal energy that damages structures such as blood vessels, bile ducts, and nerves entailing a relevant limitation to the pancreas which lies immediately adjacent to the superior mesenteric artery, portal vein, and common bile duct (Bower et al. 2011). In fact many cases of hemorrhages have been reported after the RFA procedure and that makes it a very difficult technique to be implemented in current practice. By contrast, irreversible electroporation is a non-thermal technique that it has been shown to preserve the vital structures within the IRE-ablated zone such are gross blood vessels, ducts and nerves (Maor and Rubinsky 2010; Li et al. 2011), what makes it suitable for pancreatic cancer treatment.

Although additional studies are required, the work presented in this thesis shows the potential of IRE in the treatment of non-metastatic pancreatic tumors and it can be considered as an alternative approach to RFA. Some of the relevant advantages of IRE are that it is a very rapid procedure and could potentially be applied to treat different nodules located in separated areas by a unique surgical procedure. Moreover the low toxic effects of the therapy could encourage the application of more than one round of IRE treatment in the subset of tumors that may present with partial responses.

CONCLUSIONS

"Todo es muy fácil antes de ser sencillo."

T. Fuller *(1610-1661)*

Escritor británico

I. Adenoviruses intraductally injected through the common bile duct efficiently target pancreatic tumors in the Ela-myc mouse model.

II. AduPARTat8TK intraductally delivered into the common bile duct, followed by GCV treatment, triggers pancreatic tumor regression in Ela-myc mice. Increased antitumoral effect is achieved by AduPARTat8TK intraductal delivery compared to intravenous administration.

III. AduPARTat8TK/GCV gene therapy ameliorates pancreatic function and hepatic tumor-associated toxicity in Ela-myc mice.

IV. The combined therapy AduPARTat8TK/GCV plus gemcitabine shows synergistic *effects* in pancreatic cancer cell lines. The two combined regimens tested in vivo did not augment the antitumor effect of individual therapies.

V. AdTATMMP fiber-modified adenovirus is activable by MMP-2 and MMP-9 and shows *in vitro* enhanced transduction efficiency in MMP rich cells. AdTATMMP rescues the infectivity of the CAR-ablated AdYTRGE.

VI. AdTATMMP systemically delivered to Ela-myc mice increased pancreatic tumor transduction in 7.3 times respect to AdYTRGE.

VII. Irreversible electroporation reduces BxPC-3-Luc orthotopic tumor growth, increases mice survival and leads to complete tumor regression in 25% of the animals at 90 days post treatment. Transient toxicity is detected but resolved at 24h post-IRE.

BIBLIOGRAPHY

Abate-Daga, D., L. Garcia-Rodriguez, L. Sumoy and C. Fillat (2010). "Cell cycle control pathways act as conditioning factors for TK/GCV sensitivity in pancreatic cancer cells." Biochim Biophys Acta **1803**(10): 1175-1185.

Aguirre, A. J., N. Bardeesy, M. Sinha, L. Lopez, D. A. Tuveson, J. Horner, M. S. Redston and R. A. DePinho (2003). "Activated Kras and Ink4a/Arf deficiency cooperate to produce metastatic pancreatic ductal adenocarcinoma." Genes Dev **17**(24): 3112-3126.

Akiyama, M., S. Thorne, D. Kirn, P. W. Roelvink, D. A. Einfeld, C. R. King and T. J. Wickham (2004). "Ablating CAR and integrin binding in adenovirus vectors reduces nontarget organ transduction and permits sustained bloodstream persistence following intraperitoneal administration." Mol Ther **9**(2): 218-230.

Al-Sakere, B., F. Andre, C. Bernat, E. Connault, P. Opolon, R. V. Davalos, B. Rubinsky and L. M. Mir (2007). "Tumor ablation with irreversible electroporation." PLoS One **2**(11): e1135.

Alemany, R. and D. T. Curiel (2001). "CAR-binding ablation does not change biodistribution and toxicity of adenoviral vectors." Gene Ther **8**(17): 1347-1353.

Artandi, S. E., S. Chang, S. L. Lee, S. Alson, G. J. Gottlieb, L. Chin and R. A. DePinho (2000). "Telomere dysfunction promotes non-reciprocal translocations and epithelial cancers in mice." Nature **406**(6796): 641-645.

Atkinson, H. and R. Chalmers (2010). "Delivering the goods: viral and non-viral gene therapy systems and the inherent limits on cargo DNA and internal sequences." Genetica **138**(5): 485-498.

Ball, C., K. R. Thomson and H. Kavnoudias (2010). "Irreversible electroporation: a new challenge in "out of operating theater" anesthesia." Anesth Analg **110**(5): 1305-1309.

Barba, D., J. Hardin, M. Sadelain and F. H. Gage (1994). "Development of anti-tumor immunity following thymidine kinase-mediated killing of experimental brain tumors." Proc Natl Acad Sci U S A **91**(10): 4348-4352.

Bardeesy, N., A. J. Aguirre, G. C. Chu, K. H. Cheng, L. V. Lopez, A. F. Hezel, B. Feng, C. Brennan, R. Weissleder, U. Mahmood, D. Hanahan, M. S. Redston, L. Chin and R. A. Depinho (2006). "Both p16(Ink4a) and the p19(Arf)-p53 pathway constrain progression of pancreatic adenocarcinoma in the mouse." Proc Natl Acad Sci U S A **103**(15): 5947-5952.

Bardeesy, N. and R. A. DePinho (2002). "Pancreatic cancer biology and genetics." Nat Rev Cancer **2**(12): 897-909.

Bardeesy, N., N. E. Sharpless, R. A. DePinho and G. Merlino (2001). "The genetics of pancreatic adenocarcinoma: a roadmap for a mouse model." Semin Cancer Biol **11**(3): 201-218.

Batty, G. D., M. Kivimaki, D. Morrison, R. Huxley, G. D. Smith, R. Clarke, M. G. Marmot and M. J. Shipley (2009). "Risk factors for pancreatic cancer mortality: extended follow-up of the original Whitehall Study." Cancer Epidemiol Biomarkers Prev **18**(2): 673-675.

Bayo-Puxan, N., M. Gimenez-Alejandre, S. Lavilla-Alonso, A. Gros, M. Cascallo, A. Hemminki and R. Alemany (2009). "Replacement of adenovirus type 5 fiber shaft heparan sulfate proteoglycan-binding domain with RGD for improved tumor infectivity and targeting." Hum Gene Ther **20**(10): 1214-1221.

Bazan-Peregrino, M., L. W. Seymour and A. L. Harris (2007). "Gene therapy targeting to tumor endothelium." Cancer Gene Ther **14**(2): 117-127.

Becker, T. C., R. J. Noel, W. S. Coats, A. M. Gomez-Foix, T. Alam, R. D. Gerard and C. B. Newgard (1994). "Use of recombinant adenovirus for metabolic engineering of mammalian cells." Methods Cell Biol **43 Pt A**: 161-189.

Beerens, A. M., A. F. Al Hadithy, M. G. Rots and H. J. Haisma (2003). "Protein transduction domains and their utility in gene therapy." Curr Gene Ther **3**(5): 486-494.

Belousova, N., V. Krendelchtchikova, D. T. Curiel and V. Krasnykh (2002). "Modulation of adenovirus vector tropism via incorporation of

polypeptide ligands into the fiber protein." J Virol **76**(17): 8621-8631.

Biliran, H., Jr., Y. Wang, S. Banerjee, H. Xu, H. Heng, A. Thakur, A. Bollig, F. H. Sarkar and J. D. Liao (2005). "Overexpression of cyclin D1 promotes tumor cell growth and confers resistance to cisplatin-mediated apoptosis in an elastase-myc transgene-expressing pancreatic tumor cell line." Clin Cancer Res **11**(16): 6075-6086.

Black, M. E., M. S. Kokoris and P. Sabo (2001). "Herpes simplex virus-1 thymidine kinase mutants created by semi-random sequence mutagenesis improve prodrug-mediated tumor cell killing." Cancer Res **61**(7): 3022-3026.

Bortolanza, S., M. Bunuales, I. Otano, G. Gonzalez-Aseguinolaza, C. Ortiz-de-Solorzano, D. Perez, J. Prieto and R. Hernandez-Alcoceba (2009). "Treatment of pancreatic cancer with an oncolytic adenovirus expressing interleukin-12 in Syrian hamsters." Mol Ther **17**(4): 614-622.

Bosma, M. J. and A. M. Carroll (1991). "The SCID mouse mutant: definition, characterization, and potential uses." Annu Rev Immunol **9**: 323-350.

Boucher, P. D. and D. S. Shewach (2005). "In vitro and in vivo enhancement of ganciclovir-mediated bystander cytotoxicity with gemcitabine." Mol Ther **12**(6): 1064-1071.

Bower, M., L. Sherwood, Y. Li and R. Martin (2011). "Irreversible electroporation of the pancreas: Definitive local therapy without systemic effects." J Surg Oncol **104**(1): 22-28.

Brugge, W. R., G. Y. Lauwers, D. Sahani, C. Fernandez-del Castillo and A. L. Warshaw (2004). "Cystic neoplasms of the pancreas." N Engl J Med **351**(12): 1218-1226.

Buchler, P., H. A. Reber, A. Ullrich, M. Shiroiki, M. Roth, M. W. Buchler, R. S. Lavey, H. Friess and O. J. Hines (2003). "Pancreatic cancer growth is inhibited by blockade of VEGF-RII." Surgery **134**(5): 772-782.

Burris, H. A., 3rd, M. J. Moore, J. Andersen, M. R. Green, M. L. Rothenberg, M. R. Modiano, M. C. Cripps, R. K. Portenoy, A. M. Storniolo, P. Tarassoff, R. Nelson, F. A. Dorr, C. D. Stephens and D. D. Von Hoff (1997). "Improvements in survival and clinical benefit with gemcitabine as first-line therapy for patients with advanced pancreas cancer: a randomized trial." J Clin Oncol **15**(6): 2403-2413.

Buxbaum, J. L. and M. A. Eloubeidi (2010). "Molecular and clinical markers of pancreas cancer." JOP **11**(6): 536-544.

Calbo, J., M. Marotta, M. Cascallo, J. M. Roig, J. L. Gelpi, J. Fueyo and A. Mazo (2001). "Adenovirus-mediated wt-p16 reintroduction induces cell cycle arrest or apoptosis in pancreatic cancer." Cancer Gene Ther **8**(10): 740-750.

Campbell, S. L., R. Khosravi-Far, K. L. Rossman, G. J. Clark and C. J. Der (1998). "Increasing complexity of Ras signaling." Oncogene **17**(11 Reviews): 1395-1413.

Carrió, M., A. Mazo, C. López-Iglesias, X. Estivill and C. Fillat (2001). "Retrovirus-mediated transfer of the herpes simplex virus thymidine kinase and connexin26 genes in pancreatic cells results in variable efficiency on the bystander killing: Implications for gene therapy." International Journal of Cancer **94**(1): 81-88.

Carrio, M., A. Romagosa, E. Mercade, A. Mazo, M. Nadal, A. M. Gomez-Foix and C. Fillat (1999). "Enhanced pancreatic tumor regression by a combination of adenovirus and retrovirus-mediated delivery of the herpes simplex virus thymidine kinase gene." Gene Ther **6**(4): 547-553.

Carrio, M., J. Visa, A. Cascante, X. Estivill and C. Fillat (2002). "Intratumoral activation of cyclophosphamide by retroviral transfer of the cytochrome P450 2B1 in a pancreatic tumor model. Combination with the HSVtk/GCV system." J Gene Med **4**(2): 141-149.

Caruso, M., Y. Panis, S. Gagandeep, D. Houssin, J. L. Salzmann and D. Klatzmann (1993). "Regression of established macroscopic liver

metastases after in situ transduction of a suicide gene." Proc Natl Acad Sci U S A **90**(15): 7024-7028.

Cascallo, M., E. Mercade, G. Capella, F. Lluis, C. Fillat, A. M. Gomez-Foix and A. Mazo (1999). "Genetic background determines the response to adenovirus-mediated wild-type p53 expression in pancreatic tumor cells." Cancer Gene Ther **6**(5): 428-436.

Cascante, A., D. Abate-Daga, L. Garcia-Rodríguez, J. R. González, R. Alemany and C. Fillat (2007). "GCV modulates the antitumoural efficacy of a replicative adenovirus expressing the TAT8-TK as a late gene in a pancreatic tumour model." Gene Therapy **14**(20): 1471-1480.

Cascante, A., M. Huch, L. G. Rodriguez, J. R. Gonzalez, L. Costantini and C. Fillat (2005). "Tat8-TK/GCV suicide gene therapy induces pancreatic tumor regression in vivo." Hum Gene Ther **16**(12): 1377-1388.

Clarke, M. F. and M. Fuller (2006). "Stem cells and cancer: two faces of eve." Cell **124**(6): 1111-1115.

Conroy, T., F. Desseigne, M. Ychou, O. Bouche, R. Guimbaud, Y. Becouarn, A. Adenis, J. L. Raoul, S. Gourgou-Bourgade, C. de la Fouchardiere, J. Bennouna, J. B. Bachet, F. Khemissa-Akouz, D. Pere-Verge, C. Delbaldo, E. Assenat, B. Chauffert, P. Michel, C. Montoto-Grillot and M. Ducreux (2011). "FOLFIRINOX versus gemcitabine for metastatic pancreatic cancer." N Engl J Med **364**(19): 1817-1825.

Costello, E. and J. P. Neoptolemos (2011). "Pancreatic cancer in 2010: new insights for early intervention and detection." Nat Rev Gastroenterol Hepatol **8**(2): 71-73.

Crocetti, L. and R. Lencioni (2008). "Thermal ablation of hepatocellular carcinoma." Cancer Imaging **8**: 19-26.

Culver, K. W., Z. Ram, S. Wallbridge, H. Ishii, E. H. Oldfield and R. M. Blaese (1992). "In vivo gene transfer with retroviral vector-producer cells for treatment of experimental brain tumors." Science **256**(5063): 1550-1552.

Cunningham, D., I. Chau, D. D. Stocken, J. W. Valle, D. Smith, W. Steward, P. G. Harper, J. Dunn, C. Tudur-Smith, J. West, S. Falk, A. Crellin, F. Adab, J. Thompson, P. Leonard, J. Ostrowski, M. Eatock, W. Scheithauer, R. Herrmann and J. P. Neoptolemos (2009). "Phase III randomized comparison of gemcitabine versus gemcitabine plus capecitabine in patients with advanced pancreatic cancer." J Clin Oncol **27**(33): 5513-5518.

Curiel, D. and J. T. Douglas (2002). Adenoviral vectors for gene therapy. Amsterdam ; Boston, Academic Press.

Curiel, T. J. (2008). "Regulatory T cells and treatment of cancer." Curr Opin Immunol **20**(2): 241-246.

Chang, K. J. and A. Irisawa (2009). "EUS 2008 Working Group document: evaluation of EUS-guided injection therapy for tumors." Gastrointest Endosc **69**(2 Suppl): S54-58.

Chang, K. J., J. G. Lee, R. F. Holcombe, J. Kuo, R. Muthusamy and M. L. Wu (2008). "Endoscopic ultrasound delivery of an antitumor agent to treat a case of pancreatic cancer." Nat Clin Pract Gastroenterol Hepatol **5**(2): 107-111.

Chen, D. and Q. Tang (2010). "An experimental study on cervix cancer with combination of HSV-TK/GCV suicide gene therapy system and 60Co radiotherapy." BMC Cancer **10**: 609.

Chevallet, M., S. Luche and T. Rabilloud (2006). "Silver staining of proteins in polyacrylamide gels." Nat Protoc **1**(4): 1852-1858.

Chou, T. C. and P. Talalay (1984). "Quantitative analysis of dose-effect relationships: the combined effects of multiple drugs or enzyme inhibitors." Adv Enzyme Regul **22**: 27-55.

Chu, G. C., A. C. Kimmelman, A. F. Hezel and R. A. DePinho (2007). "Stromal biology of pancreatic cancer." J Cell Biochem **101**(4): 887-907.

D'Onofrio, M., E. Barbi, R. Girelli, E. Martone, A. Gallotti, R. Salvia, P. T. Martini, C. Bassi, P. Pederzoli and R. Pozzi Mucelli (2010). "Radiofrequency ablation of locally advanced pancreatic

adenocarcinoma: an overview." World J Gastroenterol **16**(28): 3478-3483.

Dai, Y., E. M. Schwarz, D. Gu, W. W. Zhang, N. Sarvetnick and I. M. Verma (1995). "Cellular and humoral immune responses to adenoviral vectors containing factor IX gene: tolerization of factor IX and vector antigens allows for long-term expression." Proc Natl Acad Sci U S A **92**(5): 1401-1405.

Davalos, R. V., I. L. Mir and B. Rubinsky (2005). "Tissue ablation with irreversible electroporation." Ann Biomed Eng **33**(2): 223-231.

de Vrij, J., R. A. Willemsen, L. Lindholm, R. C. Hoeben, C. H. Bangma, C. Barber, J. P. Behr, S. Briggs, R. Carlisle, W. S. Cheng, I. J. Dautzenberg, C. de Ridder, H. Dzojic, P. Erbacher, M. Essand, K. Fisher, A. Frazier, L. J. Georgopoulos, I. Jennings, S. Kochanek, D. Koppers-Lalic, R. Kraaij, F. Kreppel, M. Magnusson, N. Maitland, P. Neuberg, R. Nugent, M. Ogris, J. S. Remy, M. Scaife, E. Schenk-Braat, E. Schooten, L. Seymour, M. Slade, P. Szyjanowicz, T. Totterman, T. G. Uil, K. Ulbrich, L. van der Weel, W. van Weerden, E. Wagner and G. Zuber (2010). "Adenovirus-derived vectors for prostate cancer gene therapy." Hum Gene Ther **21**(7): 795-805.

Deodhar, A., S. Monette, G. W. Single, Jr., W. C. Hamilton, Jr., R. H. Thornton, C. T. Sofocleous, M. Maybody and S. B. Solomon (2011). "Percutaneous Irreversible Electroporation Lung Ablation: Preliminary Results in a Porcine Model." Cardiovasc Intervent Radiol.

Dexter, D. L., G. M. Matook, P. A. Meitner, H. A. Bogaars, G. A. Jolly, M. D. Turner and P. Calabresi (1982). "Establishment and characterization of two human pancreatic cancer cell lines tumorigenic in athymic mice." Cancer Res **42**(7): 2705-2714.

Di Paolo, N. C., N. van Rooijen and D. M. Shayakhmetov (2009). "Redundant and synergistic mechanisms control the sequestration of blood-born adenovirus in the liver." Mol Ther **17**(4): 675-684.

Ding, Y., J. D. Cravero, K. Adrian and P. Grippo (2010). "Modeling pancreatic cancer in vivo: from xenograft and carcinogen-induced systems to genetically engineered mice." Pancreas **39**(3): 283-292.

Duerner, L. J., A. Schwantes, I. C. Schneider, K. Cichutek and C. J. Buchholz (2008). "Cell entry targeting restricts biodistribution of replication-competent retroviruses to tumour tissue." Gene Ther **15**(22): 1500-1510.

Dumonceau, J. M. and A. Vonlaufen (2007). "Pancreatic endoscopic retrograde cholangiopancreatography (ERCP)." Endoscopy **39**(2): 124-130.

Dumot, J. A. (2006). "ERCP: current uses and less-invasive options." Cleve Clin J Med **73**(5): 418, 421, 424-415 passim.

Edge, S. B., American Joint Committee on Cancer. and American Cancer Society. (2010). AJCC cancer staging handbook : from the AJCC cancer staging manual. New York, Springer.

Egeblad, M. and Z. Werb (2002). "New functions for the matrix metalloproteinases in cancer progression." Nat Rev Cancer **2**(3): 161-174.

Ellis, T. L., P. A. Garcia, J. H. Rossmeisl, Jr., N. Henao-Guerrero, J. Robertson and R. V. Davalos (2011). "Nonthermal irreversible electroporation for intracranial surgical applications. Laboratory investigation." J Neurosurg **114**(3): 681-688.

Essafi, M., A. D. Baudot, X. Mouska, J. P. Cassuto, M. Ticchioni and M. Deckert (2011). "Cell-penetrating TAT-FOXO3 fusion proteins induce apoptotic cell death in leukemic cells." Mol Cancer Ther **10**(1): 37-46.

Estin, D., M. Li, D. Spray and J. K. Wu (1999). "Connexins are expressed in primary brain tumors and enhance the bystander effect in gene therapy." Neurosurgery **44**(2): 361-368; discussion 368-369.

Fallaux, F. J., O. Kranenburg, S. J. Cramer, A. Houweling, H. Van Ormondt, R. C. Hoeben and A. J. Van Der Eb (1996). "Characterization of

911: a new helper cell line for the titration and propagation of early region 1-deleted adenoviral vectors." Hum Gene Ther **7**(2): 215-222.

Fatima, J., T. Schnelldorfer, J. Barton, C. M. Wood, H. J. Wiste, T. C. Smyrk, L. Zhang, M. G. Sarr, D. M. Nagorney and M. B. Farnell (2010). "Pancreatoduodenectomy for ductal adenocarcinoma: implications of positive margin on survival." Arch Surg **145**(2): 167-172.

Faulds, D. and R. C. Heel (1990). "Ganciclovir. A review of its antiviral activity, pharmacokinetic properties and therapeutic efficacy in cytomegalovirus infections." Drugs **39**(4): 597-638.

Feldmann, G., R. Beaty, R. H. Hruban and A. Maitra (2007). "Molecular genetics of pancreatic intraepithelial neoplasia." J Hepatobiliary Pancreat Surg **14**(3): 224-232.

Fidler, I. J. (1986). "Rationale and methods for the use of nude mice to study the biology and therapy of human cancer metastasis." Cancer Metastasis Rev **5**(1): 29-49.

Fillat, C., M. Carrio, A. Cascante and B. Sangro (2003). "Suicide gene therapy mediated by the Herpes Simplex virus thymidine kinase gene/Ganciclovir system: fifteen years of application." Curr Gene Ther **3**(1): 13-26.

Fillat, C., A. Jose, X. Bofill-DeRos, A. Mato-Berciano, M. V. Maliandi and L. Sobrevals (2011). "Pancreatic Cancer Gene Therapy: From Molecular Targets to Delivery Systems." Cancers **3**(1): 368-395.

Fogh, J., T. Orfeo, J. Tiso, F. E. Sharkey, J. M. Fogh and W. P. Daniels (1980). "Twenty-three new human tumor lines established in nude mice." Exp Cell Biol **48**(3): 229-239.

Folch, E., N. Prats, G. Hotter, S. Lopez, E. Gelpi, J. Rosello-Catafau and D. Closa (2000). "P-selectin expression and Kupffer cell activation in rat acute pancreatitis." Dig Dis Sci **45**(8): 1535-1544.

Fossella, F. V., S. M. Lippman, D. M. Shin, P. Tarassoff, M. Calayag-Jung, R. Perez-Soler, J. S. Lee, W. K. Murphy, B. Glisson, E. Rivera and W.

K. Hong (1997). "Maximum-tolerated dose defined for single-agent gemcitabine: a phase I dose-escalation study in chemotherapy-naive patients with advanced non-small-cell lung cancer." J Clin Oncol **15**(1): 310-316.

Freeman, S. M., C. N. Abboud, K. A. Whartenby, C. H. Packman, D. S. Koeplin, F. L. Moolten and G. N. Abraham (1993). "The "bystander effect": tumor regression when a fraction of the tumor mass is genetically modified." Cancer Res **53**(21): 5274-5283.

Freytag, S. O., K. N. Barton, S. L. Brown, V. Narra, Y. Zhang, D. Tyson, C. Nall, M. Lu, M. Ajlouni, B. Movsas and J. H. Kim (2007). "Replication-competent adenovirus-mediated suicide gene therapy with radiation in a preclinical model of pancreatic cancer." Mol Ther **15**(9): 1600-1606.

Fridlender, Z. G., J. Sun, S. Singhal, V. Kapoor, G. Cheng, E. Suzuki and S. M. Albelda (2010). "Chemotherapy delivered after viral immunogene therapy augments antitumor efficacy via multiple immune-mediated mechanisms." Mol Ther **18**(11): 1947-1959.

Fuchs, C. S., G. A. Colditz, M. J. Stampfer, E. L. Giovannucci, D. J. Hunter, E. B. Rimm, W. C. Willett and F. E. Speizer (1996). "A prospective study of cigarette smoking and the risk of pancreatic cancer." Arch Intern Med **156**(19): 2255-2260.

Gage, A. A., J. M. Baust and J. G. Baust (2009). "Experimental cryosurgery investigations in vivo." Cryobiology **59**(3): 229-243.

Gallina, G., L. Dolcetti, P. Serafini, C. De Santo, I. Marigo, M. P. Colombo, G. Basso, F. Brombacher, I. Borrello, P. Zanovello, S. Bicciato and V. Bronte (2006). "Tumors induce a subset of inflammatory monocytes with immunosuppressive activity on CD8+ T cells." J Clin Invest **116**(10): 2777-2790.

Garcia-Rodriguez, L., D. Abate-Daga, A. Rojas, J. R. Gonzalez and C. Fillat (2011). "E-cadherin contributes to the bystander effect of TK/GCV suicide therapy and enhances its antitumoral activity in pancreatic cancer models." Gene Ther **18**(1): 73-81.

Gea-Sorli, S. and D. Closa (2009). "In vitro, but not in vivo, reversibility of peritoneal macrophages activation during experimental acute pancreatitis." BMC Immunol **10**: 42.

Giannopoulos, G., K. Pavlakis, A. Parasi, N. Kavatzas, D. Tiniakos, A. Karakosta, N. Tzanakis and G. Peros (2008). "The expression of matrix metalloproteinases-2 and -9 and their tissue inhibitor 2 in pancreatic ductal and ampullary carcinoma and their relation to angiogenesis and clinicopathological parameters." Anticancer Res **28**(3B): 1875-1881.

Gidekel Friedlander, S. Y., G. C. Chu, E. L. Snyder, N. Girnius, G. Dibelius, D. Crowley, E. Vasile, R. A. DePinho and T. Jacks (2009). "Context-dependent transformation of adult pancreatic cells by oncogenic K-Ras." Cancer Cell **16**(5): 379-389.

Glasgow, J. N., G. J. Bauerschmitz, D. T. Curiel and A. Hemminki (2004). "Transductional and transcriptional targeting of adenovirus for clinical applications." Curr Gene Ther **4**(1): 1-14.

Goggins, M., M. Shekher, K. Turnacioglu, C. J. Yeo, R. H. Hruban and S. E. Kern (1998). "Genetic alterations of the transforming growth factor beta receptor genes in pancreatic and biliary adenocarcinomas." Cancer Res **58**(23): 5329-5332.

Gondi, C. S. and J. S. Rao (2009). "Therapeutic potential of siRNA-mediated targeting of urokinase plasminogen activator, its receptor, and matrix metalloproteinases." Methods Mol Biol **487**: 267-281.

Graham, F. L., J. Smiley, W. C. Russell and R. Nairn (1977). "Characteristics of a human cell line transformed by DNA from human adenovirus type 5." J Gen Virol **36**(1): 59-74.

Gravante, G., S. L. Ong, M. S. Metcalfe, N. Bhardwaj, G. J. Maddern, D. M. Lloyd and A. R. Dennison (2011). "Experimental application of electrolysis in the treatment of liver and pancreatic tumours: principles, preclinical and clinical observations and future perspectives." Surg Oncol **20**(2): 106-120.

Greenlee, K. J., D. B. Corry, D. A. Engler, R. K. Matsunami, P. Tessier, R. G. Cook, Z. Werb and F. Kheradmand (2006). "Proteomic identification of in vivo substrates for matrix metalloproteinases 2 and 9 reveals a mechanism for resolution of inflammation." J Immunol **177**(10): 7312-7321.

Grippo, P. J., P. S. Nowlin, M. J. Demeure, D. S. Longnecker and E. P. Sandgren (2003). "Preinvasive pancreatic neoplasia of ductal phenotype induced by acinar cell targeting of mutant Kras in transgenic mice." Cancer Res **63**(9): 2016-2019.

Grippo, P. J. and D. A. Tuveson (2010). "Deploying mouse models of pancreatic cancer for chemoprevention studies." Cancer Prev Res (Phila) **3**(11): 1382-1387.

Guerra, C., A. J. Schuhmacher, M. Canamero, P. J. Grippo, L. Verdaguer, L. Perez-Gallego, P. Dubus, E. P. Sandgren and M. Barbacid (2007). "Chronic pancreatitis is essential for induction of pancreatic ductal adenocarcinoma by K-Ras oncogenes in adult mice." Cancer Cell **11**(3): 291-302.

Guo, Y., Y. Zhang, R. Klein, G. M. Nijm, A. V. Sahakian, R. A. Omary, G. Y. Yang and A. C. Larson (2010). "Irreversible electroporation therapy in the liver: longitudinal efficacy studies in a rat model of hepatocellular carcinoma." Cancer Res **70**(4): 1555-1563.

Hahn, W. C., C. M. Counter, A. S. Lundberg, R. L. Beijersbergen, M. W. Brooks and R. A. Weinberg (1999). "Creation of human tumour cells with defined genetic elements." Nature **400**(6743): 464-468.

Hamdan, S., C. S. Verbeke, N. Fox, J. Booth, G. Bottley, H. S. Pandha and G. E. Blair (2011). "The roles of cell surface attachment molecules and coagulation Factor X in adenovirus 5-mediated gene transfer in pancreatic cancer cells." Cancer Gene Therapy.

Han, T., Y. Tang, H. Ugai, L. E. Perry, G. P. Siegal, J. L. Contreras and H. Wu (2007). "Genetic incorporation of the protein transduction domain of Tat into Ad5 fiber enhances gene transfer efficacy." Virology Journal **4**(1): 103.

Hanahan, D. and R. A. Weinberg (2000). "The hallmarks of cancer." Cell **100**(1): 57-70.

Harada, H., S. Kizaka-Kondoh and M. Hiraoka (2006). "Antitumor protein therapy; application of the protein transduction domain to the development of a protein drug for cancer treatment." Breast Cancer **13**(1): 16-26.

Harsha, H. C., K. Kandasamy, P. Ranganathan, S. Rani, S. Ramabadran, S. Gollapudi, L. Balakrishnan, S. B. Dwivedi, D. Telikicherla, L. D. Selvan, R. Goel, S. Mathivanan, A. Marimuthu, M. Kashyap, R. F. Vizza, R. J. Mayer, J. A. Decaprio, S. Srivastava, S. M. Hanash, R. H. Hruban and A. Pandey (2009). "A compendium of potential biomarkers of pancreatic cancer." PLoS Med **6**(4): e1000046.

Harvey, B. G., N. R. Hackett, T. El-Sawy, T. K. Rosengart, E. A. Hirschowitz, M. D. Lieberman, M. L. Lesser and R. G. Crystal (1999). "Variability of human systemic humoral immune responses to adenovirus gene transfer vectors administered to different organs." J Virol **73**(8): 6729-6742.

He, T. C., S. Zhou, L. T. da Costa, J. Yu, K. W. Kinzler and B. Vogelstein (1998). "A simplified system for generating recombinant adenoviruses." Proc Natl Acad Sci U S A **95**(5): 2509-2514.

He, Y., X. D. Liu, Z. Y. Chen, J. Zhu, Y. Xiong, K. Li, J. H. Dong and X. Li (2007). "Interaction between cancer cells and stromal fibroblasts is required for activation of the uPAR-uPA-MMP-2 cascade in pancreatic cancer metastasis." Clin Cancer Res **13**(11): 3115-3124.

Hecht, J. R., R. Bedford, J. L. Abbruzzese, S. Lahoti, T. R. Reid, R. M. Soetikno, D. H. Kirn and S. M. Freeman (2003). "A phase I/II trial of intratumoral endoscopic ultrasound injection of ONYX-015 with intravenous gemcitabine in unresectable pancreatic carcinoma." Clin Cancer Res **9**(2): 555-561.

Heinemann, V. and S. Boeck (2008). "Perioperative management of pancreatic cancer." Ann Oncol **19 Suppl 7**: vii273-278.

Heise, C. C., A. Williams, J. Olesch and D. H. Kirn (1999). "Efficacy of a replication-competent adenovirus (ONYX-015) following intratumoral injection: intratumoral spread and distribution effects." Cancer Gene Ther **6**(6): 499-504.

Hermann, P. C., S. L. Huber, T. Herrler, A. Aicher, J. W. Ellwart, M. Guba, C. J. Bruns and C. Heeschen (2007). "Distinct populations of cancer stem cells determine tumor growth and metastatic activity in human pancreatic cancer." Cell Stem Cell **1**(3): 313-323.

Hezel, A. F. (2006). "Genetics and biology of pancreatic ductal adenocarcinoma." Genes & Development **20**(10): 1218-1249.

Hidalgo, M. (2010). "Pancreatic cancer." N Engl J Med **362**(17): 1605-1617.

Hildenbrand, R., M. Niedergethmann, A. Marx, D. Belharazem, H. Allgayer, C. Schleger and P. Strobel (2009). "Amplification of the urokinase-type plasminogen activator receptor (uPAR) gene in ductal pancreatic carcinomas identifies a clinically high-risk group." Am J Pathol **174**(6): 2246-2253.

Hingorani, S. R., L. Wang, A. S. Multani, C. Combs, T. B. Deramaudt, R. H. Hruban, A. K. Rustgi, S. Chang and D. A. Tuveson (2005). "Trp53R172H and KrasG12D cooperate to promote chromosomal instability and widely metastatic pancreatic ductal adenocarcinoma in mice." Cancer Cell **7**(5): 469-483.

Hodish, I., R. Tal, A. Shaish, N. Varda-Bloom, S. Greenberger, A. Rauchwerger, E. Breitbart, L. Bangio, D. Ben-Shushan, R. Pfeffer, B. Feder, A. Waitsman, I. Barshack, I. Goldberg, S. Mazaki-Tovi, M. Peled and D. Harats (2009). "Systemic administration of radiation-potentiated anti-angiogenic gene therapy against primary and metastatic cancer based on transcriptionally controlled HSV-TK." Cancer Biol Ther **8**(5): 424-432.

Hoffmann, D. and O. Wildner (2006a). "Enhanced killing of pancreatic cancer cells by expression of fusogenic membrane glycoproteins in combination with chemotherapy." Mol Cancer Ther **5**(8): 2013-2022.

Hoffmann, D. and O. Wildner (2006b). "Restriction of adenoviral replication to the transcriptional intersection of two different promoters for colorectal and pancreatic cancer treatment." Mol Cancer Ther **5**(2): 374-381.

Hossain, M. Z. and J. S. Bertram (1994). "Retinoids suppress proliferation, induce cell spreading, and up-regulate connexin43 expression only in postconfluent 10T1/2 cells: implications for the role of gap junctional communication." Cell Growth Differ **5**(11): 1253-1261.

Hruban, R. H., N. V. Adsay, J. Albores-Saavedra, M. R. Anver, A. V. Biankin, G. P. Boivin, E. E. Furth, T. Furukawa, A. Klein, D. S. Klimstra, G. Kloppel, G. Y. Lauwers, D. S. Longnecker, J. Luttges, A. Maitra, G. J. Offerhaus, L. Perez-Gallego, M. Redston and D. A. Tuveson (2006). "Pathology of genetically engineered mouse models of pancreatic exocrine cancer: consensus report and recommendations." Cancer Res **66**(1): 95-106.

Hruban, R. H., M. Goggins, J. Parsons and S. E. Kern (2000). "Progression model for pancreatic cancer." Clin Cancer Res **6**(8): 2969-2972.

Hruban, R. H., A. Maitra, S. E. Kern and M. Goggins (2007a). "Precursors to pancreatic cancer." Gastroenterol Clin North Am **36**(4): 831-849, vi.

Hruban, R. H., M. B. Pitman, D. S. Klimstra, American Registry of Pathology. and Armed Forces Institute of Pathology (U.S.) (2007b). Tumors of the pancreas. Washington, D.C., American Registry of Pathology in collaboration with the Armed Forces Institute of Pathology.

Hruban, R. H., K. Takaori, D. S. Klimstra, N. V. Adsay, J. Albores-Saavedra, A. V. Biankin, S. A. Biankin, C. Compton, N. Fukushima, T. Furukawa, M. Goggins, Y. Kato, G. Kloppel, D. S. Longnecker, J. Luttges, A. Maitra, G. J. Offerhaus, M. Shimizu and S. Yonezawa (2004). "An illustrated consensus on the classification of pancreatic intraepithelial neoplasia and intraductal papillary mucinous neoplasms." Am J Surg Pathol **28**(8): 977-987.

Hruban, R. H., R. E. Wilentz and A. Maitra (2005). "Identification and analysis of precursors to invasive pancreatic cancer." Methods Mol Med **103**: 1-13.

Hu, J. C., R. S. Coffin, C. J. Davis, N. J. Graham, N. Groves, P. J. Guest, K. J. Harrington, N. D. James, C. A. Love, I. McNeish, L. C. Medley, A. Michael, C. M. Nutting, H. S. Pandha, C. A. Shorrock, J. Simpson, J. Steiner, N. M. Steven, D. Wright and R. C. Coombes (2006). "A phase I study of OncoVEXGM-CSF, a second-generation oncolytic herpes simplex virus expressing granulocyte macrophage colony-stimulating factor." Clin Cancer Res **12**(22): 6737-6747.

Huch, M., D. Abate-Daga, J. M. Roig, J. R. Gonzalez, J. Fabregat, B. Sosnowski, A. Mazo and C. Fillat (2006). "Targeting the CYP2B 1/cyclophosphamide suicide system to fibroblast growth factor receptors results in a potent antitumoral response in pancreatic cancer models." Hum Gene Ther **17**(12): 1187-1200.

Huch, M., A. Gros, A. Jose, J. R. Gonzalez, R. Alemany and C. Fillat (2009). "Urokinase-type plasminogen activator receptor transcriptionally controlled adenoviruses eradicate pancreatic tumors and liver metastasis in mouse models." Neoplasia **11**(6): 518-528, 514 p following 528.

Immonen, A., M. Vapalahti, K. Tyynela, H. Hurskainen, A. Sandmair, R. Vanninen, G. Langford, N. Murray and S. Yla-Herttuala (2004). "AdvHSV-tk gene therapy with intravenous ganciclovir improves survival in human malignant glioma: a randomised, controlled study." Mol Ther **10**(5): 967-972.

Infante, J. R., H. Matsubayashi, N. Sato, J. Tonascia, A. P. Klein, T. A. Riall, C. Yeo, C. Iacobuzio-Donahue and M. Goggins (2007). "Peritumoral fibroblast SPARC expression and patient outcome with resectable pancreatic adenocarcinoma." J Clin Oncol **25**(3): 319-325.

Itoh, T., M. Tanioka, H. Yoshida, T. Yoshioka, H. Nishimoto and S. Itohara (1998). "Reduced angiogenesis and tumor progression in gelatinase A-deficient mice." Cancer Res **58**(5): 1048-1051.

Izeradjene, K., C. Combs, M. Best, A. Gopinathan, A. Wagner, W. M. Grady, C. X. Deng, R. H. Hruban, N. V. Adsay, D. A. Tuveson and S. R. Hingorani (2007). "Kras(G12D) and Smad4/Dpc4 haploinsufficiency cooperate to induce mucinous cystic neoplasms and invasive adenocarcinoma of the pancreas." Cancer Cell **11**(3): 229-243.

Jacob, D., J. J. Davis, L. Zhang, H. Zhu, F. Teraishi and B. Fang (2005). "Suppression of pancreatic tumor growth in the liver by systemic administration of the TRAIL gene driven by the hTERT promoter." Cancer Gene Ther **12**(2): 109-115.

Ji, B., L. Tsou, H. Wang, S. Gaiser, D. Z. Chang, J. Daniluk, Y. Bi, T. Grote, D. S. Longnecker and C. D. Logsdon (2009). "Ras activity levels control the development of pancreatic diseases." Gastroenterology **137**(3): 1072-1082, 1082 e1071-1076.

Jimenez, R. E., W. Hartwig, B. A. Antoniu, C. C. Compton, A. L. Warshaw and C. Fernandez-Del Castillo (2000). "Effect of matrix metalloproteinase inhibition on pancreatic cancer invasion and metastasis: an additive strategy for cancer control." Ann Surg **231**(5): 644-654.

Jimenez, T., W. P. Fox, C. C. Naus, J. Galipeau and D. J. Belliveau (2006). "Connexin over-expression differentially suppresses glioma growth and contributes to the bystander effect following HSV-thymidine kinase gene therapy." Cell Commun Adhes **13**(1-2): 79-92.

Jimenez, V., E. Ayuso, C. Mallol, J. Agudo, A. Casellas, M. Obach, S. Munoz, A. Salavert and F. Bosch (2011). "In vivo genetic engineering of murine pancreatic beta cells mediated by single-stranded adeno-associated viral vectors of serotypes 6, 8 and 9." Diabetologia **54**(5): 1075-1086.

Jones, S., X. Zhang, D. W. Parsons, J. C. Lin, R. J. Leary, P. Angenendt, P. Mankoo, H. Carter, H. Kamiyama, A. Jimeno, S. M. Hong, B. Fu, M. T. Lin, E. S. Calhoun, M. Kamiyama, K. Walter, T. Nikolskaya, Y. Nikolsky, J. Hartigan, D. R. Smith, M. Hidalgo, S. D. Leach, A. P. Klein, E. M. Jaffee, M. Goggins, A. Maitra, C. Iacobuzio-Donahue, J. R. Eshleman, S. E. Kern, R. H. Hruban, R. Karchin, N.

Papadopoulos, G. Parmigiani, B. Vogelstein, V. E. Velculescu and K. W. Kinzler (2008). "Core signaling pathways in human pancreatic cancers revealed by global genomic analyses." Science **321**(5897): 1801-1806.

Jonsson, P. and K. Ohlsson (1995). "Intrapancreatic turnover of recombinant human pancreatic secretory trypsin inhibitor in experimental porcine pancreatitis." Scand J Clin Lab Invest **55**(3): 223-227.

Kalyuzhniy, O., N. C. Di Paolo, M. Silvestry, S. E. Hofherr, M. A. Barry, P. L. Stewart and D. M. Shayakhmetov (2008). "Adenovirus serotype 5 hexon is critical for virus infection of hepatocytes in vivo." Proceedings of the National Academy of Sciences **105**(14): 5483-5488.

Kallifatidis, G., B. M. Beckermann, A. Groth, M. Schubert, A. Apel, A. Khamidjanov, E. Ryschich, T. Wenger, W. Wagner, A. Diehlmann, R. Saffrich, U. Krause, V. Eckstein, J. Mattern, M. Chai, G. Schutz, A. D. Ho, M. M. Gebhard, M. W. Buchler, H. Friess, P. Buchler and I. Herr (2008). "Improved lentiviral transduction of human mesenchymal stem cells for therapeutic intervention in pancreatic cancer." Cancer Gene Ther **15**(4): 231-240.

Kamano, T., J. Tamura, T. Uchida, T. Kanno, N. Sakakibara, M. Tsutsumi, H. Maruyama and Y. Konishi (1991). "Studies by pancreatography of ductal changes induced by administration of pancreatic carcinogen in two dogs." Jpn J Clin Oncol **21**(4): 282-286.

Karmazanovsky, G., V. Fedorov, V. Kubyshkin and A. Kotchatkov (2005). "Pancreatic head cancer: accuracy of CT in determination of resectability." Abdom Imaging **30**(4): 488-500.

Kashiwagi, H., J. E. McDunn, P. S. Goedegebuure, M. C. Gaffney, K. Chang, K. Trinkaus, D. Piwnica-Worms, R. S. Hotchkiss and W. G. Hawkins (2007). "TAT-Bim induces extensive apoptosis in cancer cells." Ann Surg Oncol **14**(5): 1763-1771.

Kelly, K., S. Nawrocki, A. Mita, M. Coffey, F. J. Giles and M. Mita (2009). "Reovirus-based therapy for cancer." Expert Opin Biol Ther **9**(7): 817-830.

Kern, S. E., C. Shi and R. H. Hruban (2011). "The complexity of pancreatic ductal cancers and multidimensional strategies for therapeutic targeting." J Pathol **223**(2): 295-306.

Kessenbrock, K., V. Plaks and Z. Werb (2010). "Matrix metalloproteinases: regulators of the tumor microenvironment." Cell **141**(1): 52-67.

Kidd, S., L. Caldwell, M. Dietrich, I. Samudio, E. L. Spaeth, K. Watson, Y. Shi, J. Abbruzzese, M. Konopleva, M. Andreeff and F. C. Marini (2010). "Mesenchymal stromal cells alone or expressing interferon-beta suppress pancreatic tumors in vivo, an effect countered by anti-inflammatory treatment." Cytotherapy **12**(5): 615-625.

Kim, M. P., D. B. Evans, H. Wang, J. L. Abbruzzese, J. B. Fleming and G. E. Gallick (2009). "Generation of orthotopic and heterotopic human pancreatic cancer xenografts in immunodeficient mice." Nature Protocols **4**(11): 1670-1680.

Kinoh, H., M. Inoue, K. Washizawa, T. Yamamoto, S. Fujikawa, Y. Tokusumi, A. Iida, Y. Nagai and M. Hasegawa (2004). "Generation of a recombinant Sendai virus that is selectively activated and lyses human tumor cells expressing matrix metalloproteinases." Gene Ther **11**(14): 1137-1145.

Kleeff, J., K. Fukahi, M. E. Lopez, H. Friess, M. W. Buchler, B. A. Sosnowski and M. Korc (2002). "Targeting of suicide gene delivery in pancreatic cancer cells via FGF receptors." Cancer Gene Ther **9**(6): 522-532.

Kleiner, D. E. and W. G. Stetler-Stevenson (1994). "Quantitative zymography: detection of picogram quantities of gelatinases." Anal Biochem **218**(2): 325-329.

Ko, A., H. Youssoufian, J. Gurtler, K. Dicke, O. Kayaleh, H.-J. Lenz, M. Keaton, T. Katz, S. Ballal and E. Rowinsky (2011). "A phase II randomized study of cetuximab and bevacizumab alone or in combination with gemcitabine as first-line therapy for metastatic pancreatic adenocarcinoma." Investigational New Drugs: 1-10.

Koizumi, N., H. Mizuguchi, N. Utoguchi, Y. Watanabe and T. Hayakawa (2003). "Generation of fiber-modified adenovirus vectors containing heterologous peptides in both the HI loop and C terminus of the fiber knob." J Gene Med **5**(4): 267-276.

Kokoris, M. S., P. Sabo and M. E. Black (2000). "In vitro evaluation of mutant HSV-1 thymidine kinases for suicide gene therapy." Anticancer Res **20**(2A): 959-963.

Kuhlmann, K. F., M. A. van Geer, C. T. Bakker, J. E. Dekker, M. J. Havenga, R. P. Elferink, D. J. Gouma, P. J. Bosma and J. G. Wesseling (2009). "Fiber-chimeric adenoviruses expressing fibers from serotype 16 and 50 improve gene transfer to human pancreatic adenocarcinoma." Cancer Gene Ther **16**(7): 585-597.

Kuhnel, F., B. Schulte, T. Wirth, N. Woller, S. Schafers, L. Zender, M. Manns and S. Kubicka (2004). "Protein transduction domains fused to virus receptors improve cellular virus uptake and enhance oncolysis by tumor-specific replicating vectors." J Virol **78**(24): 13743-13754.

Kuppen, P. J., M. M. van der Eb, L. E. Jonges, M. Hagenaars, M. E. Hokland, U. Nannmark, R. H. Goldfarb, P. H. Basse, G. J. Fleuren, R. C. Hoeben and C. J. van de Velde (2001). "Tumor structure and extracellular matrix as a possible barrier for therapeutic approaches using immune cells or adenoviruses in colorectal cancer." Histochem Cell Biol **115**(1): 67-72.

Kurachi, S., K. Tashiro, F. Sakurai, H. Sakurai, K. Kawabata, K. Yayama, H. Okamoto, S. Nakagawa and H. Mizuguchi (2007). "Fiber-modified adenovirus vectors containing the TAT peptide derived from HIV-1 in the fiber knob have efficient gene transfer activity." Gene Therapy **14**(15): 1160-1165.

Lanuti, M., G. P. Gao, S. D. Force, M. Y. Chang, C. El Kouri, K. M. Amin, J. V. Hughes, J. M. Wilson, L. R. Kaiser and S. M. Albelda (1999). "Evaluation of an E1E4-deleted adenovirus expressing the herpes simplex thymidine kinase suicide gene in cancer gene therapy." Hum Gene Ther **10**(3): 463-475.

Leber, T. M. and F. R. Balkwill (1997). "Zymography: a single-step staining method for quantitation of proteolytic activity on substrate gels." Anal Biochem **249**(1): 24-28.

Lee, C. J., A. C. Spalding, E. Ben-Josef, L. Wang and D. M. Simeone (2010a). "In vivo bioluminescent imaging of irradiated orthotopic pancreatic cancer xenografts in nonobese diabetic-severe combined immunodeficient mice: a novel method for targeting and assaying efficacy of ionizing radiation." Transl Oncol **3**(3): 153-159.

Lee, E. J., Y. Gusev, J. Jiang, G. J. Nuovo, M. R. Lerner, W. L. Frankel, D. L. Morgan, R. G. Postier, D. J. Brackett and T. D. Schmittgen (2007). "Expression profiling identifies microRNA signature in pancreatic cancer." Int J Cancer **120**(5): 1046-1054.

Lee, E. W., C. Chen, V. E. Prieto, S. M. Dry, C. T. Loh and S. T. Kee (2010b). "Advanced hepatic ablation technique for creating complete cell death: irreversible electroporation." Radiology **255**(2): 426-433.

Lee, E. W., S. Thai and S. T. Kee (2010c). "Irreversible electroporation: a novel image-guided cancer therapy." Gut Liver **4 Suppl 1**: S99-S104.

Leifert, J. A. and J. L. Whitton (2003). ""Translocatory proteins" and "protein transduction domains": a critical analysis of their biological effects and the underlying mechanisms." Mol Ther **8**(1): 13-20.

Leitner, S., K. Sweeney, D. Oberg, D. Davies, E. Miranda, N. R. Lemoine and G. Hallden (2009). "Oncolytic adenoviral mutants with E1B19K gene deletions enhance gemcitabine-induced apoptosis in pancreatic carcinoma cells and anti-tumor efficacy in vivo." Clin Cancer Res **15**(5): 1730-1740.

Lencioni, R., C. Bartolozzi, D. Caramella, A. Paolicchi, M. Carrai, G. Maltinti, A. Capria, A. Tafi, P. F. Conte and G. Bevilacqua (1995). "Treatment of small hepatocellular carcinoma with percutaneous ethanol injection. Analysis of prognostic factors in 105 Western patients." Cancer **76**(10): 1737-1746.

Lencioni, R. and L. Crocetti (2005). "A critical appraisal of the literature on local ablative therapies for hepatocellular carcinoma." Clin Liver Dis **9**(2): 301-314, viii.

Levy, L. and C. S. Hill (2005). "Smad4 dependency defines two classes of transforming growth factor {beta} (TGF-{beta}) target genes and distinguishes TGF-{beta}-induced epithelial-mesenchymal transition from its antiproliferative and migratory responses." Mol Cell Biol **25**(18): 8108-8125.

Li, C., D. G. Heidt, P. Dalerba, C. F. Burant, L. Zhang, V. Adsay, M. Wicha, M. F. Clarke and D. M. Simeone (2007). "Identification of pancreatic cancer stem cells." Cancer Res **67**(3): 1030-1037.

Li, D., K. Xie, R. Wolff and J. L. Abbruzzese (2004). "Pancreatic cancer." Lancet **363**(9414): 1049-1057.

Li, W., Q. Fan, Z. Ji, X. Qiu and Z. Li (2011). "The effects of irreversible electroporation (IRE) on nerves." PLoS One **6**(4): e18831.

Liao, D. J., Y. Wang, J. Wu, N. V. Adsay, D. Grignon, F. Khanani and F. H. Sarkar (2006). "Characterization of pancreatic lesions from MT-tgf alpha, Ela-myc and MT-tgf alpha/Ela-myc single and double transgenic mice." J Carcinog **5**: 19.

Lieber, A., C. Y. He, L. Meuse, D. Schowalter, I. Kirillova, B. Winther and M. A. Kay (1997). "The role of Kupffer cell activation and viral gene expression in early liver toxicity after infusion of recombinant adenovirus vectors." J Virol **71**(11): 8798-8807.

Liu, Q. and D. A. Muruve (2003). "Molecular basis of the inflammatory response to adenovirus vectors." Gene Ther **10**(11): 935-940.

Liu, S., X. P. Wang and F. C. Brunicardi (2007). "Enhanced cytotoxicity of RIPTK gene therapy of pancreatic cancer via PDX-1 co-delivery." J Surg Res **137**(1): 1-9.

Lopes, R. B., R. Gangeswaran, I. A. McNeish, Y. Wang and N. R. Lemoine (2007). "Expression of the IAP protein family is dysregulated in pancreatic cancer cells and is important for resistance to chemotherapy." Int J Cancer **120**(11): 2344-2352.

Loukopoulos, P., K. Kanetaka, M. Takamura, T. Shibata, M. Sakamoto and S. Hirohashi (2004). "Orthotopic transplantation models of pancreatic adenocarcinoma derived from cell lines and primary tumors and displaying varying metastatic activity." Pancreas **29**(3): 193-203.

Lu, M. D., J. W. Chen, X. Y. Xie, L. Liu, X. Q. Huang, L. J. Liang and J. F. Huang (2001). "Hepatocellular carcinoma: US-guided percutaneous microwave coagulation therapy." Radiology **221**(1): 167-172.

Luo, J., Z.-L. Deng, X. Luo, N. Tang, W.-X. Song, J. Chen, K. A. Sharff, H. H. Luu, R. C. Haydon, K. W. Kinzler, B. Vogelstein and T.-C. He (2007a). "A protocol for rapid generation of recombinant adenoviruses using the AdEasy system." Nat. Protocols **2**(5): 1236-1247.

Luo, J., M. Iwasaki, M. Inoue, S. Sasazuki, T. Otani, W. Ye and S. Tsugane (2007b). "Body mass index, physical activity and the risk of pancreatic cancer in relation to smoking status and history of diabetes: a large-scale population-based cohort study in Japan--the JPHC study." Cancer Causes Control **18**(6): 603-612.

Mahadevan, D. and D. D. Von Hoff (2007). "Tumor-stroma interactions in pancreatic ductal adenocarcinoma." Mol Cancer Ther **6**(4): 1186-1197.

Maitra, A., N. Fukushima, K. Takaori and R. H. Hruban (2005). "Precursors to invasive pancreatic cancer." Adv Anat Pathol **12**(2): 81-91.

Maitra, A. and R. H. Hruban (2008). "Pancreatic cancer." Annu Rev Pathol **3**: 157-188.

Malumbres, M. and M. Barbacid (2003). "RAS oncogenes: the first 30 years." Nat Rev Cancer **3**(6): 459-465.

Maor, E. and B. Rubinsky (2010). "Endovascular nonthermal irreversible electroporation: a finite element analysis." J Biomech Eng **132**(3): 031008.

Masamune, A. and T. Shimosegawa (2009). "Signal transduction in pancreatic stellate cells." J Gastroenterol **44**(4): 249-260.

Massague, J., S. W. Blain and R. S. Lo (2000). "TGFbeta signaling in growth control, cancer, and heritable disorders." Cell **103**(2): 295-309.

Matsuyama, Y., S. Takao and T. Aikou (2002). "Comparison of matrix metalloproteinase expression between primary tumors with or without liver metastasis in pancreatic and colorectal carcinomas." Journal of Surgical Oncology **80**(2): 105-110.

Mazar, A. P., J. Henkin and R. H. Goldfarb (1999). "The urokinase plasminogen activator system in cancer: implications for tumor angiogenesis and metastasis." Angiogenesis **3**(1): 15-32.

Mazzolini, G., C. Alfaro, B. Sangro, E. Feijoo, J. Ruiz, A. Benito, I. Tirapu, A. Arina, J. Sola, M. Herraiz, F. Lucena, C. Olague, J. Subtil, J. Quiroga, I. Herrero, B. Sadaba, M. Bendandi, C. Qian, J. Prieto and I. Melero (2005). "Intratumoral injection of dendritic cells engineered to secrete interleukin-12 by recombinant adenovirus in patients with metastatic gastrointestinal carcinomas." J Clin Oncol **23**(5): 999-1010.

McAuliffe, P. F., W. R. Jarnagin, P. Johnson, K. A. Delman, H. Federoff and Y. Fong (2000). "Effective treatment of pancreatic tumors with two multimutated herpes simplex oncolytic viruses." J Gastrointest Surg **4**(6): 580-588.

McClane, S. J., N. Chirmule, C. V. Burke and S. E. Raper (1997). "Characterization of the immune response after local delivery of recombinant adenovirus in murine pancreas and successful strategies for readministration." Hum Gene Ther **8**(18): 2207-2216.

McNally, L. R., D. R. Welch, B. H. Beck, L. J. Stafford, J. W. Long, J. C. Sellers, Z. Q. Huang, W. E. Grizzle, C. R. Stockard, K. T. Nash and D. J. Buchsbaum (2010). "KISS1 over-expression suppresses metastasis of pancreatic adenocarcinoma in a xenograft mouse model." Clin Exp Metastasis **27**(8): 591-600.

Meier, O. and U. F. Greber (2004). "Adenovirus endocytosis." J Gene Med **6 Suppl 1**: S152-163.

Meng, Y., H. J. Mauceri, N. N. Khodarev, T. E. Darga, S. P. Pitroda, M. A. Beckett, D. W. Kufe and R. R. Weichselbaum (2010). "Ad.Egr-TNF and local ionizing radiation suppress metastases by interferon-beta-dependent activation of antigen-specific CD8+ T cells." Mol Ther **18**(5): 912-920.

Merl, M. Y., O. Abdelghany, J. Li and M. W. Saif (2010a). "First-line treatment of metastatic pancreatic adenocarcinoma: can we do better? Highlights from the "2010 ASCO Annual Meeting". Chicago, IL, USA. June 4-8, 2010." JOP **11**(4): 317-320.

Merl, M. Y., J. Li and M. W. Saif (2010b). "The first-line treatment for advanced pancreatic cancer. Highlights from the "2010 ASCO Gastrointestinal Cancers Symposium". Orlando, FL, USA. January 22-24, 2010." JOP **11**(2): 148-150.

Mihaljevic, A. L., C. W. Michalski, H. Friess and J. Kleeff (2010). "Molecular mechanism of pancreatic cancer--understanding proliferation, invasion, and metastasis." Langenbecks Arch Surg **395**(4): 295-308.

Miura, F., T. Takada, H. Amano, M. Yoshida, S. Furui and K. Takeshita (2006). "Diagnosis of pancreatic cancer." HPB (Oxford) **8**(5): 337-342.

Miura, Y., S. Ohnami, K. Yoshida, M. Ohashi, M. Nakano, M. Fukuhara, K. Yanagi, A. Matsushita, E. Uchida, M. Asaka, T. Yoshida and K. Aoki (2005). "Intraperitoneal injection of adenovirus expressing antisense K-ras RNA suppresses peritoneal dissemination of hamster syngeneic pancreatic cancer without systemic toxicity." Cancer Lett **218**(1): 53-62.

Mizuno, N., K. Hara, S. Hijioka, V. Bhatia, Y. Shimizu, Y. Yatabe and K. Yamao (2011). "Current concept of endoscopic ultrasound-guided fine needle aspiration for pancreatic cancer." Pancreatology **11 Suppl 2**: 40-46.

Moolten, F. L. (1986). "Tumor chemosensitivity conferred by inserted herpes thymidine kinase genes: paradigm for a prospective cancer control strategy." Cancer Res **46**(10): 5276-5281.

Moore, M. J., D. Goldstein, J. Hamm, A. Figer, J. R. Hecht, S. Gallinger, H. J. Au, P. Murawa, D. Walde, R. A. Wolff, D. Campos, R. Lim, K. Ding, G. Clark, T. Voskoglou-Nomikos, M. Ptasynski and W. Parulekar (2007). "Erlotinib plus gemcitabine compared with gemcitabine alone in patients with advanced pancreatic cancer: a phase III trial of the National Cancer Institute of Canada Clinical Trials Group." J Clin Oncol **25**(15): 1960-1966.

Morille, M., C. Passirani, A. Vonarbourg, A. Clavreul and J. P. Benoit (2008). "Progress in developing cationic vectors for non-viral systemic gene therapy against cancer." Biomaterials **29**(24-25): 3477-3496.

Morris, J. P., S. C. Wang and M. Hebrok (2010). "KRAS, Hedgehog, Wnt and the twisted developmental biology of pancreatic ductal adenocarcinoma." Nature Reviews Cancer **10**(10): 683-695.

Motoi, F., M. Sunamura, L. Ding, D. G. Duda, Y. Yoshida, W. Zhang, S. Matsuno and H. Hamada (2000). "Effective gene therapy for pancreatic cancer by cytokines mediated by restricted replication-competent adenovirus." Hum Gene Ther **11**(2): 223-235.

Mukherjee, P., G. D. Basu, T. L. Tinder, D. B. Subramani, J. M. Bradley, M. Arefayene, T. Skaar and G. De Petris (2009). "Progression of pancreatic adenocarcinoma is significantly impeded with a combination of vaccine and COX-2 inhibition." J Immunol **182**(1): 216-224.

Mulvihill, S., R. Warren, A. Venook, A. Adler, B. Randlev, C. Heise and D. Kirn (2001). "Safety and feasibility of injection with an E1B-55 kDa gene-deleted, replication-selective adenovirus (ONYX-015) into primary carcinomas of the pancreas: a phase I trial." Gene Ther **8**(4): 308-315.

Murakami, M., E. Nagai, K. Mizumoto, M. Saimura, K. Ohuchida, N. Inadome, K. Matsumoto, T. Nakamura, M. Maemondo, T. Nukiwa

and M. Tanaka (2005). "Suppression of metastasis of human pancreatic cancer to the liver by transportal injection of recombinant adenoviral NK4 in nude mice." Int J Cancer **117**(1): 160-165.

Neal, R. E., 2nd and R. V. Davalos (2009). "The feasibility of irreversible electroporation for the treatment of breast cancer and other heterogeneous systems." Ann Biomed Eng **37**(12): 2615-2625.

Nelson, A. R., J. Davydova, D. T. Curiel and M. Yamamoto (2009). "Combination of conditionally replicative adenovirus and standard chemotherapies shows synergistic antitumor effect in pancreatic cancer." Cancer Sci **100**(11): 2181-2187.

Neoptolemos, J. P., D. D. Stocken, H. Friess, C. Bassi, J. A. Dunn, H. Hickey, H. Beger, L. Fernandez-Cruz, C. Dervenis, F. Lacaine, M. Falconi, P. Pederzoli, A. Pap, D. Spooner, D. J. Kerr and M. W. Buchler (2004). "A randomized trial of chemoradiotherapy and chemotherapy after resection of pancreatic cancer." N Engl J Med **350**(12): 1200-1210.

Neves, S., H. Faneca, S. Bertin, K. Konopka, N. Duzgunes, V. Pierrefite-Carle, S. Simoes and M. C. Pedroso de Lima (2009). "Transferrin lipoplex-mediated suicide gene therapy of oral squamous cell carcinoma in an immunocompetent murine model and mechanisms involved in the antitumoral response." Cancer Gene Ther **16**(1): 91-101.

Niidome, T. and L. Huang (2002). "Gene therapy progress and prospects: nonviral vectors." Gene Ther **9**(24): 1647-1652.

Nishida, K., T. Kaneko, M. Yoneda, S. Nakagawa, T. Ishikawa, E. Yamane, B. Nishioka, Y. Miyamoto, H. Takano, T. Yoshikawa and M. Kondo (1999). "Doubling time of serum CA 19-9 in the clinical course of patients with pancreatic cancer and its significant association with prognosis." J Surg Oncol **71**(3): 140-146.

Nishihara, E., Y. Nagayama, F. Mawatari, K. Tanaka, H. Namba, M. Niwa and S. Yamashita (1997). "Retrovirus-mediated herpes simplex virus thymidine kinase gene transduction renders human thyroid

carcinoma cell lines sensitive to ganciclovir and radiation in vitro and in vivo." Endocrinology **138**(11): 4577-4583.

Oberg, D., E. Yanover, V. Adam, K. Sweeney, C. Costas, N. R. Lemoine and G. Hallden (2010). "Improved potency and selectivity of an oncolytic E1ACR2 and E1B19K deleted adenoviral mutant in prostate and pancreatic cancers." Clin Cancer Res **16**(2): 541-553.

Ocker, M., D. Neureiter, M. Lueders, S. Zopf, M. Ganslmayer, E. G. Hahn, C. Herold and D. Schuppan (2005). "Variants of bcl-2 specific siRNA for silencing antiapoptotic bcl-2 in pancreatic cancer." Gut **54**(9): 1298-1308.

Ogura, Y., K. Mizumoto, E. Nagai, M. Murakami, N. Inadome, M. Saimura, K. Matsumoto, T. Nakamura, M. Maemondo, T. Nukiwa and M. Tanaka (2006). "Peritumoral injection of adenovirus vector expressing NK4 combined with gemcitabine treatment suppresses growth and metastasis of human pancreatic cancer cells implanted orthotopically in nude mice and prolongs survival." Cancer Gene Ther **13**(5): 520-529.

Onimaru, M., K. Ohuchida, T. Egami, K. Mizumoto, E. Nagai, L. Cui, H. Toma, K. Matsumoto, M. Hashizume and M. Tanaka (2010). "Gemcitabine synergistically enhances the effect of adenovirus gene therapy through activation of the CMV promoter in pancreatic cancer cells." Cancer Gene Ther **17**(8): 541-549.

Onion, D., P. Patel, R. G. Pineda, N. James and V. Mautner (2009). "Antivector and tumor immune responses following adenovirus-directed enzyme prodrug therapy for the treatment of prostate cancer." Hum Gene Ther **20**(11): 1249-1258.

Orii, K. O., J. H. Grubb, C. Vogler, B. Levy, Y. Tan, K. Markova, B. L. Davidson, Q. Mao, T. Orii, N. Kondo and W. S. Sly (2005). "Defining the pathway for Tat-mediated delivery of beta-glucuronidase in cultured cells and MPS VII mice." Mol Ther **12**(2): 345-352.

Ornitz, D. M., R. E. Hammer, A. Messing, R. D. Palmiter and R. L. Brinster (1987). "Pancreatic neoplasia induced by SV40 T-antigen

expression in acinar cells of transgenic mice." Science **238**(4824): 188-193.

Ornitz, D. M., R. D. Palmiter, A. Messing, R. E. Hammer, C. A. Pinkert and R. L. Brinster (1985). "Elastase I promoter directs expression of human growth hormone and SV40 T antigen genes to pancreatic acinar cells in transgenic mice." Cold Spring Harb Symp Quant Biol **50**: 399-409.

Oster, S. K., C. S. Ho, E. L. Soucie and L. Z. Penn (2002). "The myc oncogene: MarvelouslY Complex." Adv Cancer Res **84**: 81-154.

Pardoll, D. (2003). "Does the immune system see tumors as foreign or self?" Annu Rev Immunol **21**: 807-839.

Patterson, E. J., C. H. Scudamore, D. A. Owen, A. G. Nagy and A. K. Buczkowski (1998). "Radiofrequency ablation of porcine liver in vivo: effects of blood flow and treatment time on lesion size." Ann Surg **227**(4): 559-565.

Pech, M., A. Janitzky, J. J. Wendler, C. Strang, S. Blaschke, O. Dudeck, J. Ricke and U. B. Liehr (2011). "Irreversible electroporation of renal cell carcinoma: a first-in-man phase I clinical study." Cardiovasc Intervent Radiol **34**(1): 132-138.

Perez-Torras, S., A. Vidal-Pla, R. Miquel, V. Almendro, L. Fernandez-Cruz, S. Navarro, J. Maurel, N. Carbo, P. Gascon and A. Mazo (2011). "Characterization of human pancreatic orthotopic tumor xenografts suitable for drug screening." Cell Oncol (Dordr).

Pezzilli, R., C. Serra, C. Ricci, R. Casadei, F. Monari, M. D'Ambra and F. Minni (2011). "Radiofrequency ablation for advanced ductal pancreatic carcinoma: is this approach beneficial for our patients? A systematic review." Pancreas **40**(1): 163-165.

Qiao, J., M. E. Black and M. Caruso (2000). "Enhanced ganciclovir killing and bystander effect of human tumor cells transduced with a retroviral vector carrying a herpes simplex virus thymidine kinase gene mutant." Hum Gene Ther **11**(11): 1569-1576.

Quaife, C. J., C. A. Pinkert, D. M. Ornitz, R. D. Palmiter and R. L. Brinster (1987). "Pancreatic neoplasia induced by ras expression in acinar cells of transgenic mice." Cell **48**(6): 1023-1034.

Raimondi, S., P. Maisonneuve, J. M. Lohr and A. B. Lowenfels (2007). "Early onset pancreatic cancer: evidence of a major role for smoking and genetic factors." Cancer Epidemiol Biomarkers Prev **16**(9): 1894-1897.

Raimondi, S., P. Maisonneuve and A. B. Lowenfels (2009). "Epidemiology of pancreatic cancer: an overview." Nature Reviews Gastroenterology & Hepatology **6**(12): 699-708.

Rao, J. S. (2003). "Molecular mechanisms of glioma invasiveness: the role of proteases." Nat Rev Cancer **3**(7): 489-501.

Ravet, E., H. Lulka, F. Gross, L. Casteilla, L. Buscail and P. Cordelier (2010). "Using lentiviral vectors for efficient pancreatic cancer gene therapy." Cancer Gene Ther **17**(5): 315-324.

Real, F. X., E. Cibrian-Uhalte and P. Martinelli (2008). "Pancreatic cancer development and progression: remodeling the model." Gastroenterology **135**(3): 724-728.

Regine, W. F., K. A. Winter, R. A. Abrams, H. Safran, J. P. Hoffman, A. Konski, A. B. Benson, J. S. Macdonald, M. R. Kudrimoti, M. L. Fromm, M. G. Haddock, P. Schaefer, C. G. Willett and T. A. Rich (2008). "Fluorouracil vs gemcitabine chemotherapy before and after fluorouracil-based chemoradiation following resection of pancreatic adenocarcinoma: a randomized controlled trial." JAMA **299**(9): 1019-1026.

Reya, T., S. J. Morrison, M. F. Clarke and I. L. Weissman (2001). "Stem cells, cancer, and cancer stem cells." Nature **414**(6859): 105-111.

Reyes, G., A. Villanueva, C. Garcia, F. J. Sancho, J. Piulats, F. Lluis and G. Capella (1996). "Orthotopic xenografts of human pancreatic carcinomas acquire genetic aberrations during dissemination in nude mice." Cancer Res **56**(24): 5713-5719.

Ritts, R. E. and H. A. Pitt (1998). "CA 19-9 in pancreatic cancer." Surg Oncol Clin N Am **7**(1): 93-101.

Robinson, K., L. Lambiase, J. Li, C. Monteiro and M. Schiff (2003). "Fatal cholestatic liver failure associated with gemcitabine therapy." Dig Dis Sci **48**(9): 1804-1808.

Roig, J. M., M. A. Molina, A. Cascante, J. Calbo, N. Carbo, U. Wirtz, S. Sreedharan, C. Fillat and A. Mazo (2004). "Adenovirus-mediated retinoblastoma 94 gene transfer induces human pancreatic tumor regression in a mouse xenograft model." Clin Cancer Res **10**(4): 1454-1462.

Rozenblum, E., M. Schutte, M. Goggins, S. A. Hahn, S. Panzer, M. Zahurak, S. N. Goodman, T. A. Sohn, R. H. Hruban, C. J. Yeo and S. E. Kern (1997). "Tumor-suppressive pathways in pancreatic carcinoma." Cancer Res **57**(9): 1731-1734.

Rubinsky, B. (2007). "Irreversible electroporation in medicine." Technol Cancer Res Treat **6**(4): 255-260.

Rubinsky, B., G. Onik and P. Mikus (2007). "Irreversible electroporation: a new ablation modality--clinical implications." Technol Cancer Res Treat **6**(1): 37-48.

Sadeghi, H. and M. M. Hitt (2005). "Transcriptionally targeted adenovirus vectors." Curr Gene Ther **5**(4): 411-427.

Saimura, M., E. Nagai, K. Mizumoto, N. Maehara, H. Okino, M. Katano, K. Matsumoto, T. Nakamura, K. Narumi, T. Nukiwa and M. Tanaka (2002). "Intraperitoneal injection of adenovirus-mediated NK4 gene suppresses peritoneal dissemination of pancreatic cancer cell line AsPC-1 in nude mice." Cancer Gene Ther **9**(10): 799-806.

Sandgren, E. P., C. J. Quaife, A. G. Paulovich, R. D. Palmiter and R. L. Brinster (1991). "Pancreatic tumor pathogenesis reflects the causative genetic lesion." Proc Natl Acad Sci U S A **88**(1): 93-97.

Sangro, B., G. Mazzolini, J. Ruiz, M. Herraiz, J. Quiroga, I. Herrero, A. Benito, J. Larrache, J. Pueyo, J. C. Subtil, C. Olague, J. Sola, B. Sadaba, C. Lacasa, I. Melero, C. Qian and J. Prieto (2004). "Phase I

trial of intratumoral injection of an adenovirus encoding interleukin-12 for advanced digestive tumors." J Clin Oncol **22**(8): 1389-1397.

Sarkar, D., Z. Z. Su, N. Vozhilla, E. S. Park, A. Randolph, K. Valerie and P. B. Fisher (2005). "Targeted virus replication plus immunotherapy eradicates primary and distant pancreatic tumors in nude mice." Cancer Res **65**(19): 9056-9063.

Sato, N., K. Mizumoto, M. Nakamura, N. Maehara, Y. A. Minamishima, S. Nishio, E. Nagai and M. Tanaka (2001). "Correlation between centrosome abnormalities and chromosomal instability in human pancreatic cancer cells." Cancer Genet Cytogenet **126**(1): 13-19.

Sato, N., K. Mizumoto, M. Nakamura, K. Nakamura, M. Kusumoto, H. Niiyama, T. Ogawa and M. Tanaka (1999). "Centrosome abnormalities in pancreatic ductal carcinoma." Clin Cancer Res **5**(5): 963-970.

Schneider, R. M., Y. Medvedovska, I. Hartl, B. Voelker, M. P. Chadwick, S. J. Russell, K. Cichutek and C. J. Buchholz (2003). "Directed evolution of retroviruses activatable by tumour-associated matrix metalloproteases." Gene Ther **10**(16): 1370-1380.

Schroder, C., A. Jacob, S. Tonack, T. P. Radon, M. Sill, M. Zucknick, S. Ruffer, E. Costello, J. P. Neoptolemos, T. Crnogorac-Jurcevic, A. Bauer, K. Fellenberg and J. D. Hoheisel (2010). "Dual-color proteomic profiling of complex samples with a microarray of 810 cancer-related antibodies." Mol Cell Proteomics **9**(6): 1271-1280.

Schwarze, S. R., A. Ho, A. Vocero-Akbani and S. F. Dowdy (1999). "In vivo protein transduction: delivery of a biologically active protein into the mouse." Science **285**(5433): 1569-1572.

Seo, D. W. (2010). "EUS-Guided Antitumor Therapy for Pancreatic Tumors." Gut Liver **4 Suppl 1**: S76-81.

Sergeant, G., H. Vankelecom, L. Gremeaux and B. Topal (2009). "Role of cancer stem cells in pancreatic ductal adenocarcinoma." Nature Reviews Clinical Oncology **6**(10): 580-586.

Sharma, C., K. M. Eltawil, P. D. Renfrew, M. J. Walsh and M. Molinari (2011). "Advances in diagnosis, treatment and palliation of pancreatic carcinoma: 1990-2010." World J Gastroenterol **17**(7): 867-897.

Shayakhmetov, D. M., A. Gaggar, S. Ni, Z. Y. Li and A. Lieber (2005). "Adenovirus Binding to Blood Factors Results in Liver Cell Infection and Hepatotoxicity." Journal of Virology **79**(12): 7478-7491.

Sherr, C. J. (2001). "The INK4a/ARF network in tumour suppression." Nat Rev Mol Cell Biol **2**(10): 731-737.

Shi, C., R. H. Hruban and A. P. Klein (2009). "Familial pancreatic cancer." Arch Pathol Lab Med **133**(3): 365-374.

Shibata, M. A., J. Morimoto, K. Akamatsu and Y. Otsuki (2008). "Antimetastatic effect of suicide gene therapy for mouse mammary cancers requires T-cell-mediated immune responses." Med Mol Morphol **41**(1): 34-43.

Short, J. J., A. A. Rivera, H. Wu, M. R. Walter, M. Yamamoto, J. M. Mathis and D. T. Curiel (2010). "Substitution of adenovirus serotype 3 hexon onto a serotype 5 oncolytic adenovirus reduces factor X binding, decreases liver tropism, and improves antitumor efficacy." Mol Cancer Ther **9**(9): 2536-2544.

Smith, H. W. and C. J. Marshall (2010). "Regulation of cell signalling by uPAR." Nat Rev Mol Cell Biol **11**(1): 23-36.

Smith, T., N. Idamakanti, H. Kylefjord, M. Rollence, L. King, M. Kaloss, M. Kaleko and S. C. Stevenson (2002). "In vivo hepatic adenoviral gene delivery occurs independently of the coxsackievirus-adenovirus receptor." Mol Ther **5**(6): 770-779.

Solbiati, L., T. Ierace, M. Tonolini, V. Osti and L. Cova (2001). "Radiofrequency thermal ablation of hepatic metastases." Eur J Ultrasound **13**(2): 149-158.

Springfeld, C., V. von Messling, M. Frenzke, G. Ungerechts, C. J. Buchholz and R. Cattaneo (2006). "Oncolytic efficacy and enhanced safety

of measles virus activated by tumor-secreted matrix metalloproteinases." Cancer Res **66**(15): 7694-7700.

Stathis, A. and M. J. Moore (2010). "Advanced pancreatic carcinoma: current treatment and future challenges." Nat Rev Clin Oncol **7**(3): 163-172.

Stefanidakis, M. and E. Koivunen (2006). "Cell-surface association between matrix metalloproteinases and integrins: role of the complexes in leukocyte migration and cancer progression." Blood **108**(5): 1441-1450.

Sternlicht, M. D. and Z. Werb (2001). "How matrix metalloproteinases regulate cell behavior." Annu Rev Cell Dev Biol **17**: 463-516.

Suzuki, E., V. Kapoor, A. S. Jassar, L. R. Kaiser and S. M. Albelda (2005). "Gemcitabine selectively eliminates splenic Gr-1+/CD11b+ myeloid suppressor cells in tumor-bearing animals and enhances antitumor immune activity." Clin Cancer Res **11**(18): 6713-6721.

Szecsi, J., R. Drury, V. Josserand, M. Grange, B. Boson, I. Hartl, R. Schneider, C. Buchholz, J. Coll and S. Russell (2006). "Targeted retroviral vectors displaying a cleavage site-engineered hemagglutinin (HA) through HA–protease interactions." Molecular Therapy **14**(5): 735-744.

Takahara, A., S. Koido, M. Ito, E. Nagasaki, Y. Sagawa, T. Iwamoto, H. Komita, T. Ochi, H. Fujiwara, M. Yasukawa, J. Mineno, H. Shiku, S. Nishida, H. Sugiyama, H. Tajiri and S. Homma (2011). "Gemcitabine enhances Wilms' tumor gene WT1 expression and sensitizes human pancreatic cancer cells with WT1-specific T-cell-mediated antitumor immune response." Cancer Immunol Immunother.

Takeuchi, M., T. Shichinohe, N. Senmaru, M. Miyamoto, H. Fujita, M. Takimoto, S. Kondo, H. Katoh and N. Kuzumaki (2000). "The dominant negative H-ras mutant, N116Y, suppresses growth of metastatic human pancreatic cancer cells in the liver of nude mice." Gene Ther **7**(6): 518-526.

Tokui, Y., J. Kozawa, K. Yamagata, J. Zhang, H. Ohmoto, Y. Tochino, K. Okita, H. Iwahashi, M. Namba, I. Shimomura and J. Miyagawa (2006). "Neogenesis and proliferation of beta-cells induced by human betacellulin gene transduction via retrograde pancreatic duct injection of an adenovirus vector." Biochem Biophys Res Commun **350**(4): 987-993.

Tominaga, K., S. Kuriyama, H. Yoshiji, A. Deguchi, Y. Kita, F. Funakoshi, T. Masaki, K. Kurokohchi, N. Uchida, T. Tsujimoto and H. Fukui (2004). "Repeated adenoviral administration into the biliary tract can induce repeated expression of the original gene construct in rat livers without immunosuppressive strategies." Gut **53**(8): 1167-1173.

Touraine, R. L., N. Vahanian, W. J. Ramsey and R. M. Blaese (1998). "Enhancement of the herpes simplex virus thymidine kinase/ganciclovir bystander effect and its antitumor efficacy in vivo by pharmacologic manipulation of gap junctions." Hum Gene Ther **9**(16): 2385-2391.

Toyoda, E., R. Doi, K. Kami, T. Mori, D. Ito, M. Koizumi, A. Kida, K. Nagai, T. Ito, T. Masui, M. Wada, M. Tagawa and S. Uemoto (2008). "Adenovirus vectors with chimeric type 5 and 35 fiber proteins exhibit enhanced transfection of human pancreatic cancer cells." Int J Oncol **33**(6): 1141-1147.

Tracy, C. R., W. Kabbani and J. A. Cadeddu (2011). "Irreversible electroporation (IRE): a novel method for renal tissue ablation." BJU Int **107**(12): 1982-1987.

Tsuji, K., M. Yang, P. Jiang, A. Maitra, S. Kaushal, K. Yamauchi, M. H. Katz, A. R. Moossa, R. M. Hoffman and M. Bouvet (2006). "Common bile duct injection as a novel method for establishing red fluorescent protein (RFP)-expressing human pancreatic cancer in nude mice." JOP **7**(2): 193-199.

Tuveson, D. A., L. Zhu, A. Gopinathan, N. A. Willis, L. Kachatrian, R. Grochow, C. L. Pin, N. Y. Mitin, E. J. Taparowsky, P. A. Gimotty, R. H. Hruban, T. Jacks and S. F. Konieczny (2006). "Mist1-KrasG12D knock-in mice develop mixed differentiation metastatic exocrine

pancreatic carcinoma and hepatocellular carcinoma." Cancer Res **66**(1): 242-247.

van Dillen, I. J., N. H. Mulder, W. Vaalburg, E. F. de Vries and G. A. Hospers (2002). "Influence of the bystander effect on HSV-tk/GCV gene therapy. A review." Curr Gene Ther **2**(3): 307-322.

Vigant, F., D. Descamps, B. Jullienne, S. Esselin, E. Connault, P. Opolon, T. Tordjmann, E. Vigne, M. Perricaudet and K. Benihoud (2008). "Substitution of hexon hypervariable region 5 of adenovirus serotype 5 abrogates blood factor binding and limits gene transfer to liver." Mol Ther **16**(8): 1474-1480.

Vile, R. G., S. Castleden, J. Marshall, R. Camplejohn, C. Upton and H. Chong (1997). "Generation of an anti-tumour immune response in a non-immunogenic tumour: HSVtk killing in vivo stimulates a mononuclear cell infiltrate and a Th1-like profile of intratumoural cytokine expression." Int J Cancer **71**(2): 267-274.

Vives, E., P. Brodin and B. Lebleu (1997). "A truncated HIV-1 Tat protein basic domain rapidly translocates through the plasma membrane and accumulates in the cell nucleus." J Biol Chem **272**(25): 16010-16017.

Vogler, M., K. Durr, M. Jovanovic, K. M. Debatin and S. Fulda (2007). "Regulation of TRAIL-induced apoptosis by XIAP in pancreatic carcinoma cells." Oncogene **26**(2): 248-257.

Vonhoff, D. (2006). "What's new in pancreatic cancer treatment pipeline?" Best Practice & Research Clinical Gastroenterology **20**(2): 315-326.

Vrionis, F. D., J. K. Wu, P. Qi, M. Waltzman, V. Cherington and D. C. Spray (1997). "The bystander effect exerted by tumor cells expressing the herpes simplex virus thymidine kinase (HSVtk) gene is dependent on connexin expression and cell communication via gap junctions." Gene Ther **4**(6): 577-585.

Wack, S., S. Rejiba, C. Parmentier, M. Aprahamian and A. Hajri (2008). "Telomerase transcriptional targeting of inducible Bax/TRAIL

gene therapy improves gemcitabine treatment of pancreatic cancer." Mol Ther **16**(2): 252-260.

Waddington, S. N., J. H. McVey, D. Bhella, A. L. Parker, K. Barker, H. Atoda, R. Pink, S. M. K. Buckley, J. A. Greig, L. Denby, J. Custers, T. Morita, I. M. B. Francischetti, R. Q. Monteiro, D. H. Barouch, N. van Rooijen, C. Napoli, M. J. E. Havenga, S. A. Nicklin and A. H. Baker (2008). "Adenovirus Serotype 5 Hexon Mediates Liver Gene Transfer." Cell **132**(3): 397-409.

Wadia, J. S. and S. F. Dowdy (2005). "Transmembrane delivery of protein and peptide drugs by TAT-mediated transduction in the treatment of cancer." Adv Drug Deliv Rev **57**(4): 579-596.

Waehler, R., S. J. Russell and D. T. Curiel (2007). "Engineering targeted viral vectors for gene therapy." Nat Rev Genet **8**(8): 573-587.

Wagner, M., F. R. Greten, C. K. Weber, S. Koschnick, T. Mattfeldt, W. Deppert, H. Kern, G. Adler and R. M. Schmid (2001). "A murine tumor progression model for pancreatic cancer recapitulating the genetic alterations of the human disease." Genes Dev **15**(3): 286-293.

Warshaw, A. L. and C. Fernandez-del Castillo (1992). "Pancreatic carcinoma." N Engl J Med **326**(7): 455-465.

Wei, D., H. Q. Xiong, J. L. Abbruzzese and K. Xie (2003). "Experimental animal models of pancreatic carcinogenesis and metastasis." Int J Gastrointest Cancer **33**(1): 43-60.

Weichselbaum, R. R. and D. Kufe (2009). "Translation of the radio- and chemo-inducible TNFerade vector to the treatment of human cancers." Cancer Gene Ther **16**(8): 609-619.

Welch, S. A. and M. J. Moore (2007). "Combination chemotherapy in advanced pancreatic cancer: time to raise the white flag?" J Clin Oncol **25**(16): 2159-2161.

Wesseling, J. G., P. J. Bosma, V. Krasnykh, E. A. Kashentseva, J. L. Blackwell, P. N. Reynolds, H. Li, M. Parameshwar, S. M. Vickers, E. M. Jaffee, K. Huibregtse, D. T. Curiel and I. Dmitriev (2001).

"Improved gene transfer efficiency to primary and established human pancreatic carcinoma target cells via epidermal growth factor receptor and integrin-targeted adenoviral vectors." Gene Ther **8**(13): 969-976.

Wolpin, B. M., A. T. Chan, P. Hartge, S. J. Chanock, P. Kraft, D. J. Hunter, E. L. Giovannucci and C. S. Fuchs (2009). "ABO blood group and the risk of pancreatic cancer." J Natl Cancer Inst **101**(6): 424-431.

Wong, A., R. A. Soo, W. P. Yong and F. Innocenti (2009). "Clinical pharmacology and pharmacogenetics of gemcitabine." Drug Metab Rev **41**(2): 77-88.

Wong, H. H. and N. R. Lemoine (2009). "Pancreatic cancer: molecular pathogenesis and new therapeutic targets." Nat Rev Gastroenterol Hepatol **6**(7): 412-422.

Xia, D., L. Henry, R. D. Gerard and J. Deisenhofer (1995). "Structure of the receptor binding domain of adenovirus type 5 fiber protein." Curr Top Microbiol Immunol **199 (Pt 1)**: 39-46.

Xu, J., C. Jin, S. Hao, G. Luo and D. Fu (2010). "Pancreatic cancer: gene therapy approaches and gene delivery systems." Expert Opin Biol Ther **10**(1): 73-88.

Yachida, S., S. Jones, I. Bozic, T. Antal, R. Leary, B. Fu, M. Kamiyama, R. H. Hruban, J. R. Eshleman, M. A. Nowak, V. E. Velculescu, K. W. Kinzler, B. Vogelstein and C. A. Iacobuzio-Donahue (2010). "Distant metastasis occurs late during the genetic evolution of pancreatic cancer." Nature **467**(7319): 1114-1117.

Yu, D., C. Jin, J. Leja, N. Majdalani, B. Nilsson, F. Eriksson and M. Essand (2011). "Adenovirus with hexon Tat-PTD modification exhibits increased therapeutic effect in experimental neuroblastoma and neuroendocrine tumors." J Virol.

Yu, Y. A., C. Galanis, Y. Woo, N. Chen, Q. Zhang, Y. Fong and A. A. Szalay (2009). "Regression of human pancreatic tumor xenografts in mice after a single systemic injection of recombinant vaccinia virus GLV-1h68." Mol Cancer Ther **8**(1): 141-151.

Zhang, Y. A., J. Nemunaitis, S. K. Samuel, P. Chen, Y. Shen and A. W. Tong (2006). "Antitumor activity of an oncolytic adenovirus-delivered oncogene small interfering RNA." Cancer Res **66**(19): 9736-9743.

Zischek, C., H. Niess, I. Ischenko, C. Conrad, R. Huss, K. W. Jauch, P. J. Nelson and C. Bruns (2009). "Targeting tumor stroma using engineered mesenchymal stem cells reduces the growth of pancreatic carcinoma." Ann Surg **250**(5): 747-753.

ANNEX

Pujal, J; Huch, M; José, A; Abasolo, I; Rodolosse, A; Duch, A; Sánchez-Palazón, L; Smith, FJ; McLean, WH; Fillat, C; Real, FX. Keratin 7 promoter selectively targets transgene expression to normal and neoplastic pancreatic ductal cells in vitro and in vivo. FASEB J. 2009 May;23(5):1366-75.

Huch, M; Gros,A ; Jose, A; Gonzalez, JR; Alemany, R; Fillat,C. Urokinase-type plasminogen activator receptor transcriptionally controlled adenoviruses eradicate pancreatic tumors and liver metastasis in mouse models. Neoplasia. 2009; 11(6): 518-528.

Fillat, C; José, A ; Bofill-De Ros, X; Mato-Berciano, A; Maliandi, M.V; Abate-Daga, D. Controlling Adenoviral Replication to Induce Oncolytic Efficacy.The Open Gene Therapy Journal. 2010; 3:15-23.

Fillat,C ; Jose,A; Bofill-DeRos,X; Mato-Berciano, A; Maliandi,M. V.;Sobrevals L. Pancreatic Cancer Gene Therapy: From Molecular Targets to Delivery Systems. Cancers. 2011; 3(1): 368-395.

Irreversible electroporation shows efficacy against pancreatic carcinoma without systemic toxicity in mouse models.

Anabel José [1,2,‡], Luciano Sobrevals [1,2‡,], Antoni Ivorra [3*], Cristina Fillat [1,2*]

[1]Institut d'Investigacions Biomèdiques August Pi i Sunyer-IDIBAPS. [2]Centro de Investigación Biomédica en Red de Enfermedades Raras (CIBERER), Barcelona. [3]Department of Information and Communication Technologies, Universitat Pompeu Fabra (UPF). Barcelona. Spain.

‡ Anabel José and Luicano Sobrevals equally contributed to this work.

Under second revision in Cancer Letters.

ABSTRACT

Pancreatic Ductal Adenocarcinoma (PDAC) therapies show limited success. Irreversible electroporation (IRE) is an innovative loco-regional therapy in which highvoltage pulses are applied to induce plasma membrane defects leading to cellular death. In the present study we evaluated the feasibility of IRE against PDAC. IRE treatment exhibited significant antitumor effects and prolonged survival in mice with orthotopic xenografts. Extensive tumor necrosis, reduced tumor cell proliferation and disruption of microvessels were observed at different days post-IRE. Animals had transient increases in transaminases, amylase and lipase enzymes that normalized at 24h post-IRE. These results suggest that IRE could be an effective treatment for locally advanced pancreatic tumors.